SpringerWienNewYork

Progress in the Chemistry
of Organic Natural Products

Founded by L. Zechmeister

94

Progress in the Chemistry of Organic Natural Products

Authors:
S.S. Ebada, N. Lajkiewicz, J.A. Porco Jr,
M. Li-Weber, and P. Proksch
M.A.R.C. Bulusu, K. Baumann, and A. Stuetz
R.I. Misico, V.E. Nicotra, J.C. Oberti, G. Barboza,
R.R. Gil, and G. Burton

SpringerWienNewYork

Prof. A. Douglas Kinghorn, College of Pharmacy,
Ohio State University, Columbus, OH, USA

em. Univ.-Prof. Dr. H. Falk, Institut für Organische Chemie,
Johannes-Kepler-Universität, Linz, Austria

Prof. Dr. J. Kobayashi, Graduate School of Pharmaceutical Sciences,
Hokkaido University, Sapporo, Japan

SpringerWienNewYork is a part of
Springer Science + Business Media
springer.at

Typesetting: SPI, Chennai

Printed on acid-free and chlorine-free bleached paper
SPIN: 80022757

With 45 (partly coloured) Figures and 4 coloured Plates

ISSN 0071-7886
ISBN 978-3-7091-0747-8 e-ISBN 978-3-7091-0748-5
DOI 10.1007/978-3-7091-0748-5
SpringerWienNewYork

Contents

Contributors ix

Chemistry and Biology of Rocaglamides (= Flavaglines) and Related Derivatives from *Aglaia* Species (Meliaceae) 1
Sherif S. Ebada, Neil Lajkiewicz, John A. Porco Jr., Min Li-Weber, and *Peter Proksch*

1. Introduction 2
2. Structural Classification of Rocaglamides and Related Compounds 5
   2.1. Rocaglamide Derivatives 5
   2.2. Aglain Derivatives 12
   2.3. Aglaforbesin Derivatives 17
   2.4. Forbagline Derivatives 18
3. Biosynthesis of Rocaglamides and Related Metabolites 20
4. Pharmacological Significance of Rocaglamides and Related Compounds 23
   4.1. Insecticidal Activity 23
   4.2. Anti-inflammatory Activity 26
   4.3. Anticancer Activity 28
5. Chemical Synthesis of Cyclopenta[*b*]benzofurans 34
   5.1. First Approaches to the Synthesis of Rocaglamides 34
   5.2. The First Total Synthesis of Rocaglamide 36
   5.3. Syntheses of Rocaglamide and Related Natural Products 37
   5.4. New Approaches to Rocaglamide and Related Natural Products 39
   5.5. Syntheses of Silvestrol 44
   5.6. Development of Rocaglates and Analogues as Therapeutic Agents 47
6. Concluding Remarks 51

References 51

Chemistry of the Immunomodulatory Macrolide Ascomycin and Related Analogues 59
Murty A.R.C. Bulusu, Karl Baumann, and *Anton Stuetz*

1. Introduction 59
   1.1. Ascomycin and Related Natural Products 60
   1.2. Ascomycin Derivatives, a Novel Class of Anti-inflammatory Compounds 62
   1.3. Structural Features of Ascomycin 66
2. Synthesis Aspects 70
   2.1. Synthesis of the Four Diastereomeric "Furano-Ascomycins" 70
   2.2. Synthesis of ^{13}C Labelled Ascomycin 72
   2.3. Reactivity of the Binding Domain 75
   2.4. Modifications in the Effector and Cyclohexyl Domains 94
3. Summary 116
References 118

Withanolides and Related Steroids 127
Rosana I. Misico, Viviana E. Nicotra, Juan C. Oberti, Gloria Barboza, Roberto R. Gil, and *Gerardo Burton*

1. Introduction 128
2. Withanolides in the Plant Kingdom 129
   2.1. Solanaceous Genera Containing Withanolides 129
   2.2. Non-Solanaceous Genera Containing Withanolides 132
3. Classification of Withanolides 132
   3.1. Withanolides with a δ-Lactone or δ-Lactol Side Chain 132
   3.2. Withanolides with a γ-Lactone Side Chain 134
4. Withanolides with an Unmodified Skeleton 135
   4.1. The Withania *Withanolides* 135
   4.2. Other Withanolides with an Unmodified Skeleton 143
5. Withanolides with Modified Skeletons 157
   5.1. Withanolides with Additional Rings Involving C-21 157
   5.2. Physalins and Withaphysalins 163
   5.3. Withanolides Containing an Aromatic Ring and Related Steroids 168
   5.4. Withanolides with a γ-Lactone Side Chain 172
   5.5. 18-Norwithanolides 181
   5.6. Spiranoid Withanolides at C-22 184
6. Chemical and Bio-transformations of Withanolides 185
   6.1. Chemical Transformations 186
   6.2. Photochemical Transformations 188
   6.3. Biotransformations 189
7. Biological Activities of the Withanolides 192
   7.1. Insecticidal Activities 193

7.2. Phytotoxic Activities 196
7.3. Antiparasitic Activities 197
7.4. Antimicrobial Activities 199
7.5. Anti-inflammatory and Glucocorticoid Related Activities 200
7.6. Cancer-Related Activities 203
7.7. CNS-Related Activities 208
8. Chemotaxonomic Considerations 209
8.1. Tribe Physaleae 210
8.2. Tribes Hyoscyameae, Lycieae, and Solaneae 213
8.3. Tribe Datureae 213
8.4. Genera with Uncertain Positions in the Solanaceae Taxonomic System 213
References 216

Author Index 231

Subject Index 249

Listed in PubMed

Contributors

Gloria Barboza Departamento de Farmacia and IMBIV (CONICET), Facultad de Ciencias Químicas, Universidad Nacional de Córdoba, Ciudad Universitaria, Córdoba 5000, Argentina, gbarboza@imbiv.unc.edu.ar

Karl Baumann Novartis Institutes for BioMedical Research Vienna, Muthgasse 11/2, A-1190, Vienna, Austria

Murty A.R.C. Bulusu Novartis Institutes for BioMedical Research Vienna, Muthgasse 11/2, A-1190, Vienna, Austria

Gerardo Burton Departamento de Química Orgánica and UMYMFOR (CONICET-UBA), Facultad de Ciencias Exactas y Naturales, Universidad de Buenos Aires, Ciudad Universitaria, Pabellón 2, Buenos Aires C1428EGA, Argentina, burton@qo.fcen.uba.ar

Sherif S. Ebada Institute of Pharmaceutical Biology and Biotechnology, Heinrich-Heine University of Duesseldorf, Universitaetsstrasse 1, D-40225, Duesseldorf, Germany; Department of Pharmacognosy and Phytochemistry, Faculty of Pharmacy, Ain-Shams University, Organization of African Unity 1, 11566 Cairo, Egypt, sherif.elsayed@uni-duesseldorf.de

Roberto R. Gil Department of Chemistry, Carnegie Mellon University, 4400 Fifth Ave Pittsburgh, PA 15213, USA, rgil@andrew.cmu.edu

Neil Lajkiewicz Department of Chemistry and Center for Chemical Methodology and Library Development (CMLD-BU), Boston University, Commonwealth Avenue 590, Boston, MA 02215, USA, neiljl@bu.edu

Min Li-Weber Tumor Immunology Program (D030), German Cancer Research Center (DKFZ), Im Neuenheimer Feld 280, D-69120, Heidelberg, Germany, m.li-weber@dkfz-heidelberg.de

Rosana I. Misico Departamento de Química Orgánica and UMYMFOR (CONICET-UBA), Facultad de Ciencias Exactas y Naturales, Universidad de Buenos Aires, Ciudad Universitaria, Pabellón 2, Buenos Aires C1428EGA, Argentina, misicori@qo.fcen.uba.ar

Viviana E. Nicotra Departamento de Química Orgánica and IMBIV (CONICET), Facultad de Ciencias Químicas, Universidad Nacional de Córdoba, Ciudad Universitaria, Ciencias Químicas II, Córdoba 5000, Argentina, vnicotra@mail.fcq.unc.edu.ar

Juan C. Oberti Departamento de Química Orgánica and IMBIV (CONICET), Facultad de Ciencias Químicas, Universidad Nacional de Córdoba, Ciudad Universitaria, Ciencias Químicas II, Córdoba, Argentina, jco@mail.fcq.unc.edu.ar

John A. Porco Jr. Department of Chemistry and Center for Chemical Methodology and Library Development (CMLD-BU), Boston University, Commonwealth Avenue 590, Boston, MA 02215, USA, porco@bu.edu

Peter Proksch Institute of Pharmaceutical Biology and Biotechnology, Heinrich-Heine University of Duesseldorf, Universitaetsstrasse 1, D-40225, Duesseldorf, Germany, proksch@uni-duesseldorf.de

Anton Stuetz Novartis Institutes for BioMedical Research Vienna, Muthgasse 11/2, A-1190, Vienna, Austria, anton.stuetz@novartis.com

About the Authors

Sherif S. Ebada was born on September 1, 1978 in Cairo (Egypt). He received his B.Sc. and M.Sc. in Pharmaceutical Sciences (Pharmacognosy) from Ain-Shams University, Cairo (Egypt) under the guidance of Professors Ayoub, Singan, and Al-Azizi. In 2007, he joined the research group of Prof. Dr. Peter Proksch at the Institute of Pharmaceutical Biology and Biotechnology in the University of Duesseldorf as a doctoral candidate where he studied the isolation, structural elucidation, and structure-activity relationships of bioactive secondary metabolites from marine organisms. In 2010, he received his Ph.D. degree from the University of Duesseldorf, followed by a postdoctoral fellowship with Professor Proksch until the present.

Neil Lajkiewicz was born on November 23, 1983 in New York City, USA. He received his B.Sc. in chemistry at Boston University in 2005 and joined Lundbeck Research, USA after graduation. In 2008, he joined Sirtis Pharmaceuticals and in 2009 matriculated at Boston University for Ph.D. studies in organic synthesis. He is currently a second year graduate student in Professor John A. Porco Jr.'s laboratory studying photocycloadditions to achieve the synthesis of flavaglines and related products.

John A. Porco Jr. was born in Danbury, CT (USA) in 1963. He received his Ph.D. in 1992 from Harvard University under the direction of Professor Stuart L. Schreiber. John joined the Department of Chemistry at Boston University in 1999 as Assistant Professor after a period in industry and was promoted to Professor of Chemistry in September 2004. Professor Porco's current research is focused in two major areas: the development of new synthesis methodologies for efficient chemical synthesis of complex natural products and synthesis of complex chemical libraries.

Min Li-Weber was born on May 8, 1948 in Phnom Penh, Cambodia. She received her Master's in Biochemistry in 1975 from Peking (Beijing) University (China). From 1976 to 1979, she was a researcher at the Institute of Microbiology, Chinese Academy of Science in Beijing. From 1979 to 1980, she was a visiting scientist at the University of Utah (USA). From 1980 to 1982, she was a research assistant at the Max-Planck-Institute for cell biology (Germany). She received her Ph.D. in Biology on January 1985 from University of Heidelberg (Germany). From 1985 to 1986, she was a post-doctoral at the Max-Planck-Institute for cell biology. Since November 1986, she has been a project leader at the German Cancer Research Center (DKFZ) (Germany), where she works in the field of immunology and molecular and cellular aspects of apoptosis. She was guest professor at University of Salzburg (Austria) in 2003. Her current research is focused on the molecular mechanisms of apoptosis sensitivity and resistance in cancers and discovering and developing new anticancer drugs from natural products. She has published over 65 original research articles and several scientific review papers in the field of cancer research.

Peter Proksch was born on December 6, 1953 in Leipzig (Germany). He received his Ph.D. in Biology in 1980 from the University of Cologne. From 1980 to 1982 he was a postdoctoral at the University of California, Irvine (USA). From 1982 to 1985 he was at the University of Cologne and from 1986 to 1990 at the University of Braunschweig where he received his venia legendi for Pharmaceutical Biology. In 1990 he became Professor for Pharmaceutical Biology at the University of Wuerzburg and in 1999 he moved to his present position as Professor of Pharmaceutical Biology and Biotechnology and Head of the Institute at the University of Duesseldorf. His fields of research are bioactive natural products from marine invertebrates, higher plants and endophytic fungi. He has authored or coauthored over 300 publications and holds visiting professorships at the Universities of Beijing and Qingdao (P.R. China).

Dr. Murty Bulusu studied chemistry at Andhra University Waltair and obtained a Ph.D. degree from the Indian Institute of Technology Kanpur, India in 1983. Subsequently, he worked as Alexander von Humboldt Fellow with Prof. H. Prinzbach at the University of Freiburg i. Br., Germany, and then with Prof. A. Vasella at the University of Zürich, Switzerland. In 1989, he joined Sandoz Research Institute Vienna as a laboratory head, which later became Novartis Institutes for Biomedical Research Vienna, and then continued with its spinoff companies Sandoz AntiBiotic Research Institute (ABRI) and the New AntiBiotic Research Institute Vienna Austria (NABRIVA), and finally with the Albany Molecular Research Institute (AMRI) Hungary in 2010.

Dr. Bulusu's research interests have been on cage molecules, such as dodecahedrane, polysaccharides, such as lipid A, ascomycin and related macrolides, pleuromutilin and β-lactam antibiotics, and other low-molecular-weight classes of compounds, in various medicinal chemistry programs. He has contributed 25 research publications to peer-reviewed journals and holds five patents.

Dr. Karl Baumann studied chemistry at the Technical University in Vienna, Austria, and obtained a Ph.D. degree in organic chemistry. After a postdoctoral fellowship from 1984 to 1986 with Prof. A. Eschenmoser at the Swiss Federal Institute of Technology (ETH) in Zürich, Switzerland, he joined the Chemie Linz AG in Linz, Austria. In 1988 he joined the Sandoz Research Institute Vienna, which later became Novartis Institutes for Biomedical Research Vienna, where he worked as head of a medicinal chemistry laboratory until 2009.

Dr. Baumann invented the ascomycin derivative, SDZ 281–240, which was the first topical calcineurin inhibitor to show efficacy in patients with inflammatory skin disease. These data provided the first proof of concept and thus a milestone in the identification of this new class of topical non-steroids. He is author/coauthor of 32 publications and 20 abstracts, and the holder of 18 patents in the fields of β-lactam and quinolone-type antibiotics, natural products, labeling of organic compounds, and the development of synthetic methods.

Dr. Anton Stuetz studied chemistry and physics at the University of Vienna and obtained a Ph.D. degree in organic chemistry in 1972. After postdoctoral studies in molecular biology at the Max Planck Institute for Biophysical Chemistry, Göttingen, Germany, in 1974 he joined the Sandoz Research Institute Vienna, Austria, as head of laboratory. In 1986, he took over the responsibility of establishing dermatology research within Sandoz and became head of this new department. In 1995–1996, he served as acting head of the institute, which was renamed Novartis Research Institute Vienna after the merger of Sandoz and Ciba-Geigy. At present, he is Executive Director of Dermatology within the Disease Area Autoimmunity, Transplantation, and Inflammation as part of the Novartis Institutes for BioMedical Research, located in Vienna, Austria.

Dr. Stuetz invented terbinafine (Lamisil) in 1980, which after a worldwide launch during 1991–1997 has become the global standard for the treatment of fungal infections of the skin and nails (onychomycosis). Under his leadership a

new class of anti-inflammatory agents later termed "topical calcineurin inhibitors" were pioneered, including the use of topical tacrolimus for the treatment of skin diseases, and pimecrolimus invented and its pharmacological profile established. Tacrolimus ointment (Protopic) and pimecrolimus cream (Elidel) are the first therapeutically effective and registered topical non-steroid agents for treatment of atopic dermatitis.

Dr. Stuetz is the author/coauthor of 89 publications and 170 abstracts, and holds 35 patents in the fields of synthetic and medicinal chemistry, antifungal chemotherapy, immunology, inflammation, dermatology, and translational research. He is a frequently invited speaker at international congresses and universities.

In 1994, Dr. Stuetz was appointed as professor for pharmaceutical chemistry at the University of Vienna. In 2004, he was awarded the Erwin Schrödinger Prize by the Austrian Academy of Sciences. He has served as a member of the Board of Directors of the Society for Investigative Dermatology for the period 2005–2010. In February 2011, he received the Eugene J. Van Scott Award for Innovative Therapy of the Skin and the Philipp Frost Leadership Lecture Award from the American Academy of Dermatology.

Rosana I. Misico was born in Córdoba, Argentina. She obtained her Ph.D. in chemistry (natural products) at the National University of Córdoba under the supervision of Prof. Juan C. Oberti. She then spent a postdoctoral year at the University of Illinois at Chicago working with Prof. A. Douglas Kinghorn. In 2001, she joined the group of Professor Gerardo Burton at the University of Buenos Aires. She is currently a senior researcher of the National Research Council of Argentina (CONICET). Her current research interests are on the synthesis of bioactive naphthoquinones and natural products.

Viviana E. Nicotra was born and raised in Cordoba, Argentina. She received a Pharmacy degree from the Cordoba National University, Cordoba, Argentina in 1987, a Masters in Biological Chemistry from the National University of Comahue, Neuquen, Argentina in 1988, and the Ph.D. in Chemistry (Natural Products) from Cordoba National University, under the supervision of Prof. Juan C. Oberti. She had a brief postdoctoral stay at the Instituto Universitario de Bioorganica (IUBO) at the Universidad de La Laguna, La Laguna, Canary Islands, Spain, under the supervision of Prof. Angel Gutierrez Ravelo, in 2008. Since 1999, she has been working at the Department of Chemistry of the Cordoba National University with a teaching instructor position and a senior researcher position within the research track of the National Research Council of Argentina (CONICET). Her current research interest is on the search of bioactive steroidal lactones (withanolides) from South American Solanaceae, as well as studies of montmorillonite-tetracycline interactions by circular dichroism.

Juan Carlos M. Oberti was born in the city of Paran, Entre Rios province, Argentina. He received degrees in Biochemistry (1965) and Pharmacy (1968), and a Ph.D. in 1974 under the supervision of Professor Ramón Juliani, on the topic "Alkaloids from Prosopis ruscifolia", all from Córdoba National University, Córdoba, Argentina. He spent a short postdoctoral stay at the Department of Organic Chemistry of the University of Buenos Aires with Prof. Eduardo Gros, where he also participated in the team that officially performed anti-doping tests for the soccer matches during the 1978 FIFA World Cup in Argentina. Since 1979, he has led the Natural Products research group at the Department of Chemistry of the College of Chemistry, Córdoba National University, focusing mainly on the search for sesquiterpene lactones from South American Compositae and steroidal lactones (withanolides) from South American Solanaceae. Prof. Oberti retired from Cordoba National University in 2005, where he remains as Consulting Professor, and is still active in research with a research position from the National Research Council of Argentina (CONICET). He is currently working on withanolides, as well as on sesquiterpene agarofuran alkaloids and quinones from the Celastraceae.

Gloria E. Barboza was born and raised in Salta, Argentina. She received a degree in Biology from the National University of Tucuman (Argentina) in 1985 and a Ph.D. in Biology from the National University of Cordoba (Argentina) in 1989, where she worked under the supervision of Prof. Armando T. Hunziker, a recognized specialist on the Solanaceae. Since 1990, she has held a permanent position as a researcher in the National Research Council of Argentina (CONICET) working at the Instituto Multidisciplinario de Biología Vegetal (IMBIV) in Córdoba. In 1994, she was appointed to a Professor position in Botany at the Pharmacy Department (Chemical Sciences College). Her current research interests are on the systematics of the Solanaceae, especially the South American genera, and on Argentine medicinal plants.

Roberto R. Gil was born in Catamarca, Argentina in 1961. He received the degrees of B.S./M.S. in Organic Chemistry (1983) and Ph.D. in Natural Products Chemistry (1989) from the University of Córdoba, Córdoba, Argentina. In 1992 he received an external postdoctoral fellowship from the National Research Council of Argentina (CONICET) to work with Professors Geoffrey A. Cordell and A. Douglas Kinghorn at the University of Illinois at Chicago in the field of bioactive natural products from plants. In 1995, he returned to the University of Córdoba where he started his own research group as Assistant Professor. In 2000 he spent a year as Visiting Professor at Carnegie Mellon University working in Protein NMR with Professor Miguel Llins. In 2002, he moved to Pittsburgh, Pennsylvania, where he currently holds the position of Associate Research Professor and Director of the NMR Laboratory of the Department of Chemistry at Carnegie Mellon University. His research interest is aimed at the development and application of NMR methodologies to the analysis of the structural and physical properties of bioactive natural products, nucleic acids, peptides and synthetic polymers.

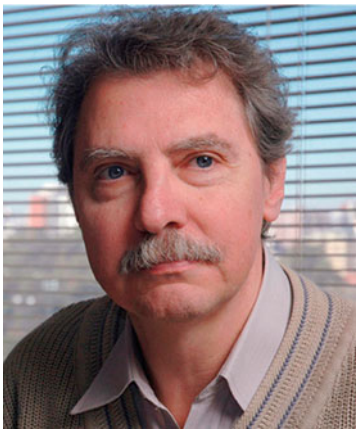

Gerardo Burton was born in Buenos Aires, Argentina. He obtained a doctoral degree in organic chemistry from the University of Buenos Aires in 1977, where he worked on the biosynthesis of steroidal lactones of animal origin with Prof. E. G. Gros. After a postdoctoral stay at the Department of Chemistry, Texas A&M University (USA) with Prof. A. Ian Scott working on porphyrin biosynthesis and biological NMR, he returned to Argentina in 1980. There he joined the faculty of the Organic Chemistry Department (Facultad de Ciencias Exactas y Naturales), University of Buenos Aires as an Assistant Professor, and started research on the design and synthesis of steroid hormone analogs. He is currently a Plenary Professor in that Department and an Investigator of the National Research Council of Argentina (CONICET). He was Chairman of the Organic Chemistry Department (University of Buenos Aires) on two occasions, and has been Director of UMYMFOR, a research institute and spectroscopic and analytical facility of CONICET, since 2001. His current research interests are in the area of organic synthesis and medicinal chemistry, specifically the design and synthesis of new bioactive steroids and their interaction with nuclear receptors.

Chemistry and Biology of Rocaglamides (= Flavaglines) and Related Derivatives from *Aglaia* Species (Meliaceae)

Sherif S. Ebada, Neil Lajkiewicz, John A. Porco Jr., Min Li-Weber, and *Peter Proksch*

Contents

1. Introduction 2
2. Structural Classification of Rocaglamides and Related Compounds 5
   2.1. Rocaglamide Derivatives 5
   2.2. Aglain Derivatives 12
   2.3. Aglaforbesin Derivatives 17
   2.4. Forbagline Derivatives 18
3. Biosynthesis of Rocaglamides and Related Metabolites 20

John A. Porco, Min Li-Weber, and Peter Proksch contributed equally to the writing of this chapter. Dedicated to Dr. Bambang Wahyu Nugroho, a pioneer of rocaglamide research (*9*, *14*, *16*, *17*, *27*, *54–56*, *58*, *59*, *75*, *84*, *85*) who passed away far too early.

S.S. Ebada
Institute of Pharmaceutical Biology and Biotechnology, Heinrich-Heine University of Duesseldorf, Universitaetsstrasse 1, D-40225, Duesseldorf, Germany
Department of Pharmacognosy and Phytochemistry, Faculty of Pharmacy, Ain-Shams University, Organization of African Unity 1, 11566 Cairo, Egypt
e-mail: sherif.elsayed@uni-duesseldorf.de

N. Lajkiewicz • J.A. Porco Jr.
Department of Chemistry and Center for Chemical Methodology and Library Development (CMLD-BU), Boston University, Commonwealth Avenue 590, Boston, MA 02215, USA
e-mail: neiljl@bu.edu; porco@bu.edu

M. Li-Weber
Tumor Immunology Program (D030), German Cancer Research Center (DKFZ), Im Neuenheimer Feld 280, D-69120, Heidelberg, Germany
e-mail: m.li-weber@dkfz-heidelberg.de

P. Proksch (✉)
Institute of Pharmaceutical Biology and Biotechnology, Heinrich-Heine University of Duesseldorf, Universitaetsstrasse 1, D-40225, Duesseldorf, Germany
e-mail: proksch@uni-duesseldorf.de

A.D. Kinghorn, H. Falk, J. Kobayashi (eds.), *Progress in the Chemistry of Organic Natural Products, Vol. 94*, DOI 10.1007/978-3-7091-0748-5_1,

4. Pharmacological Significance of Rocaglamides and Related Compounds 23
4.1. Insecticidal Activity 23
4.2. Anti-inflammatory Activity 26
4.3. Anticancer Activity 28
5. Chemical Synthesis of Cyclopenta[*b*]benzofurans 34
5.1. First Approaches to the Synthesis of Rocaglamides 34
5.2. The First Total Synthesis of Rocaglamide 36
5.3. Syntheses of Rocaglamide and Related Natural Products 37
5.4. New Approaches to Rocaglamide and Related Natural Products 39
5.5. Syntheses of Silvestrol 44
5.6. Development of Rocaglates and Analogues as Therapeutic Agents 47
6. Concluding Remarks 51
References 51

1. Introduction

Throughout the ages, humans have relied on Nature for fulfilling their basic needs for foodstuffs, shelter, clothing, means of transportation, fertilizers, flavors and fragrances, and, last but not least, medicines. Natural products have played, for thousands of years, an important role throughout the world in treating and preventing human diseases. Natural product medicines have come from various source materials including terrestrial plants, terrestrial microorganisms, marine organisms, and terrestrial vertebrates and invertebrates (*1*). The importance of natural products in modern medicine can be assessed using three criteria: (a) the rate of introducing new chemical entities of wide structural diversity, which may serve as templates for semisynthetic and total synthetic modification, (b) the number of diseases treated or prevented by these substances, and (c) their frequency of use in the treatment of disease (*2*, *3*). An analysis of the origin of drugs developed between 1981 and 2007 indicated that almost half of the drugs approved since 1994 were based on natural products (*2*, *3*). Over 20

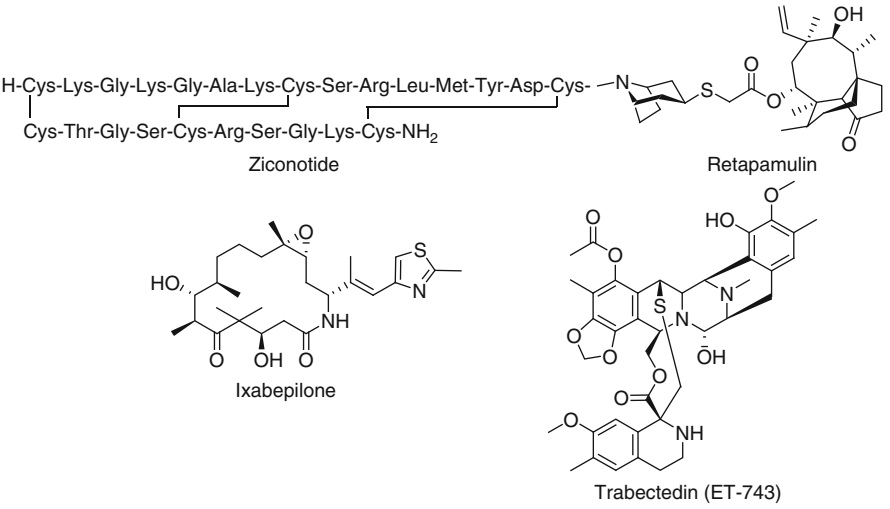

Fig. 1. Chemical structures of ziconotide, ixabepilone, retapamulin, and trabectedin (ET-743)

new drugs launched into the pharmaceutical market between 2000 and 2005 represent natural products (*2*, *3*), whereas more than 13 natural-product-related drugs were approved from 2004 to 2007; four of them represent the first members of new classes of drugs: the peptide ziconotide, and the small molecules ixabepilone, retapamulin, and trabectedin (ET-743) (Fig. 1) (*3*, *4*). Interestingly, over a hundred natural-product-derived compounds are currently undergoing clinical trials and at least a hundred similar substances are under preclinical development, with most of these derived from leads from plant and microbial sources (*3*). In spite of challenges facing drug discovery from plants, including the legal and logistical difficulties involved in the procurement of plant materials, and the lengthy and costly process of bioassay-guided fractionation and compound isolation, plants still provide new drug leads that prove to be of potential preclinical and/or clinical use against serious ailments such as cancer, malaria, *Alzheimer*'s disease, and AIDS (*5*).

The family Meliaceae (= Mahogany family, order Sapindales) is an angiosperm plant family of mostly trees and shrubs together with a few herbaceous plants. This family includes about 50 genera and 550 species, with a panotropical geographical distribution. Two genera, namely, *Swietenia* (Mahogany) and *Khaya* (African mahogany), are important sources of high-quality woods for building shelters and furniture due to their physical properties and also due to their resistance to insect invasion (*6*).

The genus *Aglaia* Lour. (Fig. 2) is the largest genus of the family Meliaceae, comprising about 120 woody species ranging from small to large trees up to 40 m

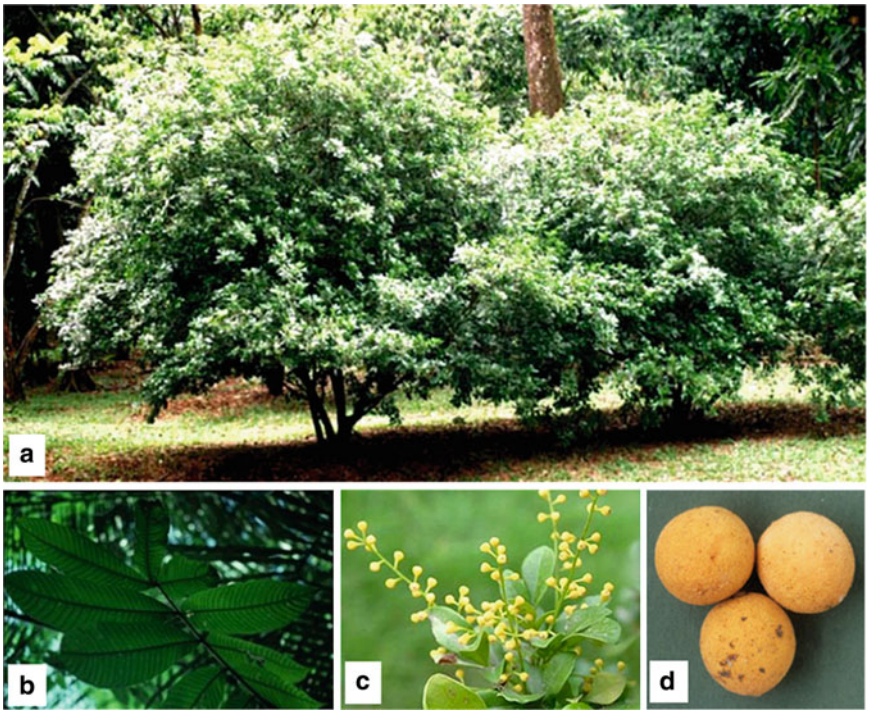

Fig. 2. *Aglaia* Lour. (family Meliaceae). (a): Entire tree of *Aglaia odorata*, (b): leaves of *A. tomentosa*, (c): flowers of *A. odorata*, (d): fruits of *A. forbes*ii (photos by Dr. *B. W. Nugroho* and from http://dps.plants.ox.ac.uk/bol/aglaia and http://www.rareflora.com/aglaiaodo.html)

high, mainly distributed in the tropical rainforests of southeast Asia from Sri Lanka and India, through Burma, south China and Taiwan, Vietnam, Malaysia, Indonesia, the Philippines, New Guinea, the Solomon Islands, Vanuatu (New Hebrides), New Caledonia, Australia (Queensland, Northern Territory and Western Australia), Fiji, as far east as the island of Samoa in Polynesia and north to the Marianne Islands (Saipan, Roti and Guam), and the Caroline Islands (Palau and Ponape) in Micronesia (*7*). A molecular phylogeny has demonstrated that the genus is divided into three sections, section *Amoora*, section *Neoaglaia*, and section *Aglaia* (*8*). They are distinguishable morphologically, mainly on fruit characteristics and the numbers of flower parts (*8*). Like the two genera *Swietenia* (Mahogany) and *Khaya*, the timber of many *Aglaia* species is used locally for house-building, fence-posts, canoes, paddles, axe-handles, spear-shafts, and firewood. The fragrant flowers are used for scenting tea and are kept in cupboards to perfume and to protect clothing from moths. They produce sweet, fleshy fruits that are cultivated in villages in Thailand and peninsular Malaysia and are eaten in the forest by indigenous forest peoples.

The fruits of *Aglaia* (Fig. 2) are also a source of food for birds and mammals in the forests of the Indo-Malayan and Australasian regions where they occur. In West Malaysia, the fruits of species in the section *Aglaia* are indehiscent and primates break open the orange, yellow or brown, fibrous, inedible pericarp and extract the one or two seeds from within. The translucent, sweet aril adheres firmly to the seed, and the seed is often swallowed whole. Analysis of the nutrient content of the aril reveals that it contains sugars and other sweet-tasting constituents and it is thought that these are attractive to the gibbons that disperse the seeds (*7*). The fruits of sections *Amoora* and *Neoaglaia* are dehiscent and contain up to three seeds. The outer pericarp is pink or reddish-brown and contrasts with the white inner pericarp and the red aril surrounding the seed. The aril is easily detached from the testa and is removed by the action of a bird's gizzard, without destroying the rest of the seed. The aril, surrounding a relatively large seed, is rich in lipids and provides the birds that disperse the large seed with a high-calorie reward (*7*).

Several species of the genus *Aglaia*, such as *A. odorata*, are used traditionally in folk medicine for heart stimulant and febrifuge purposes, and for the treatment of coughs, diarrhea, inflammation, and injuries (*9*). Extracts have also been used as bactericides, insecticides, and in perfumery (*10*).

During the last few decades, species in the genus *Aglaia* Lour. have received an increasing scientific focus due to their bioactivity potential. Phytochemical interest in the natural constituents of *Aglaia* Lour. can be traced back to the discovery in 1982 of the first cyclopenta[*b*]benzofuran derivative, rocaglamide (**1**), from *A. elliptifolia* (*11*). To date, more than a hundred naturally occurring rocaglamide-type (= flavagline) compounds have been isolated from over 30 *Aglaia* species (*9, 12*). Rocaglamides exhibit potent insecticidal (*13–18*) and antiproliferative (*12, 19–21*) activities. In addition, antiviral (*22*), antifungal (*23*), and anti-inflammatory (*24, 25*) activities were also reported for these compounds, which are so far only known from *Aglaia* species. Other classes of natural products occurring in *Aglaia* include lignans (*13, 26–29*), flavonoids, and bisamides (*18, 22, 26, 30–36*). Some of these

metabolites exhibit cytotoxic and antiviral properties as well (*22*, *30*). Furthermore, many terpenoids have been reported from the genus *Aglaia* Lour. (*10*, *36–51*).

The present contribution surveys the group of the rocaglamide derivatives (also known as "flavaglines" or "rocaglate derivatives") and related compounds obtained from the genus *Aglaia*, with an emphasis on their structural diversity, and highlights their potential pharmacological significance, which is the main reason for attracting a greater attention by natural product chemists and cell biologists to this class of natural products and provides a comprehensive overview on their total synthesis.

2. Structural Classification of Rocaglamides and Related Compounds

2.1. Rocaglamide Derivatives

Rocaglamide (**1**), a 1*H*-2,3,3a,8b-tetrahydrocyclopenta[*b*]benzofuran, was first structurally elucidated in 1982 by *King et al*. through single-crystal X-ray analysis (Fig. 3) (*11*). Its absolute stereochemistry was determined unambiguously to be (1*R*,2*R*,3*S*,3a*R*,8b*S*) using enantioselective synthesis in 1990 by *Trost et al*. (*52*). Comparative MS and 1D and 2D NMR spectroscopic data of rocaglamide (**1**) and

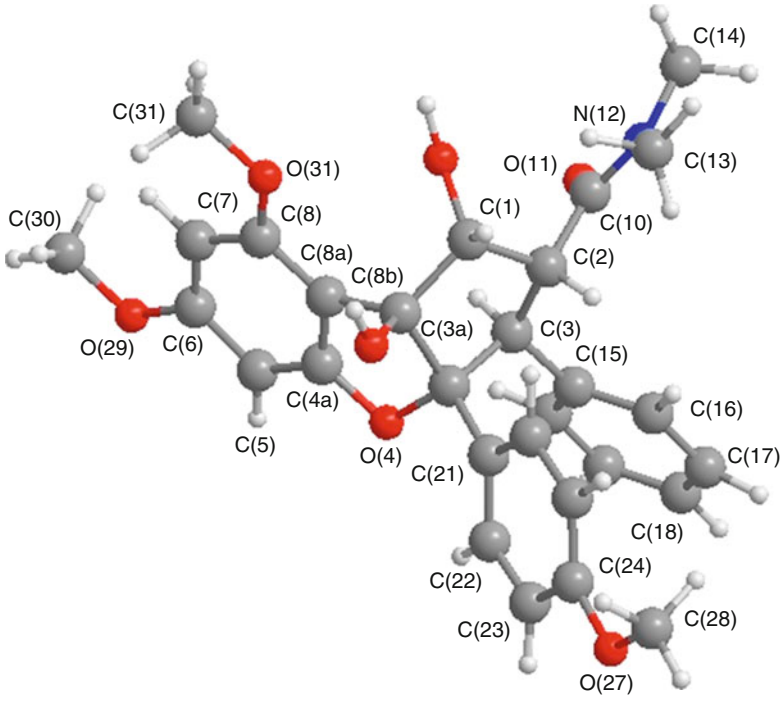

Fig. 3. X-ray crystal structure of rocaglamide (**1**) (*11*)

its analogues, desmethylrocaglamide (**7**), methyl rocaglate (**18**), and rocaglaol (**28**) were first presented in 1993 by *Ishibashi et al.* (*53*). Rocaglamide congeners differ basically with regard to their substituents at C-1, C-2, C-8b, and C-3′ at ring B. Major variations in the substitution pattern occur at C-2 while the hydroxy substituents at C-1 or C-8b can either be acetylated, methylated, or ethylated (*e.g.* congeners **4**, **5**, and **6**). The position C-3′ is either hydroxylated or methoxylated (*e.g.* congeners **2** and **3**). However, oxidation (*16*) and esterification (*17*) of the hydroxy group at C-1 have been also reported. The structures of rocaglamides known so far are summarized in Fig. 4.

The mass spectra of rocaglamide and its derivatives often show characteristic pairs of fragments at *m*/*z* 300 and 313 dependent on the substitution pattern. Plausible structures for the ions *m*/*z* 300 and 313 arising from fragmentation of rocaglamide-type compounds under EI conditions have been described (*54*), as summarized in Fig. 5. Changes in the fragmentation pattern in the range *m*/*z* 300–343 indicate the type of substitution at ring B and C-8b of the furan ring. For example, the presence of a hydroxy substituent at C-3′ shifts the characteristic pair of fragments at *m*/*z* 300 and 313 (as in rocaglamide) to *m*/*z* 316 and 329 while a methoxy substituent at the same position gives rise to fragments at *m*/*z* 330 and 343 in the EI mass spectrum of the respective derivative (*55*). Modification of the hydroxy substituent at C-8b (*e.g.* methylation) can also be determined initially by comparison of its diagnostic fragments to those of the more common structural analogues featuring a hydroxy group at that position (*56*). Rocaglamide analogues exhibit ^{1}H and ^{13}C NMR signals for aromatic protons and aromatic methoxy groups typical for those of substituted phenols. Investigation of the ^{1}H NMR spectra of several rocaglamide derivatives showed empirically that hydroxylation at C-3′ causes a deshielding effect on the aromatic protons at ring B in the following order: H-2′ > H-6′ > H-5′. Consequently, methylation of the hydroxy group at C-3′ causes a deshielding of the aromatic protons accordingly: H-6′ > H-5′ > H-2′. Moreover, substitution at C-3′ changes the symmetrical ^{1}H NMR resonance pattern for the AA′BB′ system for the *para*-substituted ring B to an ABC pattern of methines comparable to a threefold substituted phenyl ring system. Assignment of the relative configuration at C-2 has also been deduced by inspection of their ^{1}H NMR spectra. The vicinal coupling constant values of the methine protons at the C-1, C-2, and C-3 positions ($J_{1,2}$ *ca.* 5–7 Hz and $J_{2,3}$ *ca.* 13–14 Hz) indicated the 1α,2α,3β configuration as well as the *cis*-BC ring junction (*53*). N*O*ESY experiments have been used to confirm the stereochemical relationship of the substituents from different carbon ring junctions. The N*O*ESY spectrum showed a N*O*E correlation peak between H-2′ and both H-1α and H-2α but not between H-2′ and H-3β (*53*).

The CD spectra of the rocaglamides show prominent negative *Cotton* effects between 217 and 220 nm as the most characteristic feature (*54*). Their CD spectra are dominated by the nature of the cyclopenta[*b*]tetrahydrobenzofuran moiety forming the backbone of the rocaglamide derivatives with stereocenters at C-1, C-2, C-3, C-3a, and C-8b and thus by the 3D array of the main molecular chromophores, the three aromatic rings. However, the asymmetric carbon C-2 apparently can influence the CD spectra of rocaglamide congeners, as exemplified by the α-sugar-substituted

Fig. 4. Rocaglamide derivatives isolated from *Aglaia* species

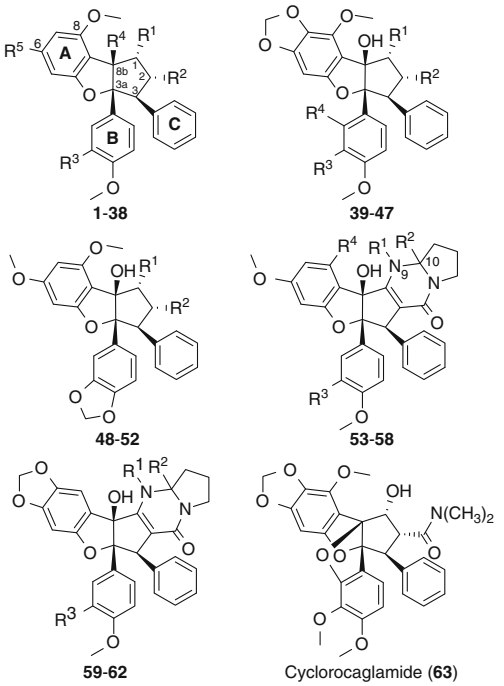

Cpd.	Trivial Name	R^1	R^2	R^3	R^4	R^5	Ref.
1	Rocaglamide	OH	$CON(CH_3)_2$	H	OH	OCH_3	(*11*, *60*)
2		OH	$CON(CH_3)_2$	OH	OH	OCH_3	(*55*)
3	Aglaroxin E	OH	$CON(CH_3)_2$	OCH_3	OH	OCH_3	(*55*, *57*)
4	1-*O*-Acetylrocaglamide	$OCOCH_3$	$CON(CH_3)_2$	H	OH	OCH_3	(*58*)
5		$OCOCH_3$	$CON(CH_3)_2$	OH	OH	OCH_3	(*55*)
6		OH	$CON(CH_3)_2$	OH	OC_2H_5	OCH_3	(*56*)
7	Desmethyl-rocaglamide	OH	$CONHCH_3$	H	OH	OCH_3	(*53*, *60*)
8		OH	$CONHCH_3$	OH	OH	OCH_3	(*14*)
9		$OCOCH_3$	$CONHCH_3$	H	OH	OCH_3	(*58*)
10		$OCOCH_3$	$CONHCH_3$	OH	OH	OCH_3	(*59*)
11		OH	$CONHCH_3$	OH	OC_2H_5	OCH_3	(*56*)
12	*N*,*N*-Didesmethyl-*N*-4-hydroxybutyl-rocaglamide	OH	$CONH(CH_2)_4OH$	H	OH	OCH_3	(*54*)
13		$OCOCH_3$	$CONH(CH_2)_4OH$	H	OH	OCH_3	(*54*)
14		OH	Ring[1]	H	OH	OCH_3	(*54*)
15	Didesmethyl-rocaglamide	OH	$CONH_2$	H	OH	OCH_3	(*60*)
16		OH	$CONH_2$	OH	OH	OCH_3	(*59*)
17		$OCOCH_3$	$CONH_2$	H	OH	OCH_3	(*56*)
18	Methyl rocaglate (Aglafoline)	OH	$COOCH_3$	H	OH	OCH_3	(*53*, *60*–*62*)

Fig. 4. continued

Cpd.	Trivial Name	R^1	R^2	R^3	R^4	R^5	Ref.
19	3'-Hydroxyaglafoline	OH	$COOCH_3$	OH	OH	OCH_3	(*14*)
20		OH	$COOCH_3$	OCH_3	OH	OCH_3	(*17*)
21		$OCOCH_3$	$COOCH_3$	H	OH	OCH_3	(*56*)
22		$OCOCH_3$	$COOCH_3$	OH	OH	OCH_3	(*59*)
23	1-*O*-Formylaglafoline	OCHO	$COOCH_3$	H	OH	OCH_3	(*17*)
24		OCHO	$COOCH_3$	OH	OH	OCH_3	(*17*)
25		=NOH	$COOCH_3$	OCH_3	OH	OCH_3	(*14*)
26		OH	$COOCH_3$	H	OCH_3	OCH_3	(*58*)
27	Rocagloic acid	OH	COOH	H	OH	OCH_3	(*63*)
28	Rocaglaol (Aglaiastatin A)	OH	H	H	OH	OCH_3	(*53*, *60*, *65*)
29		OH	H	OCH_3	OH	OCH_3	(*59*)
30		OH	H	Sugar[2]	OH	OCH_3	(*54*)
31		OH	H	Sugar[3]	OH	OCH_3	(*67*)
32		OH	H	H	OC_2H_5	OCH_3	(*60*)
33		OH	H	H	OCH_3	OCH_3	(*58*)
34	1-*O*-Acetylrocaglaol	$OCOCH_3$	H	H	OH	OCH_3	(*42*)
35	Silvestrol (5'''*R*)	OH	$COOCH_3$	H	OH	Ring[4]	(*68*)
36	Episilvestrol (5'''*S*)	OH	$COOCH_3$	H	OH	Ring[4]	(*68*)
37	1-*O*-Formylrocagloic acid	OCHO	COOH	H	OH	OCH_3	(*70*)
38	3'-Hydroxyrocagloic acid	H	COOH	OH	OH	OCH_3	(*70*)
39	Aglaroxin A	OH	$CON(CH_3)_2$	H	H	-	(*16*, *57*)
40	Aglaroxin B	OH	$CON(CH_3)_2$	OCH_3	H	-	(*57*, *71*)
41	Aglaroxin F	OH	$CON(CH_3)_2$	OCH_3	OH	-	(*57*)
42	Aglaroxin A 1-*O*-acetate	$OCOCH_3$	$CON(CH_3)_2$	H	H	-	(*72*)
43	1-*O*-Acetyl-3'-methoxyaglaroxin A	$OCOCH_3$	$CON(CH_3)_2$	OCH_3	H	-	(*72*)
44	Pannellin	OH	$COOCH_3$	H	H	-	(*13*, *71*)
45	1-*O*-Acetylpannellin	$OCOCH_3$	$COOCH_3$	H	H	-	(*13*)
46	3'-Methoxypannellin	OH	$COOCH_3$	OCH_3	H	-	(*13*)
47	Isothapsakon A	=O	Chain[5]	H	H	-	(*71*)
48	4'-Demethoxy-3',4'-methylenedioxy-methyl rocaglate	OH	$COOCH_3$	-	-	-	(*20*)
49		OH	H	-	-	-	(*20*)
50	1-Oxo-11,12-methylendioxyrocaglaol	=O	H	-	-	-	(*20*)
51		OCHO	$COOCH_3$	-	-	-	(*20*)
52		$OCOCH_3$	$COOCH_3$	-	-	-	(*17*)
53		$\Delta^{9,10}$		H	-	-	(*73*)
54		$\Delta^{9,10}$		OH	-	-	(*56*)
55	Algaroxin D (Aglaiastatin)	H	H	H	-	-	(*54*, *57*, *74*)
56	Marikarin	$\Delta^{9,10}$		H	OH	-	(*18*)
57	3'-Hydroxymarikarin	$\Delta^{9,10}$		OH	OH	-	(*18*)
58	Aglaiformosanin	$\Delta^{9,10}$		OCH_3	OCH_3	-	(*75*)
59	Algaroxin C	$\Delta^{9,10}$		H	-	-	(*57*)
60	Algaroxin G	$\Delta^{9,10}$		OCH_3	-	-	(*57*)
61	Algaroxin H	H	H	OCH_3	-	-	(*57*)
62	Algaroxin I	H	H	H	-	-	(*57*)

Fig. 4. continued

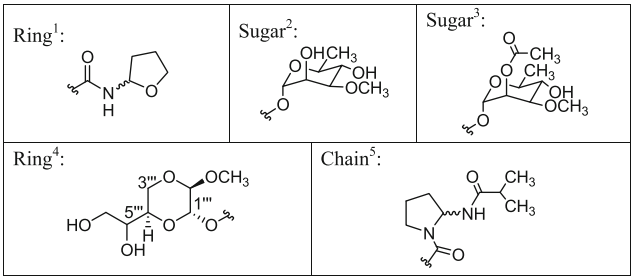

Fig. 5. Plausible structures of fragment ions *m/z* 316 and 329 of compound **2** under EI–MS

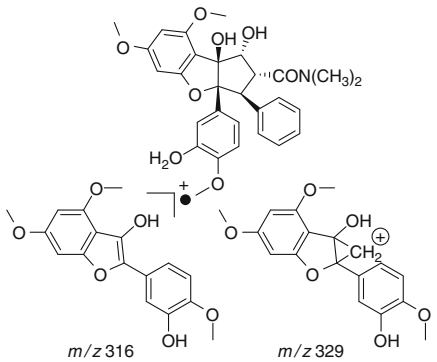

derivative **30** (*54*), which shows virtually the same CD spectrum as rocaglamide (**1**), but it lacks the stereocenter at C-2.

Considering rocaglamide (**1**) as the parent compound, major modifications in the substitution patterns occur at C-2, which in **1** is attached to a dimethylamino substituent characterized by two NCH_3 resonance signals at *ca*. 2.90–3.40 ppm in the ^1H NMR spectrum. Derivatives **2**, **5**, and **6**, with a hydroxy function at C-3′ of ring B, were isolated from the twigs (*55*) and flowers (*56*) of the Vietnamese species *Aglaia duperreana* while its methoxylated form known as aglaroxin E (**3**) was purified from the bark of the Sri Lankan species *A. roxburghiana* (*57*). Compounds with an acetoxy function at C-1 (**4** and **5**) (*55*, *58*) and ethoxylated substituent at C-8b (**6**) (*56*) were obtained from the same *A. duperreana* specimen.

N-Desmethylrocaglamide congeners **7**–**11** feature a $–CONHCH_3$ group at C-2. *N*-Desmethylrocaglamide (**7**) was isolated from twigs and leaves of *A. odorata* (*14*, *53*), whereas congeners with an acetylated hydroxy function at C-1 have been isolated from the flowers of *A. odorata* (*59*) and the roots of *A. duperreana* (*58*) collected in Vietnam. An ethylated form of substitution at C-8b occurs in compound **11**, which was obtained from the flowers of the same collection (*56*). Derivatives with an amino acyl substituent at C-2, as in congeners **12** and **13**, were isolated from *Aglaia harmsiana* (*54*). From the same species, the cyclized form of the amino acyl chain yielding the tetrahydrofuran ring, which is present in congener **14**, was isolated

in its two stereoisomeric configurations. The *N*-didesmethylrocaglamide derivatives **15–17** are widely distributed among various *Aglaia* species from different geographical origins, *e.g*. *A. odorata* from Indonesia (*59*), *A. argentea* from Malaysia (*60*), and *A. duperreana* from Vietnam (*56*).

The methyl rocaglate congeners **18–26** were identified by their methyl ester functionality at C-2, which is indicated by a ^{13}C NMR resonance at *ca*. 170 ppm as well as by a three-proton singlet at *ca*. 3.70 ppm in its ^{1}H NMR spectrum. Methyl rocaglate (**18**) was isolated initially from *Aglaia odorata* (*53*), then later from *A. forbesii* (*60*) and *A. elaeagnoidea* (*61*). Methyl rocaglate was also named aglafoline (*62*). Compounds with acetylated substituents at C-1 (**21** and **22**) were isolated from *A. duperreana* (*56*), and also from *A. odorata* (*59*) while the formylated congeners **23** and **24** were obtained from the bark of *A. spectabilis* collected from Vietnam (*17*). An unusual C-1 oxime derivative **25** of a rocaglate was isolated from the leaves of *A. odorata* (*14*), which was exemplified by a large downfield shift of 153.0 ppm as compared to the C-1 resonance for methyl rocaglate at 80.6 ppm in addition to the loss of the H-1 resonance at 4.90 ppm. The H-2 resonance in congener **25** was observed as a doublet that coupled only with H-3, instead of a double doublet as observed in methyl rocaglate (**18**).

Rocagloic acid (**27**) is the demethylated form of methyl rocaglate or the acid congener of this series of cyclopenta[*b*]tetrahydrobenzofuran compounds. It was obtained from the leaves of the Taiwanese species *Aglaia elliptifolia* (*63*) and also from the leaves of *A. dasyclada* (*64*) collected in Yunnan Province (China). The ^{1}H NMR and ^{13}C NMR spectra of **27** are comparable to those of methyl rocaglate (**18**), with the exception of the loss of methyl ester resonance signals.

The rocaglaol derivatives **28–32** are unsubstituted at C-2. Rocaglaol (**28**) itself was first isolated from the leaves of *A. odorata* (*53*) and later proved to be identical to ferrugin, which was reported from *A. ferruginaea* (*65*) but had been initially assigned a different structure (*66*). The ^{13}C NMR spectra of compounds **28–32** exhibit no signal indicative of a carbonyl group (usually in the range of 171–175 ppm), whereas they do feature an aliphatic methylene signal at *ca*. 38 ppm for C-2, as detected from the DEPT-135 spectrum (*54*). In their ^{1}H NMR spectra, the resonances for the methylene protons at *ca*. 2.15 and 2.80 ppm appear as a pair of geminally coupled multiplets splitting as a *ddd* due to coupling with the vicinal methine protons, H-1 and H-3. Modification of the substitution pattern for compounds **28–32** occurs either at C-3′ or C-8b. Methoxylation (**29**) and glycosidation (**30**) at C-3′ have been reported for compounds isolated from the flowers of *A. odorata* (*59*) and leaves of *A. harmsiana* (*54*). Inspection of the ^{1}H NMR spectrum of the glycoside congener **30** revealed an α-linked modified rhamnose unit with a methoxy group at the C-3″ position as confirmed by N*O*E experiments (*54*). This sugar-substituted rocaglaol derivative **30** was the first rocaglamide glycoside isolated from Nature. From the leaf extract of the Malaysian species *A. laxiflora*, a similar rocaglaol rhamnoside, **31**, was isolated, which was reported to contain an additional acetyl group at the C-2″ position of the modified rhamnose unit as confirmed by HMBC (*67*). Methylation (**32**) and ethylation (**33**) of the hydroxy group at C-8b occur in compounds isolated from the roots of *A. duperreana* (*58*) and the bark of *A. forbesii* (*60*).

The three cyclopenta[*b*]tetrahydrobenzofuran derivatives **34**–**36** were isolated by *Kinghorn et al*. from two specimens of *Aglaia* species collected in Indonesia (*42*, *68*, *69*). 1-*O*-Acetylrocaglaol (**34**) was isolated from the twigs of *A. rubiginosa* (*42*). The absolute stereochemistry of **34** was deduced by a comparison of the CD spectrum with that of rocaglamide (**1**). Two methyl rocaglate congeners with an unusual dioxyanyloxy unit at C-6, silvestrol (**35**) and episilvestrol (**36**), were obtained from the fruits and twigs of *A. foveolata* (*68*). The CD spectrum of silvestrol (**35**) was very similar to that of methyl rocaglate (**18**) implying that the tricyclic cores of both molecules have the same stereochemistry. However, the relative configuration of the dioxyanyloxy unit was difficult to confirm from the available NMR data. Accordingly, the absolute configuration of **35** was established by a single-crystal X-ray analysis of its 5‴,6‴-di-*p*-bromobenzoate derivative, and was found to be (1*R*,2*R*,3*S*,3a*R*,8b*S*,1‴*S*,2‴*R*,4‴*R*,5‴*R*) (*68*). From a comparison of its 2D NMR data with those of silvestrol (**35**), compound **36** was assigned as the C-5‴ epimer of **35** (*68*). Initially, the plant material was wrongly identified as *Aglaia silvestris* (M. Roemer) Merrill, hence the name silvestrol was given to **35**. However, the species was later re-identified as *A. foveolata* Pannell (*69*).

From the fruits of *Aglaia spectabilis* (syn. *Amoora cucullata*) (Meliaceae) collected from Thailand in 2004, two rocaglamide derivatives, namely, 1-*O*-formylrocagloic acid (**37**) and 3′-hydroxyrocagloic acid (**38**) were isolated (*70*). The absolute stereochemistry of **37** was defined as having the (1*R*,2*R*,3*S*,3a*R*,8b*S*)-configuration by comparing its CD spectrum, which revealed a prominent negative *Cotton* effect at 274 nm, with that of rocaglamide (**1**) (*70*).

The group of 6,7-methyenedioxy rocaglamide analogues (**39**–**41**) was isolated from the stem bark of the Sri Lankan species *Aglaia roxburghiana* (*57*) and were accorded the trivial names aglaroxins A, B, and F. Compared to the fundamental structure of the rocaglamides, the ^{1}H NMR resonances for OCH_3-6 and H-7 were absent and instead replaced by a methylenedioxy singlet at *ca*. 5.90 ppm. The doublet for H-5 at *ca*. 6.30 ppm in the ^{1}H NMR spectrum of rocaglamide (**1**) was replaced by a singlet (*13*). The resonance for OCH_3-8 was also shifted downfield from δ 3.85 to δ 4.10 ppm due to the deshielding effect of the adjacent methylenedioxy function. The presence of a methylenedioxy function was also evident from a triplet resonance at *ca*. 103 ppm as revealed in its DEPT spectra (*16*). The absolute configuration of aglaroxin A (**39**) was first determined by calculation of its CD spectrum using molecular dynamics (MD) simulations (*16*). Variations for the analogues occur at ring B in which aglaroxin B (**40**) was methoxylated at C-3′ while aglaroxin F (**41**) was both methoxylated and hydroxylated at C-3′ and C-4′ (*57*). Two further aglaroxin A analogues, the 1-*O*-acetate (**42**) and the 3′-methoxy-1-*O*-acetate (**43**), were isolated from an Indonesian collection of the bark of *A. edulis* (*71*).

The pannellins **44**–**46** were isolated from *Aglaia elaeagnoidea* collected from Thailand (*13*). For this group of analogues, the amide function at C-2 in aglaroxins A, B, and F was replaced by a methyl ester. Pannellin-1-*O*-acetate (**45**) is the acetylated product of **44** while 3′-methoxypannellin (**46**) is characterized by an additional –OCH_3 function in ring B.

Proksch et al. described the isolation of a similar group of congeners from the twigs of a Vietnamese collection of *A. oligophylla*, including isothapsakon A (**47**), a C-1-oxo derivative of aglaroxin A (**39**), bearing a bisamide side chain at C-2 that is derived from piriferine (*16*). The ketone substituent at C-1 was identified by the carbon resonance at δ 206 ppm consequently resulting in a downfield shift of H-2, which appeared as a doublet coupling only with H-3.

Derivatives **48**–**52**, featuring a 3′,4′-methylenedioxy substitution in the B ring, have been first reported from *Aglaia elliptica* (*20*) collected in Thailand and the Vietnamese species *A. spectabilis* (*17*) while the congeners **39**–**47** possess the same 3′,4′-methylenedioxy functionality but in ring A.

The last group of rocaglamide congeners (**53**–**62**) is characterized by a pyrimidinone subunit fused at C-1 and C-2. The resulting pentacyclic skeleton can be considered conceptually as a rocaglamide with a 2-aminopyrrolidine amide substituent at C-2 linked to C-1 via the primary amino group. This pyrimidinone-type rocaglamide **53** was first isolated from the roots of *A. odorata* collected in Thailand and was elucidated structurally by X-ray crystallography (*72*). Later, **53** was also isolated from the leaves and twigs of the Vietnamese species *A. duperreana* (*55*) while its flowers yielded the 3′-hydroxy derivative **54** (*56*). Aglaroxin D (aglaiastatin) (**55**), the dihydro derivative of **53**, has been isolated from the leaves of *A. duperreana* (*55*) and *A. odorata* (*73*) and from the stem bark of the Sri Lankan species *A. roxburghiana* (*57*). The latter collection yielded four further pyrimidinone analogues with an additional 6,7-methylenedioxy substituent in ring A, known as aglaroxins C (**59**) and G–I (**60**–**62**) (*57*).

Three further pyrimidinone-type congeners, marikarin (**56**) and 3′-hydroxy-marikarin (**57**), were isolated from the root bark of *Aglaia gracilis* collected in Fiji (*18*), while aglaiformosanin (**58**) was obtained from the stem bark of *A. formosana* collected in Taiwan (*74*). In 2003, aglaroxin F (**41**) was isolated from *A. oligophylla* twigs collected in Vietnam together with its 8b,10-anhydro analogue, cyclorocaglamide (**63**) (*75*). Cyclorocaglamide (**63**) was identified as the first bridged cyclopenta[*b*]benzofuran between C-8b and C-2′ of ring B, whereas to the best of our knowledge aglaroxin F (**41**) represents the only rocaglamide derivative with three oxygen functions in the B ring, bearing an additional hydroxy group at C-2′.

2.2. *Aglain Derivatives*

Aglains (see Fig. 6) are characterized by a cyclopenta[*bc*]benzopyran(2,5-methano-1-benzoxepin) skeleton, thought to be derived biogenetically from the addition of a flavonoid precursor and a bisamide such as odorine (**103**), odorinol (**104**), or piriferine (**105**) (Fig. 6) (*14*, *60*). Formally, rocaglamides can also be considered as derivatives from aglains by cleaving the C-C bond between C-10 and C-5a, and linking C-10 and C-5a instead. The nature of the ring system of aglains was proven unambiguously by X-ray crystallography of the first congener of this group, aglain

Fig. 6. Aglain derivatives isolated from *Aglaia* species

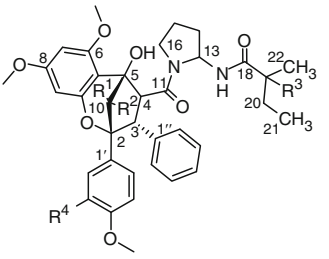

64-80

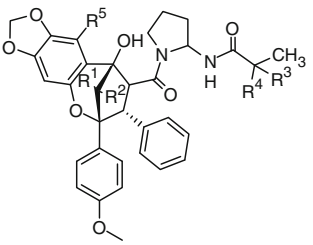

81-89

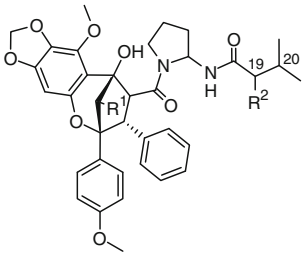

90-92

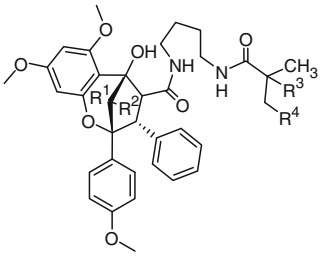

93, **94**

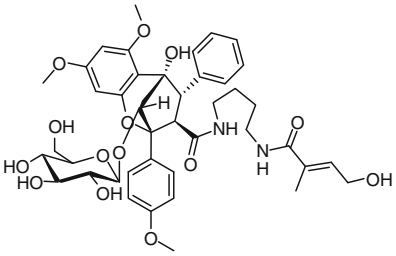

95

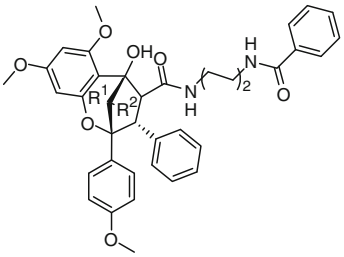

96-100

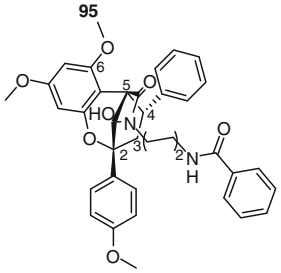

Cyclofoveoglin (**101**)

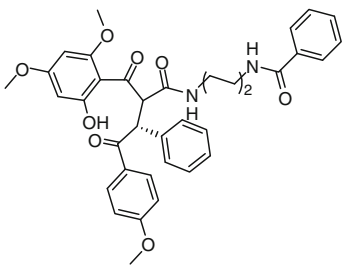

Secofoveoglin (**102**)

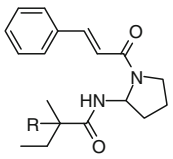

R = H: Odorine (**103**)
R = OH: Odorinol (**104**)

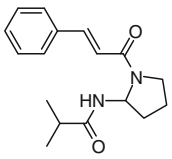

Piriferine (**105**)

Fig. 6. continued

Cpd.	Trivial Name	R^1	R^2	R^3	R^4	R^5	H-3, H-4	Ref.
64	Aglain A	$OCOCH_3$	H	H	H	-	*β,α*	(*60*)
65	4-Epiaglain A	$OCOCH_3$	H	H	H	-	*β,β*	(*80*)
66	Desacetylaglain A	OH	H	H	H	-	*β,α*	(*18*)
67	Aglain B	H	OH	H	H	-	*β,α*	(*60*)
68	10-*O*-Acetylaglain B	H	$OCOCH_3$	H	H	-	*β,α*	(*80*)
69	Aglain C	H	OH	H	H	-	*α,β*	(*60*)
70		H	OH	H	OH	-	*α,β*	(*14*)
71		H	OH	OH	OH	-	*α,β*	(*14*)
72		H	OH	OH	OCH_3	-	*α,β*	(*14*)
73		H	OH	H	OH	-	*β,α*	(*14*)
74	Aglaxiflorin A	$OCOCH_3$	H	OH	H	-	*β,α*	(*67*)
75	Aglaxiflorin B	$OCOCH_3$	H	OH	H	-	*α,β*	(*67*)
76	Aglaxiflorin D	H	OH	OH	H	-	*α,β*	(*67*)
77	Elliptifoline	H	OH	$\Delta^{19,20}$	H	-	*α,β*	(*63*)
78	Aglaroxin J	H	$OCOCH_3$	H	H	-	*α,β*	(*57*)
79	Aglaroxin L	H	OH	OH	H	-	*α,β*	(*57*)
80		H	OH	OH	H	-	*β,α*	(*57*)
81		H	OH	OH	C_2H_5	H	*β,α*	(*57*)
82		H	$OCOCH_3$	H	C_2H_5	H	*β,α*	(*57*)
83	(13*S*)-Thapsakin B	H	OH	H	CH_3	OCH_3	*β,α*	(*15*)
84	(13*R*)-Thapsakin B	H	OH	H	CH_3	OCH_3	*β,α*	(*15*)
85	Isothapsakin B	OH	H	H	CH_3	OCH_3	*β,α*	(*15*)
86	Homothapsakin A	H	OH	H	C_2H_5	OCH_3	*α,β*	(*15*)
87	10-*O*-Acetylthapsakin A	H	$OCOCH_3$	H	CH_3	OCH_3	*α,β*	(*15*)
88	Thapsakon A	=O		H	CH_3	OCH_3	*α,β*	(*15*)
89	Thapsakon B	=O		H	CH_3	OCH_3	*β,α*	(*15*)
90	Edulirin A	OH	H	-	-	-	*β,α*	(*72*)
91	10-*O*-Acetyledulirin A	$OCOCH_3$	H	-	-	-	*β,α*	(*72*)
92	19,20-Dehydroedulirin A	OH	$\Delta^{19,20}$	-	-	-	*β,α*	(*72*)
93	Grandiamide A	$OCOCH_3$	H	$\Delta^{19,20}$	CH_3	-	*α,β*	(*89*)
94		*O*-glc	H	$\Delta^{19,20}$	CH_2OH	-	*α,β*	(*75*)
96	Pyrimidaglain A	H	$OCOCH_3$	-	-	-	*β,α*	(*36*)
97	Pyrimidaglain B	$OCOCH_3$	H	-	-	-	*α α*	(*36*)
98	Desacetylpyrimidaglain A	H	OH	-	-	-	*α,β*	(*46*)
99	Desacetylpyrimidaglain C	OH	H	-	-	-	*α,β*	(*46*)
100	Desacetylpyrimidaglain D	H	OH	-	-	-	*β,α*	(*46*)

A (**64**), thus also revealing the relative configuration (*60*). The aglain skeleton was confirmed through key HMBC correlations including H-10 to C-5, C-5a, H-4 to C-11, C-5, C-5a, and H-3 to C-2″/6″, C-2, C-5 (*60*).

The aglains, aglaforbesins as well as the forbaglins contain bisamide side chains that are derived from a cinnamic acid bisamide. These low molecular weight precursors, namely, odorine (**103**) (*76, 77*), odorinol (**104**) (*19, 76*), and piriferine (**105**) (*78*), are composed of cinnamic acid, the bifunctional amine 2-aminopyrrolidine, and 2-methylbutanoic acid (in odorine), 2-hydroxy-2-methylbutanoic acid (in odorinol) or 2-methylpropanoic acid (in piriferine). In 33 of the total of 37 aglain derivatives isolated so far, the bisamide side chain is directly analogous to a naturally occurring cinnamic acid bisamide, odorine (**103**), odorinol (**104**), or piriferine (**105**). The four remaining compounds, **77** and **92–94**, can be formally obtained by dehydration of the hydroxy group at C-19 resulting in a double bond between C-19 and C-20. Aglains differ in regard to their configuration at C-19, which can be either (*R*) or (*S*), but more often remains uncertain. This finding parallels the situation of the cinnamic acid bisamides, which also occur as diastereomers at the analogous position. Similarly, the configuration at C-13 can either be (*R*) or (*S*), which again is consistent with the occurrence of both (+)- or (−)-forms of odorine (**103**), odorinol (**104**), and piriferine (**105**) in Nature. It is noteworthy that this aminal position is prone to epimerization in low molecular weight precursors (*77*), and, frequently, aglains are isolated as diastereomeric mixtures (*15*).

In their cyclic core, aglains display structural variability at the following positions: the bridging carbon atom, C-10, nearly always carries one proton as well as one oxygen-containing substituent, the latter being either a hydroxy, an acetoxy, or a sugar moiety. The substituents can be either *endo* or *exo* with regard to ring A. Only two derivatives, **88** and **89**, are known to feature a carbonyl group at C-10. In the oxepine ring, H-3 and H-4 are mostly *trans*-oriented, but both possible diastereomeric forms, *i.e.* H-3α, H-4*β* as well as H-3*β*, H-4α, occur more or less evenly distributed in Nature. For compounds with the opposite configuration at C-10, N*O*E correlation peaks are observed between the *β*-protons, H-3 or H-4, and OH-10 (in aprotic solvent) or $OCOCH_3$-10. Furthermore, these N*O*Es have also been used to assign the relative configurations of the H-3 and H-4 stereocenters. Additionally, the vicinal coupling constant between H-3 and H-4 can be utilized to confirm their configurations. For the H-3*β*, H-4α configuration, the ^{1}H NMR vicinal coupling constant varies between 5 and 6 Hz, while for the H-3α, H-4*β* configuration, the coupling constant amounts to 9–11 Hz (*14, 60, 67*). One exception is 4-epiaglain A (**65**), which features the *β*-configuration for both H-3 and H-4, and displays a coupling constant of 7.4 Hz (*79*).

As in the case of rocaglamides, ring A of aglains is usually substituted by two *m*-positioned methoxy groups at C-6 and C-8, but is also known to carry a 7,8-methylenedioxy substituent, mostly in addition to the methoxy group at C-6 except for congeners **81** and **82**, which feature no methoxy group at C-6. Ring B always carries a 4′-methoxy substituent, in some cases accompanied by a hydroxy or a methoxy group at C-3′, while ring C is always unsubstituted. These substitution patterns are again parallel to those of rocaglamide, whereas a methylenedioxy substituent in ring B has not been encountered in aglains so far.

In spite of the numerous structural analogies between rocaglamides and aglains, and the postulated similar biogenetic pathways leading to both classes of

compounds, it is interesting to note that bisamide-derived side chains occur mainly in aglains (and in aglaforbesins as well as in forbaglins, see below), but are rarely encountered in rocaglamides such as in isothapsakon A (**47**). It may be speculated that bulky substituents, such as those present in odorine (**103**), odorinol (**104**), or piriferine (**105**), cannot easily be incorporated into rocaglamides, and thus are usually replaced by simpler amide or nitrogen-free side chains.

The assignment of the relative configuration of aglain A (**64**), the parent compound of this series of cyclopenta[*bc*]benzopyran derivatives, was determined from N*O*ESY NMR correlations (*60*). In 2000, the first X-ray structure of this type of compounds was obtained for aglaxiflorin A (**74**), thus confirming the relative stereochemistry (*67*). Previously, the relative configuration of aglains had been assigned from 2D N*O*E data, while the absolute configuration was deduced on the grounds of biogenetic comparison with rocaglamide (**1**). According to *Greger* and colleagues, formal conversion of cyclopenta[*bc*]benzopyran into cyclopenta[*b*] benzofuran would leave the absolute configuration at C-2 (C-3a in rocaglamides) unchanged, as was deduced by inspecting *Dreiding* models (*15*). Thus, the structures of aglain derivatives are commonly drawn with the methylene bridge (C-10) oriented upwards, while the aromatic ring B and OH-5 are oriented downwards (*9*).

Aglains A (**64**), B (**67**), and C (**69**) were isolated from the leaves of *Aglaia argentea* collected in Malaysia (*60*), while 4-epiaglain A (**65**) and 10-*O*-acetylaglain B (**68**) were obtained from an Indonesian collection of *A. elliptica* leaves (*79*). The relative configurations of **65** and **68** were solved using N*O*ESY NMR data. Deacetylaglain A (**66**), isolated from the leaves of *A. gracilis* collected in Fiji (*18*), is very similar to aglain A (**64**), except for the hydroxy group at C-10. Recently, ponapensin, the only congener featuring a methoxy group at C-13 instead of the amide side chain in aglain B (**67**), was isolated from the Micronesian species *Aglaia ponapensis* (*80*).

In thapsakones A (**88**) and B (**89**), obtained from the root bark of *Aglaia edulis* (southwest Thailand), which lack a proton at C-10, the stereochemistry of H-3 and H-4 was deduced in an elegant manner by observing a shift stronger than a lanthanide-induced shift (LIS) to the respective *β*-proton (4 in **88**, 3 in **89**) (*15*). The configuration of the aminal proton H-13 was assigned as being (13*S*) by observing N*O*Es between H-4 and H-13 as well as between the terminal methyl group(s) H-21 (and H-20 in the case of piriferine-derived side chains) and H-2″/6″, while no such N*O*E correlations were detected for (13*R*)-derivatives as confirmed by close inspection of *Dreiding* models (*15*, *60*).

Edulirin A (**90**), 10-*O*-acetyledulirin A (**91**), and 19,20-dehydroedulirin A (**92**), together with aglaroxin A analogues **42** and **43**, were reported from an Indonesian collection of the bark of *Aglaia edulis* (*71*).

The two glycosidic derivatives **94** and **95** have been isolated from the leaves of *Aglaia dasyclada* collected in Yunnan Province, People's Republic of China (*64*). These two compounds have a hydroxytiglic amidic putrescine moiety instead of the cinnamic acid bisamides previously found as the amine substituents in other aglain derivatives.

The last group of aglain congeners with compounds **96–100** exhibits a benzoyl-1,4-butanebisamide moiety at C-4 along with the open oxepine ring congener, secofoveoglin (**101**). Pyrimidaglain A (**96**) and B (**97**) were the first congeners of this group isolated from the leaves of *Aglaia andamanica* collected in Thailand (*36*). Recently, three further congeners, desacetylpyrimidaglains A, C, and D (**98–100**), have been reported from the leaves of *A. forbesii* collected also in Thailand (*46*). The latter has been given the trivial name, isofoveoglin, and was isolated together with the open oxepine ring congener, secofoveoglin (**102**), from the leaves and stem bark of *A. foveolata* (Indonesia) (*81*). The only difference between the pyrimidaglains **96** and **97** and the desacetylpyrimidaglains **98–100** is the lack of acetylation of the OH-10 function in the latter compounds. The relative configurations of the deacetyated pyrimidaglains has been proven through the observation of the characteristic N*O*ESY cross peaks H-3 to H-4, N*H*-12, H-2′/6′, and H-2″/6″, H-4 to H-3, OH-10, N*H*-12, and H-2″/6″, and H-10 to H-2′/6′, and the most important cross peak between OH-10 and H-4, which directly proved the relative configuration at C-3, C-4, and C-10 (*46*). Cyclofloveoglin (**101**), isolated from the leaves and stem bark of *A. foveolata* (Indonesia) (*81*), represents a hitherto unprecedented five membered-cyclic amide moiety among the rocaglamide-type compounds isolated from the genus *Aglaia* so far (*9, 12*). The structure of **101** was proposed through the DEPT NMR spectrum, which revealed a quaternary carbon resonance at δ 90.6 ppm that replaced the signal of a hydroxymethine carbon at position C-10 in **100**. Furthermore, a HMBC spectrum confirmed the structure of cyclofloveoglin through correlations between the quaternary carbon, C-10, with H-4 and H-13, indicating that N-12 is bonded to C-10 (*81*).

2.3. Aglaforbesin Derivatives

The aglaforbesins are closely related to the aglains, but with a cinnamic acid bisamide-derived side chain at C-3 and the unsubstituted phenyl ring C at C-4 mutually interchanging (as in congener **95**). This structural feature was evidenced by HMBC correlations from H-3 to C-11 as well as H-4 to C-2″/6″ (*60*). To date, only ten aglaforbesin derivatives (see Fig. 7) have been described from Nature, which differ with regard to the substitution pattern of ring A as well as in the stereochemistry at C-3, C-4, and C-13. Unlike the aglains, no structural variants from the 4′-methoxy substituted ring B are known, however, in ring A, a methylendioxy functionality between C-7 and C-8 has been reported in the three congeners **109–111** (*16, 71*). Side chains are derived from odorine (**103**) (in **106** and **107**) (*60*), odorinol (**104**) (in **108**) (*67*), and piriferine (**105**) (in **109**) (*16*). However, foveoglins A (**112**) and B (**113**) feature a benzoyl-1,4-butanebisamide moiety at C-3 (*71, 81*) unlike the pyrimidaglains **96–100**, which exhibit the same moiety at C-4 (*36, 46*).

Assignment of the stereochemistry of aglaforbesins is based on the same principles as for aglains. Consequently, the configuration of the aminal proton H-13 was deduced as being (*R*) in aglaforbesins A (**106**) and B (**107**) due to

Fig. 7. Aglaforbesin derivatives isolated from *Aglaia* species

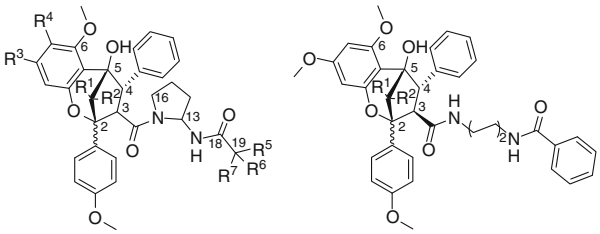

Cpd.	Trivial Name	R^1	R^2	R^3	R^4	R^5	R^6	R^7	H-3, H-4	Ref.
106	Aglaforbesin A	OH	H	OCH_3	H	C_2H_5	H	CH_3	*α,β*	(*60*)
107	Aglaforbesin B	H	OH	OCH_3	H	C_2H_5	H	CH_3	*α,β*	(*60*)
108	Aglaxiflorin C	H	$OCOCH_3$	OCH_3	H	C_2H_5	OH	CH_3	*α,β*	(*67*)
109		H	OH	-OCH_2O-		CH_3	H	CH_3	*β,α*	(*71*)
110	Isoedulirin A	H	OH	-OCH_2O-		H	H	$CH(CH_3)_2$	*α,β*	(*72*)
111	Edulirin B	H	OH	-OCH_2O-		H	H	$CH(CH_3)_2$	*β,α*	(*72*)
112	Foveoglin A	OH	H	-	-	-	-	-	*α,β*	(*82*)
113	Foveoglin B	H	OH	-	-	-	-	-	*α,β*	(*82*)

N*O*Es observed between H-3 and H-13 as well as between H-21 and H-2″/6″ (*60*). Interestingly, the H-3*α*/H-4*β* configuration leads to a pronounced upfield shift of OCH_3-6 (δ approx. 3.1 ppm), since in this case the methoxy group is placed inside the shielding zone of the unsubstituted benzene ring at C-4*α* (*60*, *67*), while a normal chemical shift (δ approx. 4.1 ppm) is observed in the case of reversed stereochemistry at C-3 and C-4 (*16*). By analogy to the aglains, configurations at their respective positions are also reflected by the magnitude of the vicinal coupling constant: $^3J_{(H\text{-}3,\ H\text{-}4)}$ amounts to 10–11 Hz when H-3 is *α* and H-4 is *β* (*60*, *67*), while the coupling constant is 6–7 Hz when in the opposite configuration (*16*).

2.4. *Forbagline Derivatives*

Forbaglines are benzo[*b*]oxepines naturally occurring in the genus *Aglaia*, in which the pyran ring of the aglains is replaced by an oxepine ring. The benzo[*b*]oxepine skeleton of the forbagline derivatives can be formally obtained from the aglains by oxidative cleavage at the methylene bridge between C-5 and C-10 (*60*). As for the aforementioned groups of rocaglamide-type compounds, the aromatic rings A, B, and C share common characteristics with their benzofuran and benzopyran counterparts. The aromatic ring A can carry either an 8-methoxy or a 7,8-methylenedioxy substituent in addition to a 6-methoxy group, while ring B may show a *p*-methoxy (as in **114**–**124**) or a *p*-hydroxy (as in **125**) substituent, and ring C is unsubstituted. The benzo[*b*]oxepine core is conserved in all but derivative **125**,

which has a carboxylic acid functional group instead of the methyl ester group at C-10 (*64*). The only major variation in the skeleton occurs in the type of the bisamide side chain substituent at C-4.

The structure of the first derivative, forbaglin A (**114**), was established by X-ray crystallographic analysis, thus revealing the relative stereochemistry (*60*). The configurations at H-3 and H-4 of the forbagline derivatives reflect those of the aglains and aglaforbesins with only *trans* isomers having been isolated so far. By analogy to the benzopyran series, the magnitude of the vicinal coupling constant $^{3}J_{(\text{H-3, H-4})}$ can be used to determine the relative stereochemistry at C-3 and C-4.

To date, 12 forbagline derivatives (see Fig. 8) have been isolated, including the 7 derivatives **114–120** with an odorine or a piriferine side chain. The other 5 analogues **121–125** revealed bisamide side chains derived from substituents other than odorine or piriferine (*64, 82*). Both derivatives **124** and **125** have a hydroxytiglic amidic putrescine moiety similar to that of **94** and **95**, and all of them were isolated from the same *Aglaia* species (*64*). Compound **124** is the only forbagline glucoside derivative isolated so far, with the glucose attached to C-21 (the bisamide side chain), whereas compound **125** has a very similar structure to **124** except for

Fig. 8. Forbagline derivatives isolated from *Aglaia* species

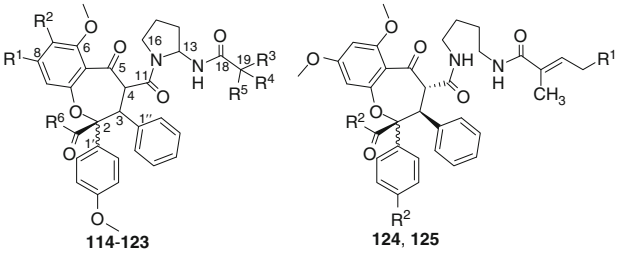

Cpd.	Trivial Name	R^1	R^2	R^3	R^4	R^5	R^6	H-3, H-4	Ref.
114	Forbaglin A (13*R*)	OCH_3	H	CH_3	H	C_2H_5	CH_3	*α,β*	(*60*)
115	Forbaglin B (13*S*)	OCH_3	H	CH_3	H	C_2H_5	CH_3	*α,β*	(*60*)
116	(13*S*)-Thapoxepine A	-OCH_2O-		CH_3	H	CH_3	CH_3	*α,β*	(*15*)
117	(13*R*)-Thapoxepine A	-OCH_2O-		CH_3	H	CH_3	CH_3	*α,β*	(*15*)
118	Homothapoxepine A	-OCH_2O-		CH_3	H	C_2H_5	CH_3	*α,β*	(*15*)
119	(13*S*)-Thapoxepine B	-OCH_2O-		CH_3	H	CH_3	CH_3	*β,α*	(*15*)
120	(13*R*)-Thapoxepine B	-OCH_2O-		CH_3	H	CH_3	CH_3	*β,α*	(*15*)
121	Edulisone A (13*R*)	-OCH_2O-		H	H	$CH(CH_3)_2$	OCH_3	*α,β*	(*83*)
122	Edulisone B (13*S*)	-OCH_2O-		H	H	$CH(CH_3)_2$	OCH_3	*α,β*	(*83*)
123	19,20-Dehydroedulisone	-OCH_2O-		$\Delta^{19,20}$		$C(CH_3)_2$	OCH_3	*α,β*	(*72*)
124		*O*-glc	OCH_3	-	-	-	-	*α,β*	(*64*)
125		OH	OH	-	-	-	-	*α,β*	(*64*)

the absence of the sugar moiety at C-21, and the presence of a carboxylic acid and a hydroxy functional group at positions C-10 and C-4′ (*64*).

Edulisones A (**121**), B (**122**), and 19,20-dehydroedulisone A (**123**) were isolated from the bark of *Aglaia edulis* collected in Indonesia (*71, 82*). The relative stereochemistry of edulisone A (**121**) was determined by single-crystal X-ray diffraction analysis, revealing the (*R*) configuration at C-13 (*82*). Furthermore, the two epimers **121** and **122** showed different ^{1}H NMR chemical shifts for protons close to the C-13 epimeric site, which may be used to assign the relative stereochemistry at C-13. For the (13*R*)-epimer **121**, H-14a and H-14b displayed two signals in the ^{1}H NMR spectrum, while for the (13*S*)-epimer, these two protons were overlapped in a relatively upfield region (*82*). For H-16a and H-16b of the (13*R*)-epimer, the two protons overlapped in the ^{1}H NMR spectrum, while for the (13*S*)-epimer, these two protons were clearly separated, one at a higher field and one at a lower field relative to those of its (13*R*)-counterparts (*82*). The same phenomenon was also observed in forbaglins A ((13*R*), **114**) and B ((13*S*), **115**) (*60*).

3. Biosynthesis of Rocaglamides and Related Metabolites

The cyclopenta[*b*]benzofurans (rocaglamides), and the two structurally related groups, the cyclopenta[*bc*]benzopyrans (including the aglains and aglaforbesins), and the benzo[*b*]oxepines (known also as the "forbaglines"), are considered characteristic secondary metabolites of the genus *Aglaia*, because they have been only isolated from this taxon (*9*). Therefore, the collective name "flavagline" has been proposed for these compounds because their mutual biogenetic origin has been postulated to arise from common structurally related precursors that include cinnamic acid amides and the flavonoid nucleus (*9, 13–15*). A postulated biosynthetic origin was firstly proposed by *Nugroho et al*. in 1999 as depicted in Fig. 9 (*14*). According to this hypothesis, the initial *C*-*C*-connecting step (step A) between C-2 of the flavonoid **I** and C-3 of the cinnamic acid amide **II** is a *Michael*-type 1,4-addition of the enolate subunit of **I** to the α,*β*-unsaturated amide **II**. The C-2 atom of the resulting amide enolate of **III** can now attack C-4 of the previous flavonoid, which has now become a strongly activated carbonyl group, to yield a five-membered ring, giving rise to **IV** (step B). According to this concept, **IV** constitutes the biosynthetic key intermediate and precursor both to aglain and rocaglamide derivatives. Moreover, **IV** can already be considered as a dehydroaglain derivative, and a simple reduction step (*e.g.* with $[H]^-$ possibly through NADPH or a related H-nucleophile), will yield the corresponding aglain derivative **V**' (step C').

This reduction to give **V** stabilizes the strained molecule **IV**, which, as the key intermediate, may otherwise undergo a rearrangement by an intramolecular migration of the electron-rich substituted (phloroglucinol-type) aromatic ring from the previous C-4 to C-3 of the flavonoid. Mechanistically, this can be considered as an electrophilic aromatic *ipso*-substitution via the cyclopropyl derivative **V** as the

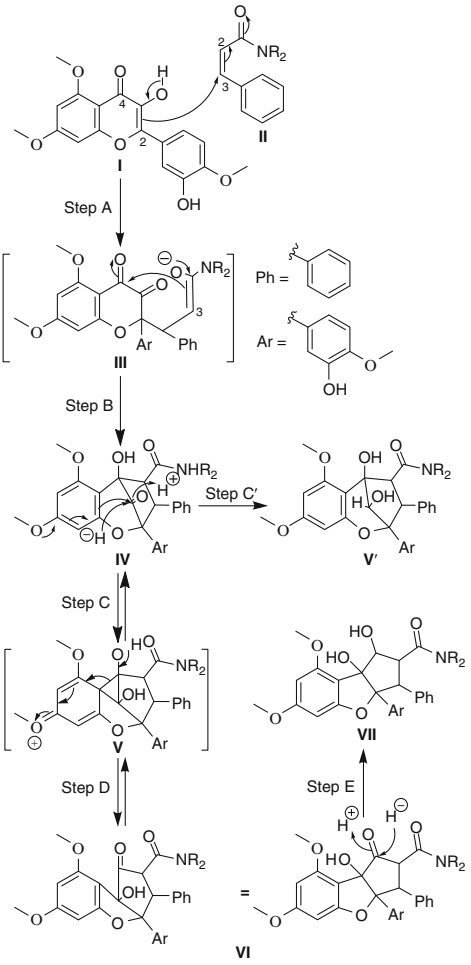

Fig. 9. Postulated joint biosynthesis scheme of rocaglamide (= flavagline)-type compounds isolated from *Aglaia* species (*14*)

σ-complex (steps C and D), thus ultimately transforming the hydroxyketone **IV** into the isomeric hydroxyketone **VI**, which is already a dehydrorocaglamide derivative. Again, this is possibly a reversible process, which becomes definite by a stabilizing final reduction step (step E), to give rise to rocaglamide derivatives **VII**.

Although aglaforbesin derivatives are not depicted in Fig. 9, they also fit into the biogenetic scheme proposed, but differ in comparison to the aglains by the opposite orientation of the cinnamic acid amide **II** with respect to flavonoid **I**. In addition, forbaglines can be proposed as being biosynthesized through oxidative cleavage between C-5 and C-10 of hydroxyketone **IV** (numbering as in aglains and aglaforbesins). Apparently, the addition of **II** to **I** is neither regio- nor stereoselective, since all four possible stereoisomers do exist in Nature, *i.e.* both (H-3α,H-4β) and (H-3β, H-4α) derivatives have been reported.

From these aforementioned considerations, a search for the probably unstable, possibly interconverting, intermediates **IV** and **VI** of the postulated biosynthesis pathway of dehydroaglain and rocaglamide derivatives, would provide further support for the hypothetical biogenetic scheme and be rewarding, if successful.

For the bisamide-containing flavaglines, a proposed biosynthesis pathway is depicted in Fig. 10, in which a similar initial *C-C*-addition occurs between C-2 of

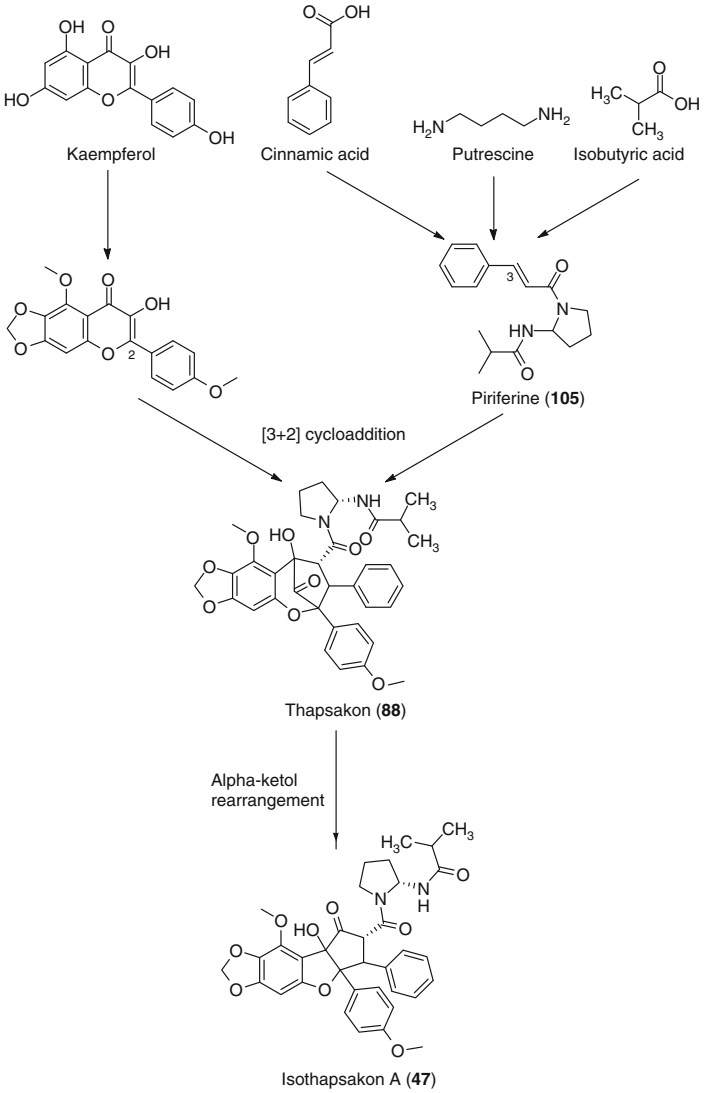

Fig. 10. Proposed biosynthetic origin of isothapsakon A (**47**) and thapsakon (**88**) as bisamide-containing rocaglamide-type derivatives

the flavonoid and C-3 of piriferine (**105**), odorine (**103**), or odorinol (**104**). This step leads to the formation of the aglain derivative, thapsakon A (**88**), which can be transformed into isothapsakon A (**47**) through an α-ketol rearrangement similar to steps (C–E) in Fig. 9.

4. Pharmacological Significance of Rocaglamides and Related Compounds

4.1. Insecticidal Activity

The first report on the remarkable insecticidal activity of extracts from *Aglaia* species in the literature originates from 1985, when Chiu *et al*. (*83*) described the antifeedant properties of a crude extract derived from *A. odorata* towards larvae of the cabbage worm, *Pieris rapae*. The active principles of *A. odorata* responsible for the strong antifeedant properties of the respective crude extracts against *P. rapae* and against other insects, however, were only identified in 1993 when *Ishibashi et al*. (*53*) reported on the bioassay-guided isolation of rocaglamide (**1**) and three of its congeners using larvae of the polyphagous noctuid, *Peridroma saucia*, as experimental insects. Interestingly, rocaglamide (**1**) had already previously been isolated in 1982 from *A. elliptifolia* and described as having inhibitory properties against a human epidemoid carcinoma of the nasopharynx (KB) cell line *in vitro* ($IC_{50} = 8.7\ \mu M$) (*11*), thereby providing an early hint to the parallelism between insecticidal and antiproliferative properties of rocaglamide and its derivatives that became even more obvious in subsequent studies (*84*, *85*).

Sparked by these findings, a more directed search for new rocaglamide derivatives from Nature aiming also at a better understanding of their pronounced insecticidal properties commenced, which up to now has led to the isolation of more than 60 naturally occurring rocaglamide congeners as well as numerous other biogenetically related compounds isolated from over 30 different *Aglaia* species collected mainly in Indonesia, the People's Republic of China, Thailand, and Vietnam.

The majority of the 63 naturally occurring rocaglamide derivatives known so far were analyzed for their insecticidal activity employing various Lepidopteran larvae including *Peridroma saucia* (*53*), *Ostrinia nubilalis* (*86*), *Helicoverpa armigera* (*87*), or *Spodoptera littoralis* as experimental insects. Most of these studies, however, have been performed with larvae of the polyphagous pest insect *Spodoptera littoralis* (*14*, *16*, *17*, *54–56*, *58*, *59*) thereby permitting the formulation of preliminary structure-activity relationships based on a larger set of data obtained with the same insect species. In the studies with *S. littoralis*, different rocaglamide derivatives were usually added at a range of concentrations to artificial diet, which was subsequently offered to newly hatched larvae in a no choice chronic feeding bioassay. From the larval survival rates, LC_{50} values can be calculated for

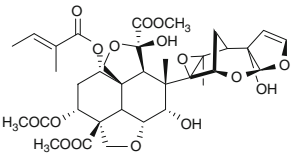

Fig. 11. Chemical structure of azadirachtin from *Azadirachta indica* (family Meliaceae)

the various rocaglamide congeners and compared to other insecticides of natural origin, such as azadirachtin from *Azadirachta indica* (family Meliaceae) (Fig. 11). With only a few exceptions, all naturally occurring rocaglamide congeners evaluated exhibited potent insecticidal activity toward the larvae of *S. littoralis*. The most active compounds, including the parent compound rocaglamide (**1**) itself or its didesmethyl analogue **15**, exhibited LC_{50} values ranging between 1 and 2 ppm, so their insecticidal activity was thus comparable to that of azadirachtin (*14*, *54*, *55*, *59*).

Acylation of the OH group at C-1 (*e.g.* with formic or acetic acid) led to a reduction of insecticidal activity, as exemplified by comparison of the LC_{50} values of compound **2** (1.5 ± 0.7 ppm) and its acetyl derivative **5** (8.0 ± 1.4 ppm) or of congener **12** (1.1 ± 0.6 ppm) and its acetyl derivative **13** (14.7 ± 2.8 ppm) (*14*, *54*, *55*). On the other hand, the nature of the amide substituent present at C-2 showed little or no influence on the insecticidal activity of the resulting rocaglamide congeners, even when the dimethylamino group present in the parent compound rocaglamide (**1**) (LC_{50} of 0.9 ± 0.4 ppm) was exchanged for a rather bulky group, as, for example, in compound **14** (LC_{50} of 1.6 ± 0.6 ppm). The same findings were true when the amide group was exchanged to an ester substituent, which likewise had no significant effect on the resultant insecticidal activity of the respective compounds. However, a diminution in insecticidal activity by a factor of 5 or 6 was usually observed for rocaglamide derivatives featuring an unsubstituted C-2 when compared to analogues with an amide or carboxylic acid ester substituent at this particular position (*14*, *54*, *55*, *59*).

In rings A or B, the occurrence of an additional oxygen substituent, when compared to the substitution pattern of the parent compound, rocaglamide (**1**), revealed only marginal influences on the insecticidal activity of the respective products (*54*). However, a dramatic effect with regard to structure-activity relationships of rocaglamide derivatives was observed for analogues with a substituted OH group at C-8b. For example, compounds featuring a methoxy group at C-8b that were isolated from the roots of *A. duperreana* proved to be completely inactive as insecticides even when tested at concentrations of more than 100 ppm. Thus, these results point out the presence of a free OH group at C-8b as being the most important structural prerequisite for insecticidal activity of rocaglamide analogues determined so far (*56*, *58*).

It is difficult to decide whether the mortality of the *S. littoralis* larvae observed in chronic feeding bioassays described above is mainly caused by starvation due to feeding deterrence or by a direct toxicity of the rocaglamide derivatives evaluated

or from a combination of both effects. When neonate larvae of *S. littoralis* were given the choice between an artificial diet treated with rocaglamide (**1**) and a control diet, they avoided the former and showed a clear preference for the latter (the IC_{50} values in these experiments varied between 0.2 and 0.25 ppm), indicating that **1** and its congeners have strong antifeedant properties (*54, 55*). The toxicity of rocaglamide (**1**) was proven by injecting known amounts of this cyclopenta[*b*] benzofuran derivative into the hemolymph of last instar larvae of *S. littoralis*. In these experiments, the LC_{50} of rocaglamide varied between 5.6 and 7.5 ppm (*54, 55*). Further proof for the effects of **1** on a cellular level was obtained using *in vitro* cultures of *Spodoptera frugiperda* cells. Addition of rocaglamide (**1**) to the *in vitro* cultures resulted in an arrest of cellular division as indicated by the severely reduced incorporation of [^{3}H]-thymidine. The IC_{50} of **1** amounted to 1.9 μg/cm^3 (= 3.8 μ*M*) (*84, 85*).

A more recent study was conducted to assess the insecticidal activity of rocaglamide (**1**) isolated from *Aglaia elaeagnoidea* against the gram pod borer, *Helicoverpa armigera* (Hübner) (*87*). In this study, rocaglamide was added to an artificial diet and this led to growth retardation of neonate larvae in a dose-dependent manner with an IC_{50} value of 0.76 ppm, which could be compared to that of azadirachtin (IC_{50} = 0.23 ppm). However, azadirachtin (Fig. 11) was determined as being more potent than rocaglamide in inducing growth inhibition via oral administration to the first stadium larvae utilized. By topical application, rocaglamide (**1**) was found to have LD_{50} and LD_{95} values of 0.40 and 1.02 μg per larvae against third instar larvae 96 h post-treatment, whereas the analogous values for azadirachtin were 8.16 and 25.8 μg per larva for the same period (*87*).

In spite of the severe morphological larval deformities observed in azadirachtin-treated larvae during the process of ecdysis, the cytotoxic nature of rocaglamide (**1**) was established by evaluating dietary utilization, for which the results did not implicate any antifeedant effect, but rather a toxicity-mediated effect due to the reduced efficiency of the conversion of ingested food. Conclusively, feeding deterrence was deduced not to be the primary mode of insecticidal activity of rocaglamide, with this compound having instead a centrally mediated effect, which could be due to induced cytotoxicity at non-specific cellular levels (*87*).

However, the molecular target of rocaglamide (**1**) and its congeners in insects is still unknown, and the insecticidal activity of these compounds can be linked to distinct structural features, such as the OH group at C-8b, which is an indispensable prerequisite for bioactivity. Interestingly, rocaglamide derivatives often co-occur in *Aglaia* species with biogenetically closely related compounds of the aglain, aglaforbesin, or forbagline type (*14, 16, 60*). In these latter compounds, the oxygen heterocycle of the dihydrobenzofuran nucleus in rocaglamides is replaced by a bridged pyran or by an oxepine ring. These structural differences, however, lead to a complete loss of insecticidal activity for aglain, aglaforbesin, or forbagline derivatives (*14, 16*). The putative biogenetic precursors of rocaglamides as well as aglains, aglaforbesins, and forbaglines – methylated flavonoids and 2-aminopyrrolidines, such as odorine (**103**) – are likewise devoid of any significant

insecticidal activity (*54*, *55*), implying that the integrity of the cyclopenta[*b*]-tetrahydrobenzofuran moiety of the rocaglamide skeleton is essential for the insecticidal activity of this unique group of natural products.

4.2. Anti-inflammatory Activity

In several countries of Southeast Asia (*e.g.* Vietnam), the leaves and flowers of *A. duperreana* and *A. odorata* are used in traditional medicine for the treatment of asthma and inflammatory skin diseases. Inflammatory diseases arise from inappropriate activation of the immune system, leading to abnormal expression of genes encoding pro-inflammatory cytokines and tissue-destructive enzymes (*88*). Overproduction of cytokines such as TNF-α and IFN-γ has been shown to be tightly associated with autoimmune and inflammatory diseases, whereas, uncontrolled expression of the cytokine IL-4 causes allergic disorders including asthma (*88*, *89*). It has been shown that rocaglamide (**1**), 1-*O*-acetylrocaglamide (**4**), and 1-oxo-11,12-methylendioxyrocaglaol (**50**) can inhibit TNF-α, IFN-γ, and IL-4 production in human peripheral blood T cells at very low doses (25–50 n*M*) (*25*). This effect may partially explain the anti-inflammatory and anti-asthmatic activities of *Aglaia* species. Importantly, at the concentrations required for inhibition of cytokine expression, these compounds do not show obvious toxicities on primary blood T cells (*21*, *25*).

Many inflammatory cytokine genes including IL-4 are regulated at the transcriptional level by pro-inflammatory transcription factors, such as NF-κB and AP-1 and by nuclear factor of activated T cells (NF-AT) (*89*–*91*). Several rocaglamide derivatives were reported to have an inhibitory effect on the activity of NF-κB. It was shown that at n*M* concentrations, rocaglamide (**1**), desmethyl-rocaglamide (**7**), *N*,*N*-didesmethyl-*N*-4-hydroxybutyl-rocaglamide (**12**), and didesmethyl-rocaglamide (**15**) inhibited NF-κB-mediated transcription induced by TNF-α or phorbol 12-myristate 13-acetate (PMA) in Jurkat leukemic T cells by more than 90%, as determined by a stably transfected NF-κB-regulated luciferase reporter gene (*24*). This effect, however, was not seen in non-lymphoid cells transiently transfected with the NF-κB-regulated luciferase reporter gene (*24*). The authors concluded that rocaglamide derivatives may be potent inhibitors of NF-κB in T lymphocytes but not in other types of cells. The NF-κB pathway can be activated by various stimuli. In resting T cells, NF-κB is sequestered in an inactive state by the cytoplasmic inhibitor of NF-κB (IκB). Stimulation of T cells, *e.g.* through the T cell receptor, the TNF receptor, or using PMA, leads to rapid activation of the IκB kinases (IKKs) and results in phosphorylation, ubiquitylation, and subsequent degradation of IκB proteins, which allows the nuclear translocation of NF-κB (*92*). Rocaglamide (**1**) probably interferes with the NF-κB activation pathway upstream of the IKK complex but downstream of the TNF receptor-associated proteins (*24*).

Recently, several rocaglamide derivatives were reported to inhibit NF-AT activity in a more sensitive and selective way than NF-κB (*25*). It was shown that rocaglamide (**1**), 1-*O*-acetylrocaglamide (**4**), and 1-oxo-11,12-methylendioxy-

rocaglaol (**50**) inhibit NF-AT-dependent transcription at doses that did not impair NF-κB- and AP1-mediated transcription in Jurkat T cells stimulated with PMA and ionomycin (*25*). Rocaglamide (**1**), which was previously reported to inhibit PMA-induced NF-κB activation in Jurkat T cells at concentrations of 25–100 n*M* (*24*), did not show inhibition of PMA-induced IκB degradation and also did not block PMA-induced nuclear translocation of p65 (a subunit of NF-κB) (*21, 25*). Instead, at concentrations <100 n*M*, rocaglamide (**1**), as well as 1-*O*-acetylrocaglamide (**4**) and 1-oxo-11,12-methylendioxy-rocaglaol (**50**), even substantially increased NF-κB-mediated transcription (*25*). In addition, using an enzyme-based NF-κB activity readout it was shown that rocaglamide (**1**) inhibited NF-κB activity only at a high dose (IC_{50} = 2 μ*M*) (*80*). Since rocaglamide also inhibits protein synthesis (see below), it is, therefore, unclear whether the observed inhibition of NF-κB activity at high concentrations of this compound is due to inhibition of NF-κB activation signalling pathway or is rather the consequence of translation inhibition. Apparently, the latter studies do not support rocaglamide as a potent NF-κB inhibitor. Nevertheless, a newly identified compound of the group of aglain derivatives named ponapensin, which is the only congener featuring a methoxy group at C-13 instead of an amide side chain in aglain B (**67**), was shown to inhibit NF-κB activity with an IC_{50} of 60 n*M* determined by the NF-κB ELISA method (*80*). So far, there are no further studies on whether and how ponapensin inhibits NF-κB activity in cells.

Members of the NF-AT family of proteins are calcium- and calcineurin-regulated transcription factors. In resting T cells, NF-AT proteins are phosphorylated and reside in the cytoplasm. T cell activation leads to activation of the calcium-dependent phosphatase calcineurin, resulting in rapid dephosphorylation of NF-AT which leads to its nuclear translocation and the induction of NF-AT-mediated gene transcription. NF-AT activities are negatively controlled by several kinases including glycogen-synthase kinase 3 (GSK3) and casein kinase 1 (CK1), which maintain NF-AT in a phosphorylated state in the cytosol (maintenance kinases), and inducible MAPKs p38 (the mitogen-activated protein kinases) and JNK (the stress-activated c-Jun N-terminal protein kinase), which induce the re-phosphorylation of nuclear NF-AT to expose a nuclear-export signal and translocate NF-AT back to the cytosol (export kinases) (*91*). Investigation of the molecular mechanism by which rocaglamide (**1**), 1-*O*-acetylrocaglamide (**4**), and 1-oxo-11,12-methylendioxyrocaglaol (**50**) inhibit NF-AT activation in Jurkat T cells revealed that these compounds can enhance T-cell-activation-induced p38 and JNK activity (*25*). Increase of p38 and JNK activity resulted in acceleration of nuclear export of NF-AT. Prevention of NF-AT nuclear translocation in activated Jurkat T cells was visualized by confocal laser scan microscopy after rocaglamide (**1**) treatment (*25*). These data suggest that rocaglamide derivatives may function as immunosuppressive agents by targeting NF-AT activity in T cells. However, later studies revealed that, in contrast to malignant T cells, rocaglamides do not activate p38 and JNK in normal T cells and have apparently little effect on the NF-AT-dependent transcription in normal T cells (*21*). How the expression of TNF-α, IFN-γ, and IL-4 in normal T cells are suppressed by rocaglamide remains unknown.

4.3. Anticancer Activity

4.3.1. Antitumor Activities *In Vivo* in Mouse Tumor Models

In 1982, rocaglamide (**1**) was shown for the first time to increase lifespan of tumor-bearing mice in a leukemic model using P388 murine lymphocytic leukemia cells (*11*). In this study, administration of rocaglamide (**1**) at a dose of 1 mg/kg/day was shown to prolong survival with a T/C value (median survival time of treated *vs*. control group) of 156% (*11*). This observation has attracted the attention of scientists and more and more newly isolated rocaglamide derivatives have been evaluated for their antitumor potential in different cancer cell lines. A battery of rocaglamide derivatives has been found to have potent inhibitory effects on proliferation in different tumor cell lines *in vitro* (summarized in Ref. (*12*)). The IC_{50} values of the antiproliferative activities of most of the rocaglamide derivatives range from 1 to 200 n*M* depending on the cell line investigated (*12*). Several rocaglamide derivatives were further tested *in vivo* in mice tumor models (*21, 68, 93, 94*). For instance, intraperitoneal treatment with 4′-demethoxy-3′,4′-methylenedioxy-methyl rocaglate (**48**) at 10 mg/kg body weight three times per week was shown to lead to delayed growth of the xenografted human breast cancer cell line BC1 in athymic mice (*93*). Treatment with silvestrol (**35**) at 2.5 mg/kg/injection, when given intraperitoneally for five consecutive days in the ip P388 murine leukemia model, afforded a lifespan increase corresponding to a T/C of 150% (*68*). Silvestrol (**35**) was also shown to inhibit growth of the xenografted human breast cancer cells MDA-MB-231 at doses of 0.5 mg/kg/day for 8 days (*94*). Significant delay in growth and tumor size (P value = 0.021) of the mouse lymphoma RMA was observed after 16 days intraperitoneal treatment with desmethyl-rocaglamide (**7**) at 5 mg/kg three times per week (*21*). These animal studies have confirmed the anticancer activities of rocaglamide derivatives. All animal studies showed that these compounds had no toxicity to liver evaluated by glutamate pyruvate transaminase (GPT) activity and showed also no body weight loss.

4.3.2. Cytostatic Activity and Inhibition of Translation

Since rocaglamide (**1**) and its derivatives have been found to have anticancer activities in experimental animal models, efforts have been taken to explore the molecular mechanisms of their actions. In several early publications, rocaglamide derivatives were reported to function mainly in a cytostatic rather than a directly cytotoxic manner (*11, 84, 85, 93*). It was shown that treatment of the human lung carcinoma cells Lu1 with 4′-demethoxy-3′,4′-methylenedioxy-methyl rocaglate (**48**) resulted in inhibition of tumor cell proliferation with cell accumulation in the G1/G0 phase of the cell cycle with only marginal cell death (*93*). Thereafter, didesmethyl-rocaglamide (**15**), aglaroxin D (aglaiastatin) (**55**), and silvestrol (**35**) were shown to inhibit cell proliferation of different human malignant cell lines

with the cell cycle blocked at the G2/M phase with negligible death (*85*, *95*, *96*). Furthermore, 4′-demethoxy-3′,4′-methylenedioxy-methyl rocaglate (**48**) was found to strongly inhibit protein biosynthesis in tumor cells as determined by ^{3}H-leucine incorporation (*93*). Based on these observations, it was thought that inhibition of translation is the key mode of action by which cyclopenta[*b*]benzofurans exert their antitumor activities.

Although rocaglamide (**1**) was found to inhibit translation more than 10 years ago, its mode of function was only recently explored. Translational control involves a highly regulated process (schematically depicted in Fig. 12).

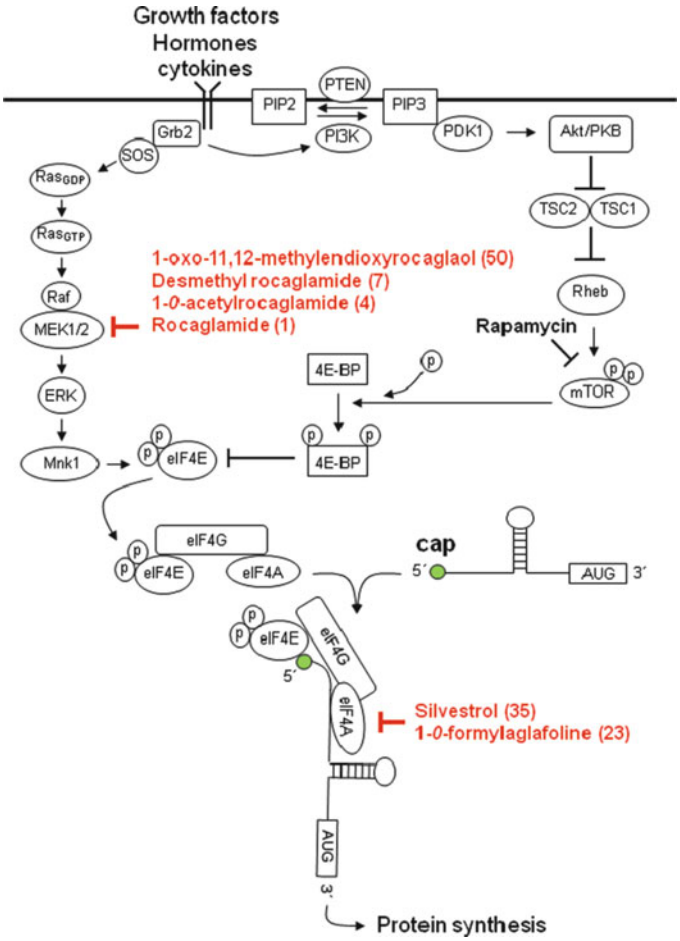

Fig. 12. Inhibition of protein synthesis by rocaglamides. The Ras-Raf-MEK-ERK and the PI3K-AKT-mTOR pathways play a central role in regulation of cap-dependent translation by activation of the eukaryotic translation initiation factor 4E (eIF4E). eIF4E binds to the 5′ cap structure and assembles eIF4G and eIF4A to initiate translation. Rocaglamide congeners **23** and **35** directly bind to and inhibit eIF4A function. Rocaglamides **1**, **4**, **7** and **50** block the MEK-REK pathway and inhibit eIF4E cap binding activity

Translation is initiated by binding of the initiation factor eIF4E to the mRNA 5′ cap structure. After binding to the 5′ cap structure, eIF4E interacts with eIF4G, which serves as a scaffold protein for the assembly of eIF4E and eIF4A to form the eIF4F complex. The eIF4F complex is then directed to the 5′ terminus of the mRNA and unwinds the mRNA 5′ secondary structure to facilitate ribosome binding and promotes ribosome recruitment and translation (*97*). Using a small molecule screening approach, 1-*O*-formylaglafoline (**23**) and silvestrol (**35**) were found to inhibit translation by interfering with eIF4A activity (*98*). It is thought that eIF4A exists as a free form or as part of the eIF4F complex and recycles through the eIF4F complex during translation initiation. 1-*O*-Formylaglafoline (**23**) and silvestrol (**35**) were shown to stimulate the RNA-binding activity of eIF4A and this action prevents incorporation of free eIF4A into the eIF4F complex (*98*).

In eukaryotes, most mRNAs are translated in a cap-dependent manner. The rate-limiting step of translation is largely controlled by binding of the initiation factor eIF4E to the mRNA 5′ cap structure. The activity of eIF4E is regulated by two major signalling pathways: the Ras-ERK-Mnk1 pathway and the PI3K-mTOR (mammalian target of rapamycin) pathway (*97*) (Fig. 12). In the Ras-ERK-Mnk1 pathway, the extracellular signal-regulated kinase ERK, activated by growth factors through Ras, phosphorylates the kinase Mnk1, which, in turn, phosphorylates eIF4E. Phosphorylation of eIF4E increases its affinity for the 5′ cap structure. The activity of eIF4E is also regulated by the PI3K-mTOR pathway. The assembly of the translation initiation complex eIF4F is inhibited by the translational repressor of eIF4E-binding proteins (4E-BP1). 4E-BP1 interacts with eIF4E in its hypophosphorylated state and prevents the recognition and binding of eIF4E to the 5′ cap mRNA structure. PI3K activates mTOR, which in turn phosphorylates 4E-BP1 leading to disruption of the interaction between 4E-BP1 and eIF4E and allowing eIF4E binding to the 5′ cap structure (Fig. 12). Most recently, 1-oxo-11,12-methylendioxyrocaglaol (**50**) was found to strongly inhibit protein synthesis ($IC_{50} = 30$ n*M*) in living cells, but had no inhibitory effect on protein synthesis *in vitro* in the rabbit reticulocyte cell free system (*99*). This finding indicates **50** does not directly inhibit the translational machinery, but rather acts through inhibition of the signaling pathway that is required for translation. Further investigation revealed **50** suppresses ERK phosphorylation and thereby inhibits ERK-Mnk1-mediated phosphorylation of eIF4E (*99*) (Fig. 12). Indeed, several rocaglamide derivatives, *e.g.* rocaglamide (**1**), 1-*O*-acetylrocaglamide (**4**), and 3′-hydroxyaglafoline (**19**), have been shown to inhibit ERK phosphorylation (*100*). Interestingly, these compounds do not inhibit ERK activity in normal lymphocytes (*100*). It is well known that the Ras-ERK-Mnk1 and the PI3K-mTOR pathways are frequently over-activated in many types of cancers due to gain of function mutations. Also the eIF4E, eIF4G, and eIF4A expression or activities are up-regulated in many cancers (*97*). Thus, targeting translational pathways is one of the mechanisms by which rocaglamide derivatives exert their antitumor functions.

4.3.3. Apoptosis Induction

Induction of apoptosis is now known to be also an important mechanism of rocaglamide (**1**)-mediated anticancer activity. Apoptotic cell death can be triggered through two main pathways: the extrinsic (also termed receptor-mediated) and the intrinsic (also termed mitochondrial-mediated) pathway (Fig. 13). The extrinsic apoptotic pathway is initiated by binding of ligands (*e.g.* CD95L and TRAIL) to their specific death receptors on the cell surface, which leads to the formation of the death inducing signaling complex (DISC) containing the FAS-associated death domain adaptor protein FADD and pro-caspase-8. Activation of caspase-8 at the DISC leads to activation of the effector caspase, caspase-3, which cleaves a number of target death proteins such as poly (ADP-ribose) polymerase (PARP) leading to apoptosis (*101*). The intrinsic pathway is initiated by various stimuli that directly or indirectly activate the mitochondrial pathway by inducing the release of

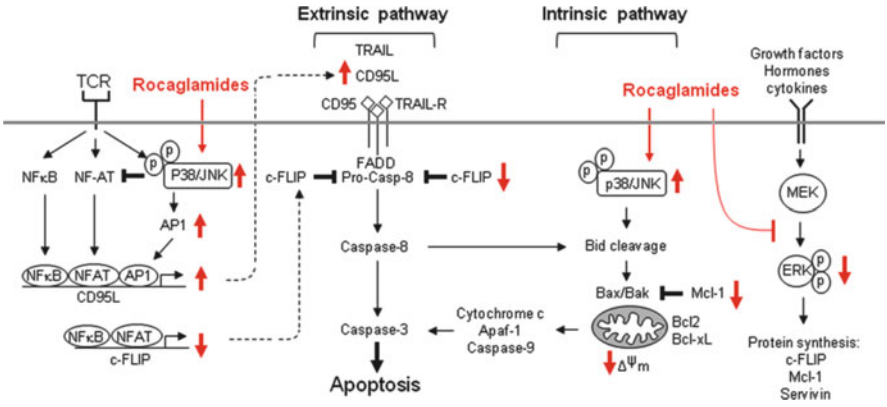

Fig. 13. Apoptosis pathways affected by rocaglamides. Apoptotic cell death is regulated by two main pathways: extrinsic (receptor-mediated) and intrinsic (mitochondria-mediated) pathways. The extrinsic pathway involves ligation of death receptors (*e.g.* CD95 and TRAIL-R) with their ligands (*e.g.* CD95L and TRAIL) resulting in a sequential activation of caspase-8 and -3, which cleave target proteins leading to apoptosis. This pathway is negatively regulated by the anti-apoptotic protein c-FLIP. Intrinsic stimuli (*e.g.* anticancer drugs) directly or indirectly activate the mitochondrial pathway by inducing release of cytochrome c and activation of caspase-9. Caspase-9, in turn, activates caspase-3. This death pathway is largely controlled by the pro-apoptotic (*e.g.* Bax and Bak) and anti-apoptotic (*e.g.* Mcl-1, Bcl-2 and Bcl-xL) proteins. Activated caspase-8 may induce cleavage of Bid, which induces translocation of Bax and/or Bak to the mitochondrial membrane and amplifies the mitochondrial apoptosis pathway. Bid cleavage can be also induced by activated p38 and JNK. Several rocaglamides can activate p38 and JNK leading to Bid cleavage. Rocaglamides can also directly inhibit protein synthesis by interfering with eIF4A (see Fig. 9) or indirectly through inhibition of the MEK-ERK-eIF4E pathway. Protein synthesis inhibition will lead to down-regulation of short-lived anti-apoptotic proteins such as c-FLIP and Mcl-1. Furthermore, rocaglamides may further increase T-cell-receptor (TCR)-mediated activation of p38 and JNK leading to down-regulation of NF-AT activity and up-regulation of AP-1 activity. This event results in up-regulation of CD95L promoter activity and suppression of c-FLIP promoter activity leading to enhancing activation-induced-cell-death

cytochrome c and the formation of the apoptosome complex with Apaf-1 and pro-caspase-9. Caspase-9 is then activated at the apoptosome and, subsequently, activates pro-caspase-3 (*102*). Activated caspase-8 may induce cleavage of Bid, which links the extrinsic death pathway to the intrinsic death pathway by induction of the translocation of the proapoptotic Bcl-2 family proteins Bax and/or Bak to the mitochondrial membrane. One major negative regulator of receptor-mediated apoptosis is the cellular caspase-8 (FLICE)-inhibitory protein (c-FLIP), which blocks processing and activation of caspase-8 at the DISC level (*101*). In the intrinsic apoptosis pathway, death and life of cells are largely controlled by pro-apoptotic, *e.g.* Bax and Bak, and anti-apoptotic proteins, *e.g.* Bcl-2, Bcl-X_L, XIAP, and myeloid cell leukemia-1 (Mcl-1) (*102*).

The first observation that rocaglamide derivatives could induce apoptotic cell death in cancer cells was reported in 2002 (*24*). It was shown that a fraction of the human leukemic CEM T cells die by apoptosis after treatment with didesmethyl-rocaglamide (**15**). It was also shown that didesmethyl-rocaglamide (**15**) could enhance apoptotic cell death induced by other apoptotic stimuli such as TNF-α and cisplatin (*24*). Thereafter, silvestrol (**35**) was also reported to have a pronounced cytotoxic rather than cytostatic effect on the human prostate carcinoma LNCaP cells (*103*). It was shown that treatment of LNCaP cells with silvestrol (**35**) resulted in cytochrome c release and consequently activation of caspase-9. However, no caspase-3 and caspase-7 activation were detected although the apoptotic cell death induced by silvestrol (**35**) could be inhibited by a pan-caspase inhibitor, Boc-D-Fmk (*103*).

Solid evidence supporting rocaglamide derivatives as being potent apoptosis inducers was provided by the study of rocaglamide (**1**) and 1-*O*-acetylrocaglamide (**4**) in leukemic cells (*100*). In this investigation, rocaglamide (**1**) treatment was shown to induce depolarization of the mitochondrial membrane potential and to trigger caspase-mediated apoptosis involving caspase-9, -8, -3, and -2 in different leukemic cell lines, *e.g.* the human acute T cell leukemia Jurkat, the human T cell lymphoma Hut78, the EBV-transformed human B lymphoblast SKW, and also primary tumor cells freshly isolated from patients having acute myeloid (AML), acute lymphoblastic (ALL), and chronic myeloid (CML) leukemias. Interestingly, rocaglamide (**1**) showed no or very low toxicities to normal peripheral blood T and B lymphocytes and had also very little toxicity to human bone marrow stem cells (*100*). Investigation of the molecular mechanisms by which rocaglamide (**1**) and 1-*O*-acetylrocaglamide (**4**) killed tumors but not normal cells revealed that these compounds preferentially induce apoptosis in malignant cells by differential modulation of the activities of ERK, p38, and JNK. It has been shown that p38 is involved in mitochondria-mediated apoptosis by promoting mitochondrial translocation of the pro-apoptotic Bcl2 family protein Bax *via* inducing Bid cleavage (*104, 105*). The protein kinase p38 has been also linked to activation of the mitochondrial pathway by directly phosphorylating Bax (*106*), Bim (*107*), and Bcl-2 (*108*) and by down-regulation of Bad phosphorylation (*109*). Consistent with those studies, activation of p38 and JNK by rocaglamide (**1**) and 1-*O*-acetylrocaglamide (**4**) was shown to correlate with Bid cleavage (*100*).

Extensive studies in the past have established that ERK is an important survival factor and, particularly, ERK has been found to be constitutively activated in the majority of cancers. Thus, targeting the ERK pathway has been considered to be one of the important strategies in anticancer therapy (*110*). Rocaglamide (**1**) and 1-*O*-acetylrocaglamide (**4**) were shown to induce activation of p38 and JNK accompanied by a long-term suppression of ERK activity (*100*). The critical role of p38/JNK and ERK in apoptosis induction in tumor cells was further demonstrated by the rocaglamide derivative 3′-hydroxylafoline (**19**), which differs from rocaglamide (**1**) and 1-*O*-acetylrocaglamide (**4**) only in having -OH at the C-3′ position. 3′-Hydroxylafoline (**19**) had a very weak effect on the activities of p38 and ERK in tumor cells and showed only a slight apoptosis induction. In addition, malignant cells that lost their ability to respond to rocaglamide-induced activation of p38/JNK or suppression of ERK were resistant to apoptosis induction by rocaglamide (*110*). Furthermore, rocaglamide (**1**) and 1-*O*-acetylrocaglamide (**4**) do not affect the activities of p38, JNK, and ERK in normal lymphocytes and therefore have no or only small effects on apoptosis induction in normal lymphocytes (*100*).

Inhibition of protein synthesis may affect expression levels of pro- and antiapoptotic proteins, in particular, those having a short half-life. Therefore, rocaglamide-mediated translational inhibition may cause imbalances of pro- and anti-apoptosis protein levels in a tumor cell. For instance, reduced expression of the anti-apoptotic proteins Mcl-1 and survivin were observed in human breast cancer MDA-MB-231 cells after exposure to silvestrol (**35**) (*94*). Also, down-regulation of c-FLIP, the major inhibitor of caspase-8, was detected in tumor cells treated with rocaglamide (**1**), desmethyl-rocaglamide (**7**), 1-*O*-acetylrocaglamide (**4**), and 1-oxo-11,12-methylendioxyrocaglamide (**50**) (*21, 99*). Expression of the c-FLIP proteins is controlled at multiple levels. The ERK and the PI3K signaling pathways have been shown to regulate c-FLIP expression (*111–113*). In addition, c-FLIP protein turnover is actively regulated by ubiquitin-mediated proteasomal degradation (*114*). Therefore, c-FLIP proteins are short-lived proteins and are required to be constitutively synthesized in tumor cells. As described before, rocaglamide derivatives can inhibit translation (Fig. 12). Inhibition of *de novo* protein synthesis will lead to down-regulation of the expression levels of short-lived anti-apoptotic proteins such as c-FLIP. This effect is well demonstrated by a recent study showing that 1-oxo-11,12-methylendioxyrocaglamide (**50**) inhibits expression of c-FLIP at the translational level by blocking the ERK signalling pathway and thereby breaks CD95 and TRAIL resistance in human T-cell leukemia virus type-1 (HTLV-1)-associated adult T-cell leukemia/lymphoma (ATL) (*99*) (Fig. 13). One can predict that 1-*O*-acetylrocaglamide (**4**), desmethyl-rocaglamide (**7**), 1-*O*-formylaglafoline (**23**), silvestrol (**35**), 4′-demethoxy-3′,4′-methylenedioxy-methyl rocaglate (**48**), and 1-oxo-11,12-methylendioxyrocaglamide (**50**) may be also capable of sensitizing receptor-mediated apoptosis by down-regulation of c-FLIP expression.

CD95L and its receptor CD95 are the most intensively studied apoptotic system of the extrinsic pathway (Fig. 13). A well-known phenomenon is that a fraction of T cells die after activation by a so called activation-induced-cell-death (AICD). AICD

in T cells is mediated predominantly by CD95L and CD95 (*101*). CD95 is abundantly expressed in many types of cells. In contrast, expression of CD95L is more restricted to certain types of cells and predominantly expressed in activated T cells. In resting T cells, CD95L is expressed at an undetectable level and its expression is rapidly up-regulated upon T cell activation. Thus, the rate of CD95-mediated apoptosis is largely determined by the levels of CD95L expression. Expression of CD95L in activated T cells is regulated by multiple inducible transcription factors such as NF-AT, NF-κB, and AP-1 (Fos/Jun) (*115*). However, expression of c-FLIP in T cells is also regulated by NF-κB and NF-AT (*116, 117*). Therefore, T cell activation leads not only to induction of CD95L but also c-FLIP expression. Up-regulation of c-FLIP expression during T cell activation correlates with resistance to CD95/CD95L-mediated apoptosis and rescue of T cells from AICD. Rocaglamide (**1**) and desmethyl-rocaglamide (**7**) were shown to enhance CD95L-mediated AICD in malignant T cells by up-regulation of CD95L but down-regulation of c-FLIP expression (*21*). As mentioned in Sect. 4.2., rocaglamide (**1**) and several derivatives, such as 1-*O*-acetylrocaglamide (**4**) and 1-oxo-11,12-methylendioxyrocaglaol (**50**), can enhance T-cell-activation-induced p38 and JNK activity and thereby suppress NF-AT activity by promoting NF-AT nuclear export (*25*). The CD95L promoter is strongly regulated by JNK/AP-1 (*115*). Increase of p38/JNK activity leads to increase of AP-1 activity and consequently enhanced CD95L promoter activity (*21*). In contrast, c-FLIP expression in T cells is strongly regulated by NF-AT (*117*). Rocaglamide-mediated suppression of NF-AT resulted in down-regulation of c-FLIP expression (*21*) (Fig. 13). These studies suggest that rocaglamide derivatives may serve as adjuvants for death receptor-based anticancer therapies in the future.

5. Chemical Synthesis of Cyclopenta[*b*]benzofurans

Rocaglamide (**1**) and congeners pose an intriguing synthetic chemistry challenge: multiple functionalities, a hepta-substituted cyclopenta[*b*]benzofuran scaffold, and five contiguous, stereogenic centers. The following syntheses, presented largely in chronological order, are significant because of the daring synthetic maneuvers employed, efficiency of the transformations, and development of asymmetric processes.

5.1. First Approaches to the Synthesis of Rocaglamides

Before (−)-rocaglamide was synthesized, there were two significant approaches published. In 1987, *Richard J. K. Taylor* and coworkers first accessed the tricyclic rocaglate core employing the benzofuranone intermediate **126** (Fig. 14) (*118, 119*). The rocaglate skeleton was subsequently assembled *via* an intramolecular, 1,3-dithianyl anion-carbonyl condensation. However, in this case the 1,3-dithiane

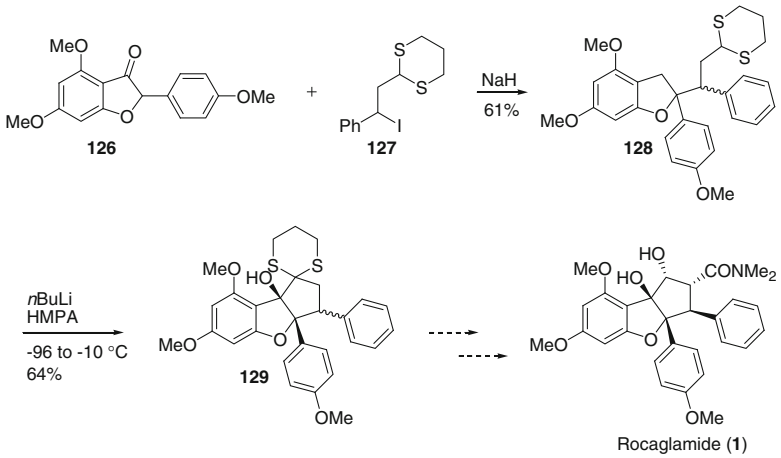

Fig. 14. *Taylor*'s approach to the rocaglate skeleton (*119*)

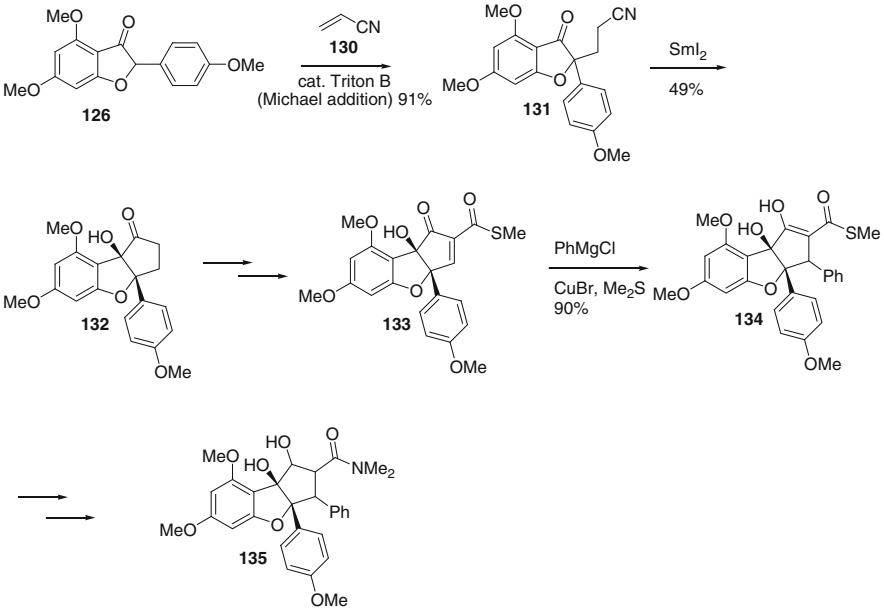

Fig. 15. *Kraus*'s synthesis of a rocaglamide di-*epi*-analogue (*120*)

group proved difficult to remove. Later syntheses, including *Taylor*'s total synthesis, have adapted the use of key intermediate **126** as starting material.

Taylor's work towards the rocaglate skeleton was then followed by *Kraus* and coworkers' synthesis of the di-*epi*-analogue of rocaglamide (Fig. 15) (*120*). Like *Taylor*'s approach, the investigators began their synthesis with the known

intermediate **126**. The first significant step in this synthesis is a *Michael* addition of acrylonitrile (**130**) with **126**. Next, a samarium-mediated reductive cyclization was performed to afford rocaglate skeleton **132**. Later in the synthesis, a cuprate addition was conducted on unsaturated thioester **133** to provide the enol intermediate **134**, which through X-ray crystal structure analysis was shown to be the *trans*-phenyl-aryl isomer. Accordingly, the cuprate had added unexpectedly to the concave face of the bicyclic ring system. Subsequent amidation and reduction of **134** yielded rocaglamide isomer **135** that did not possess the same NMR spectra as natural rocaglamide. Although the natural product was not synthesized, *Kraus* established two key steps (*Michael* addition of acrylonitrile and the reductive cyclization using SmI_2) that paved the way for future investigations in the field.

5.2. The First Total Synthesis of Rocaglamide

The first total synthesis of rocaglamide (**1**) was accomplished by *Barry Trost* and coworkers in 1990 (Fig. 16) (*52*). Asymmetric [3 + 2] cycloaddition of trimethylsilylmethyl precursor **136** and chiral oxazepinedione **137** afforded cyclopentene **138**, a transformation which established the absolute configuration at C_4. Following removal of the chiral auxiliary and ozonolysis (*not shown*), cyclopentanone **139**

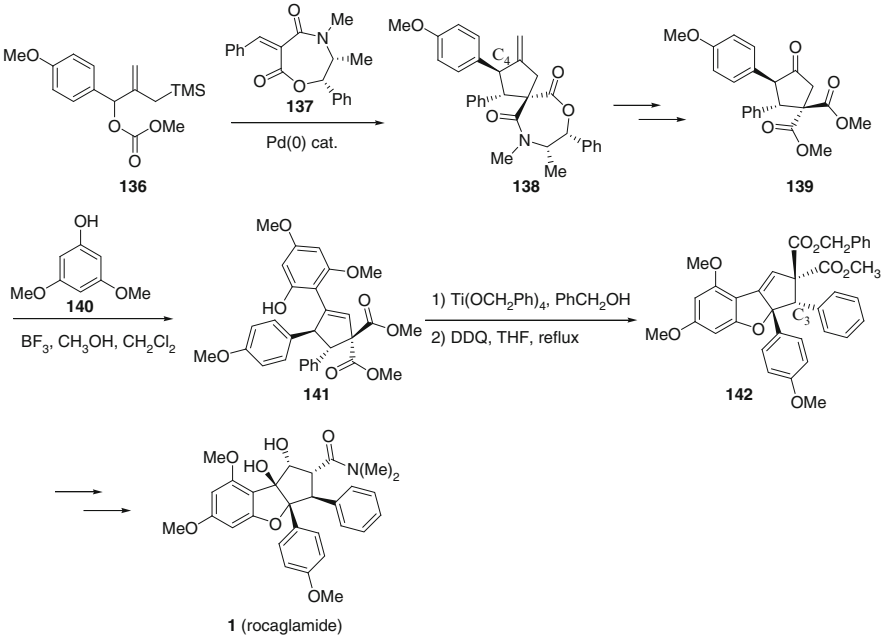

Fig. 16. *Trost*'s synthesis of (−)-rocaglamide (*52*)

was next condensed with dimethylphloroglucinol **140** to furnish intermediate **141**. Regioselective transesterification of **141** with benzyl alcohol was then performed that was followed by oxidative cyclization with DDQ to furnish intermediate **142**. With the rocaglate skeleton in hand, several reactions were performed to fully functionalized intermediate **142** and also invert stereochemistry at C_3. The synthesis was completed in 16 steps and fully established the absolute configuration of the natural product.

5.3. Syntheses of Rocaglamide and Related Natural Products

Shortly after the *Trost* synthesis, in 1991 *Taylor* and coworkers reported their synthesis of racemic rocaglamide (**1**) in eight steps from the benzofuran intermediate **126** (Fig. 17) (*121*). The key steps utilized were (1) *Michael* addition of *trans*-cinnamaldehyde (**144**) and benzofuran **126**; and (2) intramolecular, keto-aldehyde pinacolic coupling (reductive cyclization) mediated by SmI_2. This step afforded high diastereoselectivity (6:1) in construction of the rocaglate scaffold. Advanced intermediate **146** was then oxidized *via Swern* oxidation and was then transformed to a dimethylamide. The synthesis was completed with a hydroxy-directed, diastereoselective reduction of the α-hydroxy ketone **149** using $NMe_4BH(OAc)_3$ to afford (±)-rocaglamide (**1**). In 1992, *Taylor* and coworkers published another synthesis of rocaglamide involving hydrolysis of the dithiane group used in his original approach (*122*). These syntheses by *Taylor* are a beautiful fusion of his original

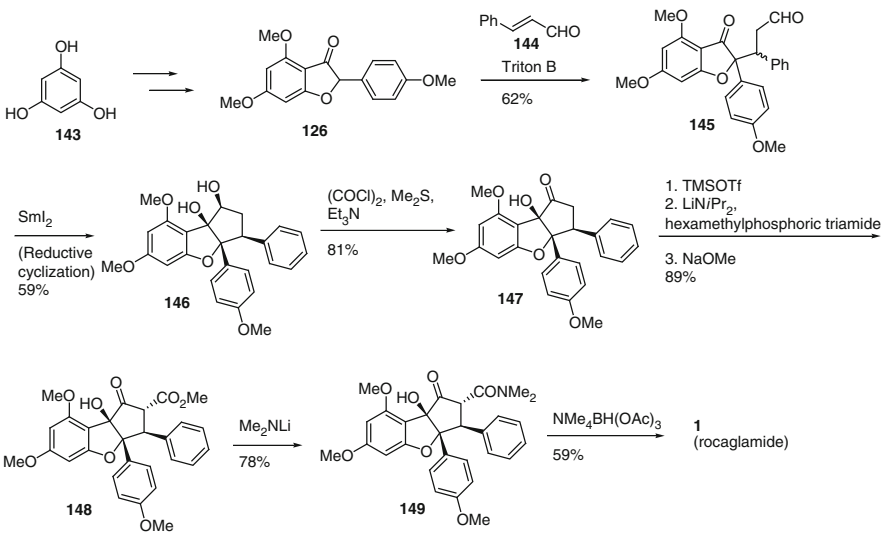

Fig. 17. *Taylor*'s racemic synthesis of rocaglamide (**1**) (*121*)

approach and the *Kraus* approach to the rocaglamide skeleton and are also frequently cited and used in later syntheses of rocaglamide and related natural products.

Inspired by the approaches of *Kraus*, *Taylor*, and *Trost*, *Takumi Watanabe* and coworkers achieved the racemic synthesis of aglaiastatin, a natural product related to rocaglamide (Fig. 18) (*123*). As the synthesis of ABC ring system had already been developed by *Taylor*, *Watanabe* began with advanced intermediate **150** (*122*). Carboxylic acid **150** was subsequently coupled with 4,4-diethoxybutanamine to form amide **151**. After the secondary alcohol was selectively oxidized, anhydrous HCl was used to form an acyl iminium species, in which case excess ammonium formate in formic acid served to form the enamine leading to cyclization with an iminium ion intermediate to afford (±)-aglaiastatin (**154**) (*dr* = 2:1).

In 2001, *Dobler* and coworkers reported a total synthesis of racemic rocaglamide using the *Michael* addition performed by *Taylor*. However, instead of using SmI_2, *Dobler* converted aldehyde **145** to a cyanohydrin intermediate in quantitative yield (Fig. 19) (*124*). Acyloin (**147**) was then initiated *via* addition of LDA, followed by deprotection with K_2CO_3, a marked improvement from preexisting methods.

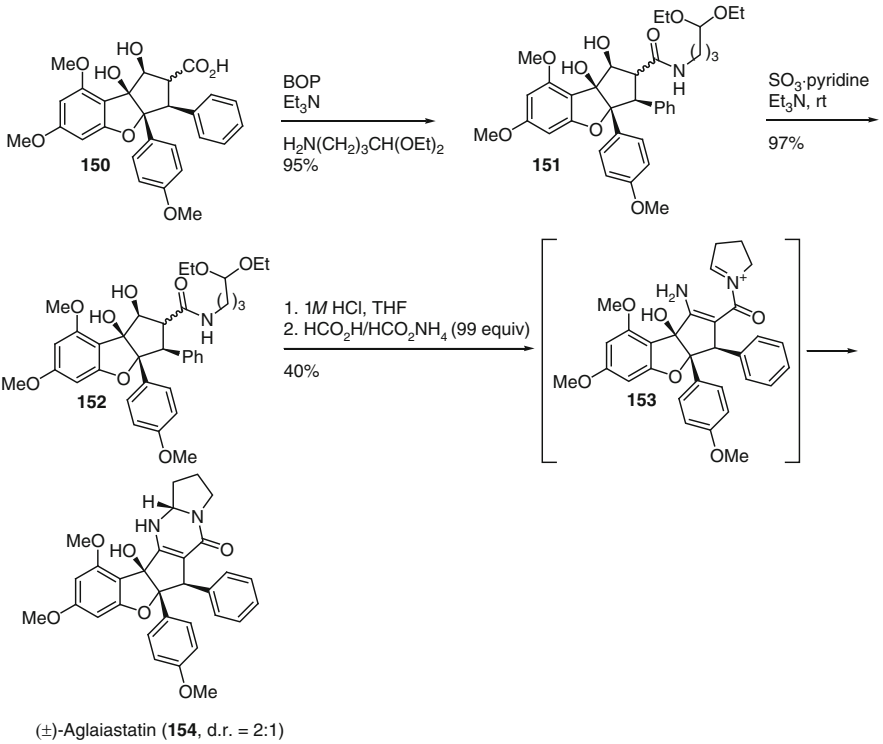

Fig. 18. *Watanabe*'s synthesis of (±)-aglaiastatin (**154**) (*123*)

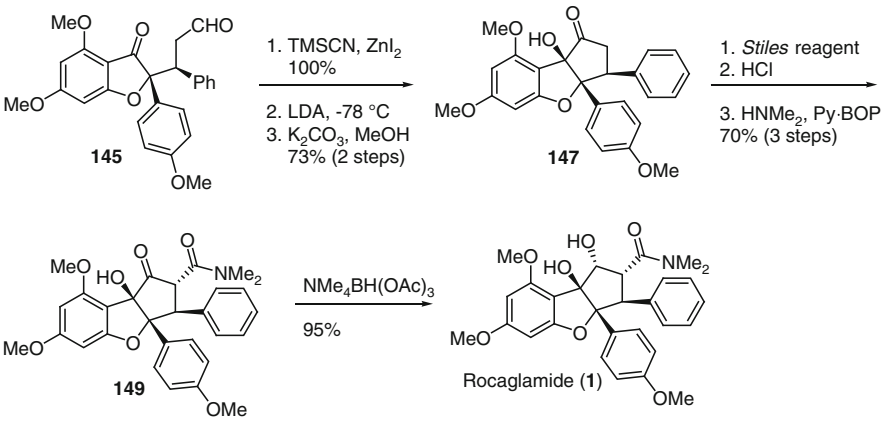

Fig. 19. *Dobler*'s synthesis of racemic rocaglamide (**1**) (*124*)

Additionally, *Stiles* carboxylation following the keto-aldehyde acyloin ring closure made the synthesis more efficient than previously reported.

5.4. *New Approaches to Rocaglamide and Related Natural Products*

The year 2004 saw a new synthetic approach to rocaglamide and related natural products employing 3-hydroxyflavones, *Porco* and coworkers found that upon photoirradiation of 3-hydroxyflavones (*e.g.* intermediate **155**), an oxidopyrylium species derived from excited-state intramolecular proton transfer (ESIPT) could be trapped with a dipolarophile (*e.g.* *trans*-methyl cinnamate **156**) (Fig. 20) (*125*) resulting in an overall [3 + 2] photocycloaddition to afford aglain intermediate **157**. The approach may mimic the proposed biosynthesis of the rocaglamides (*cf.* *13–15*). Forbaglin natural products (**158**) were also accessed through oxidation of the aglain intermediate, while rocaglamide and related natural products such as methyl rocaglate were obtained through an α-ketol shift, followed by an hydroxyl-directed reduction of the α-hydroxy ketone **159**. The methodology was then used to synthesize (±)-methyl rocaglate (Fig. 21) (*125*). Photoirradiation of 3-hydroxyflavone (**161**) and methyl cinnamate (**156**) afforded the aglain (**162**) as well as a benzo[*b*]-cyclobutapyran-8-one (**163**), which were then subjected to basic conditions to provide α-ketol rearrangement product **148**. Hydroxyl-directed reduction of α-hydroxyketone **148** yielded racemic methyl rocaglate (**18**).

To further improve their methodology, *Porco* and coworkers developed an enantioselective [3 + 2] photocycloaddition that was then used to synthesize the natural enantiomer (−)-methyl rocaglate, (−)-rocaglamide, and (−)-rocaglaol (Fig. 22) (*126*). Using functionalized TADDOL (*127*) derivatives, chiral *Brønsted* acids to enhance excited state intramolecular proton transfer, asymmetry was

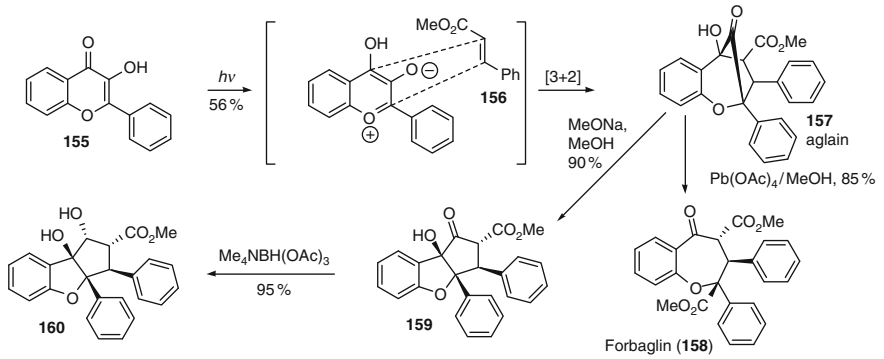

Fig. 20. *Porco*'s unified approach to the aglains, forbaglins, and rocaglamides (*125*)

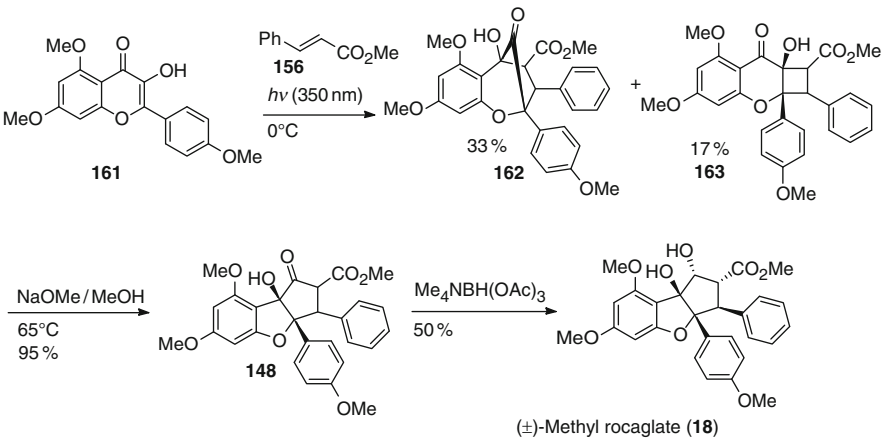

Fig. 21. *Porco*'s synthesis of (±)-methyl rocaglate (**18**) (*125*)

successfully induced with an enantiomeric excess (*ee*) of 86% using the TADDOL **164**. Recrystallization of methyl rocaglate (**18**) enhanced the *ee* to 94%, with 86% recovery. (−)-Rocaglaol (**28**) was also obtained through decarboxylation followed by diastereoselective reduction of intermediate **148**. Likewise, (−)-rocaglamide (**1**) was synthesized from **148** through a reduction/saponification/amide coupling sequence.

The work of *Thede* and *Ragot* in 2004 and 2005 focused on the synthesis of rocaglaol and analogues. While *Taylor's* approach to rocaglate natural products was quite viable, access to very electron-rich benzofuranones derived from *Hoesch* or *Friedel Crafts* reactions was limited. Using methods for unsymmetrical 3,4-diaryl-cyclopent-2-enones (*128*), *Thede* and *Ragot* published an imaginative approach to the molecule, which was highlighted by intramolecular epoxide ring opening (Fig. 23) (*129*). Although the method did not afford the natural product, it did allow for preparation of 3-*epi*-rocaglaol (**170**) and analogues through variation of aryl boronic acids on the western portion of the molecule. In 2005, *Thede* and *Ragot*

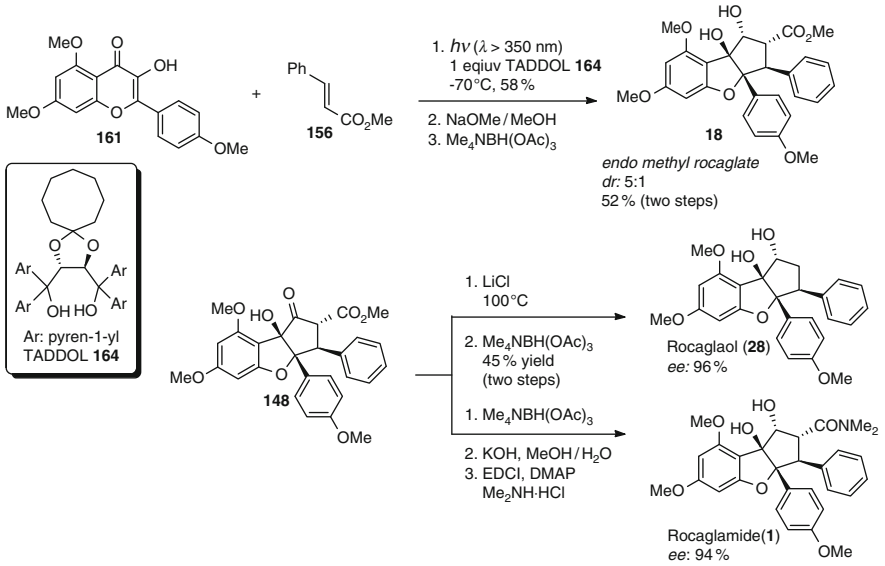

Fig. 22. *Porco*'s enantioselective methodology for the synthesis of (−)-methyl rocaglate (**18**), (−)-rocaglaol (**28**), and (−)-rocaglamide (**1**) (*126*)

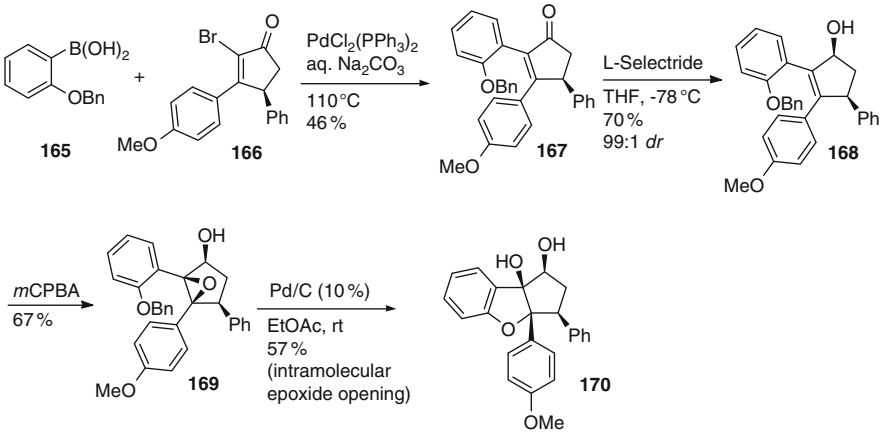

Fig. 23. *Thede* and *Ragot*'s stereoselective synthesis of (±)-rocaglaol analogues (*129*)

developed an alternative method to synthesize rocaglaol (**28**) and alteration of the benzofuran moiety to create rocaglaol analogues (Fig. 24) (*130*). This was achieved through the α-arylation of ketones using *Taylor*'s method to synthesize the skeleton. The α-arylation entailed *Suzuki*-type reaction of brominated silyl enol ethers with aryl boronic acids, allowing broad variation of the benzofuran moiety.

Control of stereochemistry of the adjacent phenyl and *para*-methoxyphenyl (PMP) groups is a difficulty frequently encountered in the synthesis of rocaglates and analogues. *Philip Magnus* and coworkers synthesized (±)-1,2-anhydro methyl

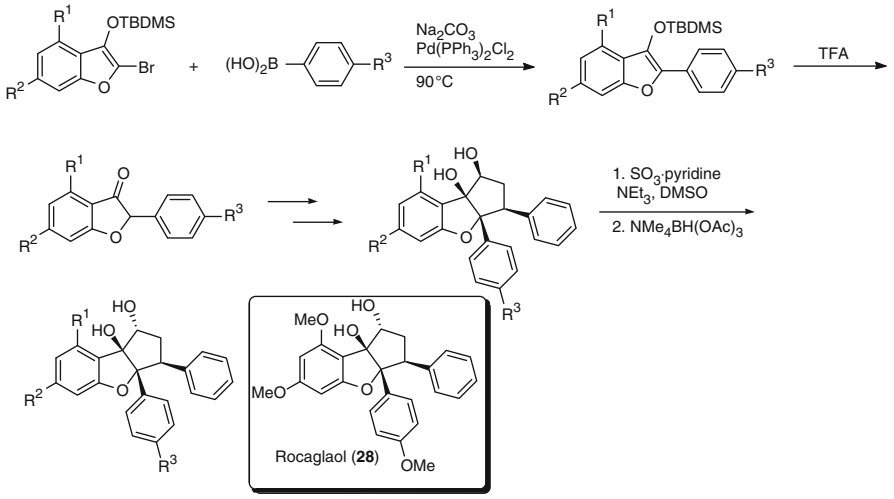

Fig. 24. *Thede* and *Ragot*'s stereoselective synthesis of (±)-rocaglaol (**28**) and analogues (*130*)

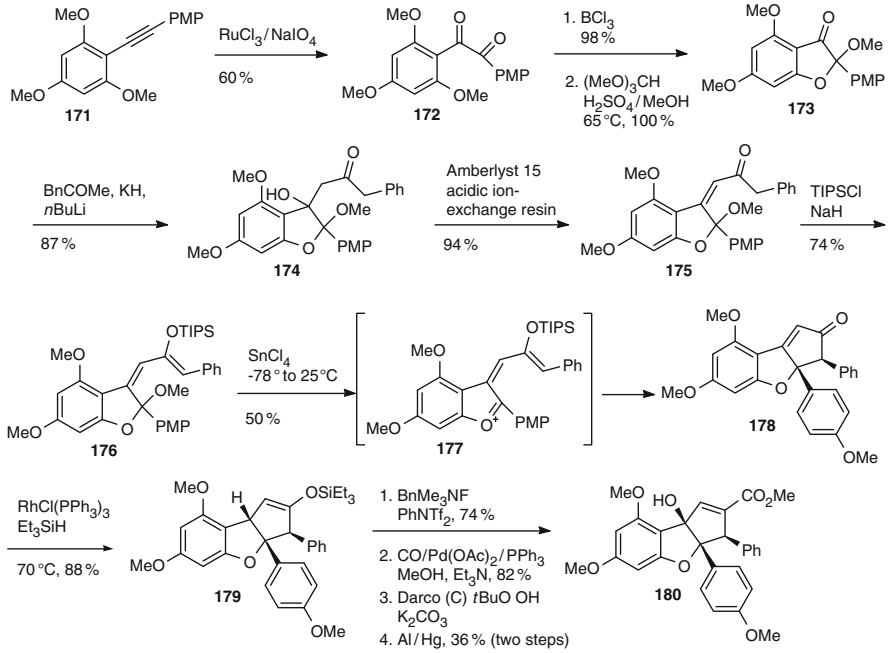

Fig. 25. *Magnus*'s stereospecific synthesis of (±)-1,2-anhydro methyl rocaglate (**180**) (*131*)

rocaglate stereospecifically in which the stereocontrol was generated through an *Isler-Mukaiyama* aldol reaction (conrotatory *Nazarov* reaction) (Fig. 25) (*131*). The synthesis commenced with coupling of 2,4,6-trimethoxyiodobenzene with

4-methoxyphenylacetylene under *Sonogashira* coupling conditions to afford intermediate **171**. Next, an oxidation was carried out with catalytic ruthenium chloride/sodium periodate to provide dione **172**, which was then treated with boron trichloride to selectively demethylate and simultaneously form a hemiketal. The hemiketal was subsequently methylated using trimethoxymethane and sulfuric acid to afford benzofuranone (**173**). Benzofuranone (**173**) was then alkylated to give substrate **174**, which was then exposed to Amberlyst 15 ion-exchange resin to afford **175**. Treatment with base and TIPSCl produced the substrate used in the conrotatory *Nazarov* cyclization. Since the reaction is stereospecific, only *cis*-aryl-phenyl diastereomer **178** was formed. Using *Wilkinson*'s catalyst, **178** was hydrosilated to give **179**, which was then desilylated and trapped with *N*-phenyltriflamide. This intermediate was then subjected to *Ortar* reaction conditions to afford a methyl ester intermediate that was further oxidized to a *tert*-butyl peroxide and subsequently reduced to yield (±)-1,2-anhydro methyl rocaglate (**180**).

In 2008, *Qin* and coworkers reported the shortest synthesis of (±)-rocaglamide and its 2,3-di-*epi*-analogue to date (Fig. 26) (*132*). A methoxycarbonyl group was introduced into *Michael* acceptor **181**, thus making the synthesis immensely more efficient. Samarium (II)-mediated reductive cyclization afforded keto-methyl rocaglate (**148**) which was then converted to the amide **149** and reduced with tetramethylammonium triacetoxyborohydride to afford the natural product **1**.

The most recent synthesis of rocaglamide was accomplished by *Alison Frontier* and coworkers (Fig. 27) (*133*). Benzofuran (**126**) was first alkylated with vinyl magnesium bromide and then oxidized to form aldehyde **183**. Subsequent alkylation with

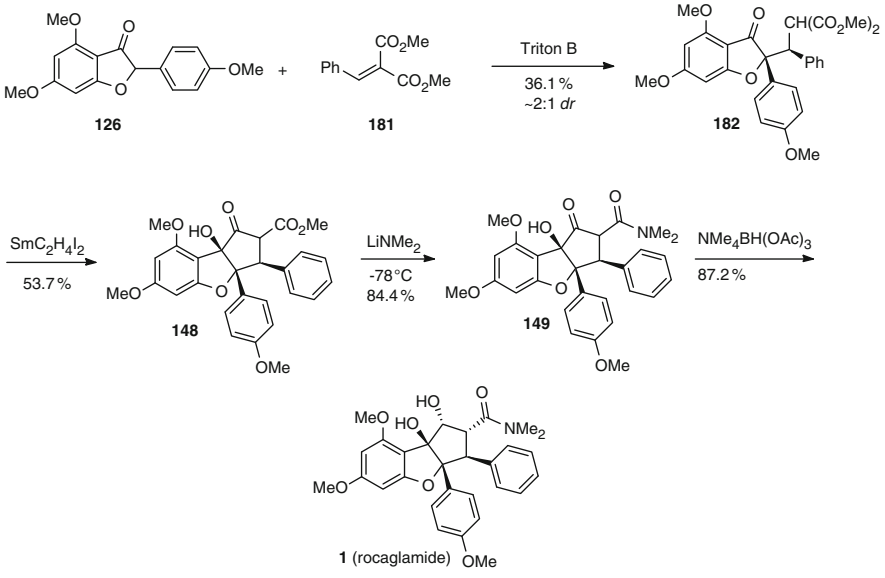

Fig. 26. *Qin*'s racemic synthesis of rocaglamide (**1**) (*132*)

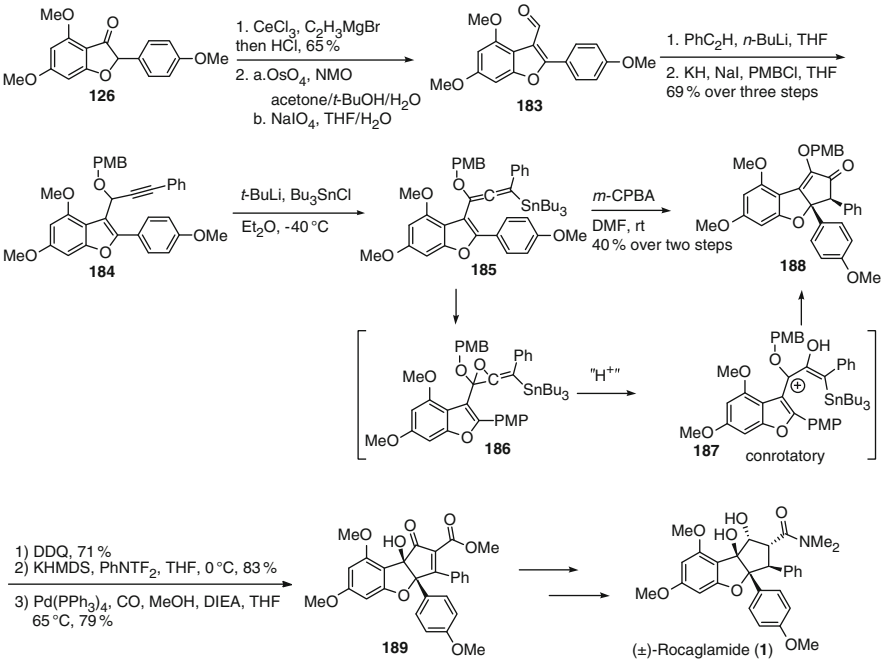

Fig. 27. *Frontier*'s synthesis of (±)-rocaglamide (**1**) *via Nazarov* cyclization (*133*)

phenylacetylene and protection of the propargyl alcohol afforded propargyl ether **184**. Next, **184** was deprotonated with *tert*-butyllithium and the resulting allenyl anion trapped with tri-*n*-butyltin chloride to afford stannyl alkoxyallene **185**. In a key step, the allenol ether was oxidized with *meta*-chloroperbenzoic acid (*m*-CPBA) forming an epoxide intermediate **186**, which opened to form the pentadienyl cation **187** necessary for the *Nazarov* cyclization under acidic conditions. Treatment of intermediate **188** with excess DDQ led to a production of a diosphenol intermediate, which was subsequently converted to a triflate, and the latter was then carbonylated to afford intermediate **189** and further advanced to racemic rocaglamide.

5.5. *Syntheses of Silvestrol*

The enantioselective synthesis of the complex rocaglate silvestrol was reported by *Porco* and coworkers in 2007 (Fig. 28) (*134*). Through a convergent strategy, the rocaglate intermediate **191** and dioxanyloxy fragment **193** were connected and subsequently deprotected to form the natural product. Methoxy methyl ether protected 3-hydroxyflavone **190** was photo-excited to its oxidopyrylium tautomer

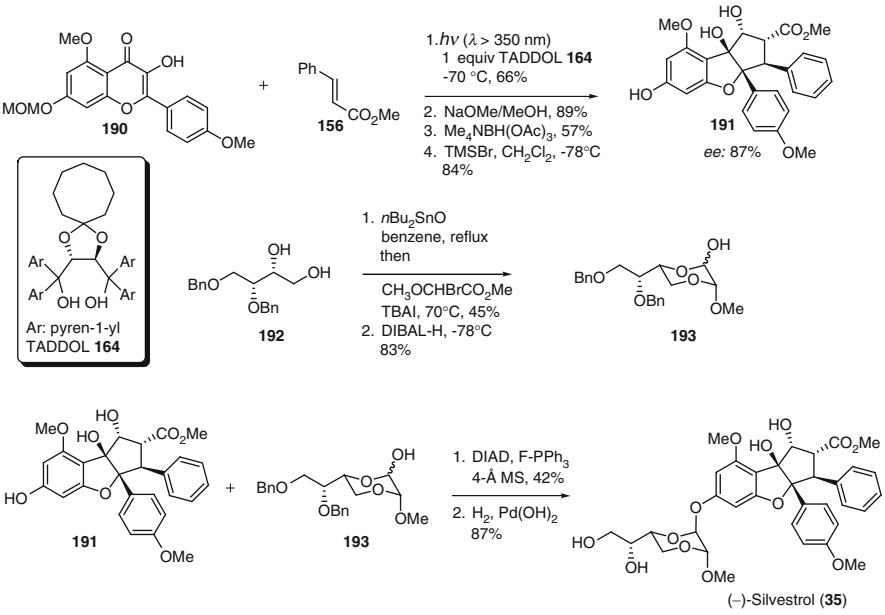

Fig. 28. *Porco*'s enantioselective synthesis of (−)-silvestrol (**35**) (*134*)

and then trapped with methyl cinnamate (**156**) mediated by TADDOL (**164**). After a ketol rearrangement/hydroxyl directed reduction sequence, the resulting cyclopenta[*b*,*c*]benzofuran intermediate was deprotected using TMSBr to remove the methoxymethyl ether (MOM), which afforded rocaglate intermediate **191** in 87% *ee* after recrystallization. Intermediate **192** was used to form an *O*-stannylene acetal, which was then combined with 2-bromo-2-methoxy acetate to afford a dioxanylone intermediate. Reduction of the dixoanylone intermediate with diisobutylaluminum hydride (DIBAL-H) afforded the dioxanyloxy fragment **193**. Using *Mitsunobu* conditions, fragments **191** and **193** were successfully coupled. Finally, hydrogenation of the coupled product gave (−)-silvestrol (**35**).

Rizzacasa and coworkers synthesized *epi*-silvestrol and silvestrol in a convergent fashion employing a method similar to their published pilot studies (*135*). Their plan was to connect the 1,4-dioxanyloxy fragment **199** with the cyclopentabenzofuran **191** core *via Mitsunobu*-type coupling to access *epi*-silvestrol (**36**), which was subsequently converted to silvestrol (**35**) using a *Mitsunobu* reaction (Fig. 29) (*136*). The synthesis of the 1,4-dioxanyloxy fragment **199** commenced with glycosylation of bromide **194** using *para*-methoxybenzyl alcohol, followed by removal of the acetates *via* methanolysis. Subsequent benzylidene formation afforded acetal **195**, which was treated with BH_3·THF and $Cu(OTf)_2$ to selectively cleave the benzylidene and afforded the protected sugar **196**. Periodate cleavage, followed by selective reduction of the newly formed aldehyde-lactol, yielded the

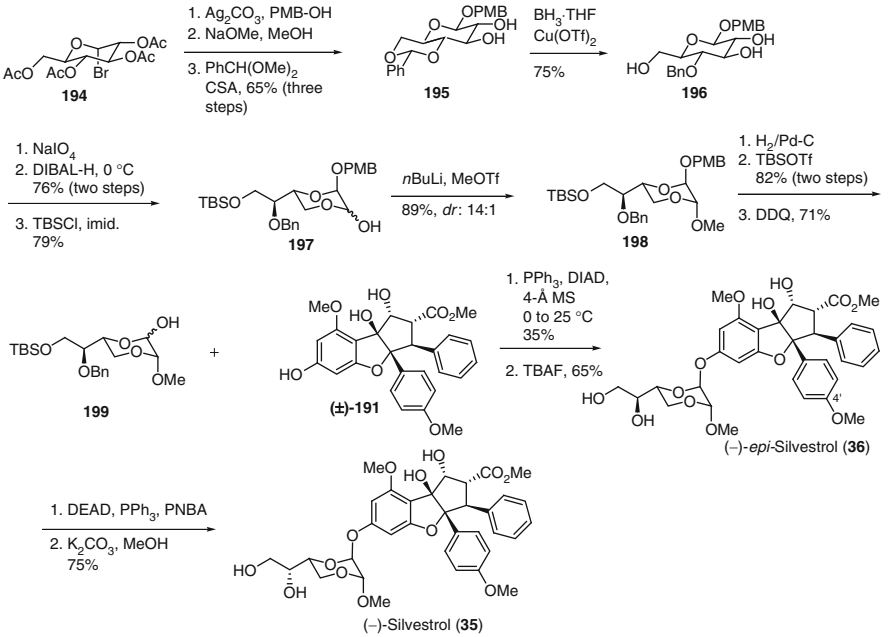

Fig. 29. *Rizzacasa*'s syntheses of (−)-silvestrol (**35**) and (−)-*epi*-silvestrol (**36**) (*136*)

lactol as a 1:3 mixture of anomers. The resultant lactol was then selectively protected at the primary alcohol to afford TBS ether **197**, which was then methylated with high selectivity to provide axial product **198**. DDQ was then used to remove the *para*-methoxybenzyl protecting group to afford the 1,4-dioxanyloxy fragment **199**. Racemic rocaglate core **191** was synthesized using the methods developed by *Porco* and coworkers, which was then coupled with optically pure fragment **199** to afford two major axial diastereomers in equal amounts, and two equatorial diastereomers in equal amounts (2:1 ratio axial:equatorial products) in 35% overall yield. The diastereomers were then deprotected to afford (−)-*epi*-silvestrol (**36**). (−)-Silvestrol (**35**) was then achieved through a selective "double *Mitsunobu*" reaction of (−)-*epi*-silvestrol (**36**). Future studies by *Rizzacasa* and coworkers disclosed a method to resolve racemic **191** using (−)-menthol, as well as an improved *Mitsunobu* coupling of **191** and **199** using (di-2-methoxyethyl azodicarboxylate) (*137*).

Aside from their complexity and synthetic challenge, silvestrol and *epi*-silvestrol displayed potent anticancer activity in A549 lung cancer proliferation assays with IC_{50} values of 33 n*M* and 30 n*M* (*137*). The synthetic analogue 4′-desmethoxy-*epi*-silvestrol was also found to be highly potent against LIM1215 colon cancer cells proliferation with an IC_{50} of 10 n*M*, foreshadowing the development of cytotoxic flavagline analogues that are more potent than their parent counterparts.

5.6. *Development of Rocaglates and Analogues as Therapeutic Agents*

Recently, *Laurent Désaubry* and coworkers discovered the first synthetic rocaglamide-type compound that inhibits cell proliferation and viability at lower doses than the parent compound, rocaglaol (**28**) (Fig. 30) (*138*). Using *Dobler*'s

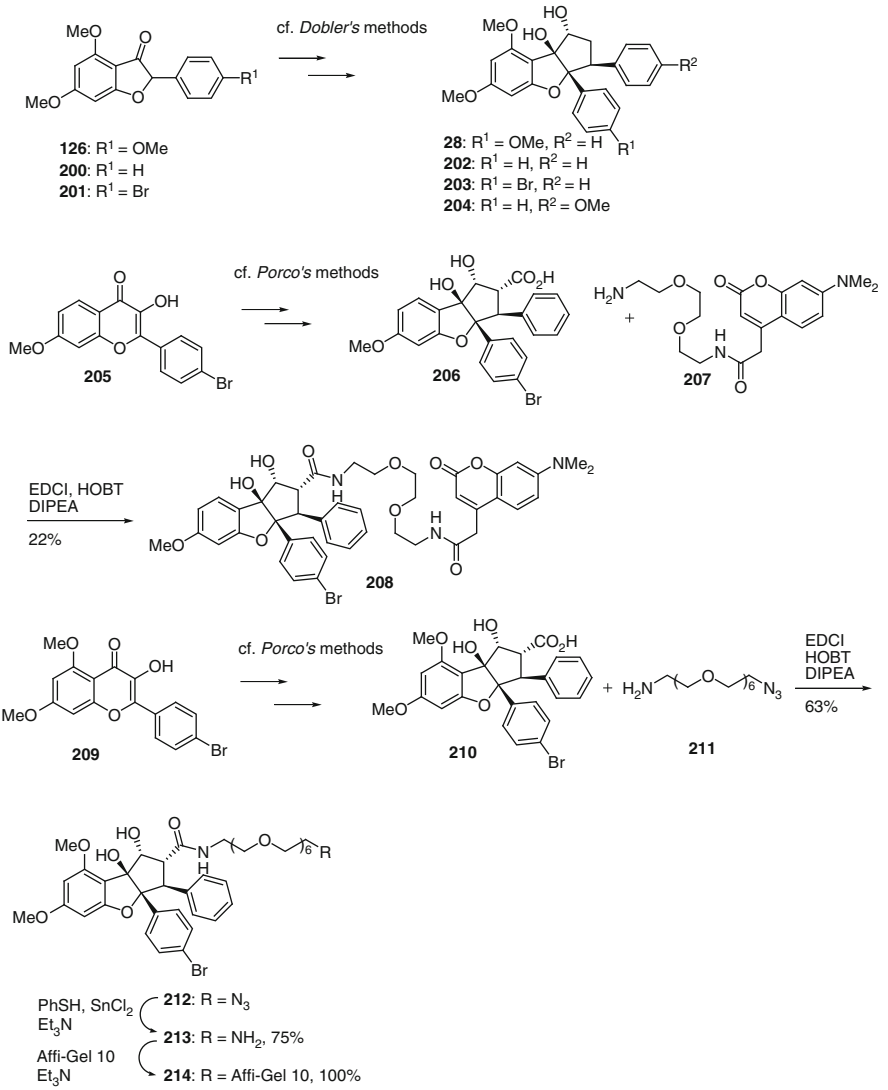

Fig. 30. *Désaubry*'s synthetic rocaglaol derivatives **28** and **202–204**, fluorescent probe **208**, and affinity ligand **214** (*138*)

procedure for the preparation of rocaglamides, the synthesis of racemic rocaglaol (**28**) and rocaglaol derivatives **202**, **203**, and **204** were achieved. These compounds were tested on a variety of human cancer cell lines. In all cases, brominated rocaglaol **203** was the most potent, having IC_{50} values lower than 1 n*M* for KB (nasopharynx), MCF7R (breast), HCT116 (colon), and HL60 (neutrophil) human cancer cell lines. No aryl substituents manifested a decrease in potency, while rocaglaol derivative **204** was highly inactive (methoxy group on the other aryl ring). Fluorescent probe **208** was synthesized from an amide coupling between fluorescent coumarin intermediate **207** and rocagloic acid intermediate **206**. The synthesis of affinity ligand **214** was initiated by amide coupling between fragments **210** and **211** to afford azide **212**, which was converted to amine **213** using $SnCl_2$ and benzene thiol. Then, **213** was conjugated to Affi-Gel 10 to afford the affinity ligand **214** used in pull down experiments that did not reveal any interaction between **214** and eukaryotic initiation factor 4A (eiF4A). Fluorescent probe **208** was shown to accumulate in the endoplasmic reticulum (ER), implying that rocaglamides bind to their target in the ER, inducing the death of cancer cells *via* activation of the AIF and caspase-12 pathways.

Porco and coworkers, using optimized reaction conditions and sequences, displayed the broad scope of their photocycloaddition methodology in the syntheses of rocaglate analogues (Fig. 31) (*139*). Using a variety of dipolarophiles, novel cycloadducts were obtained including thioester **216b**, *Weinreb* amide **216e**, and amide **216f**. The aglain intermediates were then converted to cyclopenta[*b*,*c*]-benzofurans using two methods. Cycloadducts bearing a methyl ester moiety were readily converted into rocaglate isomers, but in many cases a *Lewis* acid-catalyzed method was found to be necessary. When 25 compounds were tested for *in vitro* potency as inhibitors of eukaryotic translation, six compounds had IC_{50} values lower than 10 μ*M*. Compounds **217e** and **217f** were found to be the most potent with IC_{50} values of 300–400 n*M*. The positive control, silvestrol, had an IC_{50}

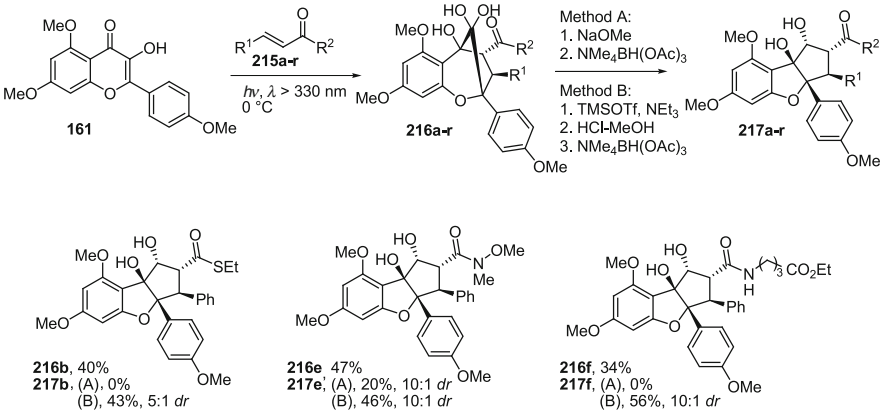

Fig. 31. Scope of [3 + 2] photocycloaddition to produce analogues of rocaglamide (*139*)

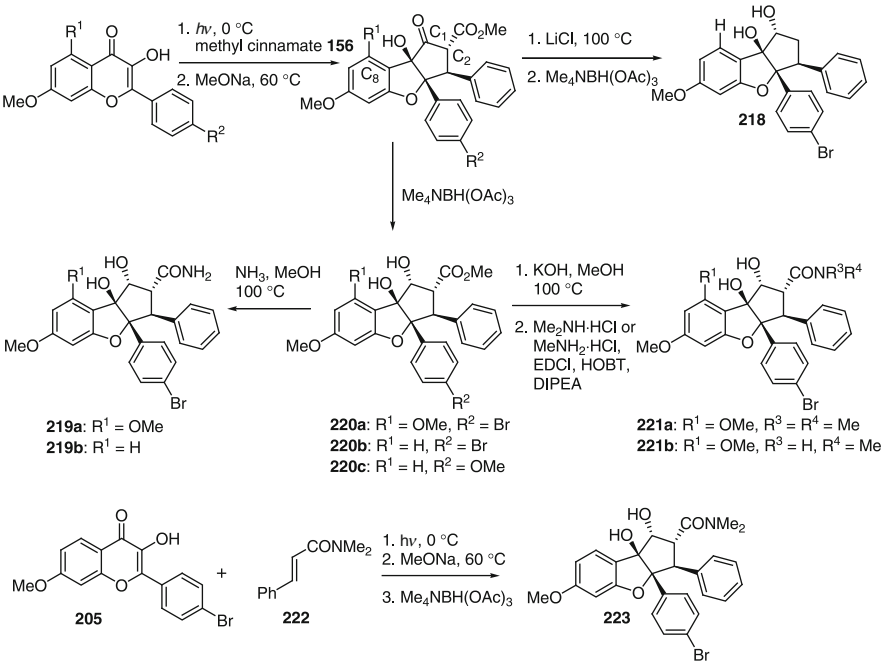

Fig. 32. *Désaubry*'s rocaglamide and rocaglaol analogues (*140*)

of 100 n*M* in the same assay, demonstrating excellent potency from the synthetic analogues. When tested *in vivo*, hydroxamate **217e** was the most potent, inhibiting 85% of protein synthesis over the course of an hour, similar to silvestrol.

With knowledge that bromine substituted at the C-4′ position improves cancer cell cytotoxicity, *Désaubry* and coworkers studied structure activity relationships (SAR) when C-1 and C-2 substituents are varied, and how the C-8 methoxy affected activity. The rocaglamide core was constructed through [3 + 2] photocycloaddition, followed by acyloin rearrangement (Fig. 32) (*140*). Compound **218** was prepared by decarboxylation and subsequent reduction. Methyl rocaglate analogues **220a-220c** were tested, and from **220a** and **220b**, amide analogues **219a** and **219b** were achieved through nucleophilic displacement using ammonia. Compounds **221a** and **221b** were prepared from **220a** and **220b** by KOH hydrolysis followed by amide coupling. Using modified 3-hydroxyflavone **205** and cinnamic amide **222**, synthetic rocaglamide **223** was efficiently prepared using a [3 + 2] photocycloaddition, ketol rearrangement, and subsequent reduction. With the C-2 analogues in hand, C-1 analogues were constructed from α-hydroxyketone **224** (Fig. 33) (*140*). Reduction with $Me_4NBH(OAc)_3$ afforded rocaglaol analogue **225**, which was esterified to afford analogues **226**, **227**, and **228**. When **224** was treated with sodium borohydride, *Désaubry* observed opposite selectivity from $Me_4NBH(OAc)_3$, forming *cis*-diol **229**, which was esterified to afford **230**. Oxime methyl ether **231** was reduced

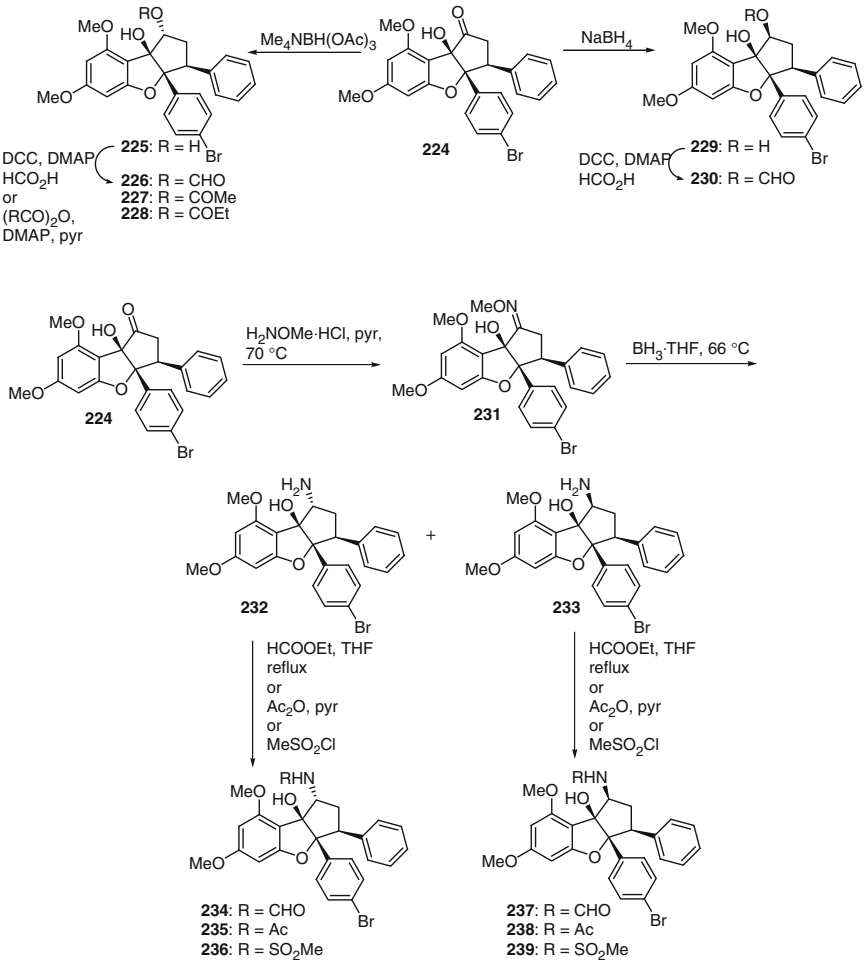

Fig. 33. *Désaubry*'s rocaglamide and rocaglaol analogues varied at C-1 (*140*)

using BH_3 to give two diasteromers **232** and **233**, which were then acylated to give corresponding esters and sulfonic esters.

An SAR investigation tested cytotoxic activity of these novel analogues against a variety of human cancer cell lines, and found that 8-demethoxy compounds **218**, **219b**, **220b**, **220c**, and **223** were less active than their 8-methoxy counterparts, suggesting a preference of a methoxy group for cytotoxicity. It was also determined that having an amide or ester substituent at C-2 was detrimental for activity against HL60R cells, suggesting a detriment to multidrug resistance as well. Although configuration of the hydroxy at C-1 was not crucial for activity, formamide analogue **237** had better activity in comparison to diastereomer **234**. Compound **237**

also proved to be the best therapeutic candidate from *in vitro* studies. *In vivo* studies were then performed on mice with xenografted 3LL tumors using **237**, and reduced the growth of the tumor by 65% without any visible toxicity in the mice.

6. Concluding Remarks

The present review surveys and summarizes the rocaglamides (= flavaglines) and related derivatives isolated from the genus *Aglaia* (family Meliaceae). Both the unique unprecedented chemical skeleton and the interesting pharmacological properties of rocaglamides have attracted the attention of natural product chemists, cell biologists, and pharmacologists alike. The overwhelming research interests placed on the genus *Aglaia* have led to the isolation of more than 120 congeners since the first report of the prototype compound, rocaglamide (**1**), in 1982 by King *et al.* (*11*).

In addition to their insecticidal activity, rocaglamide derivatives revealed several other bioactivities of interest, such as anti-inflammatory, *in vitro* and *in vivo* antiproliferative, and apoptosis induction activities. While rocaglamides are unlikely to be developed into a commercial insecticide, their anti-tumor and apoptosis induction activities make them potential oncology drug candidates.

Acknowledgements Preparation of this chapter was supported by a grant of BMBF (to *P.P.*). A scholarship granted and financed by the Egyptian government (predoctoral fellowship for *S.S.E.*) is gratefully acknowledged.

References

1. Newman DJ, Cragg GM, Snader KM (2000) The Influence of Natural Products upon Drug Discovery. Nat Prod Rep **17**: 215
2. Chin Y-W, Balunas MJ, Chai HB, Kinghorn AD (2006) Drug Discovery from Natural Sources. AAPS J **8**: e239
3. Butler MS (2008) Natural Products to Drugs: Natural Product-Derived Compounds in Clinical Trials. Nat Prod Rep **25**: 475
4. Altmann K-H, Höfle G, Müller R, Mulzer J, Prantz K (2009) The Epothilones: an Outstanding Family of Anti-Tumor Agents – From Soil to the Clinic. Prog Chem Org Nat Prod 90, 1
5. Balunas MJ, Jones WP, Chin Y-W, Mi Q, Farnsworth NR, Soejarto DD, Cordell GA, Swanson SM, Pezzuto JM, Chai H-B, Kinghorn AD (2006) Relationships between Inhibitory Activity against a Cancer Cell Line Panel, Profiles of Plants Collected, and Compound Classes Isolated in an Anticancer Drug Discovery Project. Chem Biodiversity **3**: 897
6. Isman MB, Gunning PJ, Spollen KM (1997) Tropical Timber Species as Sources of Botanical Insecticides. In: Hedin PA, Hollingworth RM, Masler EP, Miyamoto J, Thompson DG (eds.) Phytochemicals for Pest Control, Symposium Series 658, p. 27. ACS Books, Washington, DC
7. Pannell CM (2007) *Aglaia*. In: Soepadmo E, Saw LG, Chung RCK, Kiew R (eds.) Tree Flora of Sabah and Sarawak, p. 24. Ampang Press Sdn Bhd, Kuala Lumpur

8. Muellner AN, Samuel R, Chase MW, Pannell CM, Greger H (2005) *Aglaia* (Meliaceae): An Evaluation of Taxonomic Concepts Based on DNA Data and Secondary Metabolites. Am J Bot **92**: 534
9. Proksch P, Edrada RA, Ebel R, Bohnenstengel FI, Nugroho BW (2001) Chemistry and Biological Activity of Rocaglamide Derivatives and Related Compounds in *Aglaia* species (Meliaceae). Curr Org Chem **5**: 923
10. Janaki S, Vijayasekaran V, Viswanathan S, Balakrishna K (1999) Anti-Inflammatory Activity of *Aglaia roxburghiana* var. *beddomei* Extract and Triterpenes Roxburghiadiol A and B. J Ethnopharmacol **67**: 45, and references cited therein
11. King ML, Chiang C-C, Ling H-C, Fujita E, Ochiai M, McPhail AT (1982) X-Ray Crystal Structure of Rocaglamide, a Novel Antileukemic 1*H*-Cyclopenta[*b*]benzofuran from *Aglaia elliptifolia*. J Chem Soc Chem Commun: 1150
12. Kim S, Salim AA, Swanson SM, Kinghorn AD (2006) Potential of Cyclopenta[*b*]benzofurans from *Aglaia* Species in Cancer Chemotherapy. Anticancer Agents Med Chem **6**: 319
13. Brader G, Vajrodaya S, Greger H, Bacher M, Kalchhauser H, Hofer O (1998) Bisamides, Lignans, Triterpenes, and Insecticidal Cyclopenta[*b*]benzofurans from *Aglaia* Species. J Nat Prod **61**: 1482
14. Nugroho BW, Edrada, RA, Wray V, Witte L, Bringmann G, Gehling M, Proksch P (1999) An Insecticidal Rocaglamide Derivative and Related Compounds from *Aglaia odorata* (Meliaceae). Phytochemistry **51**: 367
15. Bacher M, Hofer O, Brader G, Vajrodaya S, Greger H (1999) Thapsakins: Possible Biogenetic Intermediates towards Insecticidal Cyclopenta[*b*]benzofurans from *Aglaia edulis*. Phytochemistry **52**: 253
16. Dreyer M, Nugroho BW, Bohnenstengel FI, Ebel R, Wray V, Witte L, Bringmann G, Mühlbacher J, Herold M, Hung PD, Kiet LC, Proksch P (2001) New Insecticidal Rocaglamide Derivatives and Related Compounds from *Aglaia oligophylla*. J Nat Prod **64**: 415
17. Schneider C, Bohnenstengel FI, Nugroho BW, Wray V, Witte L, Hung PD, Kiet LC, Proksch P (2000) Insecticidal Rocaglamide Derivatives from *Aglaia spectabilis* (Meliaceae). Phytochemistry **54**: 731
18. Greger H, Pacher T, Brem B, Bacher M, Hofer O (2001) Insecticidal Flavaglines and Other Compounds from Fijian *Aglaia* Species. Phytochemistry **57**: 57
19. Hayashi N, Lee K-H, Hall IH, McPhail AT, Huang H-C (1982) Structure and Stereochemistry of (−)-Odorinol, an Antileukemic Diamide from *Aglaia odorata*. Phytochemistry **21**: 2371
20. Cui B, Chai H, Santisuk T, Reutrakul V, Farnsworth NR, Cordell GA, Pezzuto JM, Kinghorn AD (1997) Novel Cytotoxic 1*H*-Cyclopenta[*b*]benzofuran Lignans from *Aglaia elliptica*. Tetrahedron **53**: 17625
21. Zhu JY, Giaisi M, Köhler R, Müller WW, Mühleisen A, Proksch P, Krammer PH, Li-Weber M (2009) Rocaglamide Sensitizes Leukemic T Cells to Activation-Induced Cell Death by Differential Regulation of CD95L and c-FLIP Expression. Cell Death Differen **16**: 1289
22. Saifah E, Suttisri R, Shamsub S, Pengsuparp T, Lipipum V (1999) Bisamides from *Aglaia edulis*. Phytochemistry **52**: 1085
23. Engelmeier D, Hadacek F, Pacher T, Vajrodaya S, Greger H (2000) Cyclopenta[*b*] benzofurans from *Aglaia* Species with Pronounced Antifungal Activity against Rice Blast Fungus (*Pyricularia grisea*). J Agric Food Chem **48**: 1400
24. Baumann B, Bohnenstengel F, Siegmund D, Wajant H, Weber C, Herr I, Debatin K-M, Proksch P, Wirth T (2002) Rocaglamide Derivatives are Potent Inhibitors of NF-κB Activation in T-Cells. J Biol Chem **277**: 44791
25. Proksch P, Giaisi M, Treiber MK, Palfi K, Merling A, Spring H, Krammer PH, Li-Weber M (2005) Rocaglamide Derivatives are Immunosuppressive Phytochemicals that Target NF-AT Activity in T cells. J Immunol **174**: 7075
26. Greger H, Pacher T, Vajrodaya S, Bacher M, Hofer O (2000) Infraspecific Variation of Sulfur-Containing Bisamides from *Aglaia leptantha*. J Nat Prod **63**: 616

27. Wang B-G, Ebel R, Nugroho BW, Prijono D, Frank W, Steube KG, Hao X-J, Proksch P (2001) Aglacins A–D, First Representatives of a New Class of Aryltetralin Cyclic Ether Lignans from *Aglaia cordata*. J Nat Prod **64**: 1521
28. Wang B-G, Ebel R, Wang C-Y, Wray V, Proksch P (2002) New Methoxylated Aryltetrahydronaphthalene Lignans and a Norlignan from *Aglaia cordata*. Tetrahedron Lett **43**: 5783
29. Wang B-G, Ebel R, Wang C-Y, Edrada RA, Wray V, Proksch P (2004) Aglacins I–K, Three Highly Methoxylated Lignans from *Aglaia cordata*. J Nat Prod **67**: 682
30. Saifah E, Puripattanavong J, Likhitwitayawuid K, Cordell GA, Chai H, Pezzuto JM (1993) Bisamides from *Aglaia* Species: Structure Analysis and Potential to Reverse Drug Resistance with Cultured Cells. J Nat Prod **56**: 473
31. Saifah E, Suparakchinda N (1998) Bisamide from *Aglaia rubiginosa*. Planta Med **64**: 682
32. Inada A, Shono K, Murata H, Inatomi Y, Darnaedi D, Nakanishi T (2000) Three Putrescine Bisamides from the Leaves of *Aglaia grandis*. Phytochemistry **53**: 1091
33. Seger C, Pacher T, Greger H, Saifah E, Hofer O (2002) Aglairubine: Structure Revision of a Chemotaxonomically Interesting Bisamide in *Aglaia* (Meliaceae). Monatsh Chem **133**: 97
34. Duong TN, Edrada RA, Ebel R, Wray V, Frank W, Duong AT, Lin WH, Proksch P (2007) Putrescine Bisamides from *Aglaia gigantea*. J Nat Prod **70**: 1640
35. Greger H, Hofer M, Teichmann K, Schinnerl J, Pannell CM, Vajrodaya S, Hofer O (2008) Amide-Esters from *Aglaia tenuicaulis* – First Representatives of a Class of Compounds Structurally Related to Bisamides and Flavaglines. Phytochemistry **69**: 928
36. Puripattanavong J, Weber S, Brecht V, Frahm AW (2000) Phytochemical Investigation of *Aglaia andramanica*. Planta Med **66**: 740
37. Mohamad K, Martin M-T, Leroy E, Tempête C, Sévenet T, Awang K, Païs M (1997) Argenteanones C–E and Argenteanols B–E, Cytotoxic Cycloartanes from *Aglaia argentea*. J Nat Prod **60**: 81
38. Roux D, Martin M-T, Adeline M-T, Sevenet T, Hadi AHA, Païs (1998) Foveolins A and B, Dammarane Triterpenes from *Aglaia foveolata*. Phytochemistry **49**: 1745
39. Mohamad K, Sévenet T, Dumontet V, Païs M, Tri MV, Hadi H, Awang K, Martin M-T (1999) Dammarane Triterpenes and Pregnane Steroids from *Aglaia lawii* and *A. tomentosa*. Phytochemistry **51**: 1031
40. Mohamad K, Martin M-T, Najdar H, Gaspard C, Sévenet T, Awang K, Hadi H, Païs M (1999) Cytotoxic 3,4-Secoapotirucallanes from *Aglaia argentea* Bark. J Nat Prod **62**: 868
41. Weber S, Puripattanavong J, Brecht V, Frahm AW (2000) Phytochemical Investigation of *Aglaia rubiginosa*. J Nat Prod **63**: 636
42. Rivero-Cruz JF, Chai H-B, Kardono LBS, Setyowati FM, Afriastini JJ, Riswan S, Farnsworth NR, Cordell GA, Pezzuto JM, Swanson SM, Kinghorn AD (2004) Cytotoxic Constituents of the Twigs and Leaves of *Aglaia rubiginosa*. J Nat Prod **67**: 343
43. Cai X-H, Luo X-D, Zhou J, Hao X-J (2005) Dolabellane Diterpenoids from the Higher Plant *Aglaia odorata*. Helv Chim Acta **88**: 2938
44. Su B-N, Chai H, Mi Q, Riswan S, Kardono LBS, Afriastini JJ, Santarsiero BD, Mesecar AD, Farnsworth NR, Cordell GA, Swanson SM, Kinghorn AD (2006) Activity-Guided Isolation of Cytotoxic Constituents from the Bark of *Aglaia crassinervia* Collected in Indonesia. Bioorg Med Chem **14**: 960
45. Xie B-J, Yang S-P, Chen H-D, Yue J-M (2007) Agladupols A–E, Triterpenoids from *Aglaia duperreana*. J Nat Prod **70**: 1532
46. Joycharat N, Greger H, Hofer O, Saifah E (2008) Flavaglines and Triterpenoids from the Leaves of *Aglaia forbesii*. Phytochemistry **69**: 206
47. Joycharat N, Greger H, Hofer O, Saifah E (2008) Flavaglines and Triterpenes as Chemical Markers of *Aglaia oligophylla*. Biochem Syst Ecol **36**: 584
48. Pointinger S, Promdang S, Vajrodaya S, Pannell CM, Hofer O, Mereiter K, Greger H (2008) Silvaglins and Related 2,3-Secodammarane Derivatives – Unusual Types of Triterpenes from *Aglaia silvestris*. Phytochemistry **69**: 2696

49. Seger C, Pointinger S, Greger H, Hofer O (2008) Isoeichlerianic Acid from *Aglaia silvestris* and Revision of the Stereochemistry of Foveolin B. Tetrahedron Lett **49**: 4313
50. Hofer O, Pointinger S, Brecker L, Peter K, Greger H (2009) Silvaglenamin – A Novel Dimeric Triterpene Alkaloid from *Aglaia silvestris*. Tetrahedron Lett **50**: 467
51. Cai X-H, Wang Y-Y, Zhao P-J, Li Y, Luo X-D (2010) Dolabellane Diterpenoids from *Aglaia odorata*. Phytochemistry **71**: 1020
52. Trost BM, Greenspan PD, Yang BV, Saulnier MG (1990) An Unusual Oxidative Cyclization. A Synthesis and Absolute Stereochemical Assignment of (−)-Rocaglamide. J Am Chem Soc **112**: 9022
53. Ishibashi F, Satasook C, Isman MB, Towers GHN (1993) Insecticidal 1*H*-Cyclopentatetrahydro[*b*]benzofurans from *Aglaia odorata*. Phytochemistry **32**: 307
54. Nugroho BW, Güssregen B , Wray V, Witte L, Bringmann G, Proksch P (1997) Insecticidal Rocaglamide Derivatives from *Aglaia elliptica* and *A. harmsiana*. Phytochemistry **45**: 1579
55. Nugroho BW, Edrada RA, Güssregen B, Wray V, Witte L, Proksch P (1997) Insecticidal Rocaglamide Derivatives from *Aglaia duperreana*. Phytochemistry **44**: 1455
56. Chaidir, Hiort J, Nugroho BW, Bohnenstengel FI, Wray V, Witte L, Hung PD, Kiet LC, Sumaryono W, Proksch P (1999) New Insecticidal Rocaglamide Derivatives from Flowers of *Aglaia duperreana* (Meliaceae). Phytochemistry **52**: 837
57. Molleyres L-P, Rindlisbacher A, Winkler T, Kumar V (1999) Insecticidal Natural Products: New Rocaglamide Derivatives from *Aglaia roxburghiana*. Pestic Sci **55**: 494
58. Hiort J, Chaidir, Bohnenstengel FI, Nugroho BW, Schneider C, Wray V, Witte L, Hung PD, Kiet LC, Proksch P (1999) New Insecticidal Rocaglamide Derivatives from the Roots of *Aglaia duperreana*. J Nat Prod **62**: 1632
59. Güssregen B, Fuhr M, Nugroho BW, Wray V, Witte L, Proksch P (1997) New Insecticidal Rocaglamide Derivatives from Flowers of *Aglaia odorata*. J Biosci (Z Naturforsch) **52c**: 339
60. Dumontet V, Thoison O, Omobuwajo OR, Martin M-T, Perromat G, Chiaroni A, Riche C, Païs M, Sévenet T, Hadi AHA (1996) New Nitrogenous and Aromatic Derivatives from *Aglaia argentea* and *A. forbesii*. Tetrahedron **52**: 6931
61. Fuzzati N, Dyatmiko W, Abdul Rahman, Achmad F, Hostettman K (1996) Triterpenoids, Lignans and a Benzofuran Derivative from the Bark of *Aglaia elaeagnoidea*. Phytochemistry **42**: 1395
62. Ko F-N, Wu T-S, Liou M-J, Huang T-F, Teng C-M (1992) PAF Antagonism In Vitro and In Vivo by Aglafoline from *Aglaia elliptifolia* Merr. Eur J Pharmacol **218**: 129
63. Wang S-K, Cheng Y-J, Duh C-Y (2001) Cytotoxic Constituents from Leaves of *Aglaia elliptifolia*. J Nat Prod **64**: 92
64. Chaidir, Lin WH, Ebel R, Edrada RA, Wray V, Nimtz M, Sumaryono W, Proksch P (2001) Rocaglamides, Glycosides, and Putrescine Bisamides from *Aglaia dasyclada*. J Nat Prod **64**: 1216
65. Mulholland DA, Naidoo N (1998) A Revision of the Structure of Ferrugin from *Aglaia ferruginaea*. Phytochemistry **47**: 1163
66. Dean FM, Monkhe TV, Mulholland DA, Taylor DAH (1993) An Isoflavanoid from *Aglaia ferruginaea*, an Australian Member of the Meliaceae. Phytochemistry **34**: 1537
67. Xu Y-J, Wu X-H, Tan BKH, Lai Y-H, Vittal JJ, Imiyabir Z, Madani L, Khozirah KS, Goh SH (2000) Flavonol–Cinnamate Cycloadducts and Diamide Derivatives from *Aglaia laxiflora*. J Nat Prod **63**: 473
68. Hwang BY, Su B-N, Chai H, Mi Q, Kardono LB, Afriastini JJ, Riswan S, Santarsiero BD, Mesecar AD, Wild R, Fairchild CR, Vite GD, Rose WC, Farnsworth NR, Cordell GA, Pezzuto JM, Swanson SM, Kinghorn AD (2004) Silvestrol and Episilvestrol, Potential Anticancer Rocaglate Derivatives from *Aglaia silvestris*. J Org Chem **69**: 3350
69. Hwang BY, Su B-N, Chai H, Mi Q, Kardono LB, Afriastini JJ, Riswan S, Santarsiero BD, Mesecar AD, Wild R, Fairchild CR, Vite GD, Rose WC, Farnsworth NR, Cordell GA, Pezzuto JM, Swanson SM, Kinghorn AD (2004) Silvestrol and Episilvestrol, Potential Anticancer Rocaglate Derivatives from *Aglaia silvestris*. J Org Chem **69**: 6156

70. Chumkaew P, Kato S, Chantrapromma K (2006) Potent Cytotoxic Rocaglamide Derivatives from the Fruits of *Amoora cucullata*. Chem Pharm Bull **54**: 1344
71. Kim S, Chin Y-W, Su B-N, Riswan S, Kardono LBS, Afriastini JJ, Chai H, Farnsworth NR, Cordell GA, Swanson SM, Kinghorn AD (2006) Cytotoxic Flavaglines and Bisamides from *Aglaia edulis*. J Nat Prod **69**: 1769
72. Kokpol U, Venaskulchai B, Simpson J, Weavers RT (1994) Isolation and X-ray Structure Determination of a Novel Pyrimidinone from *Aglaia odorata*. J Chem Soc Chem Commun (6):773
73. Ohse T, Ohba S, Yamamoto T, Koyano T, Umezawa K (1996) Cyclopentabenzofuran Lignan Protein Synthesis Inhibitors from *Aglaia odorata*. J Nat Prod **59**: 650
74. Wang S-K, Duh C-Y (2001) Cytotoxic Cyclopenta[*b*]benzofuran Derivatives from the Stem Bark of *Aglaia formosana*. Planta Med **67**: 555
75. Bringmann G, Mühlbacher J, Messer K, Dreyer M, Ebel R, Nugroho BW, Wray V, Proksch P (2003) Cyclorocaglamide, the First Bridged Cyclopentatetrahydro-benzofuran, and a Related "Open Chain" Rocaglamide Derivative from *Aglaia oligophylla*. J Nat Prod **66**: 80
76. Shiengthong D, Ungphakorn A, Lewis DE, Massy-Westropp RA (1979) New Nitrogenous Compounds – Odorine and Odorinol. Tetrahedron Lett **24**: 2247
77. Purushothaman KK, Sarada A, Connolly JD, Akinniyi JA (1979) The Structure of Roxburghilin, a Bis-amide of 2-Aminopyrrolidine from the Leaves of *Aglaia roxburghiana* (Meliaceae). J Chem Soc Perkin Trans I :3171
78. Saifah E, Jongbunprasert V, Kelley CJ (1988) Piriferine, a New Pyrrolidine Alkaloid from *Aglaia pirifera* leaves. J Nat Prod **51**: 80
79. Inada A, Sorano T, Murata H, Inatomi Y, Darnaedi D, Nakanishi T (2001) Diamide Derivatives and Cycloartanes from the Leaves of *Aglaia elliptica*. Chem Pharm Bull **49**: 1226
80. Salim AA, Pawlus AD, Chai H-B, Farnsworth NR, Kinghorn AD, Carcache-Blanco EJ (2007) Ponapensin, a Cyclopenta[*bc*]benzopyran with Potent NF-κB Inhibitory Activity from *Aglaia ponapensis*. Bioorg Med Chem Lett **17**: 109
81. Salim AA, Chai H-B, Rachman I, Riswan S, Kardono LBS, Farnsworth NR, Carcache-Blanco EJ, Kinghorn AD (2007) Constituents of the Leaves and Stem Bark of *Aglaia foveolata*. Tetrahedron **63**: 7926
82. Kim S, Su B-N, Riswan S, Kardono LBS, Afriastini JJ, Gallucci JC, Chai H, Farnsworth NR, Cordell GA, Swanson SM, Kinghorn AD (2005) Edulisones A and B, Two Epimeric Benzo-[*b*]oxepine Derivatives from the Bark of *Aglaia edulis*. Tetrahedron Lett **46**: 9021
83. Chiu SF (1985) Recent Research Findings on Meliaceae and Other Promising Botanical Insecticides in China. J Plant Diseases and Protection **92**: 310
84. Bohnenstengel FI, Steube KG, Meyer C, Nugroho BW, Hung PD, Kiet LC, Proksch P (1999) Structure Activity Relationships of Antiproliferative Rocaglamide Derivatives from *Aglaia* species (Meliaceae). J Biosci (Z Naturforsch) **54c**: 55
85. Bohnenstengel FI, Steube KG, Meyer C, Quentmeier H, Nugroho BW, Proksch P (1999) 1 *H*-Cyclopenta[*b*]benzofuran Lignans from *Aglaia* species Inhibit Cell Proliferation and Alter Cell Cycle Distribution in Human Monocytic Leukemia Cell Lines. J Biosci (Z Naturforsch) **54c**: 1075
86. Ewete F, Nicol RW, Hengsawad V, Sukumalanand P, Satasook C, Wiriyachitra P, Isman MB, Kahn Y, Duval F, Philogène BJR, Arnason JT (1996) Insecticidal Activity of *Aglaia odorata* Extract and the Active Principle, Rocaglamide, to the European Corn Borer *Ostrinia nubilalis* Hübn. (Lep., Pyralidae). J Appl Ent **120**: 483
87. Koul O, Kaur H, Goomber S, Wahab S (2004) Bioefficacy and Mode of Action of Rocaglamide from *Aglaia elaeagnoidea* (syn. *A. roxburghiana*) against Gram Pod Borer, *Helicoverpa armigera* (Hübner). J Appl Ent **128**: 177
88. O'Shea JJ, Ma A, Lipsky P (2002) Cytokines and Autoimmunity. Nat Rev Immunol **2**: 37
89. Li-Weber M, Krammer PH (2003) Regulation of IL4 Gene Expression by T Cells and Therapeutic Perspectives. Nat Rev Immunol **3**: 534

90. Yamamoto Y, Gaynor RB (2001) Therapeutic Potential of Inhibition of the NF-kappaB Pathway in the Treatment of Inflammation and Cancer. J Clin Invest **107**:135
91. Macian F (2005) NFAT Proteins: Key Regulators of T-Cell Development and Function. Nat Rev Immunol **5**: 472
92. Li Q, Verma IM (2002) NF-kappaB Regulation in the Immune System. Nat Rev Immunol **2**: 725
93. Lee SK, Cui B, Mehta RR, Kinghorn AD, Pezzuto JM (1998) Cytostatic Mechanism and Antitumor Potential of Novel 1*H*-Cyclopenta[*b*]benzofuran Lignans Isolated From *Aglaia elliptica*. Chem Biol Interact **115**: 215
94. Cencic R, Carrier M, Galicia-Vázquez G, Bordeleau ME, Sukarieh R, Bourdeau A, Brem B, Teodoro JG, Greger H, Tremblay ML, Porco JA Jr, Pelletier J (2009) Antitumor Activity and Mechanism of Action of the Cyclopenta[*b*]benzofuran, Silvestrol. PLoS One **4**: e5223
95. Hausott B, Greger H, Marian B (2004) Flavaglines: a Group of Efficient Growth Inhibitors Block Cell Cycle Progression and Induce Apoptosis in Colorectal Cancer Cells. Int J Cancer **109**: 933
96. Mi Q, Kim S, Hwang BY, Su BN, Chai H, Arbieva ZH, Kinghorn AD, Swanson SM (2006) Silvestrol Regulates G2/M Checkpoint Genes Independent of p53 Activity. Anticancer Res **26**: 3349
97. Silvera D, Formenti SC, Schneider RJ (2010) Translational Control in Cancer. Nat Rev Cancer **10**: 254
98. Bordeleau ME, Robert F, Gerard B, Lindqvist L, Chen SM, Wendel HG, Brem B, Greger H, Lowe SW, Porco JA Jr, Pelletier J (2008) Therapeutic Suppression of Translation Initiation Modulates Chemosensitivity in a Mouse Lymphoma Model. J Clin Invest **8**: 2651
99. Bleumink M, Köhler R, Giaisi M, Proksch P, Krammer PH, Li-Weber M (2011) Rocaglamide Breaks TRAIL Resistance in HTLV-1-associated Adult T-cell Leukemia/Lymphoma by Translational Suppression of c-FLIP Expression. Cell Death Differ **18**: 362
100. Zhu JY, Lavrik IN, Mahlknecht U, Giaisi M, Proksch P, Krammer PH, Li-Weber M (2007) The Traditional Chinese Herbal Compound Rocaglamide Preferentially Induces Apoptosis in Leukemia Cells by Modulation of Mitogen-Activated Protein Kinase Activities. Int J Cancer **121**: 1839
101. Krammer PH, Arnold R, Lavrik IN (2007) Life and Death in Peripheral T Cells. Nat Rev Immunol **7**: 532
102. Galluzzi L, Larochette N, Zamzami N and Kroemer G (2006) Mitochondria as Therapeutic Targets for Cancer Chemotherapy Oncogene **25:** 4812
103. Kim S, Hwang BY, Su BN, Chai H, Mi Q, Kinghorn AD, Wild R, Swanson SM (2007) Silvestrol, a Potential Anticancer Rocaglate Derivative from *Aglaia foveolata*, Induces Apoptosis in LNCaP Cells Through the Mitochondrial/Apoptosome Pathway Without Activation of Executioner Caspase-3 or −7. Anticancer Res **27**: 2175
104. Zhuang S, Demirs JT, Kochevar IE (2000) p38 Mitogen-Activated Protein Kinase Mediates bid Cleavage, Mitochondrial Dysfunction, and Caspase-3 Activation During Apoptosis Induced by Singlet Oxygen but not by Hydrogen Peroxide. J Biol Chem **275**: 25939
105. Yoshino T, Kishi H, Nagata T, Tsukada K, Saito S, Muraguchi A (2001) Differential Involvement of p38 MAP Kinase Pathway and Bax Translocation in the Mitochondria-Mediated Cell Death in TCR- and Dexamethasone-Stimulated Thymocytes. Eur J Immunol **31**: 2702
106. Kim BJ, Ryu SW, Song BJ (2006) JNK- and p38 Kinase-Mediated Phosphorylation of Bax Leads to Its Activation and Mitochondrial Translocation and to Apoptosis of Human Hepatoma HepG2 Cells. J Biol Chem **281**: 21256
107. Cai B, Chang SH, Becker EB, Bonni A, Xia Z (2006) p38 MAP Kinase Mediates Apoptosis Through Phosphorylation of BimEL at Ser-65. J Biol Chem **281**: 25215
108. De Chiara G, Marcocci ME, Torcia M, Lucibello M, Rosini P, Bonini P, Higashimoto Y, Damonte G, Armirotti A, Amodei S, Palamara AT, Russo T, Garaci E, Cozzolino F

(2006) Bcl-2 Phosphorylation by p38 MAPK: Identification of Target Sites and Biologic Consequences. J Biol Chem **281**: 21353
109. Grethe S, Coltella N, Di Renzo MF, Porn-Ares MI (2006) p38 MAPK Downregulates Phosphorylation of Bad in Doxorubicin-Induced Endothelial Apoptosis. Biochem Biophys Res Commun **347**: 781
110. Balmanno K, Cook SJ (2009) Tumour Cell Survival Signalling by the ERK1/2 Pathway. Cell Death Differ **16**: 368
111. Yeh JH, Hsu SC, Han SH, Lai MZ (1998) Mitogen-Activated Protein Kinase Kinase Antagonized fas-Associated Death Domain Protein-Mediated Apoptosis by Induced FLICE-Inhibitory Protein Expression. J Exp Med **188**: 1795
112. Wang W, Prince CZ, Mou Y, Pollman MJ (2002) Notch3 Signaling in Vascular Smooth Muscle Cells Induces c-FLIP Expression via ERK/MAPK Activation. Resistance to Fas ligand-Induced Apoptosis. J Biol Chem **277**: 21723
113. Panka DJ, Mano T, Suhara T, Walsh K, Mier JW (2001) Phosphatidylinositol 3-Kinase/Akt Activity Regulates c-FLIP Expression in Tumor Cells. J Biol Chem **276**: 6893
114. Poukkula M, Kaunisto A, Hietakangas V, Denessiouk K, Katajamäki T, Johnson MS, Sistonen L, Eriksson JE (2005) Rapid Turnover of c-FLIPshort is Determined by its Unique C-Terminal Tail. J Biol Chem **280**: 27345
115. Li-Weber M, Krammer PH (2003) Function and Regulation of the CD95 (APO-1/Fas) Ligand in the Immune System. Semin Immunol **15**: 145
116. Kreuz S, Siegmund D, Scheurich P and Wajant H (2001) NF-kappaB Inducers Upregulate cFLIP, a Cycloheximide-Sensitive Inhibitor of Death Receptor Signaling. Mol Cell Biol **21**: 3964
117. Ueffing N, Schuster M, Keil E, Schulze-Osthoff K and Schmitz I (2008) Up-regulation of c-FLIP short by NFAT Contributes to Apoptosis Resistance of Short-Term Activated T Cells. Blood **112**: 690
118. Katamna C (1970) Synthesis of 2-Arylbenzofuran-3-ones. Bull Soc Chim Fr **6**: 2309
119. Davey AE, Taylor RJK (1987) A Novel 1,3-Dithiane-based Cyclopenta-annulation Procedure: Synthesis of the Rocaglamide Skeleton. J Chem Soc, Chem Commun **1**: 25
120. Kraus GA, Sy JO (1989) A Synthetic Approach to Rocaglamide via Reductive Cyclization of δ-Keto Nitriles. J Org Chem **54**: 77
121. Davey AE, Schaeffer MJ, Taylor RJK (1991) Synthesis of the Novel Antileukemic Tetrahydrocyclopenta[*b*]benzofuran, Rocaglamide. J Chem Soc, Chem Commun **16**: 1137
122. Davey AE, Schaeffer MJ, Taylor RJK (1992) Synthesis of the Novel Anti-leukemic Tetrahydrocyclopenta[*b*]benzofuran, Rocaglamide and Related Synthetic Studies. J Chem Soc, Perkin Trans 1 **20**: 2657
123. Watanabe T, Takeuchi T, Kohzuma S, Umezawa K, Otsuka M (1998) Total Synthesis of (±)-Aglaiastatin, a Novel Bioactive Alkaloid. Chem Commun **10**: 1097
124. Dobler MR, Bruce I, Cederbaum F, Cooke NG, Diorazio LJ, Hall RG, Irving E (2001) Total Synthesis of (±)-Rocaglamide and Some Aryl Analogues. Tetrahedron Lett **42**: 8281
125. Gerard B, Jones G, Porco JA (2004) A Biomimetic Approach to the Rocaglamides Employing Photogeneration of Oxidopyryliums Derived from 3-Hdroxyflavones. J Am Chem Soc **126**: 13620
126. Gerard B, Sangji S, O'Leary DJ, Porco JA (2006) Enantioselective Photocycloaddition Mediated by Chiral Brnsted Acids: Asymmetric Synthesis of the Rocaglamides. J Am Chem Soc **128**: 7754
127. McDougal NT, Schaus SE (2003) Asymmetric Morita-Baylis-Hillman Reactions Catalyzed by Chiral Brnsted Acids. J Am Chem Soc **125**: 12094
128. Schoop A, Helmut G, Axel G (2000) A New Analogue of Rocaglamide by an Oxidative Dihydrofuran Synthesis. Tetrahedron Lett **41**: 1913
129. Thede K, Diedrichs N, Ragot JP (2004) Stereoselective Synthesis of (±)-Rocaglaol Analogues. Org Lett **6**: 4595

130. Diedrichs N, Ragot JP, Thede K (2005) A Highly Efficient Synthesis of Rocaglaols by a Novel α-Arylation of Ketones. Eur J Org Chem **9**: 1731
131. Magnus P, Stent MAH (2005) Stereospecific Synthesis of (±)-1,2-Anhydro Methyl Rocaglate. Org Lett **7**: 3853
132. Li H, Fu B, Wang MA, Li N, Liu WJ, Xie ZQ, Ma YQ, Qin Z (2008) Total Synthesis and Biological Activity of (±)-Rocaglamide and its 2,3-Di-*epi* Analogue. Eur J Org Chem **10**: 1753
133. Malona JA, Cariou K, Frontier JA (2009) Nazarov Cyclization Initiated by Peracid Oxidation: the Total Synthesis of (±)-Rocaglamide. J Am Chem Soc **131**: 7560
134. Gerard B, Cencic R, Pelletier J, Porco JA (2007) Enantioselective Synthesis of the Complex Rocaglate (−)-Silvestrol. Angew Chem Int Ed **46**: 7831
135. El Sous M, Rizzacasa MA (2005) Biomimetic Synthesis of the Novel 1,4-Dioxanyloxy Fragment of Silvestrol and Episilvestrol. Tetrahedron Lett **46**: 293
136. El Sous M, Khoo M, Holloway G, Owen DJ, Scammells PJ, Rizzacasa MA (2007) Total Synthesis of (−)-Episilvestrol and (−)-Silvestrol. Angew Chem Int Ed **46**: 7835
137. Adams TE, El Sous M, Hawkins BC, Hirner S, Holloway G, Khoo ML, Owen DJ, Savage GP, Scammells PJ, Rizzacasa MA (2009) Total Synthesis of the Potent Anticancer *Aglaia* Metabolites (−)-Silvestrol and (−)-Episilvestrol and the Active Analogue (−)-4′-Desmethoxyepisilvestrol. J Am Chem Soc **131**: 1607
138. Thuaud F, Bernard Y, Turkeri G, Dirr R, Aubert G, Cresteil T, Baguet A, Tomasetto C, Svitkin Y, Sonenberg N, Nebigil CG, Désaubry L (2009) Synthetic Analogue of Rocaglaol Displays a Potent and Selective Cytotoxicity in Cancer Cells: Involvement of Apoptosis Inducing Factor and Caspase-12. J Med Chem **52**: 5176
139. Roche SP, Cencic R, Pelletier J, Porco JA (2010) Biomimetic Photocycloaddition of 3-Hydroxyflavones: Synthesis and Evaluation of Rocaglate Derivatives as Inhibitors of Eukaryotic Translation. Angew Chem Int Ed **49**: 6533
140. Thuaud F, Ribeiro N, Gaiddon C, Cresteil T, Désaubry L (2011) Novel Flavaglines Displaying Improved Cytotoxicity. J Med Chem **54**: 411

Chemistry of the Immunomodulatory Macrolide Ascomycin and Related Analogues

Murty A.R.C. Bulusu, Karl Baumann, and *Anton Stuetz*

Contents

1. Introduction 59
   1.1. Ascomycin and Related Natural Products 60
   1.2. Ascomycin Derivatives, a Novel Class of Anti-inflammatory Compounds 62
   1.3. Structural Features of Ascomycin 66
2. Synthesis Aspects 70
   2.1. Synthesis of the Four Diastereomeric "Furano-Ascomycins" 70
   2.2. Synthesis of ^{13}C Labeled Ascomycin 72
   2.3. Reactivity of the Binding Domain 75
   2.4. Modifications in the Effector and Cyclohexyl Domains 94
3. Summary 116
References 118

1. Introduction

This chapter, after giving a short overview of the natural product ascomycin and related analogues, provides a summary of the biological properties and the clinical use of the ascomycin derivative pimecrolimus, a calcineurin inhibitor, developed and registered for topical treatment of the inflammatory skin disease atopic dermatitis. This is followed by an in-depth description of the structural features of ascomycin and synthesis aspects including specific modifications in the binding region, cleavage reactions, semisynthetic approaches, and modifications in the effector and cyclohexyl regions. The literature covers journal articles up to July 2010 with emphasis on chemistry. Structure-activity relationships are mentioned only qualitatively. No attempt has been made to review the patent literature in depth.

M.A.R.C. Bulusu and K. Baumann are former employees of Novartis Institutes for BioMedical Research Vienna.

M.A.R.C. Bulusu • K. Baumann • A. Stuetz (✉)
Novartis Institutes for BioMedical Research Vienna, Muthgasse 11/2, A-1190, Vienna, Austria
e-mail: anton.stuetz@novartis.com

A.D. Kinghorn, H. Falk, J. Kobayashi (eds.), *Progress in the Chemistry of Organic Natural Products, Vol. 94*, DOI 10.1007/978-3-7091-0748-5_2,

1.1. Ascomycin and Related Natural Products

The successful application of cyclosporin A (CyA, Sandimmune®) in the prevention of transplantation rejection stimulated a worldwide search for new selective T-cell inhibitors resulting in the discovery of the macrolactam tacrolimus (**1**, FK506, Prograf®, Scheme 1) (*1–3*). Ascomycin (**2**), a compound initially referred to as FR-900520 and isolated earlier from *Streptomyces hygroscopicus* var. *ascomyceticus*, (Fig. 1) due to its antifungal activities, and for which the structure was not elucidated originally, was later shown to be a close structural analogue of tacrolimus (ethyl instead of allyl on C-21) (*4–7*). Analogues bearing other substituents, such as methyl (*5*), or propyl (*8*), on C-21, or, homologues in which several methyl groups on the macrocycle are replaced by a higher alkyl (*i.e.* ethyl) have been isolated as well (*9, 10*).

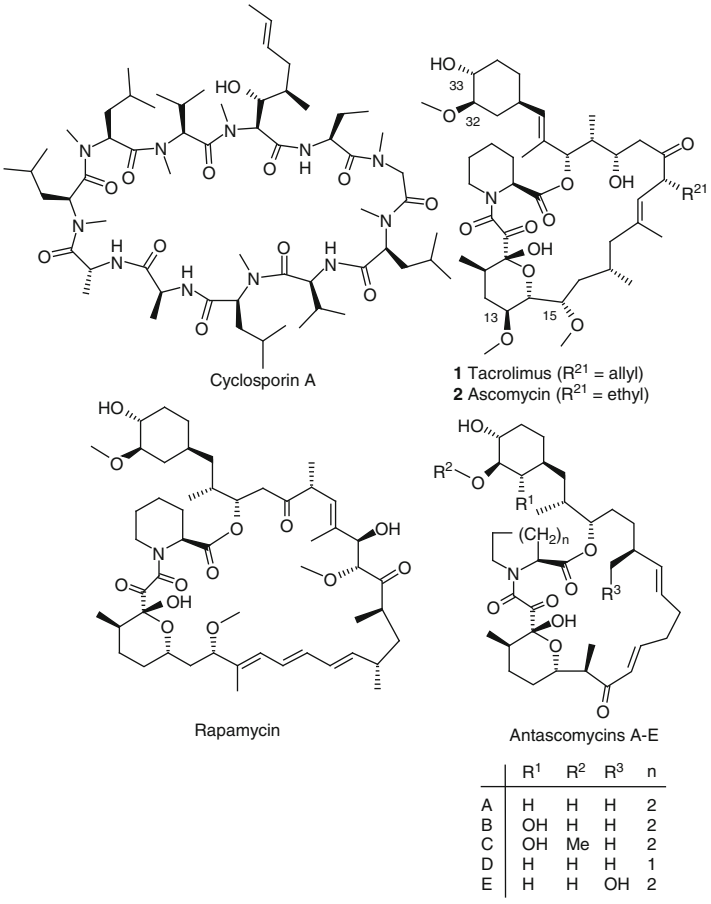

	R1	R2	R3	n
A	H	H	H	2
B	OH	H	H	2
C	OH	Me	H	2
D	H	H	H	1
E	H	H	OH	2

Scheme 1. Structures of cyclosporin A, tacrolimus (**1**), ascomycin (**2**), and related macrolactams

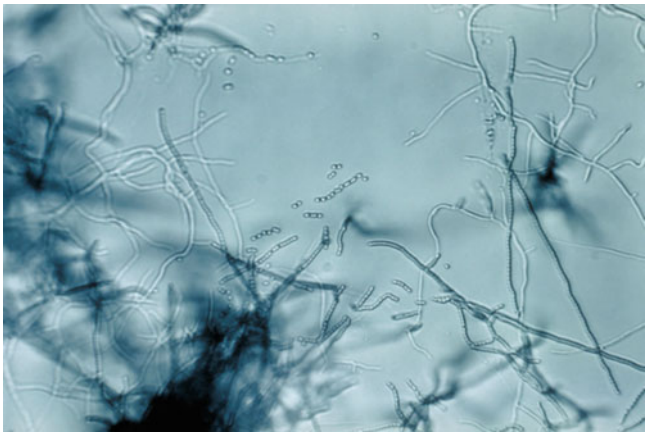

Fig. 1. Photograph of *Streptomyces* sp. grown in tap water agar. Branching filaments, abundant aerial mycelia, and long chains of small spores are visible, all of which are characteristic of the organism. Taken from en.wikipedia.org

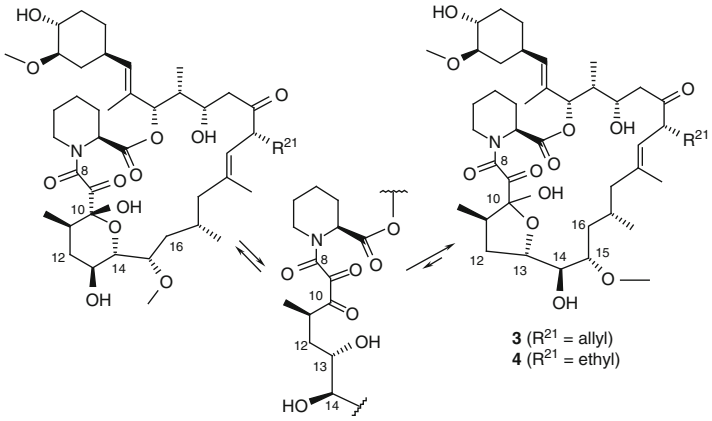

Scheme 2. Equilibria of 13-*O*-desmethyl derivatives **3** and **4** of tacrolimus (**1**) and ascomycin (**2**)

Macrolactams featuring a proline unit instead of the pipecolic acid moiety have been found as by-products in the fermentation broth of tacrolimus producer strains (*11*). Numerous 32-, 13-, and/or 15-*O*-desmethyl derivatives of ascomycin (**2**) and tacrolimus (**1**) are readily available through biotransformation (*11*–*15*). Interestingly, the 13-*O*-desmethyl-derivatives **3** and **4** exist in solution as highly complex mixtures of isomers (Scheme 2). Thus, seven different isomers of 13-*O*-desmethyl-FK506 (**3**) could be differentiated in COSY, HMBC, and HMQC experiments. The formation of these isomers could be explained by an epimerization at C-10, formation of hemiketal rings between C-10 and C-13, or, C-9 and C-13, and the occurrence of (*Z*)/(*E*)-isomers at the amide bond (*16*).

Other analogues of ascomycin that contain hydrogen, methyl, or ethyl instead of a methoxy at one or both of C-13 and C-15 have been prepared through fermentation employing a genetically modified ascomycin gene cluster (*17*). Related natural products containing an α,β-diketo-pipecolate subunit are rapamycin (Sirolimus) and the antascomycins (Scheme 1). Rapamycin, another macrolactam, had also been discovered like CyA and ascomycin in an antifungal screening of fermentation broths (*18, 19*). Although it was discovered quite early that rapamycin inhibits immune responses in rats (*20*), its therapeutic potential, however, was initially not fully recognized. It was the discovery of tacrolimus (**1**) that led to a renewed interest in rapamycin as an immunosuppressant (*21, 22*). The antascomycins A, B, C, D, and E have been isolated from a strain of *Micromonospora* (*23*). They bind strongly to macrophilin (FK506 binding protein, FKBP12) and antagonize the effects of **1** and **2** on T-cells. Their biological properties have not yet been fully explored.

1.2. Ascomycin Derivatives, a Novel Class of Anti-inflammatory Compounds

The discovery of this novel class of anti-inflammatory compounds started with reports of the high efficacy of oral cyclosporin A in the treatment of psoriasis, atopic dermatitis, and other inflammatory skin diseases. However, efforts failed to render this calcineurin inhibitor effective topically, in order to minimize its systemic immunosuppressive side effects. Using a newly developed model of allergic contact dermatitis (ACD) in pigs, calcineurin inhibitors of the tacrolimus- and ascomycin-type were shown to be highly effective after topical application. These findings provided the first pharmacological evidence of the potential of this novel class of topical agents for the treatment of inflammatory skin diseases (*24*). Topical application of the first representative of this class, SDZ 281–240 (Scheme 3), in

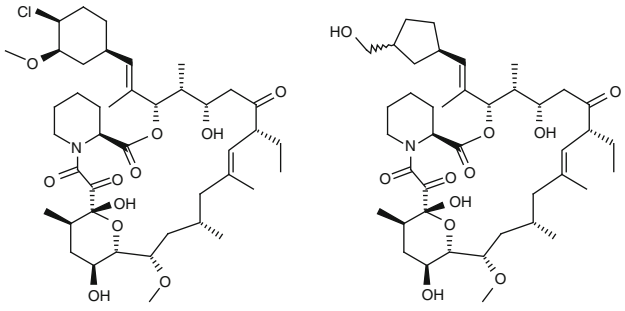

Scheme 3. Structures of the 33-*epi*-chloro-derivative of ascomycin (**2**) pimecrolimus (**2a**), and SDZ 281–240

chronic plaque psoriasis under *Finn*-chamber occlusion confirmed the validity of this concept in man (*25*). Intensive studies on structure-activity relationships and comparative pharmacological evaluations among a large number of newly synthesized derivatives to identify a compound combining high anti-inflammatory activity with minimal side effects finally resulted in the discovery and development of pimecrolimus (**2a**, SDZ ASM 981, Scheme 3) (*26, 27*). A detailed review of the discovery and development of the then new class of topical calcineurin inhibitors has been published (*28*).

1.2.1. Pimecrolimus

1.2.1.1. Pharmacology *In Vitro* and *In Vivo*

Pimecrolimus (**2a**) binds with high affinity to the cytosolic receptor macrophilin-12 and inhibits the phosphatase calcineurin, an enzyme required for the dephosphorylation of the cytosolic form of the nuclear factor of activated T-cells (NF-AT). As a consequence, it prevents in T-cells the transcription and release of both T-helper type 1 cell (TH1) and T-helper type 2 cell (TH2) inflammatory cytokines such as interleukin-2 (IL-2), interferon-γ (IFN-γ), interleukin-4 (IL-4), interleukin-5 (IL-5), interleukin-10 (IL-10), tumor necrosis factor alpha (TNF-α), and granulocyte macrophage colony-stimulating factor (GM-CSF) as well as T-cell proliferation (*29*). A graphical representation of the biological mechanism of action is shown in Fig. 2. The inhibitory effect has been shown using the Jurkat human T-cell

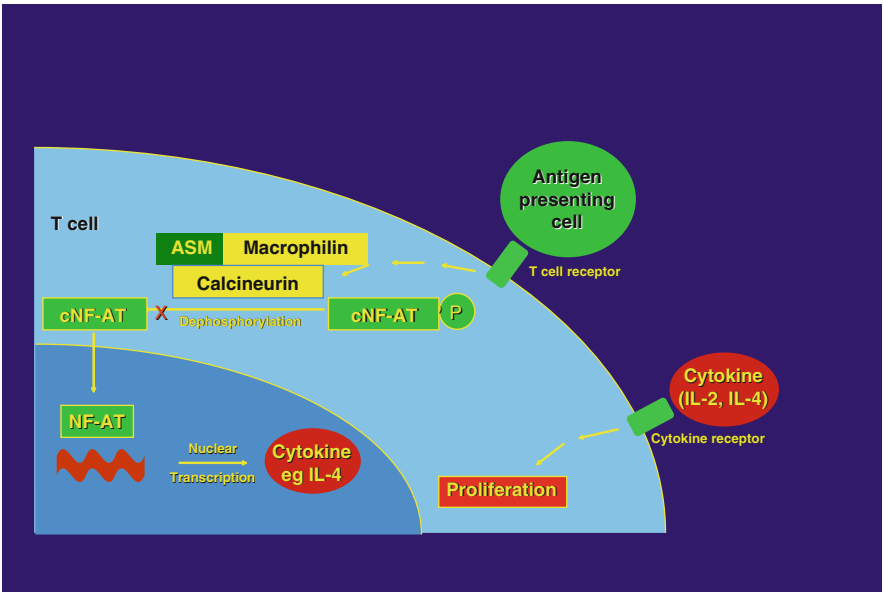

Fig. 2. Mechanism of action of pimecrolimus (ASM) on T-cells

line, peripheral blood mononuclear cells from healthy subjects, as well as human T-helper cell clones isolated from the skin of an atopic dermatitis patient. In these T-cell clones, pimecrolimus (**2a**) inhibits cytokine production at (sub)nanomolar concentrations and as potently as tacrolimus. Furthermore, pimecrolimus shows selectivity for antigen-primed memory T-cells, an effect not seen with tacrolimus (*30*). Pimecrolimus (**2a**) also prevents the production of TNF-α and the release of pro-inflammatory mediators like histamine, hexosaminidase, and tryptase in activated primary human skin mast cells and rodent mast cell lines (*31*). Pimecrolimus does not affect the proliferation of keratinocyte, endothelial, and fibroblast cell lines and has, in contrast to corticosteroids, no effect on the differentiation, maturation, functions, and viability of human dendritic cells (*32*). A recent study revealed that pimecrolimus (**2a**) increases at low nanomolar concentrations innate immune functions of human keratinocytes, such as expression of Toll-like receptors 2 and 6, as well as the production of antimicrobial peptides (cathelicidin, human beta defensin-2 and 3). Pimecrolimus (**2a**) also enhances the functional capacity of keratinocytes to inhibit the growth of *Staphylococcus aureus*. These data suggest that **2a** can amplify the cutaneous innate host defense (*33*).

Topical pimecrolimus penetrates similarly into, but permeates less through the skin *in vitro*, when compared to corticosteroids or tacrolimus. In comparison with bethamethasone, clobetasol, and difluorcortolone used as 1% solutions, pimecrolimus (**2a**) permeates less through the human skin by factors of 60–110. When comparing pimecrolimus (**2a**) and tacrolimus (**1**) in the same vehicle at the same concentration, the same skin concentrations were found with both compounds, but permeation rates of pimecrolimus through human and pig skin were lower by a factor of 9–10 (*34*). When comparing pimecrolimus cream 1% (Elidel®) and tacrolimus ointment 0.1% and 0.03% (Protopic®), similar skin concentrations were determined with pimecrolimus and tacrolimus. However, the permeation rates through the skin were found to be lower with pimecrolimus (**2a**) than those of tacrolimus (**1**), with both ointment preparations by factors of about 6 and 4, despite higher drug concentrations in Elidel® cream. In agreement with the results obtained with human skin, the permeation rate of pimecrolimus (**2a**) through normal and inflamed pig skin was found to be lower than that of tacrolimus (**1**) as well (*35*). These data indicate a lower systemic exposure to pimecrolimus after topical application as compared to tacrolimus and corticosteroids.

Pimecrolimus (**2a**) exhibits a high level of anti-inflammatory activity in animal models of skin inflammation after both topical and systemic applications (*36*). In the pig model of ACD, topical pimecrolimus is as effective as potent corticosteroids and tacrolimus ointment 0.1% (Protopic®). Unlike clobetasol, topical pimecrolimus does not cause skin atrophy nor affects blanching or skin texture in pigs. As shown in mice, topical pimecrolimus does not affect epidermal *Langerhans'* cells, antigen-presenting cells that play a critical role in the local immunosurveillance (*37, 38*). While the treatment with standard topical corticosteroids, including hydrocortisone, resulted in a reduction in MHC class II-positive *Langerhans'* cells by 96–100% in the treated skin, no effect on *Langerhans'* cells was noted. In contrast, corticosteroids greatly impair the integrity, function, and induce apoptosis of *Langerhans´*

cells (LC) in mice. A recent analysis of skin biopsies of atopic dermatitis patients has confirmed that treatment for 3 weeks with the corticosteroid ß-methasone 0.1%, but not Elidel® cream 1%, resulted in depletion of *Langerhans*' cells, while both drugs significantly reduced T-cells (*39*). These results indicate that topically applied pimecrolimus is unlikely to interfere with the function of *Langerhans*'/dendritic cells to differentiate naïve T-cells into effector T-cells, which is key for the developing immune system and maintenance of specific immunocompetence.

Pimecrolimus (**2a**) proved to be highly anti-inflammatory effective also after systemic administration to rodents. Oral and subcutaneous treatment of mice reveals pimecrolimus to be as potent as tacrolimus and more potent than cyclosporin A in inhibiting the elicitation phase, which is the clinically apparent inflammatory phase of ACD (*40*). In contrast to cyclosporin A and tacrolimus (**1**), oral treatment of mice with **2a** neither impairs the induction phase of ACD (sensitization) nor decreases weight and cellularity of draining lymph nodes, indicating that the primary immune response in ACD is not impaired by pimecrolimus (**2a**). In rat ACD, oral pimecrolimus is more potent than cyclosporin A by a factor of 4 and more potent than tacrolimus by a factor of 2 in inhibiting the elicitation phase of ACD. In contrast to tacrolimus, pimecrolimus has no effect on ongoing immune responses in the lymph nodes draining the application site of the hapten (*41*).

In comparison to cyclosporin A and tacrolimus, pimecrolimus (**2a**) has a lower potential to affect systemic immune responses. In rats, subcutaneous injections of cyclosporin A and tacrolimus suppress the localized graft-versus-host reaction 8-fold and 66-fold more potently than pimecrolimus. In the same species, the potency of tacrolimus to inhibit antibody formation against sheep red blood cells is 48-fold higher than that of pimecrolimus. Oral cyclosporin A and tacrolimus are immunosuppressive at lower doses than pimecrolimus in the rat kidney transplantation model by factors of 3 and 15, which correlates with exposure to lymph nodes (*42*).

Pimecrolimus (**2a**) may have therapeutic potential in inflammatory conditions beyond dermatological disorders as well. Results from ophthalmic studies in dogs with chronic keratokonjunctivitis sicca treated locally with experimental pimecrolimus eye drops indicate that pimecrolimus has therapeutic potential in inflammatory eye diseases in man (*43*). Studies in standard rat models of arthritis show that oral pimecrolimus (**2a**) exerts dose-dependent anti-inflammatory and disease-modifying efficacy indicating therapeutic potential for the treatment of human rheumatoid arthritis (*44*). Studies in a SCID model of inflammatory bowel disease indicate that oral pimecrolimus has therapeutic potential, superior to those of cyclosporin A and tacrolimus (*45*).

Taken together, the data suggest that pimecrolimus (**2a**) has favorable pharmacological profiles *in vitro* and *in vivo*:

- When applied topically, it has a high and selective anti-inflammatory activity in the skin, minimal percutaneous resorption, and a low potential to affect local and systemic immunosurveillance. It differs from corticosteroids by its selective action on T cells and mast cells, by a lack of effects on *Langerhans*' cells/dendritic cells, by the lack of induction of skin atrophy, and by much less permeation through the skin. It differs from tacrolimus by less permeation

through skin and by a lower potential to affect systemic immune responses, thus specifically targeting skin inflammation.
- When applied systemically, it exerts a high anti-inflammatory activity, but has a lower potential for immunosuppression and/or is better tolerated than tacrolimus or cyclosporin A (*28*).

1.2.1.2. Clinical Profile

Therapeutic efficacy and safety of topical pimecrolimus (**2a**) has been established in short-term and long-term management of atopic dermatitis in extensive double-blind, randomized, vehicle-controlled studies with patients including adults, children, and infants. In short-term studies with children, considerable efficacy was already evident at the first evaluation on day 8; significant relief from pruritus was observed also within the first week of treatment. In infants, results were similar to those obtained in the studies with children. Long-term studies were performed in children and infants (1-year treatment) and in adults (6 months). In summary, clinical trials have shown Elidel® to be highly effective in relieving the signs and symptoms of atopic dermatitis in adults, children, and infants. Clinically significant improvement was seen within 3 days of the first application. In long-term studies, Elidel® has demonstrated a unique ability to prevent disease progression if applied at the first signs or symptoms of disease.

In addition to its therapeutic efficacy, pimecrolimus (**2a**) has proven to be safe and well tolerated, as derived from animal and human studies. Topical application led to consistently low systemic exposure, irrespective of age, disease severity, or body surface treatment. Pimecrolimus cream 1% (Elidel®) was approved in the USA at the end of 2001 and in European and other countries in the autumn of 2002. Experience with more than 10 million patients treated so far in clinical practice has confirmed the high efficacy and safety elaborated in the controlled studies. Detailed reviews on clinical studies with pimecrolimus 1% cream (Elidel®) in patients with atopic dermatitis and other inflammatory skin diseases have been published (*46–51*).

In addition to topical application, pimecrolimus (**2a**) was shown to be highly effective and safe after oral treatment. In psoriasis patients, pimecrolimus down-regulated the expression of genes associated with leukocyte activation/proliferation, lymphocyte chemotaxis, and trafficking as well as inflammation. No changes in gene expression were observed that might be linked with drug-related side effects (*52*). Multicenter studies with 3-month treatments of psoriasis and atopic dermatitis patients have proven the efficacy and safety of this compound, thus confirming preclinical studies.

1.3. Structural Features of Ascomycin

As confirmed by X-ray crystal structure analysis and NMR-studies the left hand parts of ascomycin (**2**) and tacrolimus (**1**) mediate binding to their common

immunophilin macrophilin (FK506-binding protein, FKBP-12) and have therefore been termed "binding domains" (Scheme 4). The right hand parts of the macrolactams, together with elements of the immunophilin, interact with the protein-phosphatase calcineurin, which plays a key role in the Ca^{2+} dependent activation of lymphocytes, and are called "effector domains" (*53*–*58*). The X-ray crystal structure of pimecrolimus (**2a**) is shown in Fig. 3. A model of the complex of pimecrolimus and macrophilin derived from the binding complex of L-685,818 and macrophlin is presented in Fig. 4 and also as cover picture of this volume.

Ascomycin (**2**), tacrolimus (**1**), and related analogues represent highly functionalized 23-membered macrocycles, containing a pipecolate residue in an amide (C-8) and an allylic ester linkage (C-26−C-29) with a polyketide backbone. Both macrocycles feature fourteen chiral centers, an endocyclic trisubstituted double bond (C-19−C-20) with (*E*)-geometry and located in an allylic position to a ketone functionality (C-22), three methoxy groups (at C-13, C-15, and C-32), and three secondary hydroxy groups at C-33, C-14, and C-24, with one of these part of a β-hydroxy ketone unit (C-22−C-24). Most notably, within the binding domain the macrolactams feature a unique pattern of three adjacent carbonyl groups (C-8−C-10, tricarbonyl portion, α,β-diketo-amide moiety), of which one carbonyl group (C-10) is masked as a hemiketal with the secondary C-14−OH, resulting in a tetrahydropyran unit (C-10−C-14). Biosynthetically, the C-9 carbonyl is introduced at a late stage *via* C-9−hydroxylation of the corresponding 9-deoxo precursor followed by its oxidation (*59*). In $CDCl_3$-solution, ascomycin (**2**) and tacrolimus (**1**) exist as mixtures of amide bond rotamers ((*E*):(*Z*)=approx. 2:1) (*60*). In the crystalline state, tacrolimus and **2** adopt an (*E*)-amide configuration, whereas the (*Z*)-diastereomer is observed in the tacrolimus/macrophilin complex (*54*, *61*). Interestingly, due to electronic repulsion, the planes of the conjugated carbonyls (C-8/C-9) are almost orthogonally oriented. The cyclohexyl side chain and the pyran unit adopt chair conformations, whereas all substituents except the C-10−OH are oriented equatorially.

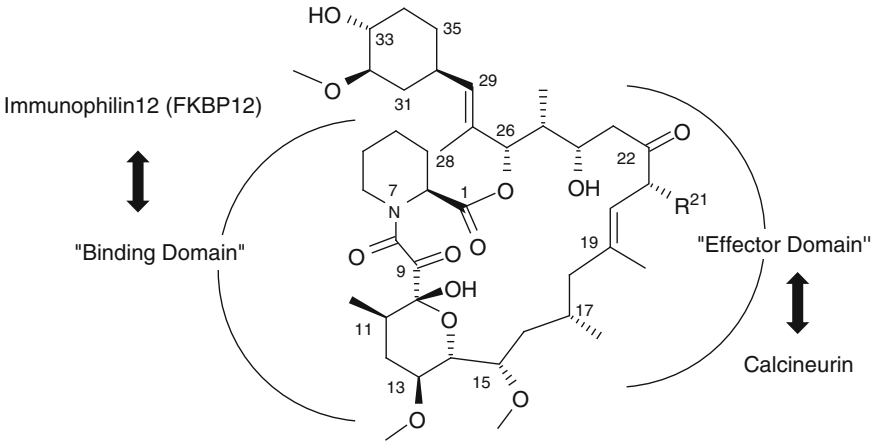

Scheme 4. Dual domain model of tacrolimus (**1**) and ascomycin (**2**)

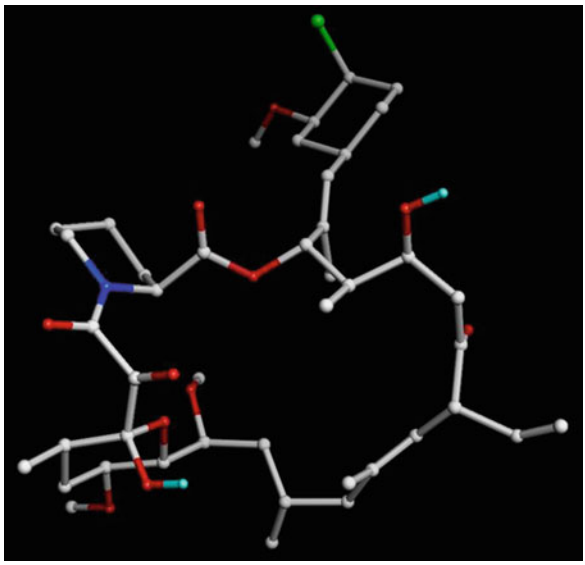

Fig. 3. View of the X-ray crystal structure of pimecrolimus (Weber HP, Sandoz, unpublished results): The ring of pimecrolimus adopts a *cis*-amide conformation and the structure is identical to the X-ray structure of ascomycin (*113*)

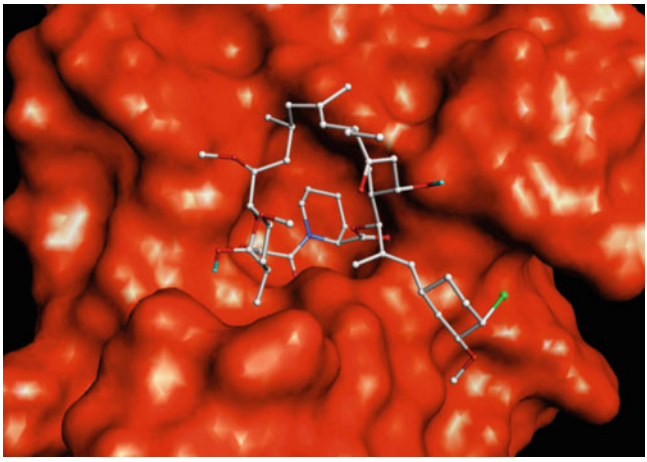

Fig. 4. Model of the complex of pimecrolimus (**2a**) and macrophilin – derived based on the X-ray structure of the native macrophilin (Burkhard P, Taylor P, Walkinshaw MD (2000) J Mol Biol **295**: 953; PDB: 1d60), and the conformation of L-685,818 (18-hydroxyascomycin) as observed in the binding complex with macrophilin (Becker JW, Rotonda J, McKeever BM, Chan HK, Marcy AI, Wiederrecht G, Hemes JD, Springer JP (1993) FK-506-binding protein: three-dimensional structure of the complex with the antagonist L-685,818 J Biol Chem **268**: 11335; PDB: 1fkd) in the trans-amide conformation. The surface of macrophilin is marked in red and pimecrolimus is represented by sticks. Contacts with macrophilin are formed by the pipecolinyl and pyranose rings and the dicarbonyl groups. The pipecolinyl ring is embedded in a deep cavity. The chlorine atom does not form strong contacts to the protein

1.3.1. Structural Flexibility of Ascomycin

Although the structure of ascomycin (**2**) shown in Scheme 4 is the main isomeric form adopted in organic solution, the close proximity of the tricarbonyl unit to C-14−OH potentially allows the formation of numerous alternative isomers (Scheme 5). Thus, liberation and enolization of the tricarbonyl portion followed by re-hemiketalizations could give rise to the four six- or seven-membered hemiketal forms **A**-**D** and their C-11−isomers 11-*epi*-**A**-**D** (not shown in the Scheme). Furthermore, anticipating a 1,4-addition of C-14−OH to the enolized tricarbonyl form **E** allows the generation of a set of isomeric "furano-ascomycins", **F1**-**F4**. In addition, in an aqueous environment, the formation of a hydrate form, **H**, could also be anticipated. Finally, each of the above potential equilibrium products could exist as a mixture of the amide bond rotamers.

Despite the numerous equilibrium products that could be formed, only the isomeric forms **B** and **C** (Scheme 5) of ascomycin (**2**) and tacrolimus (**1**) have been identified and characterized so far (*62–64*). The existence of the tricarbonyl form **T** and its hydrate form **H** has not yet been established, but is suggested by the following findings. Addition of minor amounts of water to a colorless solution of **2** in acetonitrile causes a yellow coloration indicating the formation of the free tricarbonyl form. Further addition of water to the yellow solution leads back to a colorless solution, indicating the conversion of **T** into its hydrate form **H**. An equilibrium among the tricarbonyl form **T**, the hemiketal form **A,** and an alternative hemiketal form (most probably **C**), has also been suggested by the results from reversed-phase LC/MS experiments. The major equilibrium product of ascomycin

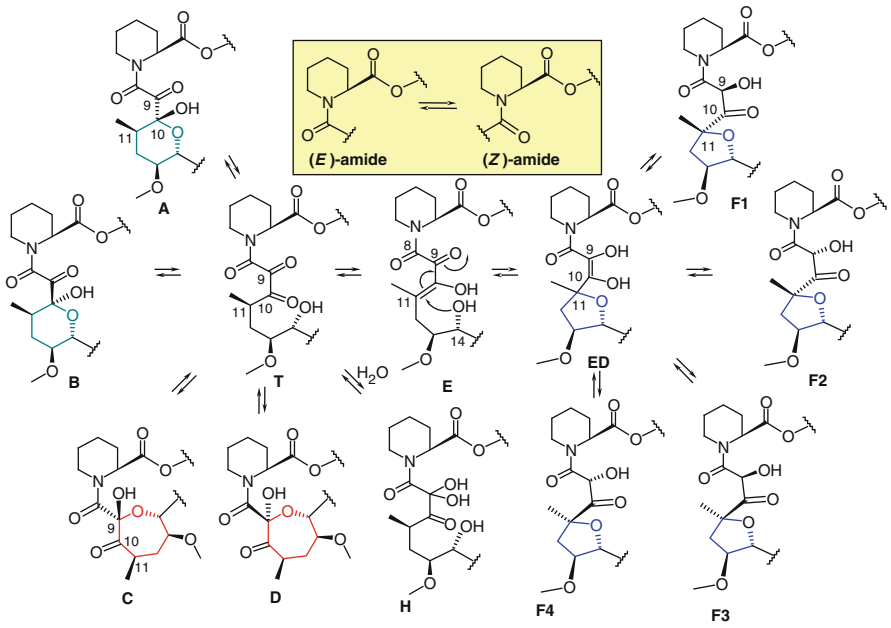

Scheme 5. (Hypothetical) structural flexibility of ascomycin (**2**) and tacrolimus (**1**)

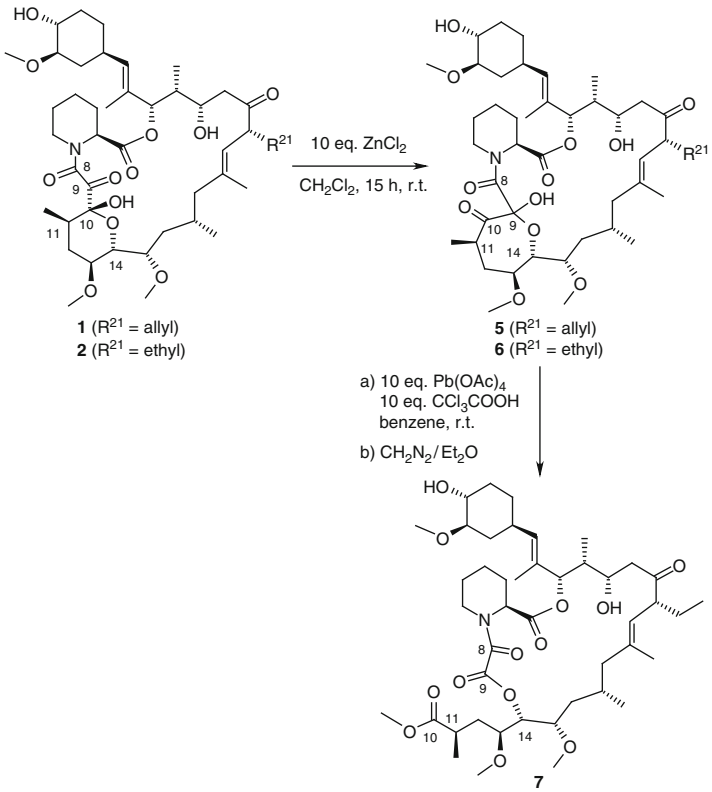

Scheme 6. Conversion of tacrolimus (**1**) and ascomycin (**2**) to their hemiketal forms **5** and **6**, and the chemical degradation of **6** to **7**

(**C**) has been isolated *via* selective crystallization and reversed-phase chromatography (*63*). Its structure has been confirmed by NMR spectroscopy and its synthesis followed by oxidative degradation (Scheme 6) (*64*). Thus, the action of *Lewis* acids (*i.e.* zinc halides) in non-protic organic solvents converts ascomycin (**2**) and tacrolimus (**1**) into the corresponding seven-membered C-9−hemiketal forms, **6** and **5**, almost quantitatively. Lead tetraacetate-mediated chemoselective α-ketol cleavage of **6**, followed by esterification of the crude product and chromatography provided the ester **7** in a 80% yield, thus confirming the C-14−O−C-9 linkage.

2. Synthesis Aspects

2.1. Synthesis of the Four Diastereomeric "Furano-Ascomycins"

An unexpected and interesting reaction occurring in the binding domain of ascomycin (**2**) could be used to synthesize the "furano-ascomycins" **F1**-**F4** (Scheme 5) from **2** (*65*). Thus, bis-silylation of **2** gave **8**, which upon action of

diiodo-triphenyl-phosphorane in the presence of imidazole in refluxing acetonitrile, gave a mixture of the silyl protected 9- and 10-deoxo-furano-ascomycins, **9a**, **9b**, **10a**, and **10b** (Scheme 7). The reaction probably proceeds through equilibration to the ene-diol form **ED**, replacement of either of the OH groups by iodide, followed by iodide ion-mediated deiodination. Starting from **10a** and **10b**, simple functional group manipulations afforded the (11*S*)-furano-ascomycins **13a** and **13b** and their (11*R*)-isomers **13c** and **13d** (Scheme 8). Thus, oxidation of the activated methylene groups in **10a** and **10b** with *Dess-Martin* periodinane in the presence of pyridine yielded the yellow tricarbonyl derivatives **11a** and **11b**, which, after desilylation, provided the derivatives **12a** and **12b**, in high yields. Chemoselective reduction of the highly activated C-9−carbonyl group of **12a** and **12b** with zinc/glacial acetic acid, followed by chromatography afforded the individual isomers **13a**-**13d** in high yields.

The furano-ascomycins **13a** and **13b** differ only at the configuration of C-9, as could be shown by equilibration under basic conditions. Analogous results

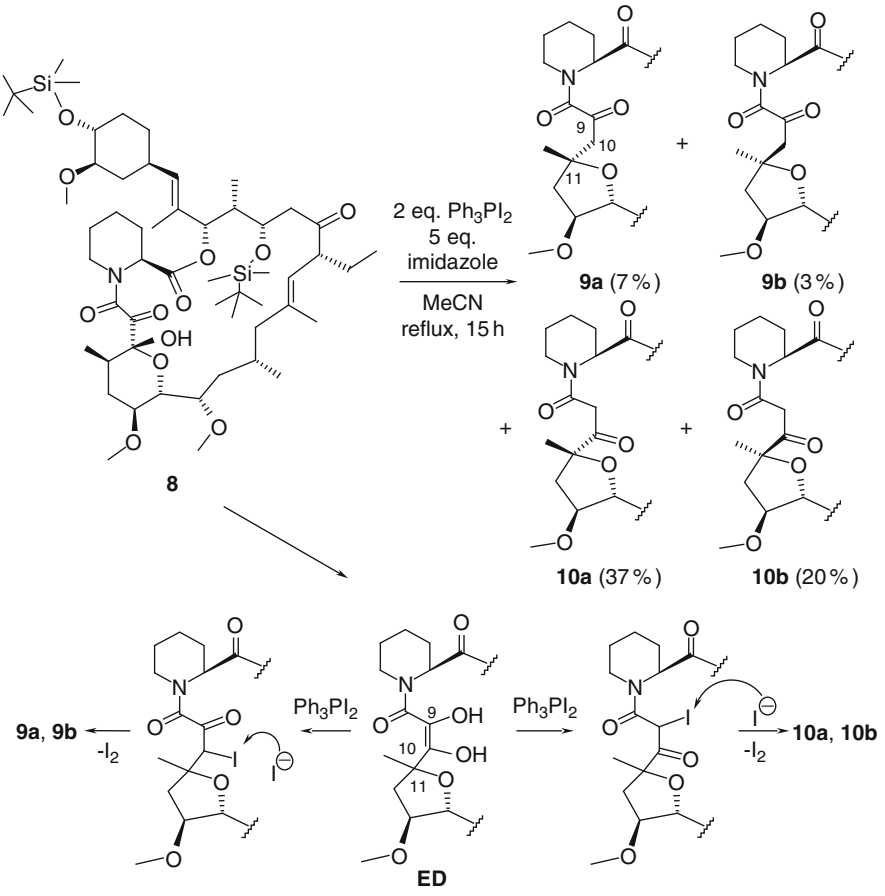

Scheme 7. Transformation of **8** to the 9-, and 10-deoxo-furano-ascomycins **9a**, **9b**, **10a**, and **10b** and a possible mechanism

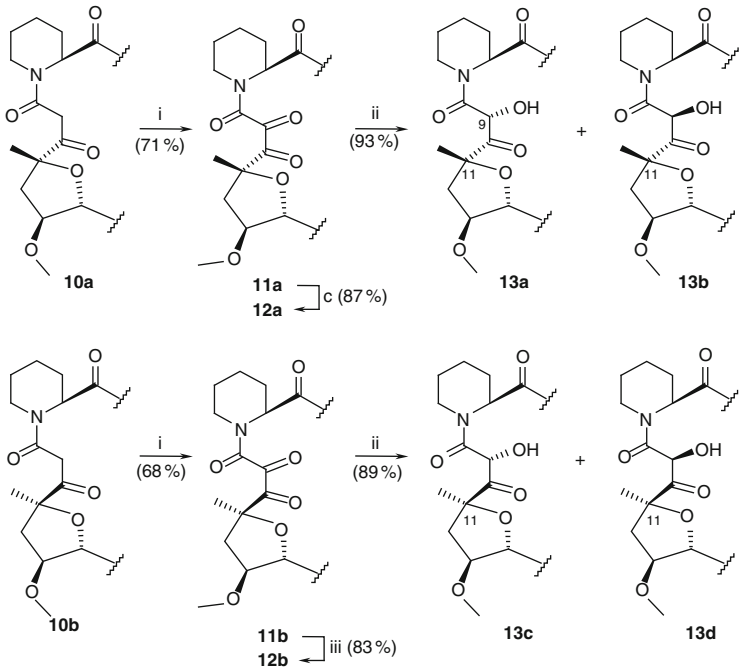

Scheme 8. Transformation of the deoxo-furano-ascomycins **10a** and **10b** to the furano-ascomycins **13a**, **13b**, **13c**, and **13d**

were obtained starting from the 11-*epi*-isomers **13c** and **13d**. The isolated pure furano-ascomycins are remarkably stable at room temperature for several months. Furthermore, no reconversion into ascomycin (**2**) in protic or aprotic solutions under neutral, basic, or acidic conditions could be seen. Also, starting from ascomycin (**2**) no formation of **13a-13d** could be demonstrated in solution. Thus, there is no evidence for equilibrium between the furano-ascomycins and the parent compound ascomycin. No biological activities of these compounds have been reported.

2.2. Synthesis of ^{13}C Labeled Ascomycin

It is essential to have appropriate tools to establish the purity of a drug substance (DS) unambiguously. In the case of an ascomycin-derived DS it is important to be able to distinguish between the "real by-products" and DS-related inherent equilibrium compounds. Researchers at Novartis succeeded in labeling **2** at the diagnostically most relevant C-9 or C-10−carbons in the binding domain (*66*). ^{13}C-Labeled ascomycin (^{13}C-n−**2**), or drug substances derived thereof, serve as versatile tools for studying equilibrium phenomena in more complex mixtures, such

as galenical formulations. For the synthesis of ^{13}C-9–**2**, a ring contraction/ring expansion strategy has been applied (Scheme 9). Thus, ascomycin (**2**) was silylated to furnish the yellow 14,24,33-tris-*O*-TBDMS- derivative **14**, bearing the unmasked tricarbonyl unit. Treatment of **14** with excess calcium hydroxide in THF-water afforded, *via* an irreversible benzilic acid-type rearrangement reaction, the ring-contracted α-hydroxy acid **15** as a >95:5 mixture of diastereoisomers in favor of the (10*S*)-enantiomer. Oxidative decarboxylation of the latter with lead tetraacetate furnished the ring contracted ketoamide **16** quantitatively, setting the stage for ring expansion. The ^{13}C-label was introduced through reaction of **16** with ^{13}C-methylene iodide and butyllithium. Further functional group manipulations

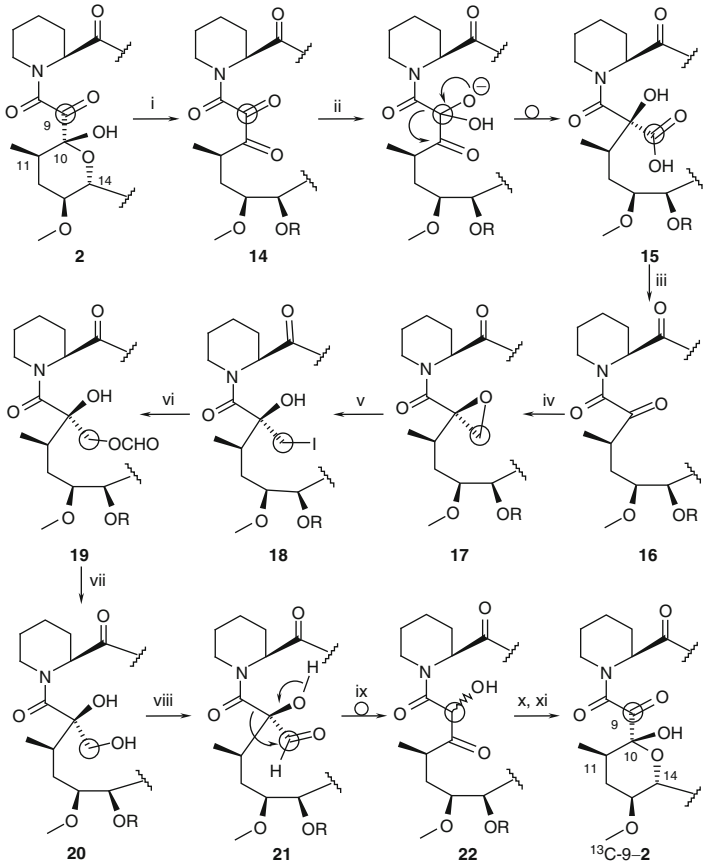

i) TBDMSOTf, 2, 6-lutidine, CH_2Cl_2, r.t.; ii) $Ca(OH)_2$, THF, water, r.t.;
iii) $Pb(OAc)_4$, C_6H_6, r.t.; iv) (^{13}C)-CH_2I_2, BuLi, THF, –78°; v) MgI_2, CH_2Cl_2, r.t.;
vi) $AgBF_4$, DMF, r.t.; vii) $ZnCl_2$, MeOH, r.t.; viii) Oxalyl chloride, DMSO, Et_3N;
ix) $ZnCl_2$,CH_2Cl_2 , r.t., or Florisil, THF, reflux; x) Oxalyl chloride, DMSO, Et_3N;
xi) aq. HF, MeCN, r.t.

Scheme 9. Synthesis of ^{13}C-labeled ascomycin (^{13}C-9–**2**)

provided the α-hydroxyaldehyde **21** as the key intermediate for the subsequent ring expansion protocol. Thus, exposure of **21** to zinc chloride in methanol at room temperature, or to magnesium silicate on silica gel (Forisil®) in refluxing THF solution, provided the ^{13}C-9−labelled 9(*R*/*S*)-dihydroascomycin **22** regioselectively. Oxidation of the secondary hydroxy group in **22**, followed by deprotection, completed the synthesis of ^{13}C-9−**2**.

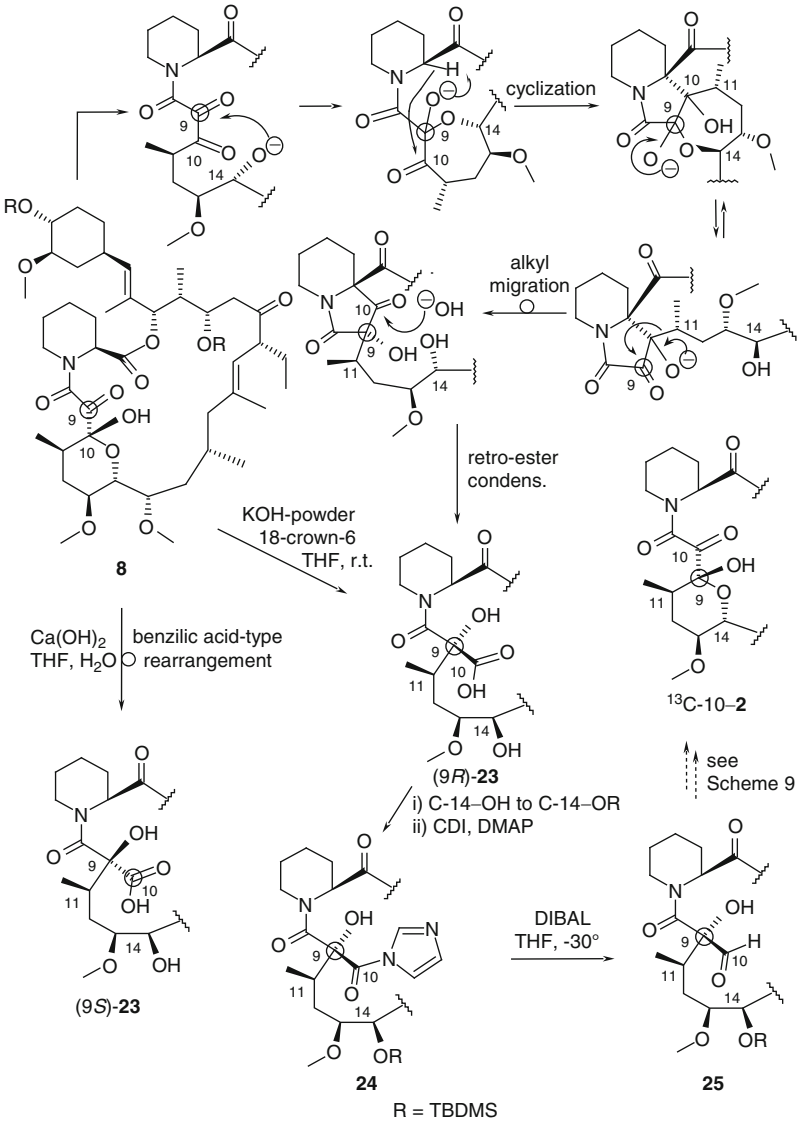

Scheme 10. Synthesis of ^{13}C-9–**25**

Potentially, ^{13}C-9−ascomycin (^{13}C-9−**2**) could be converted into ^{13}C-10−ascomycin (^{13}C-10−**2**) applying a cascade of diastereoselective rearrangement reactions (Scheme 10). As described above, treatment of 24,33-bis-*O*-TBDMS-ascomycin **8** with calcium hydroxide in THF-water solution results in a facile benzilic acid-type rearrangement to give diastereoselectively the (9*S*)-α-hydroxy acid, (9*S*)-**23**, in a quantitative yield. Remarkably, changing to anhydrous reaction conditions (powdered KOH, 18-crown-6, THF, room temperature) afforded almost exclusively (>97:3) the (9*R*)-isomer, (9*R*)-**23**, in a high yield. Quenching and trapping experiments revealed that its formation proceeds not *via* a benzilic acid-type rearrangement, but *via* a cyclization followed by an α-ketol-rearrangement involving the migration of C-11, which is then followed by a diastereoselective (retention at C-2) *retro*-ester condensation. Thus, the newly created quaternary carbon atom of the α-hydroxy-acid (9*R*)-**23** is the former C-9 carbon of ascomycin (**2**). Silylation of the C-14−OH, followed by reduction of the acid *via* its imidazolide **24** provided the (9*R*)-α-hydroxy-aldehyde **25**, which potentially could be transformed to **2** as described in Scheme 9 for the (9*S*)-isomer. Thus, provided that C-8 migrates in the ring enlargement reaction (as observed for the (9*S*)-isomer), this sequence would allow the conversion of ^{13}C-9−ascomycin (^{13}C-9−**2**) into ^{13}C-10−ascomycin (^{13}C-10−**2**).

Tritium labeled tacrolimus was prepared by a metal-catalyzed hydrogen isotope exchange procedure (*67*). The radiochemical purity was 98% and ^{3}H-NMR spectroscopy was used to identify the tritium incorporation in about 10–15 different positions. When administered to rats, HTO-formation turned out to be less than 6% of the dose, thus indicating a reasonable biological stability.

2.3. Reactivity of the Binding Domain

The structural flexibility of ascomycin (**2**) and related macrolactams in the binding domain imparts a high reactivity to this region towards a broad variety of reaction conditions. Thus, selective transformations on other parts of the molecule are often difficult to achieve without provoking concomitant changes in this unit.

2.3.1. Reactivity of Ascomycin and Tacrolimus Towards Diazomethane

Reaction of ascomycin (**2**) with excess ethereal diazomethane led to the diastereoisomeric 9-epoxides **26** and **27**, as expected, together with eight minor by-products **28**–**35** (Scheme 11; for clarity only the relevant portions of the macrocycle are drawn) (*68*–*70*). Compounds **26**–**32** result through insertion of a methylene unit, while compounds **33**–**35** arise from **31** and **32** through a second methylene insertion reaction. The formation of **26**–**31** could be rationalized through the intermediacy of the betaines **A** (keto-form) and **B** (hemiketal form) (Scheme 11). Thus, ring closure with C-9−OH leads to the formation of the oxiranes **26** and **27**. Alternatively, ring

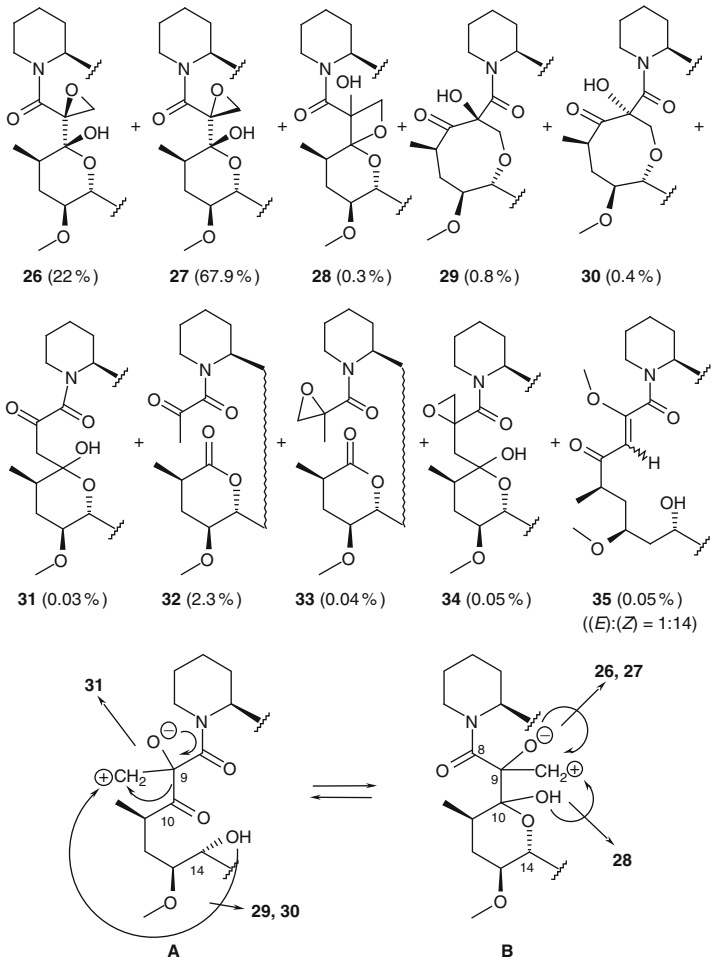

Scheme 11. Products from the reaction of ascomycin (**2**) with diazomethane and a possible mechanistic picture for the formation of the products **26**–**31**. The *long wavy lines* indicate partial structures

closure with C-10−OH or C-14−OH, leads, respectively, to the unusual *spiro*-oxetane **28**, or the oxocanone isomers **29** and **30**. The ring-enlarged derivative **31** could be formed through migration of C-10 to the positively charged carbon of the betaines **A** or **B**. Two distinct pathways could be proposed for the formation of the unusual *seco*-compound **32** (Scheme 12). Thus, starting from the betaine **B**, a *Grob*-type fragmentation would provide the enol form **C** of **32**. Alternatively, starting from the betaine **A**, ring closure to the hydroxy-epoxide **D** followed by a similar fragmentation could lead to the enol ester **E**, which after an intramolecular transesterification, leads to the *seco*-compound **32**. In fact, the enol ester **36** was isolated as a by-product from the reaction of 14,24,33-tris-*O*-TBDMS-ascomycin with diazomethane. This supports the intermediacy of compounds of type **E** in these

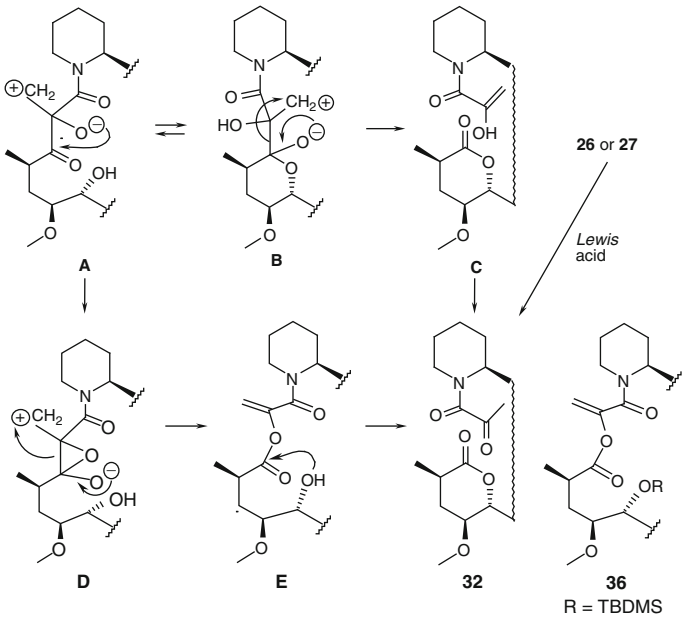

Scheme 12. Possible pathways for the formation of the product **32** in the reaction of ascomycin (**2**) with diazomethane, and the structure of the isolated intermediate **36**. The *long wavy lines* indicate partial structures

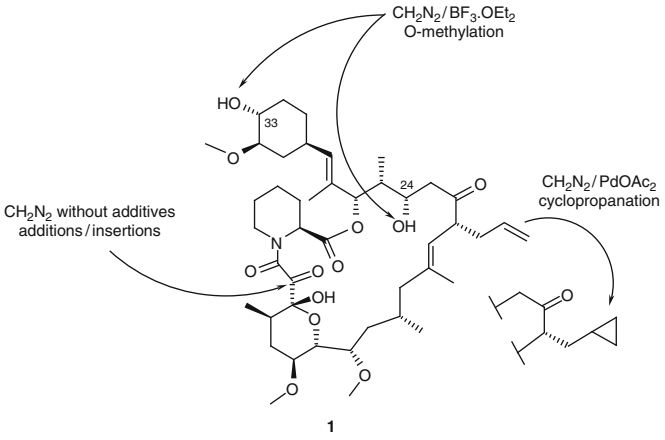

Scheme 13. Selective reactions of diazomethane with tacrolimus (**1**)

reactions. Interestingly, treatment of the oxiranes **26** and **27** with *Lewis* acids leads to the *seco*- compound **32** in an almost quantitative yield (*69*, *71*).

Although the tricarbonyl portions of ascomycin (**2**) and tacrolimus (**1**) are highly sensitive towards diazomethane, selective O-methylations on C-24−OH and C-33−OH could be achieved in the presence of catalytic amounts of $BF_3.OEt_2$ (Scheme 13). On the other hand, reaction with excess of diazomethane in the

presence of $Pd(OAc)_2$ led selectively to cyclopropanation of the double bond on the allylic side chain of tacrolimus (**1**), leading to 37,38-cyclopropano-FK506, which showed excellent macrophilin binding but somewhat weaker T-cell inhibitory activities (*26, 72–74*).

2.3.2. Rearrangement Reactions in the Binding Domain

2.3.2.1. Benzilic Acid-Type Rearrangement Reactions

Early attempts to cleave the endocyclic pipecolic ester bond by a base-catalyzed saponification procedure did not lead to the expected 1,26-*seco*- derivative, but instead to a 22-membered lactone with a rearranged C-9−C-10 region (Scheme 14). Based on labeling studies, a benzilic acid-type rearrangement occurring on the free tricarbonyl form was proposed as a mechanism for this ring-contraction reaction. More detailed studies performed at Novartis showed that the reaction conditions originally applied (*i.e.* 1.1 eq. LiOH, THF-H_2O) (*73, 75, 76*) provided not only the hydroxy acid (9*R*)-**37** but also its 9-*epi*-derivative (9*S*)-**37** (*77, 78*). Oxidative degradation of both isomers led to **38,** which after deprotection, led to the common ring-contracted *nor*-C-9 ascomycin derivative **39**, thus showing that all other chiral positions remained unchanged. Further studies showed that the derivative (9*S*)-**37** was formed *via* a distinct reaction pathway and could be prepared selectively by applying anhydrous reaction conditions. An almost exclusive formation of the 24,33-bis-*O*-TBDMS protected (9*S*)-hydroxy esters **40a** (R′=methyl) and **41a**, **42a** and **43a** (R′=ethyl, propyl, *iso*-propyl), or their unprotected congeners **40b**, **41b**, **42b** and **43b,** could be accomplished by reacting 24,33-bis-*O*-TBDMS-ascomycin (**8**) or unprotected ascomycin (**2**) in the appropriate alcohol with *Lewis* acids (*i.e.* ZnX_2, MgX_2, X=Cl, Br, I; $Ti(O\text{-}^iPr)_4$) (*71*).

2.3.2.2. Rearrangement Reactions in Aprotic Media

Treatment of unprotected **2** or 24,33-bis-*O*-TBDMS protected ascomycin (**8**) with various non-nucleophilic bases in aprotic solvents led to a set of unusual rearranged derivatives, which have been termed "cyclo-ascomycins" (Scheme 15). Thus, refluxing ascomycin with excess triethylamine and catalytic amounts of powdered KOH in acetonitrile yielded (9*S*,11*S*),2,10-cyclo-ascomycin **44** (SDZ ASD 732), together with traces of the stereoisomers **45**–**47** (*79, 80*). Separation of the diastereomers **44**–**47** was accomplished using stimulated moving bed technology or centrifugal counter-current chromatography (*81, 82*).

The isomer **44** could be transformed to 11-*epi*-ascomycin in a series of steps (Scheme 15) (*83*). Thus, silylation of **44** afforded 14,24,33-tris-*O*-TBDMS-protected **44** that on treatment with powdered KOH and 18-crown-6 under aprotic

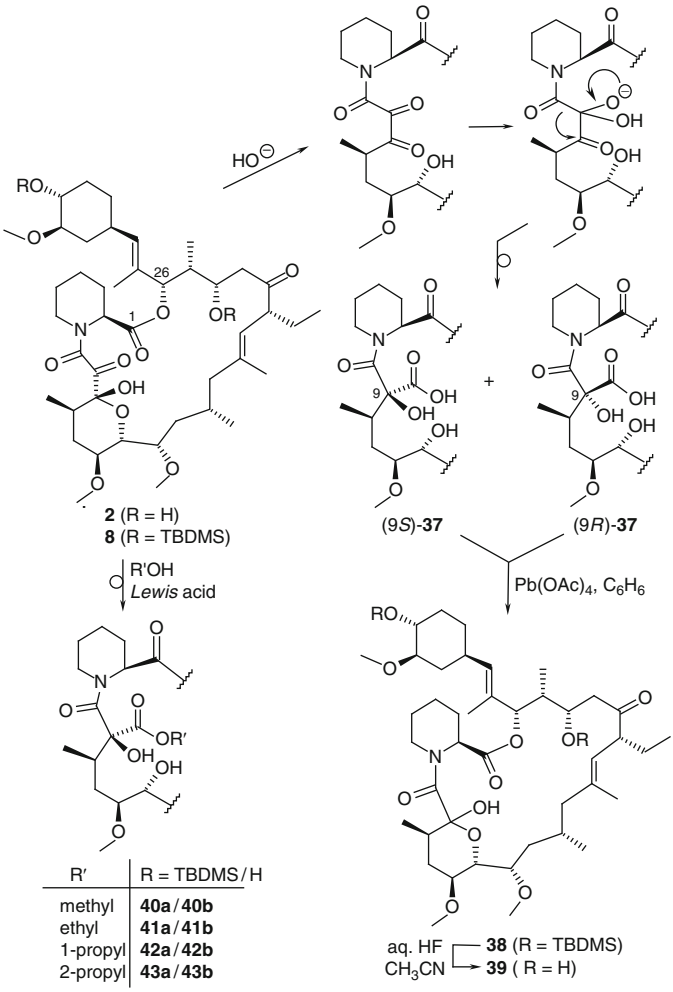

Scheme 14. Benzilic acid-type rearrangement reactions of ascomycin (**2**)

conditions led to 11-*epi*-(9*R*)-**23a**. This compound, upon further transformations analogous to those described in Scheme 10, led to 11-*epi*-ascomycin (11-*epi*-**2**). In contrast to ascomycin (**2**), which exists in $CDCl_3$ solution as a mixture of six- and seven-membered hemiketal forms (ratio 15:1), 11-*epi*-**2** adopts exclusively two diastereomeric (10*S*)- and (10*R*)-six-membered hemiketal forms in the ratio 4:1. Notably, 11-*epi*-**2** is stable to acidic conditions, but is converted completely to **2** under weakly basic conditions, whereas no conversion of **2** to 11-*epi*-**2** was observed under the same conditions or on storage under protic, aprotic, organic, or aqueous solutions. Interestingly, treatment with DBU converts 11-*epi*-**2** to **44** as the sole product. Therefore, it is likely that the formation of **44** from **2** involves

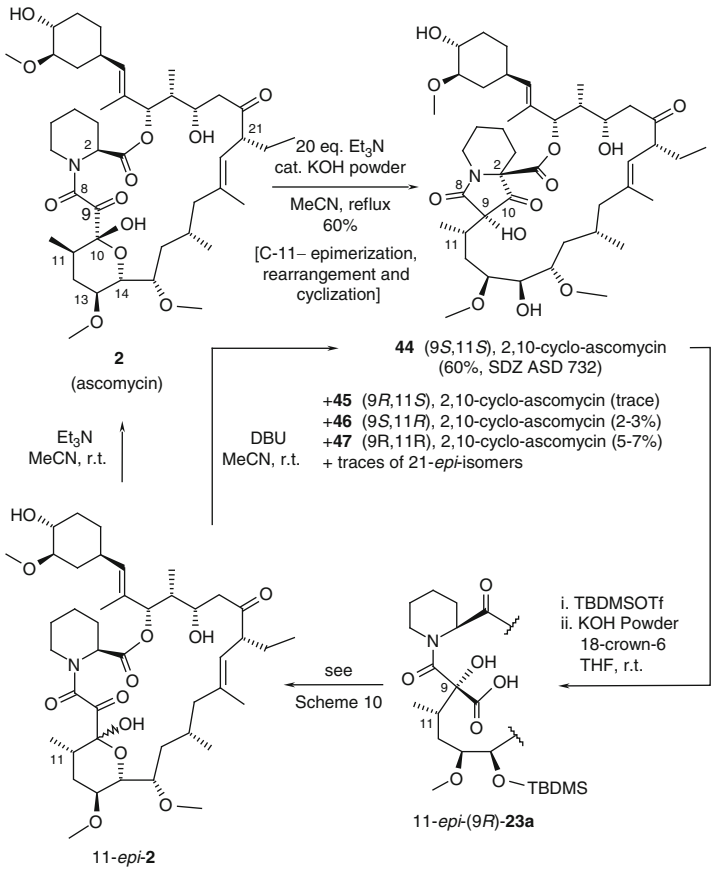

Scheme 15. Conversion of ascomycin (**2**) to the cyclo-ascomycin **44** (SDZ ASD732) and other isomers, and, transformation of **44** to 11-*epi*-ascomycin (11-*epi*-**2**) and *vice versa*

epimerization at C-11 as the first step, which is then followed by rearrangement and ring closure.

Starting from 24,33-bis-*O*-TBDMS-protected ascomycin (**8**), the isomeric cyclo-ascomycins **45**–**47** could be prepared as the sole products (*79*, *84*, *85*) (Scheme 16). Thus, treatment of **8** with the sodium salt of tosylamide provided with high stereoselectivity the cyclized compound **48** ((10*R*)-configuration), which, upon treatment with cesium carbonate, rearranged to **49**, and, after desilylation, afforded the (9*R*,11*R*),2,10-cyclo-ascomycin **47**. Alternatively, one could first carry out the rearrangement and then esterify to give **40b**, and then cyclize it to **49** (compare Scheme 14).

The isomer **46** can be prepared with a high stereoselectivity (Scheme 17). Thus, 24,33-bis-*O*-TBDMS-ascomycin (**8**) is transformed to (10*S*)-**48** with an (*S*)-configuration at C-10 using CsF in a 68% yield. Alternatively, **8** is converted

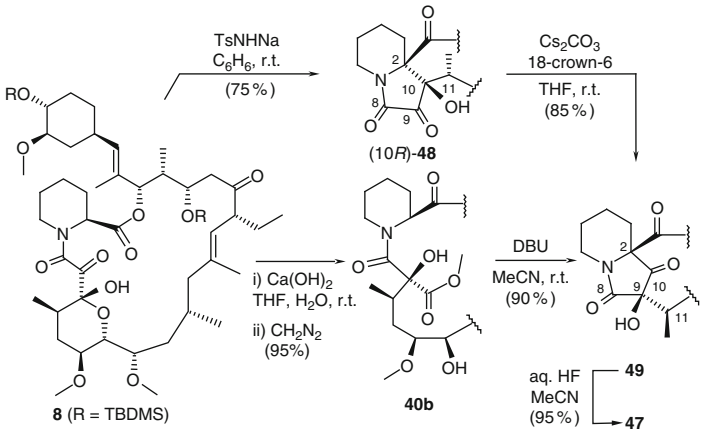

Scheme 16. Transformation of **8** to the cyclo-ascomycin **47**

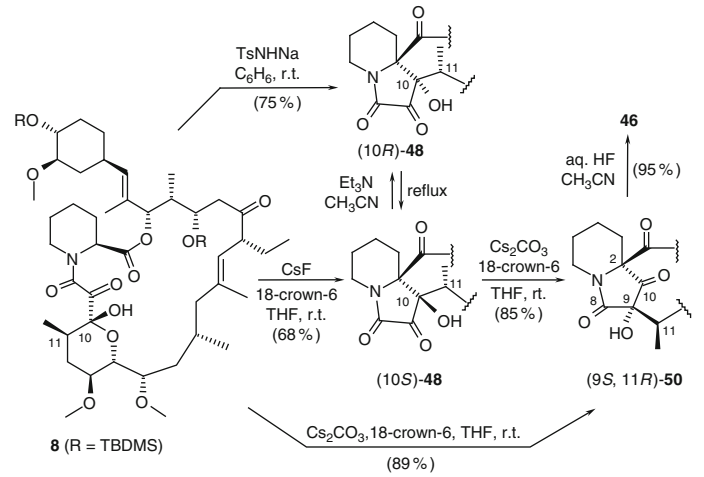

Scheme 17. Transformation of **8** to the cyclo-ascomycin **46**

first to (10*R*)-**48** and then epimerized to (10*S*)-**48**. Treatment of isolated (10*S*)-**48** with Cs_2CO_3 in the presence of 18-crown-6 in tetrahydrofuran initiates a diastereoselective alkyl migration to give the 24,33-bis-*O*-TBDMS-derivative **50**, which after desilylation affords the (9*S*,11*R*),2,10-cyclo-ascomycin **46**. More conveniently, compound **50** is also obtained in a one-pot reaction starting from **8**.

No methods are available so far for the preparation of the fourth stereoisomer (9*R*,11*S*),2,10-cyclo-ascomycin (**45**), in a good yield. The only available method involves silylation of **44** to give **51**, which is then transformed to its 9-chloro- derivative **52** by routine methods (Scheme 18). An unusual halogen/hydride exchange furnished the deoxo- derivative **53** in a low yield. Due to

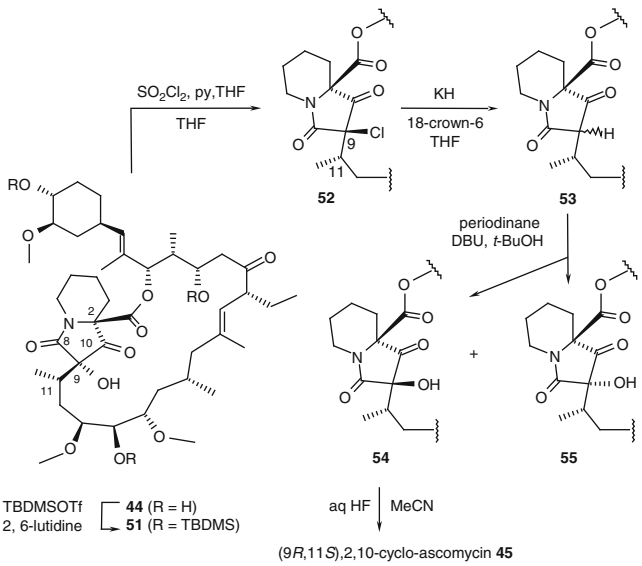

Scheme 18. Transformation of the cyclo-ascomycin **44** to the isomer **45**

keto/enol tautomerism, **53** exists in $CDCl_3$-solution as a mixture of diastereomers. Oxidation of **53** resulted in the reintroduction of the hydroxy group to give the tris-*O*-TBDMS-protected cyclo-ascomycin-derivatives **54** and **55**. Finally, desilylation of **54** afforded the desired (9*R*,11*S*),2,10-cyclo-ascomycin **45**.

In summary, four diastereoisomeric cyclo-ascomycins (**44**–**47**) can be prepared stereoselectively by simple treatment of protected or unprotected ascomycin (**2**) in aprotic media with an appropriate base. Although C-2 is clearly involved during their formation, no C-2−epimeric cyclo-ascomycins have been found so far under any of the reaction conditions, thus indicating a powerful remote stereocontrol. Interestingly, it could be shown that upon treatment with powdered KOH in the presence of 18-crown-6, the 14,24,33-tris-*O*-TBDMS-cyclo-ascomycins **54**–**57** undergo ring cleavage to the corresponding α-hydroxy acids **58**–**61**, thereby leading to, in all the four isomers, C-2 in its natural (*S*)-configuration (Scheme 19). Furthermore, **58**–**61** can be transformed to esters **62**–**65** that may then be cyclized back diastereoselectively to give **54**–**57**. The α-hydroxy acids **58**–**61** have served as versatile tools for the determination of relative configurations. Thus, oxidative decarboxylation resulted in the formation of the epimeric 14,24,33-tris-*O*-TBDMS-α-ketoamides **66** and **67** differing in their configuration at C-11, as could be shown by equilibration experiments and by their conversion to the silyl enol ether **68**. Desilylation of **67** led to the already known derivative **39**, thus giving evidence for the outlined C-11−configuration and the confirmed (*S*)-configuration at C-2 for all the α-hydroxy acids. The stereochemistry at C-2 of the cyclo-ascomycins **54**–**57** (and thus also of their deprotected congeners **44**–**47**) has been established by another chemoselective oxidative degradation protocol (Scheme 20). Thus, reaction

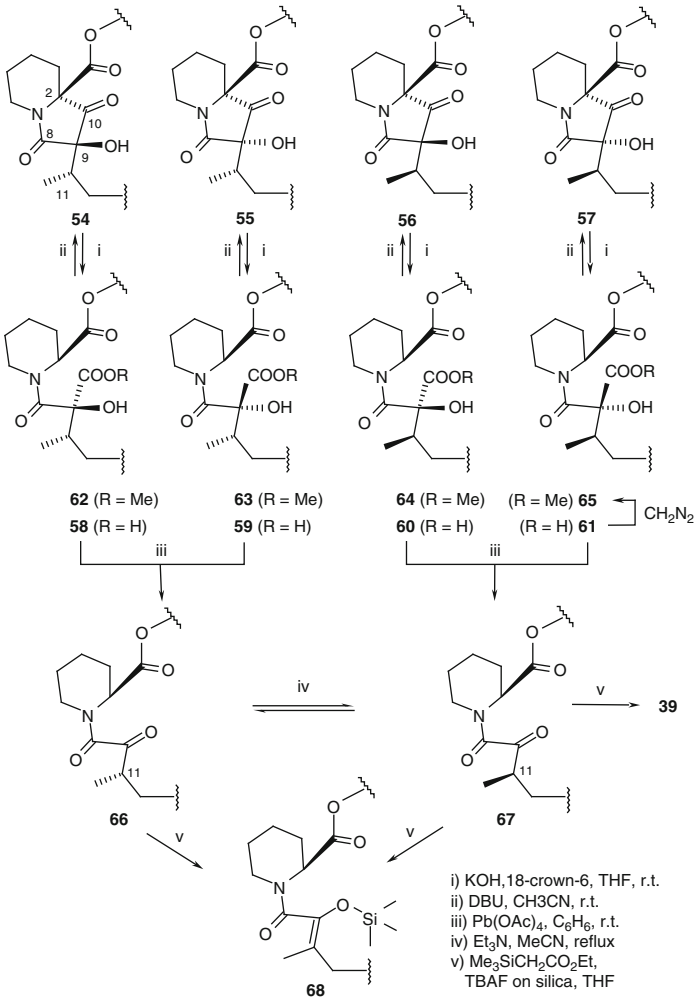

Scheme 19. Ring-cleavage reactions of the 24,33-bis-TBDMS-cyclo-ascomycins **54**–**57** and their further transformations for establishing the stereochemistry

of **54**–**57** with excess tetrapropylammonium perruthenate (TPAP) provided the two C-11−epimeric α-ketoamides **69** and **70**, bearing a carboxylic acid functionality at C-2. After treatment with diazomethane they provided the corresponding esters **71** and **72**, which in an intramolecular base-mediated transesterification event provided the enol ester derivative **73**. The latter can only exhibit the intact original C-2−configuration of the starting cyclo-ascomycins **54**–**57**. Having ascertained the relative stereochemistry at C-2, C-9, and C-11 of all cyclo-ascomycins, the absolute configurations were established by X-ray crystal structure analysis of the

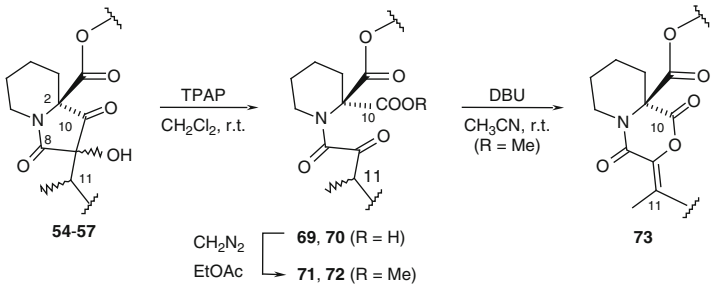

Scheme 20. Degradation reactions of the 24,33-bis-TBDMS-cyclo-ascomycins **54–57** towards establishing the C-2–configuration

unprotected (9*S*,11*S*)-derivative **44** (*71*, *84*, *85*). The biological activities of these compounds have not been reported.

2.3.3. Reduction, Deoxygenation, Imine- and Aminal-Formation in the Binding Domain

9-Dihydro-FK506 (**74**, tsukubamycin I), together with its 9-dihydro-9-*O*-methyl-congener **75** (tsukubamycin A), was first isolated as a by-product from the fermentation broth of a tacrolimus producer strain (*8*) (Scheme 21). Synthetically, chemo- and stereoselective reductions of the 9-carbonyl group of ascomycin (**2**), tacrolimus (**1**), and 24,33-bis-O-protected congeners thereof, have been accomplished using either DIBAH or *Evans*' reagent (tetramethylammonium-triacetoxyborohydride) (*74*, *86*). The absolute stereochemistry of the 9-dihydro- derivatives could be deduced by NMR spectroscopy from their corresponding rigid thiocarbonates **79** and **80**, which were prepared readily by the action of thiocarbonyl diimidazole. The latter served as versatile starting materials for further modifications. Thus, radical deoxygenation/elimination of the thiocarbonates **79** and **80** gave the (*E*)- and (*Z*)-9,10-unsaturated compounds (*E*)-**81** and (*Z*)-**81**. Different (*E*)/(*Z*) ratios were obtained when Bu_3SnH or $(Me_3Si)_3SiH$ in combination with AIBN or triethylborane were used, allowing the preparation of either isomer selectively. Hydration of the enolether **81** provided the 9-deoxo-derivative **83** as a single diastereomer, whereas hydrogenation led to the two diastereomers, (10*S*/*R*)-9-deoxo-10-deoxy-**82**. Interestingly, the unusual reduction- and deoxygenation-product **85** was obtained when ascomycin (**2**) was reacted with diphenylsilane in the presence of cesium fluoride.

Action of ammonia in methanol converts ascomycin (**2**) to a mixture of the C-10−aminal **86** and the C-9−imine **87**, whereas reaction with methylamine led to the C-9−imine **88** exclusively (Scheme 21) (*87*).

9-Deoxoascomycin (**83**), together with minor amounts of the 10-deoxo- derivative **84**, could be prepared from ascomycin (**2**) directly through reaction with hydrogen sulfide in the presence of pyridine (Scheme 22) (*88*). Notably, the

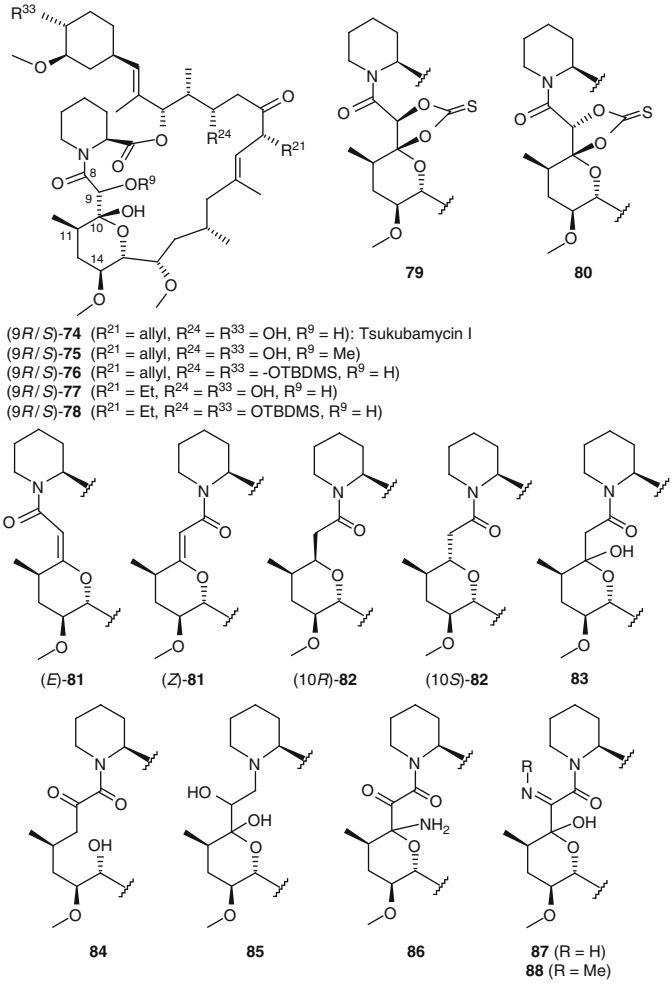

Scheme 21. Derivatives of ascomycin (**2**) and tacrolimus (**1**) with diverse modifications in the binding domain

exclusive formation of either the 9- or 10-deoxo- derivative was observed when the imine **87** or the aminal **86** was treated with hydrogen sulfide in the absence of base.

Semi-rigid derivatives of ascomycin (**2**), featuring heterocyclic structural elements in the binding region, were synthesized from the aminal **86** (*89*). The carbonyl C atoms, for example, were integrated into an oxazole ring giving **89**, and the tetrahydropyran ring of **86** was transformed into the pyridine unit in **90**.

Several of the analogues in this section have also been prepared with tacrolimus, but are omitted here for simplicity. Structure-activity relationships (SARs) have been reported (*74*) and are summarized as follows. The 9-dihydro- derivatives **74** and **77** showed good macrophilin binding but reduced inhibition of T-cell activation

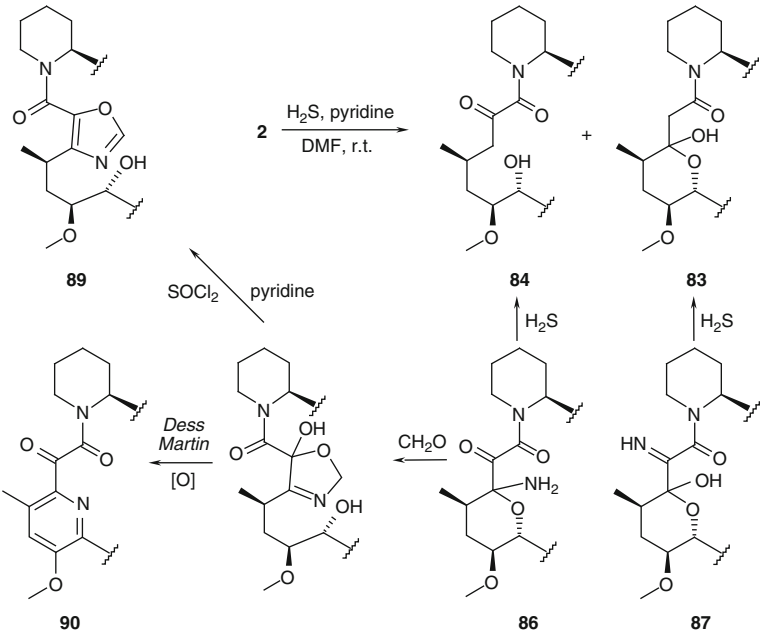

Scheme 22. Derivatives of ascomycin (**2**) featuring desoxygenations and heterocyclic rings in the binding domain

in cellular assays. The 9-desoxo derivative **83** showed lower binding affinity and reduced inhibition of T-cell activation. Interestingly, the 10-amino and 9-imino analogues **86** and **87** had higher macrophilin binding affinities than tacrolimus; the tacrolimus analogue of **86** was highly active in cellular assays. The pyridine analogue **90** was totally inactive on T-cells.

2.3.4. Modification in the Binding Domain Through Photochemistry

It has been reported that tacrolimus (**1**), on exposure to visible light (30,000 Lux) for 10 days, undergoes a rearrangement in the binding domain, leading to the oxazolidinone **91**, and degradation, affording the diastereomeric cleavage products (11*R*/*S*)-**92** (Scheme 23) (*90, 91*). The formation of **91** represents a modification on the amino acid unit, the type of which could not be achieved easily through routine chemical methods. This prompted Novartis researchers to investigate photochemical reactions in more detail.

Thus, irradiation of ascomycin (**2**) in acetonitrile using >280 nm light led to the [1,3]-sigmatropic shift product **94**, the cleavage product **96** and the oxazolidinone **97** (Scheme 24) (*92–94*). On the other hand, irradiation in methanol under the same conditions led to the methoxy derivative **93** in addition to the other products **94–96**; none of the intramolecular cyclization product **97** was observed under these

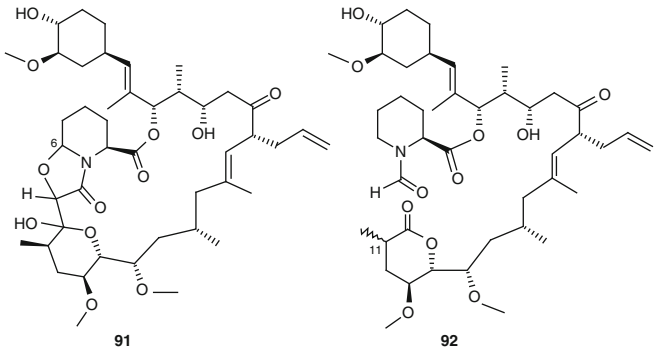

Scheme 23. Structures of the products formed after exposure of tacrolimus (**1**) to visible light

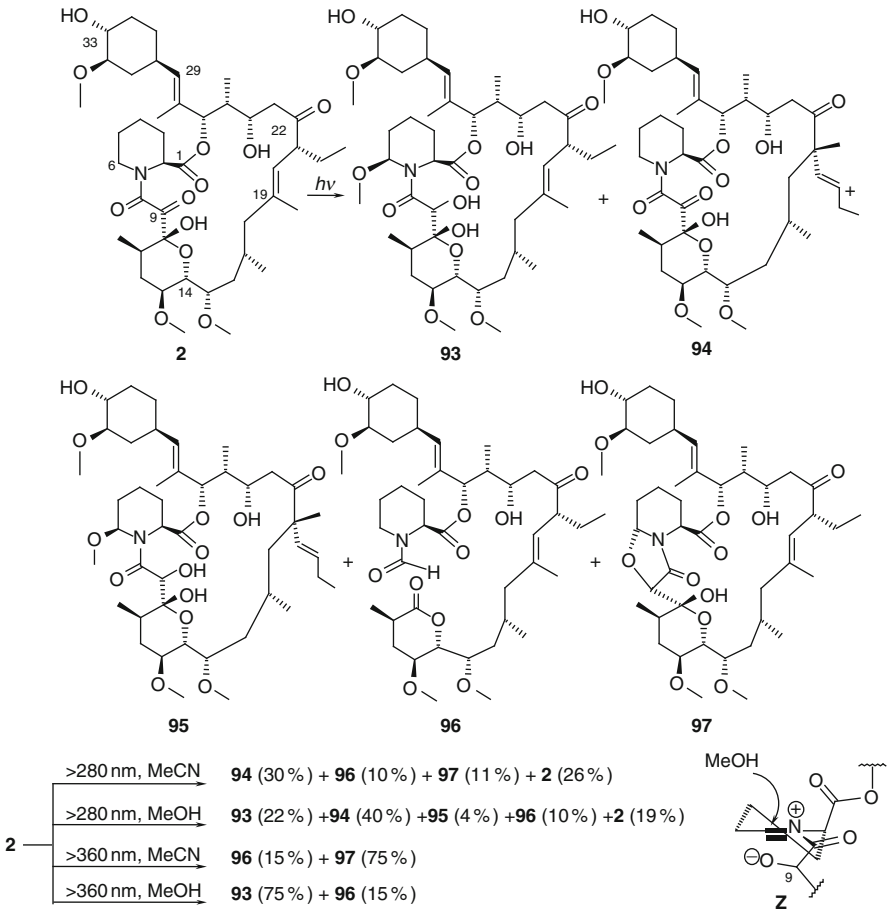

Scheme 24. Products formed upon irradiation of ascomycin (**2**) with ultraviolet light of different wavelengths in acetonitrile and methanol

reaction conditions. Interestingly, by employing light at >360 nm only the tricarbonyl chromophore is selectively excited and, hence, the formation of the [1,3]-shift product **95** could be suppressed leading to high selectivities. Thus, using these longer wavelengths the reaction in acetonitrile afforded the oxazolidinone **97**, whereas the reaction in methanol furnished the methoxy derivative **93** as the main product, hence providing preparatively useful protocols. The formation of these products could be explained through the intermediacy of the zwitterion **Z**.

The photoproduct **93** could be oxidized selectively using catalytic amounts of Cu $(OAc)_2$, pyridine, and oxygen in dichloromethane to afford 9-methoxyascomycin (**98a**) in excellent yield (Scheme 25). The ethoxy and propoxy analogues **98b** and **98c** could also be prepared analogously through irradiation of **2** in ethanol or propanol, followed by oxidation of the resulting 9-alkoxy photoproducts. On the

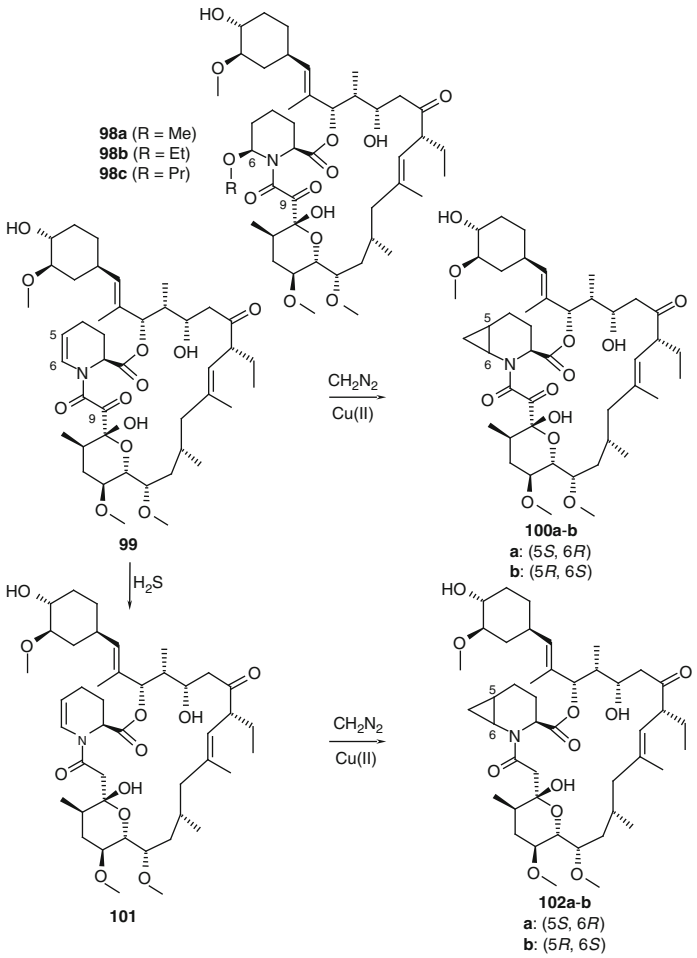

Scheme 25. 6-Alkoxy-ascomycins **98a**, **98b**, and **98c**, and 5,6-dehydroascomycin (**99**) and its further transformations

other hand, **93**, upon elimination of MeOH using ammonium chloride in DMF, gave 5,6-dehydro-9-dihydroacomycin, which after Cu(II)-catalyzed oxidation of the C-9−OH, afforded 5,6-dehydroascomycin (**99**), a close bioisostere of ascomycin in an excellent yield (*95*). Compound **99** served as a useful starting material for the preparation of 5,6-tritium labeled ascomycin in a single step through catalytic tritiation (*96*). Cu(II)-catalyzed cyclopropanation of **99** using diazomethane furnished both the α- and β- isopropano analogues **100a** and **100b** as further rigid derivatives of ascomycin (**2**). Further, **99** could be desoxygenated using hydrogen sulfide/pyridine giving the 9-desoxo analogue **101**, from which the two isomers of the cyclopropano analogues **102a** and **102b** could be obtained in low yields, in an analogous manner to the reactions described above. Starting from the proline analogue of ascomycin **103**, which is available as a side product in the fermentation of ascomycin (**2**), the 5-methoxy analogues **104** and **105**, and the 4,5-dehydro analogue **106** were prepared analogously (Scheme 26).

The hemiacetal photoproduct **93** can be hydrolyzed giving the aldehyde **107** in an excellent yield (Scheme 27). The reactivity of the aldehyde functionality can be used for preparing interesting derivatives. Thus, employing $NaClO_2$ and Cu(II)-catalyzed oxidations, *Wittig* and esterification reactions, **107** could be transformed to the linear amino acid analogues **108a**, **108b**, **109a**, and **109b** in a few steps and good yields. Furthermore, Cu(II)- catalyzed oxidation of **107** provided the corresponding C-9=O derivative, which underwent acid-catalyzed cyclization leading to the bicyclic analogues **110a** and **110b**.

For the purpose of broader derivatization in the amino acid region, the suitably protected key aldehyde **113** was synthesized starting from the easily available protected ascomycin derivative **111**, using the photoreaction described above (Scheme 28) (*97*). Thus, starting from **111** photolysis afforded the methoxy derivative **112**, which was hydrolyzed, and the C-33−*O*-silyl group that fell off was reintroduced giving **113**. Aldehyde **113** was transformed to the allyl carbonate **114** through a series of transformations. Interestingly, **114** exists exclusively as a seven-membered hemiketal in $CDCl_3$. Pd-Catalyzed cyclization of **114**, followed by desilylation and selective oxidation of the C-22−OH led to the 6-vinyl analogue **115** as an inseparable mixture of C-6−epimers. The two C-5−epimers of the 5-vinylproline analogue **116** were also synthesized starting from **113**, as individual isomers, using a similar strategy.

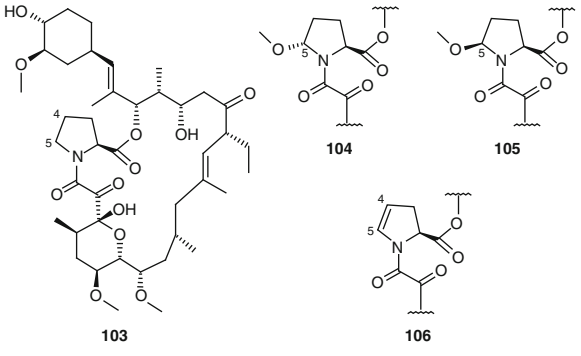

Scheme 26. 5-Alkoxy- and 4,5-dehydro- derivatives **104**, **105** and **106** of the proline analogue of ascomycin **103**

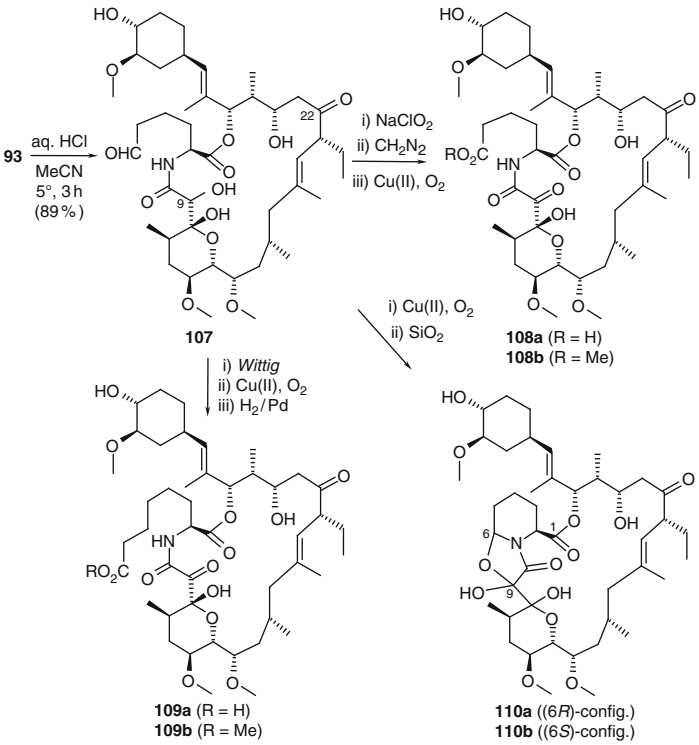

Scheme 27. Hydrolysis of the photoproduct **93** to the aldehyde **107** and its further transformations

The biological activities of these compounds resulting from photochemistry were discussed in detail in the light of the possible conformations (*92*). Briefly, the observed activities of the three 6-alkoxy derivatives **98a**, **98b**, and **98c** showed that larger alkoxy groups result in weaker binding to macrophilin. Among the cyclopropano analogues, those bearing the cyclopropano group in the α-face of the piperidine ring **100a** and **102a** showed higher activity than the β-counterparts **100b** and **102b**. The 9-oxo analogues **99**, **100a** and **100b** were more active than the 9-desoxo counterparts **101**, **102a**, and **102b**, indicating the importance of the C-9−carbonyl group to the binding with macrophilin. Other analogues, such as the vinyl analogues **115**, **116a**, **116b**, and the bridged analogues **110a** and **110b** were not active. The acyclic amino acid analogues **108a-110a** and **108b-110b** did not show any activity, reflecting on the importance of the necessity of the pipecolic acid ring structure, and hence the conformation of the macrolide. It is noteworthy that the ring-contracted butenyl analogue **94** and its saturated butyl derivative (not shown in the scheme), featuring unaltered binding domains, showed excellent binding to macrophilin, but were not active in T-cell assays. Thus, in these cases, modifications in the effector domain do not favor further interactions of the initially formed macrophilin-binding complex with calcineurin A and calcineurin B, and thus do not result in any T-cell modulatory activities. Of all these derivatives, the 5,6-dehydro-ascomycin **99** and the dehydroproline **106** showed activities close to

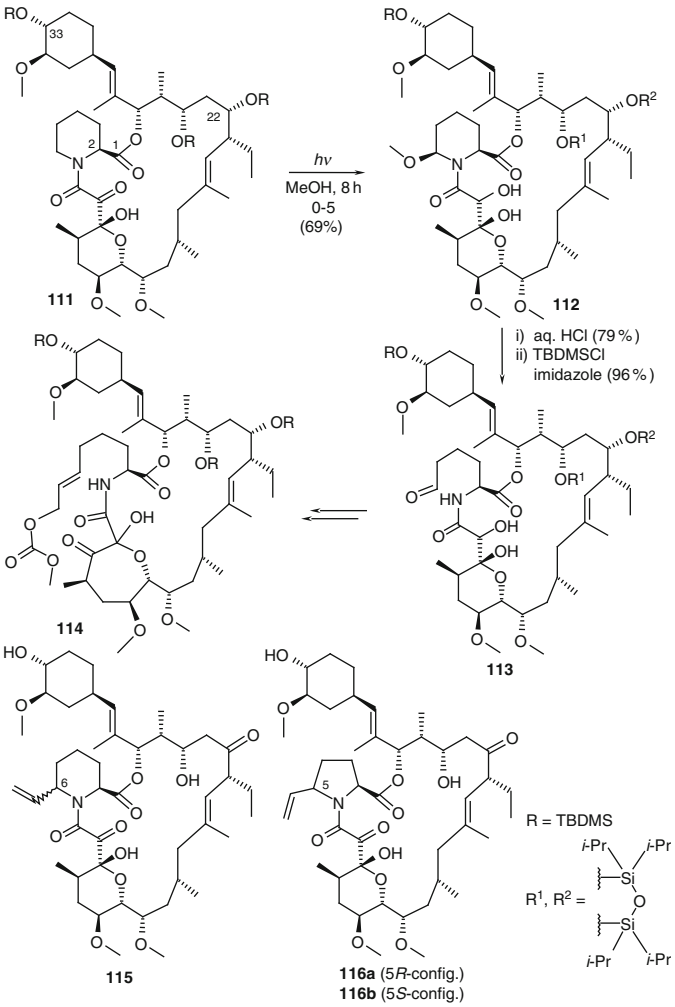

Scheme 28. Syntheses of the 6-vinyl-ascomycin **115** and the 5-vinylproline-analogues **116a** and **116b**

the parent ascomycin. Compound **99** (SDZ 283–871) had been under detailed investigations at Novartis, but its development was terminated later in preference to pimecrolimus.

2.3.5. Cleavage Reactions Within the Binding Domain: Amino Acid Exchange

In addition to the already mentioned photochemical decarbonylative cleavage and the *Lewis* acid assisted cleavage of 9-oxirane derivatives (see Scheme 12), several other cleavage protocols have been elaborated. Thus, reaction of ascomycin (**2**) or

tacrolimus (**1**) derivatives with lead tetraacetate in methanol, or with *in situ* generated LiOOH or $Ca(OOH)_2$ in THF/aq. hydrogen peroxide solution, led to a facile oxidative cleavage of the C-9−C-10 bond, affording, depending on the work-up method, *seco*- structures of the general formula **A** or **B** (Scheme 29) (*64*, *73*, *98*–*100*).

Two additional methods, allowing a reductive cleavage at the binding domain, have been described as well. Thus, reaction of tacrolimus with benzyl amine and sodium cyanoborohydride in methanol afforded the diketopiperazine **117** and a mixture of the C-10−C-34 fragments **118** and **119** (Scheme 30) (*73*). The hydroxyketone fragment **119** exists in equilibrium with its hemiketal tautomer **120**. Mechanistically, this interesting fragmentation might involve reductive amination of the C-9=O followed by an intramolecular aminolysis of the ester, and, retroaldol cleavage of the C-9−C-10 bond yielding the observed products.

Alternatively, reductive cleavage of 24,33-bis-*O*-TBDMS-ascomycin (**8**) has been achieved by the action of 9-BBN (9-bora-bicyclo[3.3.1]nonane) in THF giving the hydroxy-acetamide **121** in an excellent yield (Scheme 31) (*100*). Treatment of the latter with sodium hydride furnished the C-10−C-34 fragment **122** through an intramolecular transesterification reaction. Interestingly, **122** could also be obtained by a cyanide-induced cleavage. In the event, after addition of cyanide to the C-9−carbonyl, cleavage of the C-9−C-10 bond occurs to give the cyanohydrin **123** (*99*, *101*–*103*). Depending on the cyanide source used and the work-up conditions, either the cyanohydrin itself and/or the fragment **122** could be isolated.

The cleavage products having lost the pipecolic acid moiety could be elaborated to new analogues incorporating new amino acid units such as sarcosine, proline, D-pipecoline, *N*-methyl-alanine, 2-methyl-alanine, and β-alanine in place of the original amino acid (Schemes 32 and 33) (*100*, *104*). For example, coupling of a suitable N-protected amino acid to the most reactive, allylic C-26−OH of **122**, followed by a chemoselective reduction of the lactone unit, afforded the lactol **124**. Addition of a C_2 unit to the lactol through a *Wittig* reaction, protection of the C-14−OH and deprotection of the amine and the carboxylic acid groups followed by a macrolactamization reaction provided the enamide **125** as a key

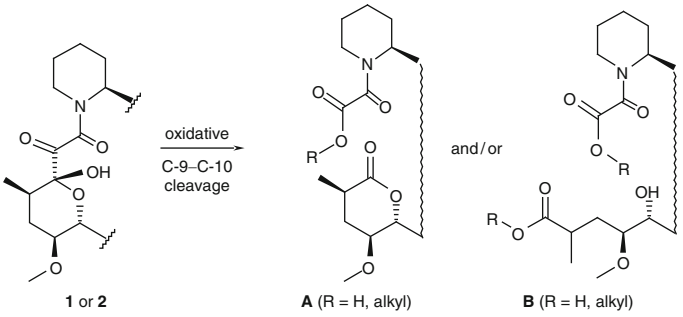

Scheme 29. Oxidative cleavage of derivatives of ascomycin (**2**) and tacrolimus (**1**). The *long wavy lines* indicate partial structures

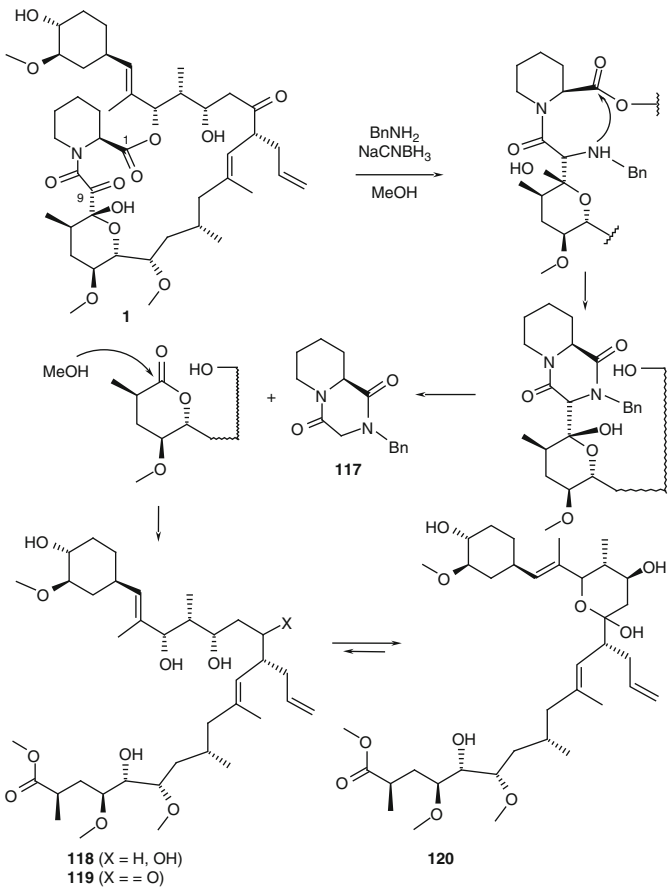

Scheme 30. Reductive cleavage of the C-1–C-9 unit of tacrolimus (**1**). The *long wavy lines* indicate partial structures

intermediate. Bishydroxylation of the C-9−C-10 double bond followed by *Dess-Martin* periodinane oxidation led to the tricarbonyl product **126**. Finally, removal of all protecting groups led to the 23-membered macrocycles **127–130** incorporating the appropriate amino acid. Interestingly, the analogues featuring 2-methyl-alanine or β-alanine exist preferentially in the seven-membered hemiketal-form.

Finally, mention must be made here of a novel photochemical amide cleavage reaction (*92, 105*). Thus, the photoproduct **112** upon oxidation of the C-9−OH gave the protected 6-methoxyascomycin analogue **131** in an excellent yield (Scheme 34). Irradiation of **131** in MeOH afforded the amide cleavage product **132** in a good yield. The reaction most probably proceeds through the zwitterionic intermediate $\mathbf{Z_3}$, which is attacked by MeOH on C-8=O instead of the usually observed attack on C-6. It is interesting to note that similar cleavage reactions have also been reported on other protected and, surprisingly, also on the unprotected ascomycin

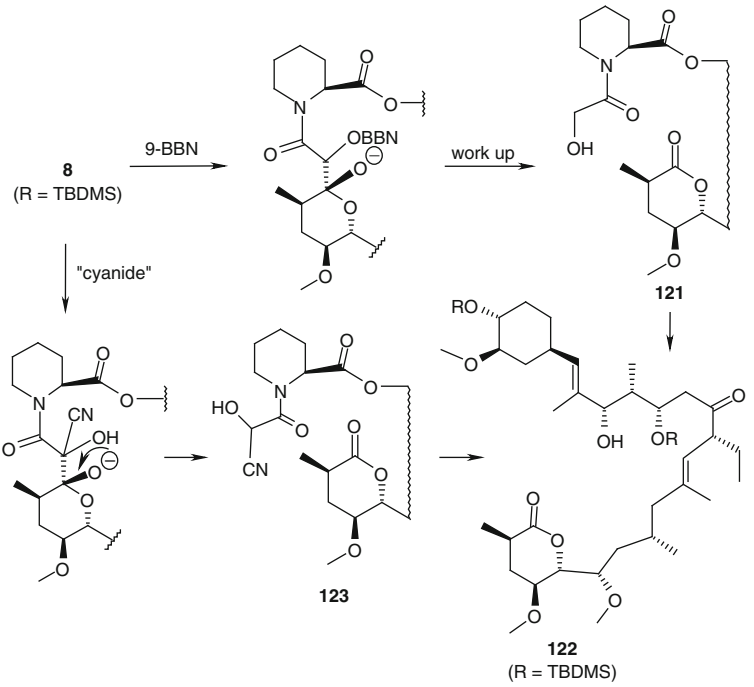

Scheme 31. Cleavage reactions in the binding domain of 24,33-bis-*O*-TBDMS-ascomycin (**8**). The *long wavy lines* indicate partial structures

analogues. The product **132** is a potentially useful intermediate for semisynthetic modifications, but this has not been explored further. Biological activities of the compounds in this section have not been reported.

2.4. Modifications in the Effector and Cyclohexyl Domains

Several modifications have been done on the effector parts of tacrolimus (**1**) and ascomycin (**2**). Whereas treatment of tacrolimus (**1**) with strong bases led to degradation of the molecule, treatment with 1,5-diazabicyclo[4,3,0]nonane (DBN) in CH_2Cl_2 at room temperature led to isomerization at C-21, affording a 1:2 equilibrium mixture of **1** and the C-21−epimer **133** (Scheme 35) (*106*). The isomer **133** was isolated and the structure established by X-ray crystal structure analysis. Compound **133** binds well to macrophilin but showed very weak immunosuppressive activities in cells (*74*). Acid-catalyzed dehydration of ascomycin (**2**) gave 23,24-dehydroascomycin (**134**), which was hydrogenated to give 24-desoxyascomycin (**135**) (*74, 107*). Whereas the dehydro derivative **134** showed only weak *in vitro* and *in vivo* activities, the desoxyascomycin **135** was as active as

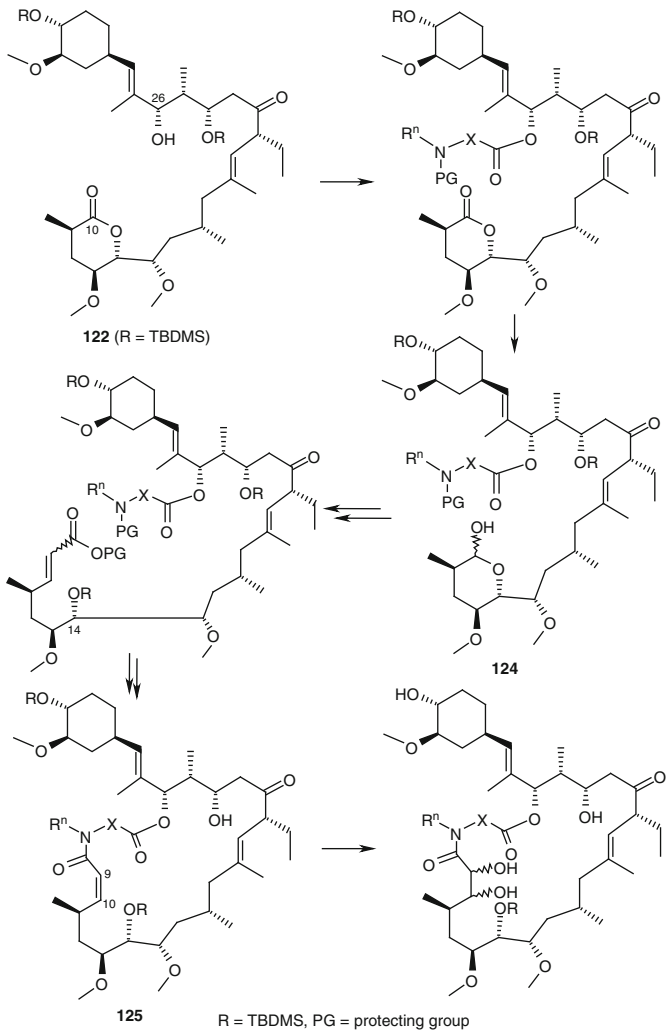

Scheme 32. Synthesis of amino acid analogues of ascomycin (**2**) starting from fragment **122**

ascomycin (**2**). NMR structures of the complexes formed between macophilin and **2** or **135** were found to be very similar, suggesting that hydrogen-bonding interactions with the C-24−OH are not important for complex formation.

Numerous derivatives of the formula **136** with modifications on the terminal carbon of the allyl group of tacrolimus (**1**) have been prepared employing the olefin cross metathesis reaction (Scheme 35). These were employed as modules for the assembly of chemical inducers of dimerization (CIDs) (*108*, *109*).

Several derivatives of **2** with modifications at C-18 were prepared through allylic oxidation (Scheme 36) (*110*). Thus, oxidation of **2** by selenium oxide and *t*-butyl

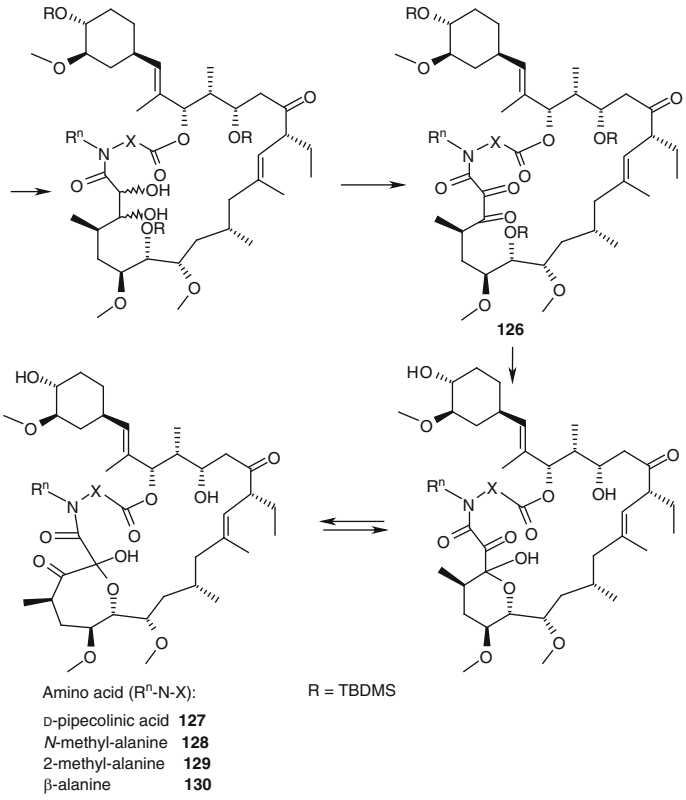

Scheme 33. Synthesis of amino acid analogues of ascomycin (**2**) starting from fragment **122**, continued from Scheme 32

hydroperoxide in dichloromethane afforded the hydroxyascomycin **137** (R=(18*S*)-OH), also referred to in literature as L-685818, in addition to side products arising through dehydration at C-23−C-24. None of the (18*R*)-isomer was formed in this reaction. On the other hand, under the same reaction conditions, oxidation of the 24,33-bis-silyl derivative **8** gave the corresponding 18-hydroxy derivatives as a mixture of isomers from which the (18*R*)-isomer **137** (R=(18*R*)-OH) could be obtained after its separation and desilylation. The 24,33-bis-silyl protected (18*R*/*S*)-OH derivatives could be oxidized and desilylated to the oxo analogue **138**. The 24,33-bis-silyl-protected (18*S*)-OH derivative could be acylated and desilylated to give (18*S*)-acetoxy, -iodoacetoxy, and -benzoyloxy derivatives of the formula **137**. Whereas 24,33-bis-silyl-ascomycin could be deprotected in excellent yield, the corresponding 24,33-bis-silyl-18-hydroxy analogues were, because of the allylic nature of the additional hydroxy group, sensitive to the usual desilylation conditions and resulted in the cyclic derivatives **139** and **140** as side products. (18*R*/*S*)-Hydroxyascomycins bind tightly to macrophilin and are potent inhibitors of rotamase (PPIase) activity, but do not show any immunomodulatory activity

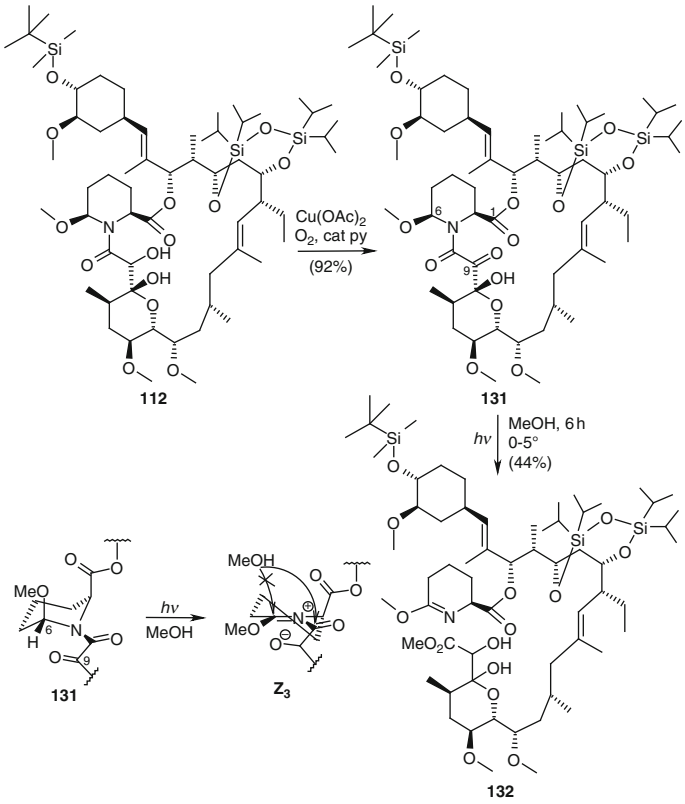

Scheme 34. A novel photochemical amide cleavage reaction of derivative **131**

in vitro or *in vivo* despite their good bioavailability. Further, they reversed the inhibition of calcineurin caused by the tacrolimus/macrophilin complex. This indicated clearly that the immunomodulatory activity has nothing to do with the inhibition of the PPIase activity of tacrolimus/macrophilin. Later, it was demonstrated that binding of the initially formed tacrolimus/macrophilin complex to calcineurins A and B is necessary for immunomodulatory activity.

Reaction of 33-*O*-TBDMS-ascomycin (**141b**) with *t*-butyldimethylsilyloxy-1-methoxyethene in the presence of $BF_3.Et_2O$ resulted in the addition of a methoxycarbonylmethyl unit to the C-22=O (Scheme 37) (*111*). The resulting aldol product upon treatment with 1 *N* HCl underwent 33-*O*-desilylation and concomitant intramolecular esterification leading to the lactone **142**. The product **142** then underwent facile acid-catalyzed dehydration to give the unsaturated lactone **143**. The enone **144**, which could be prepared through treatment of **141b** with methanesulfonyl chloride and excess of 4-dimethylaminopyridine, also underwent 1,2-addition upon treatment with *t*-butyldimethylsilyloxy-1-methoxyethane in the presence of $BF_3.Et_2O$, resulting in the corresponding silyl derivative, which could be desilylated to afford **145** as a single isomer with an unknown

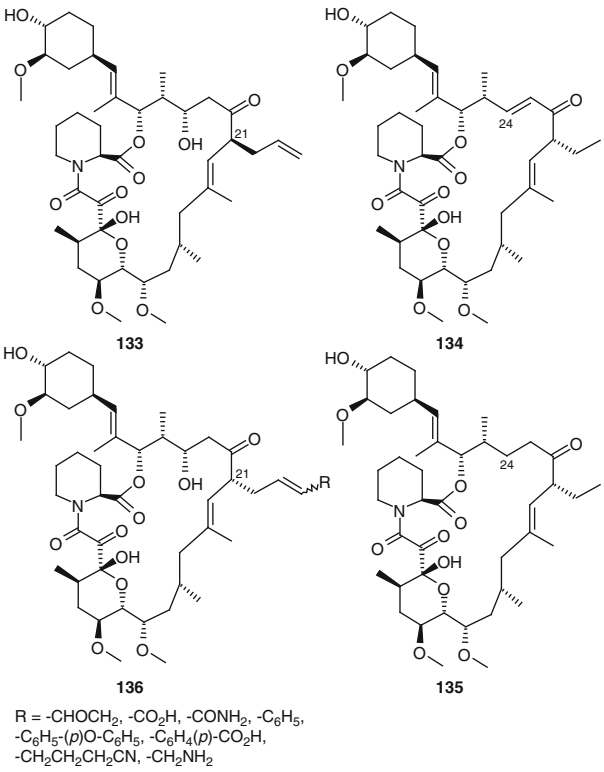

Scheme 35. 21-*epi*-FK506 (**133**), 24-desoxyascomycin (**135**) and olefin cross-metathesis derivatives of tacrolimus (**1**) **136**

C-22−configuration. On the other hand, the enone **144** underwent predominant 1,4-addition upon reaction with *t*-butyldimethylsilyloxy-1-methoxyethane in the presence of $LiClO_4$ in dichloromethane, providing the methyl ester **146** (as a single isomer of unknown stereochemistry) after desilylation (Scheme 38). Further, hydrosilylation of **144** gave the enol ether **147**, which could be employed in aldol reactions leading to **148a** and **148b**, as single isomers of unknown configuration at the newly formed stereocenters, featuring modifications at C-23.

Novel cyclopropano dervatives could be prepared using carbene chemistry. Thus, both tacrolimus (**1**) and ascomycin (**2**) were transformed to their hydrazones **149a** (62%) and **149b** (56%) (Scheme 39) (*112*). Treatment of the hydrazones **149a** and **149b** with excess manganese dioxide in dichloromethane resulted in several products. However, reaction in methanol under the same conditions led to the cyclopropano derivatives **150a** and **150b** as the main products; no biological activities are reported.

Numerous pyrazole analogues of ascomycin (**2**) have been prepared (Scheme 40) (*113*). Thus, the 33-*O*-TBDMS derivative **141b**, upon oxidation with DMSO and oxalyl chloride followed by desilylation with HF/aceteonitrile, gave a 91% yield of

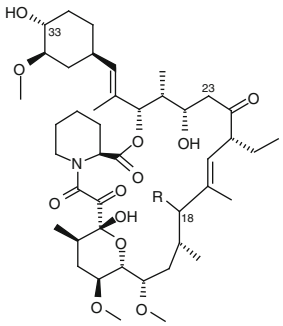

137

R = (18*R*)-OH, (18*S*)-OH, (18*S*)-OAc, (18*S*)-OBz, (18*S*)-$OCOCH_2I$

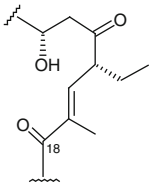

138

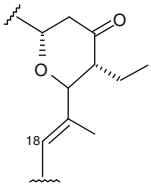

139

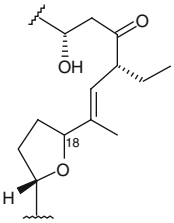

140

Scheme 36. 18-Hydroxyascomycin (**137**) and its derivatives **138–140**

151, which upon treatment with hydrazine, afforded a mixture of the isomeric pyrazoles **152** (R=H) and **153** (R=H). The substituted pyrazoles **152** and **153** were prepared either through alkylation of the 33-*O*-TBDMS-protected unsubstituted pyrazoles, or through reaction of **151** with substituted hydrazines followed by chromatographic separation of the isomers. No biological activities were reported.

Several modifications in the cyclohexyl domain have been reported. Thus, activation of C-33−OH of the 24-*O*-TBDMS-ascomycin **154** as its triflate, followed by treatment with triethyl amine in dichloromethane at 45°C for 2 days and at room temperature for 2 days, resulted in an inseparable 3:1 mixture of the two isomers **155** and **156** in a 30% yield and the enol ether **157** (3% yield) (Scheme 41) (*114*). Osmium tetroxide-catalyzed c*is*-hydroxylation of the mixture **155** + **156** using *N*-methylmorpholine *N*-oxide in THF at room temperature for 2 days, followed by separation and desilylation of the individual isomers, afforded (34*R*)-hydroxyascomycin (**158**) and the 31,32-dihydroxy-33-methoxy analogue **159**. Interestingly, the introduction of an additional hydroxy group increased the solubility of compounds **158** and **159** by 300- and 150-fold compared to ascomycin (**2**) at pH 6.5. Compound **158** showed *in vitro* and *in vivo* activities comparable to those of ascomycin.

Several 33-*epi*-amino derivatives of ascomycin and its 24-desoxy analogue have been synthesized (Scheme 42) (*115*). Thus, the C-33−OH of 24-*O*-TBDMS-ascomycin (**154**) was activated as its *o*-nitrobenzenesulfonate (*o*-nitrobenzenesulfonyl

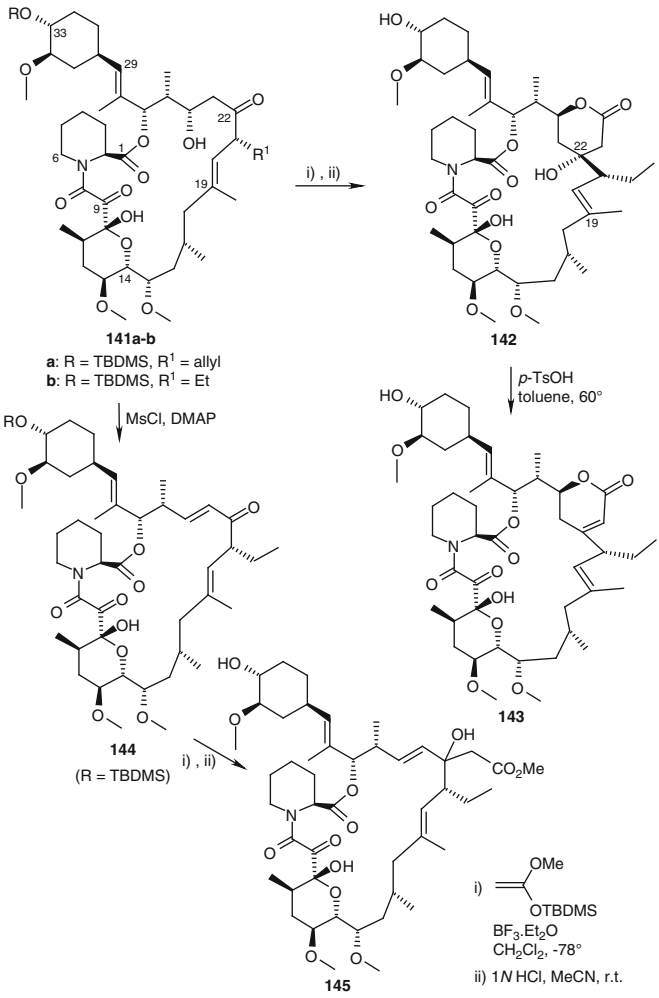

Scheme 37. Derivatives of ascomycin (**2**) with modifications in the C-22–C-24 region

chloride, triethyl amine, DMAP, CH_2Cl_2) and transformed to the 33-*epi*-azide through treatment with sodium azide in DMF at 60°C. Reduction of the azide with triphenyl phosphine in a mixture of THF and water at refluxing temperature afforded the 33-*epi*-amino-ascomycin **160** (R=H) in a 73% yield over three steps. Starting from **160** (R=H) several amides and carbamates have been synthesized. Similarly, from the 24-desoxyascomycin **135** the 33-*epi*-amino derivative **161** ($R=NH_2$) was synthesized, from which several amino analogues were prepared through condensation with aldehydes in THF, followed by reduction with sodium cyanoborohydride. The activities of these compounds in inhibiting T-cell proliferation were reported. Briefly, the 33-*epi*-amino analogue **160** (R=H) was tenfold less

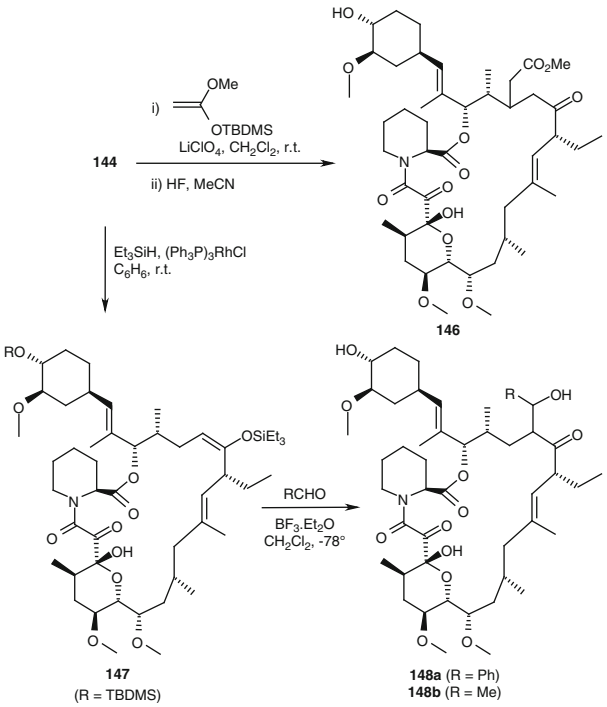

Scheme 38. Derivatives of ascomycin (**2**) with modifications in the C-22–C-24 region; continued from Scheme 37

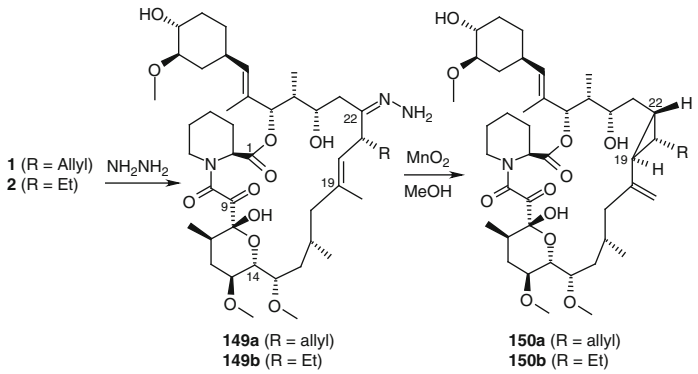

Scheme 39. Transformation of tacrolimus (**1**) and ascomycin (**2**) to the cyclopropano- analogues **150a** and **150b**

active than ascomycin; this loss was partially recovered by removing the 24-OH group. Among the carbamate derivatives, the methyl carbamate **160** (R=MeOCO-) showed activity closest to that of ascomycin.

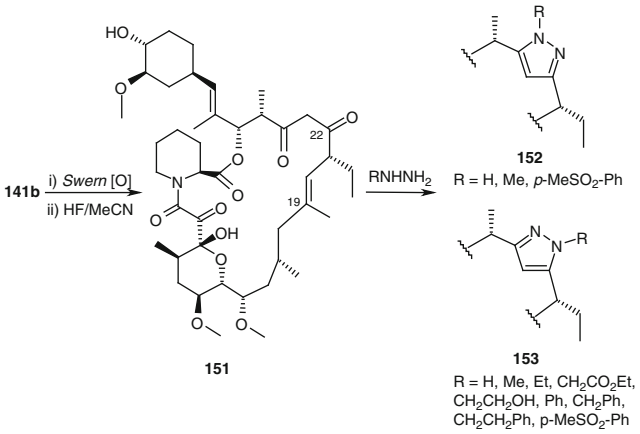

Scheme 40. Transformation of 33-*O*-TBDMS-ascomycin (**141b**) to the pyrazole analogues **152** and **153**

Pimecrolimus (**2a**) is prepared through selective chlorination of **2** using dichloro-triphenyl-phosphorane in a good yield (Scheme 43) (*116*). Other replacements of the C-33−OH of ascomycin by halogens or pseudohalogens were also reported (*116*, *117*, *118*). Further, the (33*R* or *S*)-*O*-cyano derivative **162** is easily accessible from **2** (*117*). Starting from **162** the derivatives **163**–**169** (SDZ 281–240 is a mixture of **169a** and **169b**) could be prepared easily (*117*, *118*). Of these derivatives, 33-*epi*-ascomycin (**163**) and 33-desoxy-32-oxo-ascomycin (**167**) showed good activities in a MLR (mixed lymphocyte reaction), but were, however, only weakly active in the animal models of ACD. Noteworthy is the observation that the *cis*-isomer **169b** is by a factor of 2 more active than the *trans*-isomer **169a**, in *in vitro* and *in vivo* models.

Several carbamate derivatives at C-33 have been prepared starting from 24-*O*-TBDMS-ascomycin (**154**) (Scheme 44) (*119*). Thus, reaction of **154** with the appropriate acyl isocyanate or acyl isothiocyanate followed by desilylation afforded the acylated carbamate **170a** and the acylated thiocarbamates **170b**-**h**. The hydrazide derivative **170i** was prepared through reaction of ascomycin (**2**) with triphosgene giving the corresponding 33-*O*-chloroformate selectively, followed by its reaction with phenyl hydrazine. Binding to macrophilin and the *in vitro* immunomodulatory activities were demonstrated; derivatives **170a** and **170i** showed activities similar to ascomycin (*119*).

Numerous C-33−ether derivatives were prepared by O-alkylation of 24-*O*-TBDMS-ascomycin (Scheme 44). Thus, reaction of **154** with allyl 2,2,2-trichloroacetimidate in the presence of a catalytic amount of trifluoromethane sulfonic acid gave **171a**, which after desilylation using HF in acetonitrile, afforded the allyl ether **171b** in a 75% yield (*120*). Similarly, the unsubstituted cinnamyl ether **171c** and several analogues of **171c** with electron-withdrawing and -releasing substituents on the phenyl ring have been synthesized. Further, using the same method, several analogues of **171d** featuring alkyl, alkenyl, alkynyl, aralkyl, aralkenyl, and aralkynyl units, were prepared and their binding to macrophilin

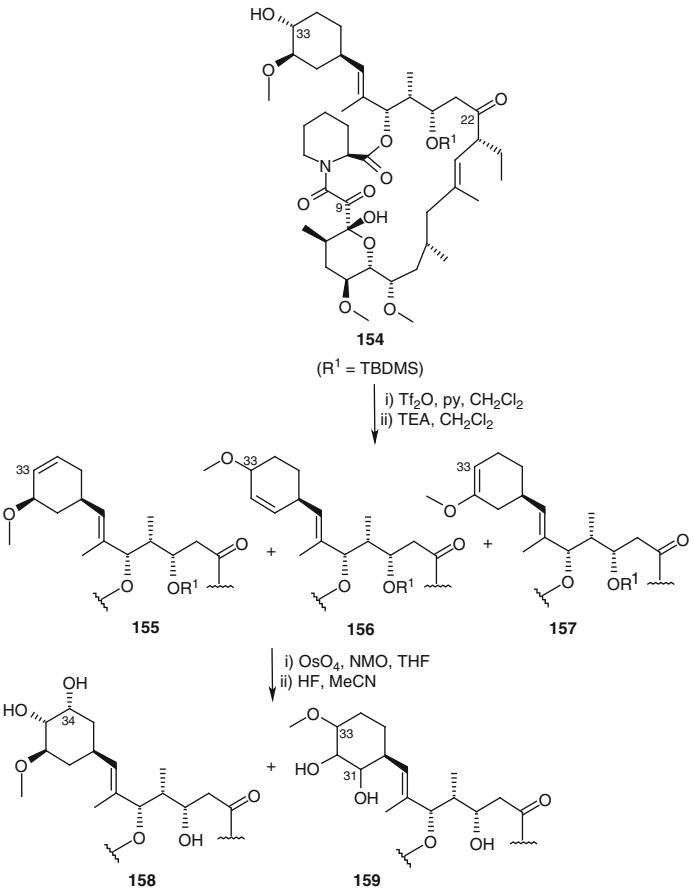

Scheme 41. Synthesis of the hydroxylated derivatives **158** and **159**

and inhibition of T-cells studied. It is interesting to note that **171c** and the corresponding *m*- and *p*-hydroxy cinnamyl ethers, in spite of their relatively weaker binding, showed inhibitory activities on T cells comparable to those of ascomycin. However, they were reported to be less efficacious *in vivo* especially upon oral administration (*121*). In further studies aimed at optimizing the linker between the C-33−O and the phenyl groups, the 24-silyl protected allyl ether **171a** was transformed to the aldehyde **171e** by osmium tetroxide-catalyzed hydroxylation followed by cleavage using sodium periodate in aqueous THF, in an overall yield of 64%. Starting from the valuable intermediate **171e**, using the sequences reductive amination followed by desilylation, or, reduction to alcohol, displacement of a trichloro acetimidate, followed by desilylation, ether derivatives of the type **172** (R=alkyl, aryl; tether=secondary amine or ether) with varying tethers were synthesized. Further, the aldehyde **171e** was transformed to several imidazol-2-yl-methyl ether derivatives of type **173** (R^1=H, Et; R^2=H, Me, Ph, substituted-Ph)

Scheme 42. Synthesis of the 33-*epi*-amino analogues **160** and **161** of ascomycin (**2**) and 24-desoxyascomycin (**135**)

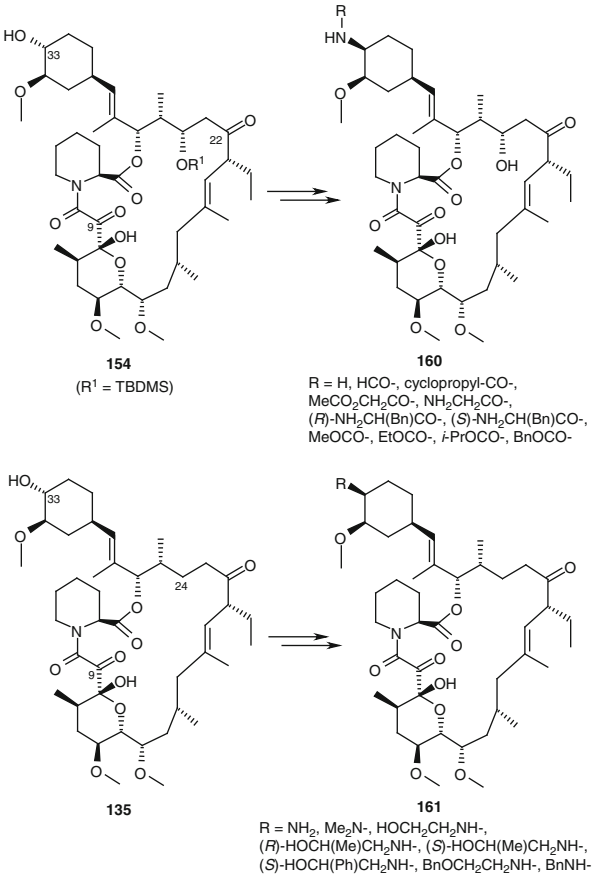

with different substituents on the imidazole ring. Among the compounds investigated, derivative **173** (R^1=H, R^2=3,5-dimethoxyphenyl), referred to as L-733,725, was reported to have *in vivo* activities comparable to those of tacrolimus and a better therapeutic index. A convergent practical synthesis was developed and was used for synthesizing multi-kilogram quantities of L-733,725 of consistently high purity (*122*). Furthermore, labelled L-733,725 carrying a ^{14}C-label on the CH_2 of the side chain was also synthesized for utilization in animal and human drug metabolism studies (*123*).

In a similar study, several 33-*O*-ether derivatives featuring a phenyl group connected through a carbon tether of varying length were synthesized (Scheme 45) (*124*). The synthesis started from the aldehyde **171e** and proceeded through addition of an organomagnesium bromide to the aldehyde, followed by transformation of the resulting alcohol to the corresponding trifluoro acetate, its elimination, selective hydrogenation of the resulting double bond and, finally, deprotection of the C-24−O−silyl group leading to the compounds **174a** (R=$PhCH_2CH_2$, $PhCH_2CH_2CH_2$); the biological data were compared with **174a** (R=Ph, $PhCH_2$)

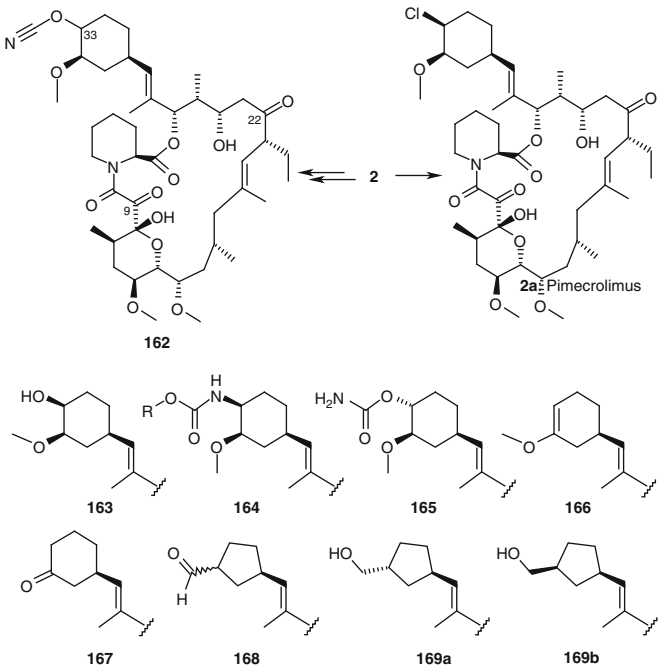

Scheme 43. Transformation of ascomycin (**2**) to several analogues *via* the 33-*O*-cyano-derivative **162**, and, synthesis of pimecrolimus (**2a**) and the individual isomers **169a** and **169b** of SDZ 281–240

(*125*). The derivatives **174b** bearing hydroxy or keto groups on the carbon tether have also been synthesized using similar strategies. A two-carbon tether provided optimum *in vitro* activity. The acetophenone derivatives **174b** (R=$PhCOCH_2$) showed efficacy in models of immunosuppression. However, it was found that they were rapidly converted to the arylhydroxy ether products when incubated in rat blood. Hence, an extensive series of substituted arylhydroxy ethers **174c** were synthesized using analogous chemistry (*126*). Several of these compounds showed potent *in vitro* and *in vivo* immunosuppressive activities. The derivative **174c** (R=2-naphthyl-$CHOHCH_2$-) was claimed to have an improved therapeutic index compared to tacrolimus (**1**) (*126*).

Using pentavalent bismuth derivatives ($Ar_3Bi(OAc)_2$, CH_2Cl_2, THF) the C-33−OH of ascomycin (**2**) could be preferentially arylated leading to compounds of type **177a** in yields ranging from 14% to 72% (Scheme 45) (*125*, *127*). Similarly, starting from the C-33−O-desmethyl analogue **176**, derivatives **177b** and **177c** could be synthesized. Among the derivatives of the type **177a** (R^1=Me, R^2=Ph), **177b** and **177c**, those with electron-donating substituents such as HO and Me_2N in the *para*- position of the phenyl group, showed better *in vitro* immunosuppressive activities. The two indole ether derivatives of the type **177a** turned out to be the best in the series, being even superior to the parent macrolide **2** by a factor of 3 in *in vitro* immunosuppression. The two derivatives **175a** and **175b**, prepared from

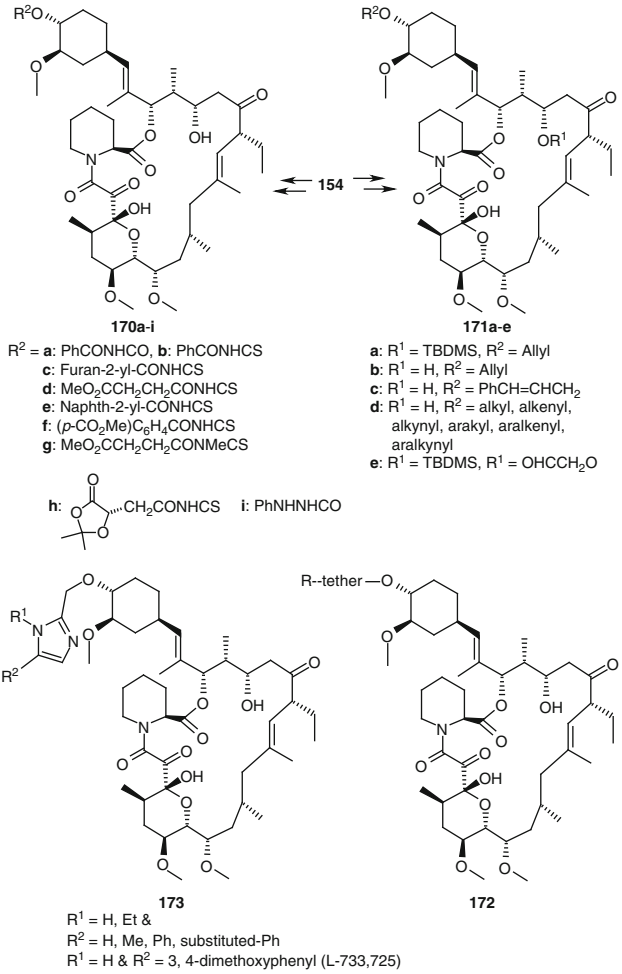

Scheme 44. Synthesis of 33-*O*-acyl, 33-*O*-thioacyl, and 33-*O*-ether derivatives of ascomycin (**2**)

(18*S*)-hydroxyascomycin (**137** (R=(18*S*)-OH) using a similar method, showed 8- to 15-fold weaker immunosuppressive activities compared to **2**.

The C-33−OH group of **2** could be etherified selectively by rhodium (II) acetate-catalyzed insertion of benzyl diazoacetate in dichloromethane affording **178** (R=Bn), from which the corresponding acid **178** (R=H) could be obtained by hydrogenolysis of the benzyl ester (Scheme 46) (*128*). Starting from the acid, ester and amide derivatives of types **178** and **179** were prepared. While the carboxylic acid **178** (R=H) did not show any *in vitro* activity, the ester and amide derivatives showed potent T-cell inhibitory activities. Surprisingly, hydrophobic amides were reported to have weakened macrophilin binding by several orders of magnitude, while maintaining potent activity to inhibit T-cell activation (*128*).

Scheme 45. Synthesis of ether derivatives at the C-31 and C-33 positions of ascomycin (**2**)

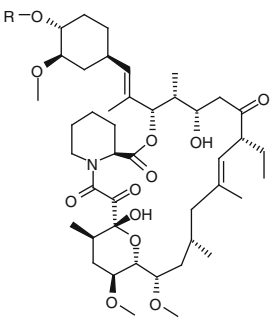

174a-c

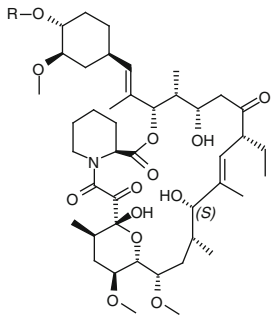

175a-b

a: R = 2-naphthyl
b: R = *N*-methyl-5-indolyl

a: R = Ph, $PhCH_2$, $PhCH_2CH_2$, $PhCH_2CH_2CH_2$
b: R = $OHCH_2CH_2$, $PhCHOHCH_2$, $PhCOCH_2$, $PhCH_2CO$, $PhC(=CH_2)CH_2$
c: R = $ArCHOHCH_2$

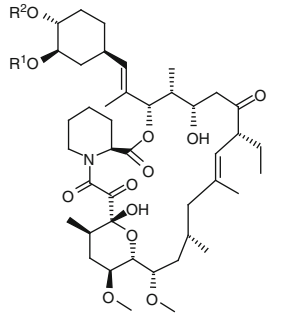

177a-c

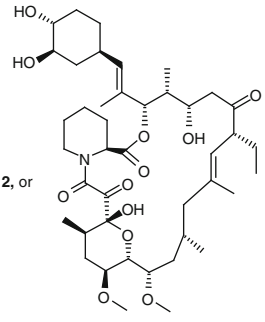

176

Prepared from **2:**
a: R^1 = Me, R^2 = substituted Ph, 2-naphthyl, 5-indolyl, *N*-methyl-5-indolyl
Prepared from **176:**
b: R^1 = H, R^2 = substituted Ph
c: R^1 = substituted Ph, R^2 = H

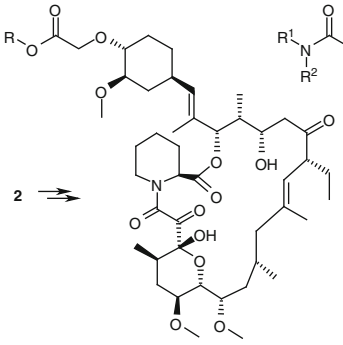

178
R = H, Et, Bn

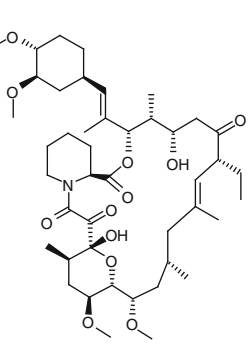

179a-b

a: R^1 = H, and R^2 = cyclohexyl, Ph, substituted aryl, Bn, CH_2CH_2Ph
b: R^1 = Me, and R^2 = Bn, CH_2CH_2Ph

Scheme 46. Diverse esters and amides of the ascomycin-33-*O*-acetic acid skeleton

Derivatives like **180** featuring a heterocycle at C-33 have been prepared through selective activation of C-33−OH as its triflate, followed by its displacement by nitrogen of a small heterocycle (Scheme 47) (*129*). Further, selective activation of C-33−OH as a *p*-nitrophenylcarbonate, followed by reaction with nitrogen nucleophiles afforded the carbamates **181**. The tetrazole **180** (R=tetrazol-1-yl), also referred to as ABT-281, was reported to be equipotent to tacrolimus (**1**) in the swine contact hypersensitivity model after topical application, despite its several-fold lower potency for inhibiting swine T cells *in vitro*. The high activity was consistent with its superior skin penetration. Further, it was found to exhibit a three- to fivefold more rapid pharmacokinetic elimination in the rat, swine, and monkey, in addition to showing a substantial reduction in potency for immunologic responses in all three species after systemic administration. These features of ABT-281 were claimed to result in both efficacy and a high margin of safety for topical therapy of skin disease as compared to tacolimus (*129*).

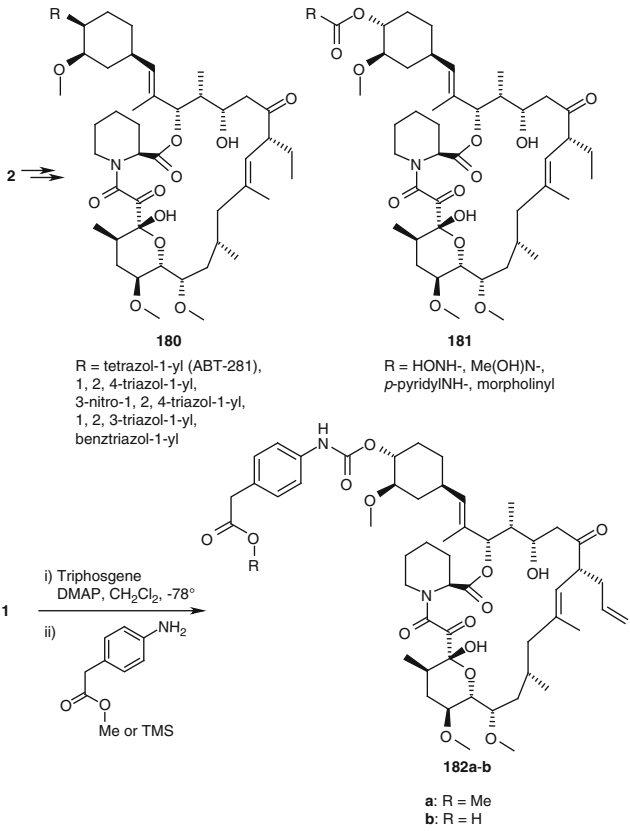

Scheme 47. Derivatives of ascomycin (**2**) featuring a heterocyclic unit on C-33, and diverse 33-*O*-carbamoyl-type derivatives of **1** and **2**

Tacrolimus was transformed to the carbamates **182a** and **182b** through activation of the C-33−OH as its chloroformate followed by reaction with *p*-amino-phenylacetic acid methyl ester, leading to **182a** in a 70% yield, or, with *p*-amino-phenylacetic acid trimethylsilyl ester followed by hydrolysis providing the acid **182b** in a 26% yield (*130*). Compound **182a** could also be prepared through activation of C-33−OH as its *p*-ntrophenyl carbonate followed by quenching with the amine. The carbamate **182a**, also referred to as MLD987, inhibited the activation, proliferation and release of cytokines from T-cells with IC_{50} values in the low nanomolar range. Furthermore, in a brown Norway rat model of allergic asthma, **182a**, when given into the airways by intertracheal administration (ED_{50} = 1 mg/kg) or by inhalation (ED_{50} = 0.4 mg/kg), potently reduced the influx of leucocytes into the bronchoalveolar fluid. Interestingly, **182a** had an appreciably

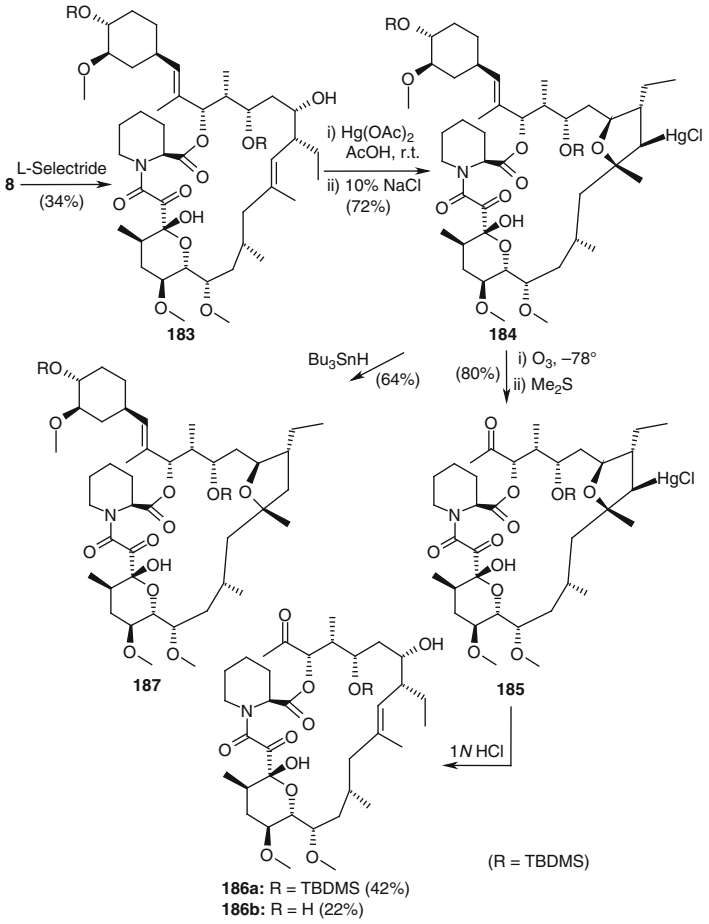

Scheme 48. Transformations using oxymercuration and ozonolysis resulting in the derivative **187** and the cleavage product **186b**

weaker activity when given orally and intravenously. Furthermore, pharmacokinetic evaluations showed that **182a** had a low oral and pulmonary bioavailability. In addition, **182a** was metabolized in the blood to the much less potent acid **182b**. These aspects indicated a potential of **182a** to serve as a soft drug after local application for therapy of asthma.

With a view to synthesizing derivatives with new substituents in place of the cyclohexyl moiety, a strategy was designed for chemoselective cleavage of the C-28 = C-29 double bond. Thus, the bis-silyl-protected ascomycin **8** was reduced stereo- and regioselectively at C-22=O giving the alcohol **183** in a 34% yield, which was then subjected to oxymercuration leading to the tetrahydrofuran **184**, thus protecting the C-19 = C-20 double bond against ozone (Scheme 48) (*131*). Ozonolysis of **184** afforded the ketone **185** in an excellent yield. Further, acidic hydrolysis of the organomercurial chloride afforded the required derivatives **186a** and **186b**. Finally, tributyl tin hydride reduction of **184** afforded the analogue **187**. The derivatives **188** and **189** could also be synthesized in an analogous manner (Scheme 49).

Starting from **8**, using K-selectride instead of L-selectride, the isomer **190** was prepared analogously to the synthesis of **186** (Scheme 50) (*132*). The C-27 = O keto group was then used for preparing derivatives of the types **191** and **192**. The required C-22 = O carbonyl could be re-established through oxidation leading to the 24-*O*-silyl derivatives **193** featuring novel replacements for the cyclohexylvinylidene unit. Several attempts to establish a carbon-carbon double bond at C-28 of **190** *via* a *Wittig* or *Wittig-Horner* olefination were unsuccessful and no reaction was observed. However, reaction of **190** with acetylmethylidenephosphorane ($CH_3COCH = PPh_3$) under forced conditions (65°C, 10 days) led to furano derivatives through reaction at the tricarbonyl region.

From the fermentation broth of *Steptomyces tsukubaensis* 9993, the novel ring-contracted metabolite *iso*-FK506 (**197a**) was isolated (Scheme 51) (*133*). A synthetic pathway for the transformation of tacrolimus to **197a** has been established (*134*). Thus, *Evans*' reduction of 33-*O*-TBMDS-FK506 (**141a**) afforded the (22*S*)-dihydro derivative **194a** in a good yield. Treatment of **194a** with DMAP in DMF

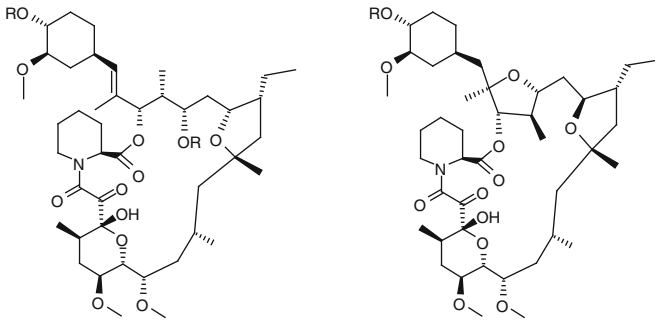

Scheme 49. Derivatives **188** and **189** prepared in an analogous manner to those in Scheme 48

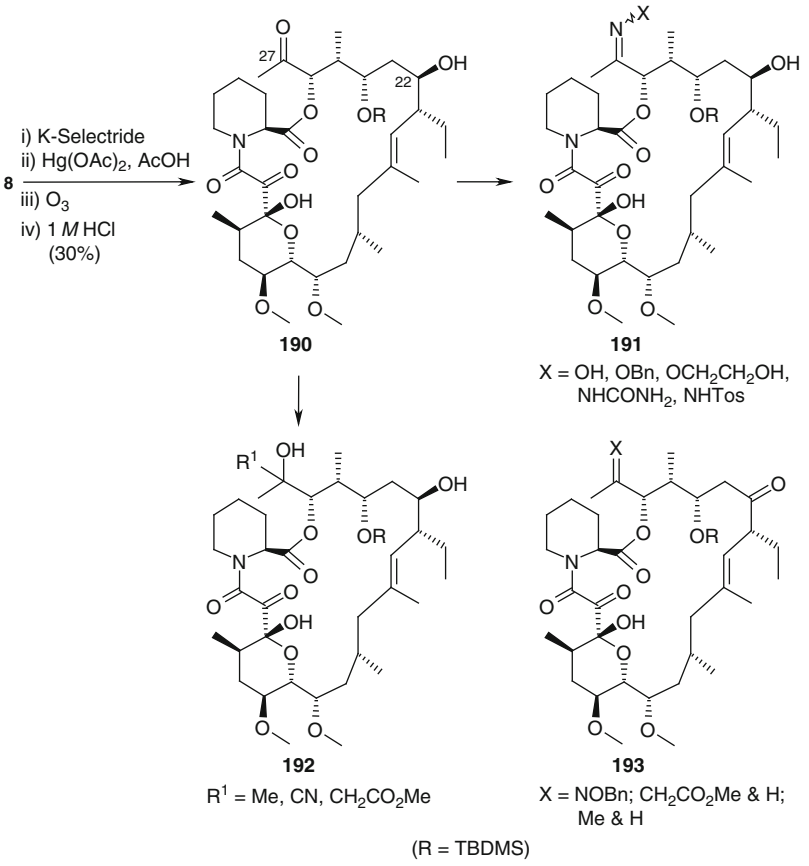

Scheme 50. Derivatives of ascomycin (**2**) featuring novel replacements for the cyclohexylvinylidene subunit

brought about acyl migration, giving **195a**. Attempts to oxidize the C-22−OH group selectively were not successful. However, after protection of the C-26−OH as its TMS derivative **196a**, oxidation using TPAP followed by desilylation afforded the *iso*-FK506 **197a**. The chemistry of the ethyl analogue **197b** followed in an analogous manner.

Under the usual desilylation conditions employing aqueous HF, the 22-dihydro *iso*-ascomycin derivative **198b** underwent intramolecular cyclization through attack of the C-22−OH on C-26 leading to the tetrahydropyran **199** in a 36% yield (Scheme 52) (*135*). On the other hand, **198a** could be desilylated using 1*N* HCl and transformed to the epoxide **200**. Interestingly, **200** upon treatment with $BF_3.Et_2O$, underwent acyl migration from 24-*O* to 22-*O*, followed by cyclization involving the released C-24−OH and the epoxide ring, affording the ring-contracted 19-membered macrolide **201** in a 38% yield.

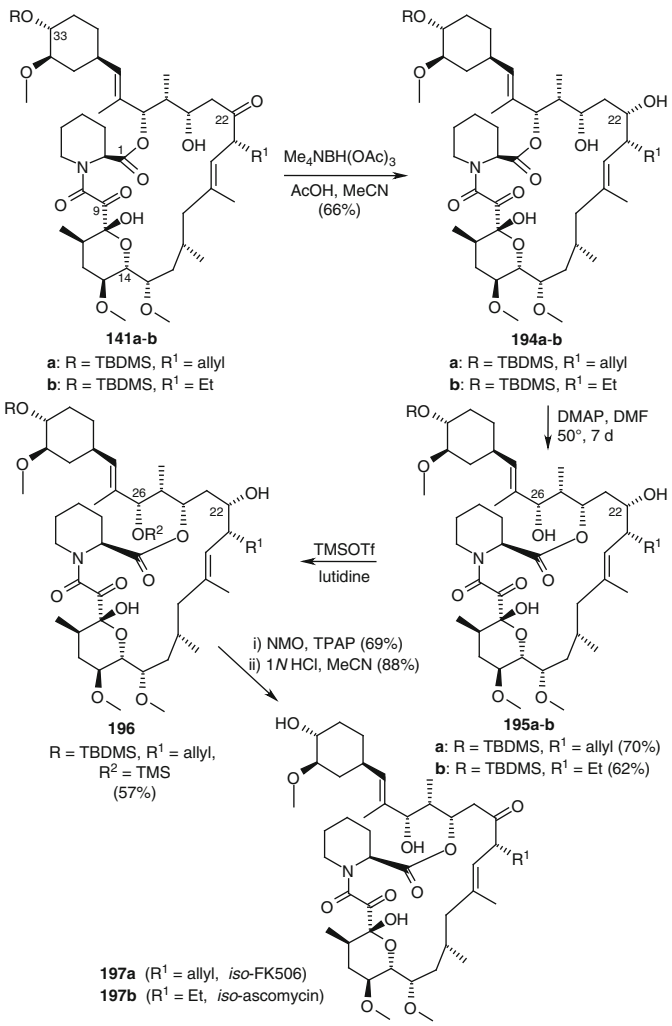

Scheme 51. Synthesis of *iso*-FK506 (**197a**) and *iso*-ascomycin (**197b**)

Several derivatives of *iso*-ascomycin featuring broad modifications in the cyclohexyl region have been synthesized. Thus, selective *cis*-hydroxylation of the C-27=C-29 double bond in a 33-*O*-TBDMS-*iso*-ascomycin (**195b**) with osmium tetraoxide led to **202** as a mixture of diastereomers, which were cleaved with periodate to give the aldehyde **203** as a valuable intermediate (Scheme 53) (*136*). Compound **203** exists predominantly as a 1:1 mixture of the anomeric hemiacetals formed through intramolecular addition of the C-22−OH to the C-26−aldehyde. The aldehyde group of **203** could be transformed to **204a** through *Wittig* reaction and to the oxime and hydrazone derivatives **204b-d** through condensation reactions.

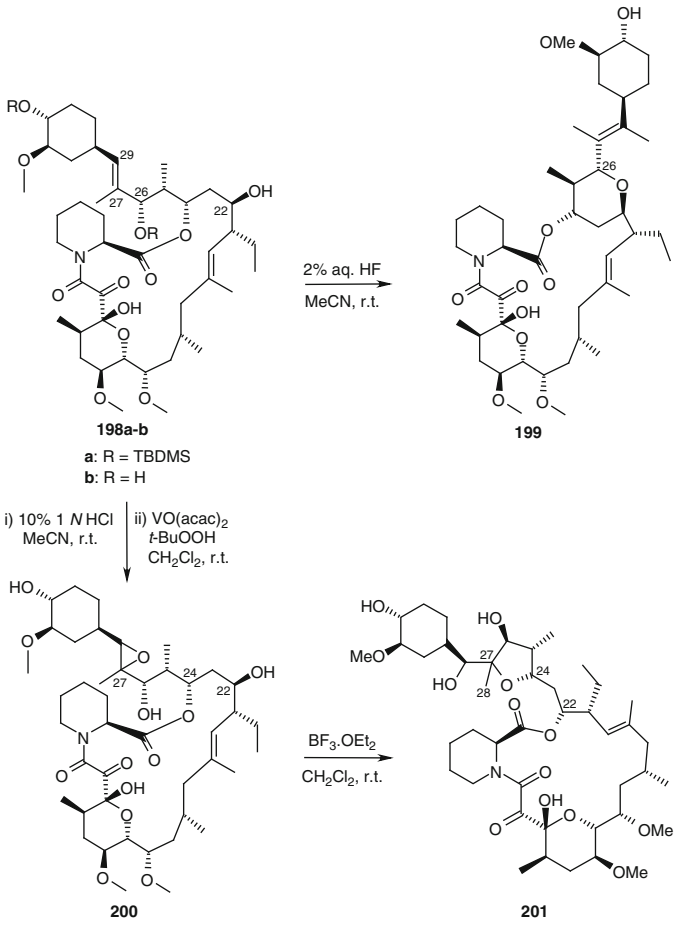

Scheme 52. Intramolecular cyclization, and ring-contraction reactions of 22-dihydro-*iso*-ascomycin (**198b**) leading to **199** and **201**

The derivatives **204a** and **204b** could be transformed to the analogues **205** (76%) and **206** (49%) through oxidation of the C-22−OH with *Dess-Martin's* periodinane.

In contrast to the chemistry observed with the (22*S*)-OH series (Scheme 52), osmium tetraoxide catalyzed dihydroxylation of the (22*R*)-dihydro-*iso*-ascomycin (**198b**) led to hydroxylation of both double bonds giving a 50% yield of the tetraol **207** as an isomeric mixture (Scheme 54) (*137*). Diol-cleavage using excess of sodium periodate led to the bis-*seco*-derivative **208**. Alternatively, **198b** could be transformed to **208** in a single step by ozonolysis followed by treatment with dimethyl sulfide.

Tacrolimus (**1**) is poorly soluble in water, and hence the conventional i.v. dosage forms contain surfactants such as cremophor EL or hydrogenated polyoxy 60 castor oil (HCO-60). Thus, towards increasing the water solubility of **1**, the methoxy-

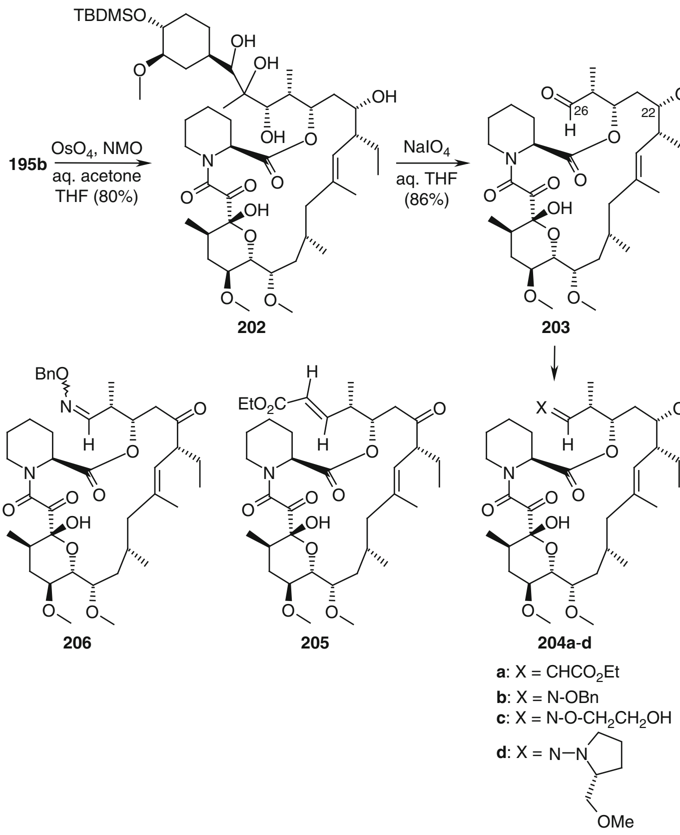

Scheme 53. Transformations of (22*S*)-diydro-33-*O*-TBDMS-*iso*-ascomycin (**195b**)

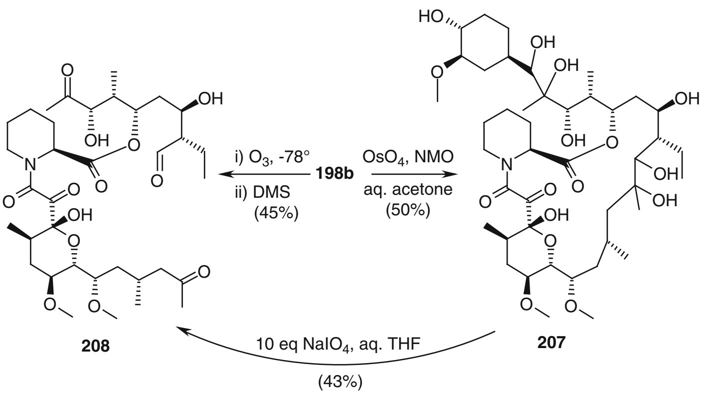

Scheme 54. Transformations of the (22*R*)-dihydro-*iso*-ascomycin **198b**

(polyethyleneglycol) (mPEG) conjugates **209d**, **209e**, and **209f** were synthesized by esterification of **1** with iodoacetic acid using dicyclohexylcarbodiimide followed by chromatographic separation giving the individual iodoacetates **209a** and **209b** and **209c**, and displacement of the iodide with mPEG-SH in a mixture of acetonitrile and 0.1 *M* aqueous sodium hydrogen carbonate (Scheme 55) (*138*). The half-life of these conjugates in phosphate buffer (pH 7.4, 37°C) was *ca*. 20 h, showing acceptable stability; in human liver homogenates they decomposed readily with a half-life of 10 min and released the drug tacrolimus (**1**). This indicates their potential as useful water-soluble prodrugs. The effects of the derivative **209d** on the proliferation of T-cells, B-cells and mast cells, and on IgG production in human B-cells, and histamine release, were investigated *in vitro* (*139*). Further, *in vivo*

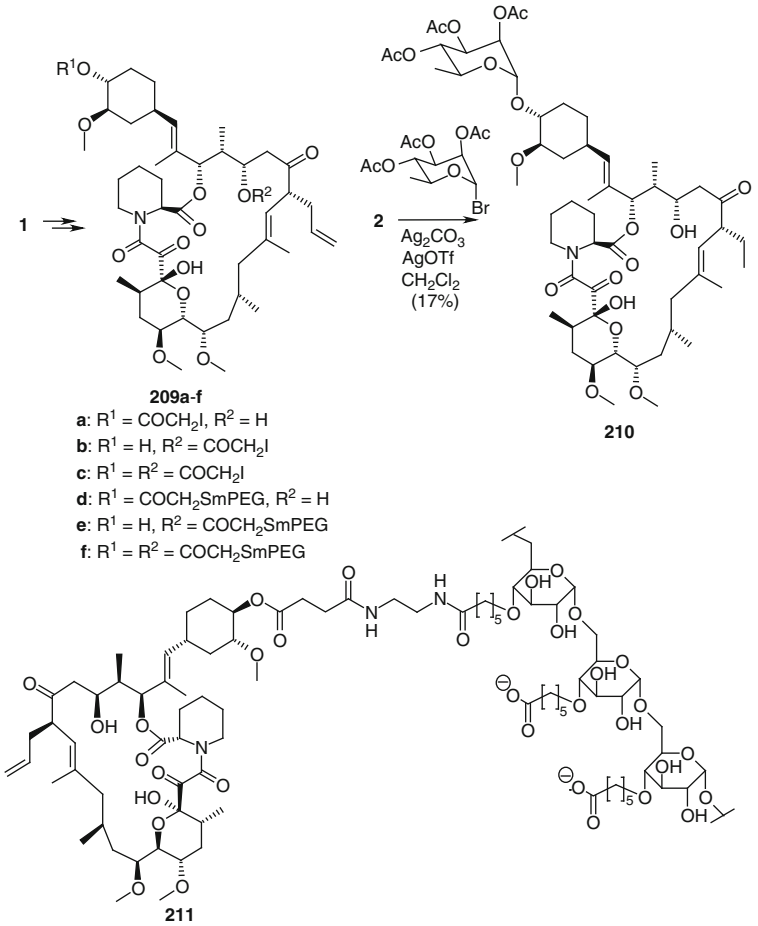

Scheme 55. Water-soluble prodrugs of tacrolimus **209d**, **209e**, **209f**, featuring methoxy-poleyethyleneglycol units attached through an ester linkage, a rhamnose derivative of ascomycin (**210**), and tacrolimus-C-6-dextran conjugate (**211**)

studies were performed on skin graft rejection in mice and in *Freund*'s adjuvant arthritis in rats. The results demonstrated that the mPEG derivative **209d** and tacrolimus have similar effects both *in vitro* an *in vivo*, thus indicating the former to be a useful prodrug with its advantageous physicochemical properties for preparing formulations for different applications.

With a view to developing a macromolecular prodrug of tacrolimus (**1**) with modified pharmacokinetic properties for systemic administration, the dextran conjugate **211** has been prepared (Scheme 55) (*140*). Thus, dextran (T-70) was O-alkylated with 6-bromohexanoic acid to give carboxy-*n*-pentyl-dextran (C6D); the free carboxylic acid groups were then modified through coupling with ethylene diamine to give C6D-ED. The free amino groups were in turn coupled through an amide bond to FK506-33-*O*-hemisuccinate, affording the conjugate **211**. The conjugate was estimated to contain 0.45% of tacrolimus (**1**) and the coupling molar ratio was approximately 1:1 (dextran:tacrolimus) (*141*). After incubation of the conjugate **211** in phosphate buffer (pH 7.4), tacrolimus was released and the half-life of the conjugate was 150 h. The *in vitro* immunosuppressive activity was reported to be almost comparable to that of free tacrolimus. *In vivo* biodistribution studies demonstrated that conjugation dramatically changes the pharmacokinetic properties of tacrolimus. After i.v. injection in rats, the AUC of the conjugate was reported to be almost 2000 times higher than that of free tacrolimus and organ uptake and clearances of the conjugate were significantly smaller than those of the free drug. However, no further activities have been reported.

Ascomycin (**2**) can be glycosylated at C-33−OH selectively using triacetyl-L-rhamnosyl bromide giving a 17% yield of the derivative **210** (Scheme 55) (*142*). Compound **210** showed good efficacy in *in vitro*, and in animal models including rat heart allograft rejection and rat adjuvant arthritis, and indicated a lower potential for neurotoxicity compared to tacrolimus.

Tacrolimus has been linked at C-33−OH through an ester or carbamate bond to several polymers for the purpose of affinity chromatography (*143*, *144*). Finally, several total syntheses (*145*–*155*) of tacrolimus and ascomycin, and also segments thereof, have been reported, and biosynthetic pathways discussed (*156*).

3. Summary

The discovery of the potent anti-inflammatory activity of the natural compounds ascomycin and tacrolimus in a new animal model of skin inflammation provided the first pharmacological evidence that calcineurin inhibitors of this type may represent a novel class for topical treatment of inflammatory skin diseases. A subsequent extensive medicinal chemistry effort finally resulted in the selection of the ascomycin derivative pimecrolimus for development, due to its favorable pharmacology and safety profile. Since 2001/2 the new class of topical calcineurin inhibitors represented by pimecrolimus cream and tacrolimus ointment has become

the first and only alternative to topical corticosteroids for treatment of inflammatory skin diseases such as atopic dermatitis.

Biological properties and clinical data of pimecrolimus are summarized. This compound differs from corticosteroids by selective action on T- and mast cells only, and by the lack of induction of skin atrophy and by less permeation through the skin. Pimecrolinus differs from other calcineurin inhibitors by specifically targeting skin inflammation, by a lower potential to affect systemic immune responses, and by its favorable skin penetration properties. Pimecrolimus cream 1% (Elidel®) has proven to be well tolerated, safe, and highly effective in extensive clinical studies in patients with atopic dermatitis and other inflammatory skin diseases.

Medicinal chemistry efforts aiming at understanding the structure-activity relationships required a detailed study of the chemical properties of the highly complex macrolactam structure of ascomycin and its derivatives, and elaboration and establishment of methodologies for selective transformations in various regions of the molecule. This chapter summarizes for the first time the chemical investigations in our laboratories and discusses the work published by others in this field as well. Furthermore, certain structure-activity relationships are described qualitatively.

Ascomycin (**2**) and tacrolimus (**1**) both exist as a mixture of several isomers in the macrophilin-binding region. Potential equilibrium products including the "furano-ascomycins" **13a**, **13b**, **13c**, and **13d** have been synthesized. The tricarbonyl moiety is highly sensitive and undergoes a benzilic acid-type of rearrangement, giving two diastereomers through two different pathways depending on the reaction conditions. Based on this, protocols were developed for the synthesis of labeled ascomycins. A new class of derivatives termed "cyclo-ascomycins" **44–47**, arising through cyclization in the binding domain, has been synthesized. In addition to other selective transformations in the binding region, photochemical investigations and further elaboration of the intermediates led to the biologically active 5,6-dehydro-ascomycin **99** and several other analogues. Using cyanide or 9-BBN, selective cleavage of C-1−C-9 was accomplished and semisynthetic strategies starting from the resulting fragment **122** led to the new analogues **127–130** featuring new amino acids. In the effector side of the molecule, several selective transformations such as allylic oxidation on C-18, epimerization of C-21, enumeration of the C-21−allyl side chain through *Grubbs*' cross metathesis reactions, and dehydration of C-24−OH leading to the enone 23,24-dehydroascomycin (**134**) were achieved. The protected enone **144** could be further transformed through selective addition reactions. Whereas the 21-*epi* derivative **133** did not show useful activities, 24-desoxyascomycin (**135**) was as active as ascomycin (**2**). On the cyclohexyl part of the molecule, demethylations, or introduction of additional hydroxy groups led to the more water-soluble derivatives **158** and **159**. Extensive derivatization of the C-33−OH has been achieved. Noteworthy is the ring contraction leading to SDZ 281–240, which was the first topical calcineurin inhibitor to demonstrate clinical proof of concept in patients with inflammatory skin disease. The cyclohexyl-methylidene group was cleaved off and new moieties could be

incorporated instead. Furthermore, *iso*-tacrolimus (**197a**), a ring-contracted derivative, also isolated from the fermentation broths, has been synthesized and its further chemistry summarized.

In conclusion, this chapter summarizes the extensive chemistry and biology studies on a natural product, which have resulted in a novel therapy approved worldwide. This helps underscore the importance of natural products as a versatile source of novel structures with unique biological activities.

Acknowledgments The authors thank Dr. *Anthony Winiski* for his assistance with the literature search and Dr. *Philipp Floersheim* for his support in the molecular modeling.

References

1. Goto T, Kino T, Hatanaka H, Okuhara M, Kohsaka M, Aoki H, Imanaka H (1991) FK506: Historical Perspectives. Transplant Proc **23**: 2713
2. Goto T, Kino T, Hatanaka H, Nishiyama M, Okuhara M, Kosaka M, Aoki H, Imanaka H (1987) Discovery of FK-506, a Novel Immunosuppressant Isolated from *Streptomyces tsukubaensis*. Transplant Proc **19**: 4
3. Tanaka H, Kuroda A, Marusawa H, Hashimoto M, Hatanaka H, Kino T, Goto T, Okuhara M (1987) Physicochemical Properties of FK-506, a Novel Immunosuppressant Isolated from *Streptomyces tskubaensis*. Transplant Proc **19** (Suppl 6): 11
4. Arai T, Koyama Y, Suenaga T, Honda H (1962) Ascomycin as Antifungal Antibiotic. J Antibiotics **15** (Ser. A): 231
5. Hatanaka H, Iwami M, Kino T, Goto T, Okuhara M (1988) FR-900520 and FR-900523, Novel Immunosuppressants Isolated from a *Streptomyces*. I. Taxonomy of the Producing Strain. J Antibiotics **41**: 1586
6. Hatanaka H, Kino T, Miyata S, Inamura N, Kuroda A, Goto T, Tanaka H, Okuhara M (1988) FR-900520 and FR-900523, Novel Immunosuppressants Isolated from a *Streptomyces*. II. Fermentation, Isolation and Physicochemical and Biological Characteristics. J Antibiotics **41**: 1592
7. Morisaki M, Arai T (1992) Identity of Immunosuppressant FR-900520 with Ascomycin. J Antibiotics **45**: 126
8. Borris RP, Wicker LS, Zink DL, Lien T (1990) Eur Pat Appl EP 358508; Chem Abstr **113**: 38913
9. Fleissner G, Haecker H, Kuesters E, Penn G (2001) PCT Int Appl WO 0190110; Chem Abstr **136**: 4783
10. Junker B, Reddy J, Olewinski R, Gailliot P, Byrne K, Gbewonyo K (1998) Secondary Metabolite Scale-Up to Minimize Homolog Impurity Levels. Biotechnol Bioengineer **59**: 595
11. Hatanaka H, Kino T, Asano M, Goto T, Tanaka H, Okuhara M (1989) FK-506 Related Compounds Produced by *Streptomyces tsukubaensis* No. 9993. J Antibiotics **42**: 620
12. Chen TS, Arison BH, Wicker LS, Inamine ES, Monaghan RL (1992) Microbial Transformation of Immunosuppressive Compounds. I. Desmethylation of FK 506 and Immunomycin (FR 900520). J Antibiotics **45**: 118
13. Haag M, Baumann K, Billich A, Bulusu M, Fehr T, Grassberger M, Haidl E, Schulz G, Sanglier JJ (1998) Bioconversion of Ascomycin and its 6-Alkoxy Derivatives. J Mol Catal B: Enzymat **5**: 389
14. Arison BH, Inamine ES, Chen SST, Wicker LS (1990) Eur Pat Appl EP 378321; Chem Abstr **115**: 112812

15. Shafiee A, Kaplan L, Dumont F, Colwell LF, Arison BH (1992) Can Pat Appl CA 2071066; Chem Abstr **118**: 253402
16. Schueler W, Christians U, Schmieder P, Schiebel HM, Holze I, Sewing KF, Kessler H (1993) 159. Structural Investigations of 13-*O*-Desmethyl-FK506 and its Isomers Generated by *in vitro* Metabolism of FK506 Using Human Liver Microsomes. Helv Chim Acta **76**: 2288
17. Revill WP, Voda J, Reeves CR, Chung L, Schirmer A, Ashley G, Carney JR, Fardis M, Carreras CW, Zhou Y, Feng L, Tucker E, Robinson D, Gold BG (2002) Genetically Engineered Analogs of Ascomycin for Nerve Regeneration. J Pharmacol Exp Ther **302**: 1278
18. Vezina C, Kudelski A, Sehgal SN (1975) Rapamycin (AY-22,989), a New Antifungal Antibiotic. I. Taxonomy of the Producing Streptomycete and Isolation of the Active Principle. J Antibiotics **28**: 721
19. Sehgal SN, Baker H, Vezina C (1975) Rapamycin (AY-22,989), a New Antifungal Antibiotic. II. Fermentation, Isolation and Characterization. J Antibiotics **28**: 727
20. Martel RR, Klicius J, Galet S (1977) Inhibition of the Immune Response by Rapamycin, a New Antifungal Antibiotic. Can J Physiol Pharmacol **55**: 48
21. Meiser BM, Wang J, Morris RE (1989) Rapamycin: A new and highly active immunosuppressive macrolide with an efficacy superior to cyclosporine. In: Melchers F (ed) Progress in Immunology, vol VII: Proceedings of the 7th International Congress of Immunology, Springer-Verlag Berlin Heidelberg, p 1195
22. Morris RE, Meiser BM, Wu J, Shorthouse R, Wang J (1991) Use of Rapamycin for the Suppression of Alloimmune Reactions *in vivo*: Schedule Dependence, Tolerance Inductions, Synergy with Cyclosporine and FK 506, and Effect of Host-Versus-Graft and Graft-Versus-Host Reactions. Transplant Proc **23**: 521
23. Fehr T, Sanglier JJ, Schuler W, Gschwind L, Ponelle M, Schilling W, Wioland C (1996) Antascomycins A, B, C, D and E. Novel FKBP12 Binding Compounds from a *Micromonospora* Strain. J Antibiotics **49**: 230
24. Meingassner JG, Stuetz A (1992) Immunosuppressive Macrolides of the Type FK506: A Novel Class of Topical Agents for Treatment of Skin Diseases? J Invest Dermatol **98**: 851
25. Rappersberger K, Meingassner JG, Födinger D, Putz E, Fialla R, Tong D, Stuetz A, Wolff K (1996) Clearing of Psoriasis by a Novel Macrolide. J Invest Dermatol **106**: 701
26. Stuetz A, Grassberger MA, Baumann K, Edmunds AJF, Hiestand P, Meingassner JG, Nussbaumer P, Schuler W, Zenke G (1993) Immunophilins as Drug Targets. In: Testa B, Kyburz E, Fuhrer W, Giger R (eds) Perspectives in Medicinal Chemistry. Verl Helvetica Chimica Acta, Basel, p 427
27. Grassberger M, Meingassner J, Stuetz A, Wolff K (1998) Ascomycins. In: Roenigk HH, Maibach HI (eds) Psoriasis, 3rd edn. Marcel Dekker, Inc. New York, Basel, Hong Kong, Chapter 66, p 769
28. Stuetz A, Baumann K, Grassberger M, Wolff K, Meingassner JG (2006) Discovery of Topical Calcineurin Inhibitors and Pharmacological Profile of Pimecrolimus. Int Arch Allergy Immunol **141**: 199
29. Grassberger M, Baumruker T, Enz A, Hiestand P, Hultsch T, Kalthoff F, Schuler W, Schulz M, Werner FJ, Winiski A, Wolff B, Zenke G (1999) A Novel Anti-inflammatory Drug, SDZ ASM 981, for the Treatment of Skin Diseases: *in vitro* Pharmacology. Br J Dermatol **141**: 264
30. Kalthoff FS, Winiski A, Fichtinger P, Schwendinger B, Wang S, Weishaeupl C, Stuetz A (2007) Differential Inhibition of Primary versus Pre-activated T Cells by Pimecrolimus but not by Tacrolimus *in vitro*. Int Arch Allergy Immunol **142**: 255
31. Hultsch T, Müller KD, Meingassner JG, Grassberger M, Schopf RE, Knop J (1998) Ascomycin Macrolactam Derivative SDZ ASM 981 Inhibits the Release of Granule Associated Mediators and of Newly Synthesized Cytokines in RBL 2 H3 Mast Cells in an Immunophilin-Dependent Manner. Arch Dermatol. Res **290**: 501
32. Kalthoff F, Chung J, Musser P, Stuetz A (2003) Pimecrolimus does not Affect the Differentiation, Maturation and Function of Human Monocyte-Derived Dendritic Cells, in Contrast to Corticosteroids. Clin Exp Immunol **133**: 350

33. Büchau A, Schauber J, Hultsch T, Stuetz A, Gallo R (2008) Pimecrolimus Enhances Antimicrobial Peptide Expression in Keratinocytes. J Invest Dermatol **128**: 2646
34. Billich A, Aschauer H, Aszody A, Stuetz A (2004) Percutaneous Absorption of Drugs Used in Atopic Eczema: Pimecrolimus Permeates Less Through Skin than Corticosteroids and Tacrolimus. Int J Pharmaceutics **269**: 29
35. Meingassner JG, Aschauer H, Stuetz A, Billich A. (2005) Pimecrolimus Permeates Less than Tacrolimus Through Normal, Inflamed or Corticosteroid Pre-treated Skin. Exp Dermatol **14**: 752
36. Meingassner JG, Grassberger M, Fahrngruber H, Moore HD, Schuurman H, Stütz A (1997) A Novel Anti-inflammatory Drug, SDZ ASM 981, for the Topical and Oral Treatment of Skin Diseases: *in vivo* Pharmacology. Br J Dermatol **137**: 568
37. Meingassner JG, Kowalsky E, Schwendinger H, Elbe-Buerger A, Stuetz A (2003) Pimecrolimus does not Affect Langerhans Cells in Murine Epidermis, in Contrast to Corticosteroids. Br J Dermatol **149**: 853
38. Hoetzenecker W, Meingassner JG, Ecker R, Stingl G, Stuetz A, Elbe-Buerger A (2004) Corticosteroids but not Pimecrolimus Affect Viability, Maturation and Immune Function of Murine Epidermal Langerhans Cells. J Invest Dermatol **122**: 673
39. Hoetzenecker W, Ecker R, Kopp T, Stuetz A, Stingl G, Elbe-Bürger A (2005) Pimecrolimus Leads to an Apoptosis-induced Depletion of T Cells but not Langerhans Cells in Patients with Atopic Dermatitis: Results from a Randomized, Double-blind, Vehicle-controlled Clinical Trial. J Allergy Clin Immunol **115**: 1276
40. Meingassner JG, Fahrngruber H, Bavandi A (2003) Pimecrolimus Inhibits the Elicitation Phase but does not Suppress the Sensitization Phase in Murine Contact Hypersensitivity, in Contrast to Tacrolimus and Cyclosporin A. J Invest Dermatol **121**: 77
41. Bavandi A, Fahngruber H, Aschauer A, Hartmann B, Meingassner JG, Kalthoff FS (2006) Pimecrolimus and Tacrolimus Differ in their Inhibition of Lymphocyte Activation During the Sensitization Phase of Contact Hypersensitivity. J Dermatol Sci **43**: 117
42. Stuetz A, Grassberger M, Meingassner JG (2001) Pimecrolimus (Elidel®, SDZ ASM 981) – Preclinical Pharmacological Profile and Skin Selectivity. Sem Cutan Med Surg **20**: 233
43. Nell B, Walde I, Billich A, Vit P, Meingassner JG (2005) The Effect of Topical Pimecrolimus on Keratoconjunctivitis Sicca and Chronic Superficial Keratitis in Dogs: Results from an Exploratory Study. Vet Ophthal **8**: 39
44. Hiestand PC, Feifel R, Stuetz A (2003) Pimecrolimus (SDZASM981, Elidel®) is Highly Effective in Two Rat Models of Rheumatoid Arthritis. Inflammat Res (Suppl. **2**): S 157
45. Moore H, Tyldesley M, Martland A, Edjlalipour M (2003) Pimecrolimus Protects Mice from Developing T Cell-induced Inflammatory Bowel Disease without Systemic Immunosuppression, in Contrast to Tacrolimus or Cyclosporine A. J Invest Dermatol **121**, Abstr. 868
46. Wolff K, Stuetz A (2004) Pimecrolimus for the Treatment of Inflammatory Skin Disease. Expert Opin Pharmacother **5**: 643
47. Grassberger M, Steinhoff M, Schneider D, Luger TA (2004) Pimecrolimus – an Anti-inflammatory Drug Targeting the Skin. Exp Dermatol **13**: 721
48. Spergel JM (2009) Pimecrolimus Cream in the Management of Patients with Atopic Eczema. Clin Cos Invest Dermatol **2**: 85
49. Erchen J, Sunderkoetter C, Luger T, Steinhoff M (2008) Calcineurin Inhibitors for Treatment of Atopic Dematitis. Expert Opin Pharmacother **9**: 3009
50. Luger T, Paul C (2007) Potential New Indications of Topical Calcineurin Inhibitors. Dermatology **215** (Suppl 1): 45
51. Hebert AA (2006) Review of Pimecrolimus Cream 1% for Treatment of Mild to Moderate Atopic Dermatitis. Clin Ther **28**: 1972
52. Rappersberger K, Komar M, Ebelin ME, Scott G, Burtin P, Greig G, Kehren J, Chibout SD, Holter W, Richter L, Oberbauer R, Cordier A, Stuetz A, Wolff K (2002) Pimecrolimus Identifies a Common Genomic Anti-inflammatory Profile, is Clinically Highly Effective in Psoriasis and is Well Tolerated. J Invest Dermatol **119**: 876
53. Van Duyne GD, Standaert RF, Karplus PA, Schreiber SL, Clardy J (1991) Atomic Structure of FKBP-FK506, an Immunophilin-Immunosuppressant Complex. Science **252**: 839

54. Lepre CA, Thomson JA, Moore JM (1992) Solution Structure of FK506 bound to FKBP-12. FEBS Lett **302**: 89
55. Van Duyne GD, Standaert RF, Karplus P, Schreiber SL, Clardy J (1993) Atomic Structures of the Human Immunophilin FKBP-12 Complexes with FK506 and Rapamycin. J Mol Biol **229**: 105
56. Griffith JP, Kim J, Kim EE, Sintchak MD, Thomson JA, Fitzgibbon MJ, Fleming MA, Caron PR, Hsiao K, Navia MA (1995) X-Ray Structure of Calcineurin Inhibited by the Immunophilin-Immunospressant FKBP12-FK506 Complex. Cell **82**: 507
57. Kissinger CR, Parge HE, Knighton DR, Lewis CT, Pelletier LA, Tempczyk A, Kalish VJ, Tucker KD, Showalter RE, Moomaw EW (1995) Crystal Structures of Human Calcineurin and the Human FKBP12-FK506-Calcineurin Complex. Nature **378**: 641
58. Liu J, Farmer JD, Lane WS, Friedman J, Weissman I, Schreiber SL (1991) Calcineurin is a Common Target of Cyclophilin-Cyclosporin A and FKBP-FK506 Complexes. Cell **66**: 807
59. Motamedi H, Shafiee A, Cai SJ, Streicher SL, Arison BH, Miller RR (1996) Characterization of Methyltransferase and Hydroxylase Genes Involved in the Biosynthesis of the Immunosuppressants FK506 and FK520. J Bacteriol **178**: 5243
60. Karuso P, Kessler H, Mierke DF (1990) Solution Structure of FK506 from Nuclear Magnetic Resonance and Molecular Dynamics. J Am Chem Soc **112**: 9434
61. Meadows RP, Nettesheim DG, Xu RX, Olejniczak ET, Petros AM, Holzman TF, Severin J, Gubbins E, Smith H, Fesik SW (1993) Three-Dimensional Structure of the FK506 Binding Protein/Ascomycin Complex in Solution by Heteronuclear Three- and Four-Dimensional NMR. Biochemistry **32**: 754
62. Namiki Y, Kihara N, Koda S, Hane K, Yasuda T (1993) Tautomeric Phenomenon of a Novel Immunosuppressant (FK506) in Solution. I. Isolation and Structure Determination of Tautomeric Compounds. J Antibiotics **46**: 1149
63. Gailliot FP, Natishan TK, Ballard JM, Reamer RA, Kuczynski D, McManemin GJ, Egan RS, Buckland BC (1994) Isolation and Characterization of the Major Equilibrium Product of FK-520. J Antibiotics **47**: 806
64. Baumann K, Oberhauser B, Grassberger MA, Haidl G, Schulz G (1995) Synthesis and Oxidative Cleavage of the Major Equilibrium Products of Ascomycin and FK506. Tetrahedron Lett **36**: 2231
65. Baumann K, Oberhauser B, Strnadt G, Knapp H, Schulz G, Grassberger MA (1999) Conversion of Ascomycin into its Furano-Isomers. Synlett **S1**: 877
66. Baumann K, Damont A, Högenauer K, Steck A (2002) Poster presented at the 1st International SPECS and BioSPECS Symposium, Delft, the Netherlands, September 18–21, Abstract book: 64
67. Shevchenko VP, Nagaev IYu, Myasoedov NF, Andres H, Moenius T, Susan A (2004) Synthesis of Tritiated Cyclosporin A and FK506 by Metal-Catalyzed Hydrogen Isotope Exchange. J Lab Comp Radiopharm **47**: 407
68. Baumann K, Haidl E, Högenauer K, Kollenz G, Schulz G, Weber HP (1996) Poster presented at the 17th European Colloquium on Heterocyclic Chemistry, Regensburg, Germany, October 6–9, Abstract book: 211
69. Högenauer K, Diploma work (1997) Department of Organic Chemistry, Karl Franzens University, Graz, Austria
70. Baumann K, Högenauer K, Knapp H, Bacher M, Steck A, Wagner T (2005) On the Reactivity of Ascomycin at the Binding Domain. Part 3: Reactivity of the Binding Domain towards Diazomethane. Tetrahedron **61**: 4819
71. Baumann K, *et al*. Novartis Institutes for BioMedical Research Vienna, Austria, unpublished results
72. Edmunds AJF, Baumann K, Grassberger M, Schulz G (1991) Highly Selective Reactions of FK506 with Diazomethane. Tetrahedron Lett **32**: 7039
73. Fisher MJ, Chow K, Villalobos A, Danishefsky SJ (1991) On the Remarkable Propensity for Carbon-Carbon Bond Cleavage Reations in the C_8-C_{10} Region of FK-506. J Org Chem **56**: 2900

74. Grassberger MA, Baumann K (1993) Macrolide Immunosuppressants. Exp Opin Ther Pat **3**: 931
75. Askin D, Reamer RA, Joe D, Volante RP, Shinkai I (1989) Chemistry of FK-506: Benzilic Acid Rearrangement of the Tricarbonyl System. Tetrahedron Lett **30**: 671
76. Askin D, Jones TK, Reamer RA, Volante RP, Shinkai I (1990) Eur Pat Appl EP 364031; Chem Abstr **113**: 152155
77. Baumann K, Bacher M, Damont A, Högenauer K, Steck A (2003) On the Reactivity of Ascomycin at the Binding Domain. Part 1: Liberation of the Tricarbonyl Portion of Ascomycin. Tetrahedron **59**: 10075
78. Baumann K, Bacher M, Steck A, Wagner T (2004) On the Reactivity of Ascomycin at the Binding Domain. Part 2: Hydroxide Mediated Rearrangement Reactions. Tetrahedron **60**: 5965
79. Baumann K (1993) Eur Pat Appl EP 569337; Chem Abstr **122**: 187265
80. Koch G, Jeck R, Hartmann O, Kuesters E (2001) Selective Synthesis of a New Ascomycin Rearrangement Product (SDZ ASD732) on a Pilot Plant Scale. Org Proc Res Devel **5**: 211
81. Wang-Fan W, Kusters E, Mak CP, Wang Y (2000) Application of Centrifugal Counter-Current Chromatography to the Separation of Macrolide Antibiotic Analogues. II. Determination of Partition Coefficients in Comparison with the Shake-Flask Method. J Liq Chomatogr Rel Technol **23**: 1365
82. Kusters E, Heuer C, Wieckhusen D (2000) Purification of an Ascomycin Derivative with Simulated Moving Bed Chromatography. A Case Study. J Chromatogr A **874**: 155
83. Baumann K, Bacher M, Damont A, Steck A (2004) Selective Transformation of Ascomycin into 11-*epi*-Ascomycin. Tetrahedron Lett **45**: 549
84. Baumann K, Strnadt G, Knapp H, Schulz G, Haidl E, Weber HP (1996) Poster presented at the 17th European Colloquium on Heterocyclic Chemistry, Regensburg, Germany, October 6–9, Abstract book: 167
85. Baumann K, Meingassner J, Schulz G, Steck A, Grassberger M (2000) Lecture given at the XVIth International Symposium on Medicinal Chemistry, Bologna, Italy, September 18–22, Abstract book: 103
86. Emmer G, Weber-Roth S (1992) Synthesis of Derivatives of FK506 and FR900520: Modifications at the Binding Domain. Tetrahedron **48**: 5861
87. Nussbaumer P, Grassberger M, Schulz G (1992) C9-Imino and C10-Amino Derivatives of Ascomycin (21-Ethyl FK506). Tetrahedron Lett **33**: 3845
88. Baumann K, Knapp H, Strnadt G, Schulz G, Grassberger MA (1999) Carbonyl to Methylene Conversions at the Tricarbonyl Portion of the Ascomycin Derivatives. Tetrahedron Lett **40**: 7761
89. Nussbaumer P, Grassberger MA, Hiestand P, Schuler W, Schulz G, Zenke G (1992) Poster presented at the XIIth International Symposium on Medicinal Chemistry, Basel, Switzerland, September 13–17, Abstract book: 347
90. Namiki Y, Kihara N (1992) PCT Int Appl WO 9213862; Chem Abstr **117**: 233717
91. Namiki Y, Kihara N (1992) Brit. Pat. Appl. GB 2249787; Chem. Abstr. **117**: 150803
92. Bulusu ARCM, Waldstaetten P, Tricotet T, Rochais C, Steck A, Bacher M, Schulz G, Meingassner JG, Hiestand P, Zenke G, Schuler W, Wagner T (2009) New Derivatives of Ascomycin with Modifications in the Amino Acid Region - Synthesis and Biological Activities and X-Ray Crystal Structure of 5,6-Dehydroascomycin. Helv Chim Acta **92**: 839
93. Bulusu ARCM, Haidl EH, Schulz G, Waldstaetten P, Grassberger M (1999) Novel Derivatives of Ascomycin through Photochemistry. Ind J Chem **38B**:1159
94. Bulusu, A.R.C.M. (1994) Eur Pat Appl EP 626385; Chem Abstr **122**: 213857
95. Bulusu M, Waldstaetten P, Schulz G, Grassberger M (2004) Novel Analogs of Ascomycin with Modifications in the Amino Acid through Photochemistry: the Synthesis of 5,6-Dehydroascomycin. Tetrahedron Lett **45**: 2523
96. Moenius T, Baumann K, Bulusu M, Schweitzer A, Voges R (2001) Labelling of Pharmacologically Active Macrocycles. In: Pleiss U, Voges R (eds) Synthesis and Applications of Isotopically Labelled Compounds, vol 7. John Wiley Sons, Chichester, UK, p 424

97. Bulusu M, Waldstaetten P, Tricotet T, Rochais C, Steck A, Bacher M (2004) Synthesis of 6-Vinyl and 5-Vinylproline Analogues of Ascomycin. Tetrahedron Lett **45**: 5833
98. Jones TK, Askin D, Mills SG, Reamer RA, Desmond R, Volante RP, Tschaen DM, Shinkai I (1990) Eur Pat Appl EP 378318; Chem Abstr **114**: 81436
99. Coleman RS, Danishefsky SJ (1989) Degradation and Manipulations of the Immunosuppressant FK506: Preparation of Potential Synthetic Intermediates. Heterocycles **28**: 157
100. Horvath A, Grassberger MA, Haidl E, Schulz G (2001) Lecture given at the Fall Meeting of the Swiss Chemical Society, October 12, Zürich, Switzerland
101. Goulet MT, Mills SG, Parsons WH, Rupprecht KM, Wyvratt MJ (1993) Chemistry of FK506. In Lukacs G (ed) Recent Progress in the Chemical Synthesis of Antibiotics and Related Microbial Products. Springer, Berlin, p 141
102. Luengo JI, Rozamus LW, Holt DA (1993) Efficient Removal of Pipecolinate from Rapamycin and FK506 by Reaction with n-$Bu_4N^+CN^-$. Tetrahedron Lett **34**: 4599
103. Cooper ME, Donald DK, Tanaka H (1991) Eur Pat Appl EP 444829; Chem Abstr **115**: 279490
104. Askin D, Reamer RA, Joe D, Volante RP, Shinkai I (1990) Synthesis of the Novel Sarcosine and Proline (FK525) Analogs of FK-506: Rearrangement of the FK506 Allylic System. J Org Chem **55**: 5448
105. Bulusu M, Waldstaetten P, Tricotett T, Schulz G (2004) Selective Photochemical Cleavage of an α-Ketoamide in a Highly Functionalised Macrolide Ascomycin. Tetrahedron Lett **45**: 2527
106. Skytte DM, Frydenvang K, Hansen L, Nielsen PG, Jaroszewski JW (2010) Synthesis and Characterization of an Epimer of Tacrolimus, an Immunosuppressive Drug. J Nat Prod **73**: 776
107. Wiedeman PE, Fesik SW, Petros AM, Nettesheim DG, Mollison KW, Lane BC, Or YS, Luly JR (1999) Retention of Immunosuppressant Activity in an Ascomycin Analogue Lacking a Hydrogen-Bonding Interaction with FKBP 12. J Med Chem **42**: 4456
108. Clemons PA, Gladstone BG, Chao ED, Seth A, Chao ED, Foley MA, Schreiber SL (2002) Synthesis of Calcineurin-Resistant Derivatives of FK506 and Selection of Compensatory Receptors. Chem Biol **9**: 49
109. Marinec PS, Evans CG, Gibbons GS, Tarnowski MA, Overbeek DL, Gestwicki JE (2009) Synthesis of Orthogonally Reactive FK506 Derivatives via Olefin Cross Metathesis. Bioorg Med Chem **17**: 5763
110. Kawai M, Lane BC, Hsieh GC, Mollison KW, Carter GW, Luly JR (1993) Structure-Activity Profiles of Macrolactam Immunosuppressant FK506 Analogues. Fed Eur Biochem Soc **316**: 107
111. Horvath A, Grassberger MA, Schulz G, Haidl E, Sperner H, Steck A (2000) Regioselective Carbon-Carbon Bond Formation in the Effector Domain of Ascomycin. Tetrahedron **56**: 7469
112. Nussbaumer P, Grassberger MA, Schulz G (1999) Synthesis of Ascomycin and FK 506 Derivatives with Modified Effector Domain. Tetrahedron Lett **40**: 3869
113. Or YS, Clark RF, Xie Q, McAlpine J, Whittern DN, Henry R, Luly JR (1993) The Chemistry of Ascomycin: Structure Determination and Synthesis of Pyrazole Analogues. Tetrahedron **49**: 8771
114. Kawai M, Gunawardana IWK, Mollison KW, Hsieh GC, Lane BC, Luly JR (1998) Studies on an Immunosuppressive Macrolactam, Ascomycin: Synthesis of a C-33 Hydroxyl Derivative. Bioorg Med Chem Lett **8**: 935
115. Ok HO, Szumiloski JL, Beattie TR, Goulet MT, Strauch MJ, Dumont FJ, Wyvratt MJ (1997) C32-Amino Derivatives of the Immunosuppressant Ascomycin. Bioorg Med Chem Lett **7**: 2199
116. Baumann K, Emmer G (1991) Can Pat. Appl CA 2029694; Chem. Abstr 116; 128509
117. Baumann K, Emmer G (1994) US Pat Appl US 5352671; Chem Abstr 122: 187265
118. Baumann K, Emmer G (1991) Eur Pat Appl EP 427680; Chem Abstr 115: 231991

119. Hersperger R, Schuler W, Zenke G (1999) Preparation and Immunosuppressive Activity of 32-(*O*)-Acylated and 32-(*O*)-Thioacylated Analogues of Ascomycin. Bioorg Med Chem Lett **9**: 227
120. Goulet MT, Hodkey DW, Staruch MJ, Dumont FJ, Cryan JG, Parsons WH, Wyvratt MJ (1994) Alkyl Ether Analogs of the FK506 Related Immunosuppressive Macrolide L-683,590 (Ascomycin). Bioorg Med Chem Lett **4**: 921
121. Goulet MT, McAlpine SR, Staruch MJ, Koprak S, Dumont FJ, Cryan JG, Wiederrecht GJ, Rosa R, Wilusz MB, Peterson LB, Wyvratt MJ, Parsons WH (1998) C(32)-*O*-Imidazol-2-yl-methyl Ether Derivatives of the Immunosuppressant Ascomycin with Improved Therapeutic Potential. Bioorg Med Chem Lett **8**: 2253
122. Song Z, DeMarco A, Zhao M, Corley EG, Thompson AS, McNamara J, Li Y, Rieger D, Sohar P, Mathre DJ, Tschaen DM, Reamer RA, Huntington MF, Ho G-J, Tsay F-R, Emerson K, Shuman R, Grabowski EJJ, Reider PJ (1999) Highly Chemoselective Trichloroacetimidate-Mediated Alkylation of Ascomycin: A Convergent, Practical Synthesis of the Immunosuppressant L-733,725. J Org Chem **64**: 1859
123. Egan MAMcE, Dean DC, Marks TM, Song Z, Melillo DG (2000) Carbon-14 Labeling of a Potential New Immunoregulant Agent. J Lab Comp Radiopharm **43**: 1095
124. Goulet MT, Sinclair PJ, Wong F, Staruch MJ, Dumont FJ, Cryan JG, Wiederrecht GJ, Wyvratt MJ, Parsons WH (1999) C32-*O*-Phenalkyl Ether Derivatives of the Immunosuppressant Ascomycin: A Tether Length Study. Bioorg Med Chem Lett **9**: 2085
125. Sinclair PJ, Wong F, Wyvratt M, Staruch MJ, Dumont F (1995) Preparation and *in vitro* Activity of Aryl Ether Derivatives of the FK506 Related Immunosuppressive Macrolides Ascomycin and L-683,742. Bioorg Med Chem Lett **5**: 1035
126. Armstrong HM, Wong F, Holmes MA, Sinclair PJ, Goulet MT, Dumont FJ, Staruch MJ, Koprak S, Peterson LB, Rosa R, Wilusz MB, Wiederrecht GJ, Cryan JG, Wyvratt MJ, Parsons WH (1999) Potent Immunosuppressive C32-*O*-Arylether Derivatives of Ascomycin with Reduced Toxicity. Bioorg Med Chem Lett **9**: 2089
127. Sinclair PJ, Wong F, Staruch MJ, Wiederrecht G, Parsons WH, Dumont F, Wyvratt M (1996) Preparation and *in vitro* Activities of Naphthyl and Indolyl Ether Derivatives of the FK506 Related Immunosuppressive Macrolide Ascomycin. Bioorg Med Chem Lett **6**: 2193
128. Wagner R, Rhoades TA, Or YS, Lane BC, Hsieh G, Mollison KW, Luly JR (1998) 32-Ascomycinyloxyacetic Acid Derived Immunosuppressants. Independence of Immunophilin Binding and Immunosuppressive Potency. J Med Chem **41**: 1764
129. Mollison KW, Fey TA, Gauvin DM, Sheets MP, Smith ML, Pong M, Krause R, Miller L, Or YS, Kawai M, Wagner R, Wiedeman PE, Clark RF, Gunawardana IWK, Rhoades TA, Henry CL, Tu NP, BaMaung NY, Kopecka H, Liu L, Xie Q, Lane BC, Trevillyan JM, Marsh K, Carter GW, Chen Y-W, Hsieh GC, Luly JR (1998) Discovery of Ascomycin Analogs with Potent Topical but Weak Systematic Activity for Treatment of Inflammatory Skin Diseases. Curr Pharm Design **4**: 367
130. Hersperger R, Buchheit KH, Cammisuli S, Enz A, Lohse O, Ponelle M, Schuler W, Schweitzer A, Walker C, Zehender H, Zenke G, Zimmerlin AG, Zollinger M, Mazzoni L, Fozard JR (2004) A Locally Active Antiinflammatory Macrolide (MLD987) for Inhalation Therapy of Asthma. J Med Chem **47**: 4950
131. Zimmer R, Grassberger MA, Baumann K, Schulz G, Haidl E (1994) Synthetic Modifications of Ascomycin – I. A Chemoselective Removal of the Cyclohexyl Residue of Ascomycin. Tetrahedron **50**: 13655
132. Zimmer R, Baumann K, Sperner H, Schulz G, Haidl E, Grassberger MA (2005) Synthetic Modifications of Ascomycin. V. Access to Novel Ascomycin Derivatives by Replacement of the Cyclohexylvinylidene Subunit. Croatica Chem Acta **78**: 17
133. Grassberger MA, Schulz G, Fehr T (1990) Ger Offen DE 3938754; Chem Abstr 115: 157124
134. Grassberger MA, Fehr T, Horvath A, Schulz G (1992) Isolation of an Isomer of FK-506 from Fermentation of *Streptomyces tsukubaensis* and its Chemical Synthesis from FK-506. Tetrahedron **48**: 413

135. Zimmer R, Baumann K, Sperner H, Schulz G, Haidl E, Grassberger MA (1999) Ring Contraction of an Ascomycin Derivative to a 19-Membered Macrolactam. Helv Chim Acta **82**: 1038
136. Zimmer R, Grassberger MA, Baumann K, Horvath A, Schulz G, Haidl E (1995) Synthetic Modifications of Ascomycin – II. A Simple and Efficient Way to Modified *iso*-Ascomycin Derivatives. Tetrahedron Lett **36**: 7635
137. Zimmer R, Grassberger MA, Baumann K, Zenke G, Schuler W (1999) Synthetic Modifications of Ascomycin: Part III – A Concise Transformation of *iso*-Ascomycin to 19,20-*seco*- Derivatives. Ind J Chem **38B**: 831
138. Chung Y, Cho H (2004) Preparation of Highly Water Soluble Tacrolimus Derivatives: Poly (Ethylene Glycol) Esters as Potential Prodrugs. Arch Pharm Res **27**: 878
139. Choi DB, Cho H (2009) Effect of Tacrolimus Derivatives on Immunosuppression. Arch Pharm Res **32**: 549
140. Yura H, Yoshimura N, Oka T, Takakura Y, Hashida M (1998) Development of a Macromolecular Prodrug of FK506: I. Synthesis of FK506-Dextran Conjugate. Transplant Proc **30**: 3598
141. Yura H, Yoshimura N, Hamashima T, Akamatsu K, Nishikawa M, Takakura Y, Hashida M (1999) Synthesis and Pharmacokinetics of a Novel Macromolecular Prodrug of Tacrolimus (FK506), FK506-dextran Conjugate. J Cont Release **57**: 87
142. Koch K, Newborg MF, Hanson DC, Cooper K, Shepard RM, Biehl ML, Biggers MS, Ramchandani M, Schulte G, Snyder JR, Ferraina RA, Donovan C, Guadliana MA, Kostek GJ, Cole SH, Connolly MJ, Sawyer PS, I T-P, Blocker LW, Meiser BM, Melvin LS (1995) The C-32 Triacetyl-L-rhamnose Derivative of Ascomycin: A Potent, Orally Active Macrolactone Immunosuppressant. J Med Chem **38**: 1255
143. Takahashi T, Shiyama T, Mori T, Hosoya K, Tanaka A (2006) Isolating the Whole Complex of Target Proteins of FK506 Using Affinity Resins from Novel Solid Phases. Anal Bioanal Chem **385**: 122
144. Takahashi T, Shiyama T, Hosoya K, Tanaka A (2006) Development of Chemically Stable Solid Phases for the Target Isolation with Reduced Nonspecific Binding Proteins. Bioorg Med Chem Lett **16**: 447
145. Fujisawa; Klinge Pharma (1992) FK506, Fujimycin, Tacrolimus, Prograf. Drugs Fut **17**: 732
146. Ireland RE, Liu L, Roper TD (1997) Total Synthesis of FK506. Part 1: Construction of the C (16)-C(34) Fragment. Tetrahedron **53**: 13221
147. Ireland RE, Liu L, Roper TD, Gleason JL (1997) Total Synthesis of FK506. Part 2: Completion of the Synthesis. Tetrahedron **53**: 13257
148. Ireland RE, Gleason JL, Gegnas LD, Highsmith TK (1996) A Total Synthesis of FK506. J Org Chem **61**: 6856
149. Smith III AB, Condon SM, McCauley JA (1998) Total Synthesis of Immunosuppressants: Unified Strategies Exploiting Dithiane Couplings and σ-Bond Olefin Constructions. Acc Chem Res **31**: 35
150. Smith III AB, Chen K, Robinson DJ, Laakso LF, Hale KJ (1994) Formal Total Synthesis of FK506. Concise Construction of the C(10)-C(34) Segment via an Effective Coupling Tactic. Tetrahedron Lett **25**: 4271
151. Batchelor MJ, Gillespie RJ, Golec JMC, Hedgecock CJR, Jones SD, Murdoch R (1994) Total Synthesis of Close Analogues of the Immunosuppressant FK506. Tetrahedron **50**: 809
152. Nakatsuka M, Ragan JA, Sammakia T, Smith DB, Uehling DE, Schreiber SL (1990) Total Synthesis of FK506 and an FKBP Probe Reagent, (C_8,C_9-$^{13}C_2$)-FK506. J Am Chem Soc **112**: 5583
153. Jones TK, Mills SG, Reamer RA, Askin D, Desmond R, Volante RP, Shinkai I (1989) Total Synthesis of Immunosuppressant (−)-FK506. J Am Chem Soc **111**: 1157
154. Jones TK, Reamer RA, Desmond R, Mills SG (1990) Chemistry of Tricarbonyl Hemiketals and Application of Evans Technology to the Total Synthesis of the Immunosuppressant (−)-FK506. J Am Chem Soc **112**: 2998

155. Jones AB, Villalobos A, Linde RG, Danishefsky SJ (1990) A Formal Synthesis of FK506: Exploration of Some Alternatives to Macrolactamisation. J Org Chem **55**: 2786
156. Reynolds KA, Demain AL (1997) Rapamycin, FK506 and Ascomycin-related Compounds. In: Strohl WR (ed) Drugs and the Pharmaceutical Sciences, vol 82 (Biotechnology of Antibiotics, 2nd ed), Marcel Dekker, Inc., New York, p 497

Withanolides and Related Steroids

Rosana I. Misico, Viviana E. Nicotra, Juan C. Oberti, Gloria Barboza, Roberto R. Gil, and *Gerardo Burton*

Contents

1. Introduction 128
2. Withanolides in the Plant Kingdom 129
   2.1. Solanaceous Genera Containing Withanolides 129
   2.2. Non-Solanaceous Genera Containing Withanolides 132
3. Classification of Withanolides 132
   3.1. Withanolides with a δ-Lactone or δ-Lactol Side Chain 132
   3.2. Withanolides with a γ-Lactone Side Chain 134
4. Withanolides with an Unmodified Skeleton 135
   4.1. The *Withania* Withanolides 135
   4.2. Other Withanolides with an Unmodified Skeleton 143
5. Withanolides with Modified Skeletons 157
   5.1. Withanolides with Additional Rings Involving C-21 157
   5.2. Physalins and Withaphysalins 163

R.I. Misico • G. Burton (✉)
Departamento de Química Orgánica and UMYMFOR (CONICET-UBA), Facultad de Ciencias Exactas y Naturales, Universidad de Buenos Aires, Ciudad Universitaria, Pabellón 2, Buenos Aires C1428EGA, Argentina
e-mail: misicori@qo.fcen.uba.ar; burton@qo.fcen.uba.ar

V.E. Nicotra • J.C. Oberti
Departamento de Química Orgánica and IMBIV (CONICET), Facultad de Ciencias Químicas, Universidad Nacional de Córdoba, Ciudad Universitaria, Ciencias Químicas II, Córdoba 5000, Argentina
e-mail: vnicotra@mail.fcq.unc.edu.ar; jco@mail.fcq.unc.edu.ar

G. Barboza
Departamento de Farmacia and IMBIV (CONICET), Facultad de Ciencias Químicas, Universidad Nacional de Córdoba, Ciudad Universitaria, Córdoba 5000, Argentina
e-mail: gbarboza@imbiv.unc.edu.ar

R.R. Gil
Department of Chemistry, Carnegie Mellon University, 4400 Fifth Ave, Pittsburgh, PA 15213, USA
e-mail: rgil@andrew.cmu.edu

A.D. Kinghorn, H. Falk, J. Kobayashi (eds.), *Progress in the Chemistry of Organic Natural Products, Vol. 94*, DOI 10.1007/978-3-7091-0748-5_3,

5.3. Withanolides Containing an Aromatic Ring and Related Steroids 168
5.4. Withanolides with a γ-Lactone Side Chain 172
5.5. 18-Norwithanolides 181
5.6. Spiranoid Withanolides at C-22 184
6. Chemical and Bio-transformations of Withanolides 185
6.1. Chemical Transformations 186
6.2. Photochemical Transformations 188
6.3. Biotransformations 189
7. Biological Activities of the Withanolides 192
7.1. Insecticidal Activities 193
7.2. Phytotoxic Activities 196
7.3. Antiparasitic Activities 197
7.4. Antimicrobial Activities 199
7.5. Anti-inflammatory and Glucocorticoid Related Activities 200
7.6. Cancer-Related Activities 203
7.7. CNS-Related Activities 208
8. Chemotaxonomic Considerations 209
8.1. Tribe Physaleae 210
8.2. Tribes Hyoscyameae, Lycieae, and Solaneae 213
8.3. Tribe Datureae 213
8.4. Genera with Uncertain Positions in the Solanaceae Taxonomic System 213
References 216

1. Introduction

Since the isolation of the first withanolides in the mid 1960s (*1*, *2*), *ca*. 650 members of this family of compounds have been described, with most of these from genera of the Solanaceae. The basic structure of withaferin A (**1**), a C_{28} ergostane with a modified side chain forming a δ-lactone between carbons 22 and 26, was considered for many years the basic template for withanolides (Fig. 1). Nowadays this has given place to a considerable number of related structures that are considered part of the withanolide family. Withanolides have shown to possess many biological activities that include anti-inflammatory, antitumor, cytotoxic, immunomodulating, and cancer chemopreventive as well as antibacterial and antifungal properties. Extracts from *Withania somnifera*, known by its Sanskrit name "Ashwagandha" or "Indian ginseng", have been used for over 3,000 years in traditional medicine in India (Ayurvedic system). Many of the curative properties of this extract may be

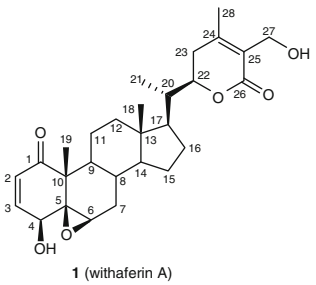

1 (withaferin A)

Fig. 1. Structure of withaferin A (**1**) and numbering scheme

associated with the presence of withanolides. Several withanolides also exhibit insecticidal activities, mostly as feedant deterrents, and selective phytotoxicity. A number of review articles have dealt with structural aspects of this group of compounds (*3*–*5*) as well as with their biological activities (*6*, *7*). The present chapter covers developments and findings in the chemistry and bioactivity of withanolides and related compounds since 1994.

2. Withanolides in the Plant Kingdom

2.1. Solanaceous Genera Containing Withanolides

The Solanaceae, also known as the nightshade or potato family, is one of the largest flowering plant families in containing nearly 100 genera and *ca*. 2,500 species, with a worldwide distribution in temperate and tropical continents (*8*–*10*). However, they are much more diversified in the Andean/Amazonian regions of South America in habitats that vary dramatically. The Solanaceae is also the third most important plant taxon economically and the most valuable in terms of vegetable crops, including the tuber-bearing potato, a number of fruit-bearing vegetables (tomato, eggplant, peppers), ornamental plants (petunias, *Nicotiana*, *Nierembergia*), plants with edible leaves (*Solanum aethiopicum*, *S. macrocarpon*), and medicinal plants (*e.g*. *Atropa*, *Capsicum*, *Datura*).

A modern traditional classification of the Solanaceae, predominantly based on morphological evidence with a minor emphasis on chemistry, recognizes six subfamilies (*9*). However, a recently proposed phylogenetic classification of the Solanaceae provides a different framework to the morphological system, with the inclusion of genera traditionally excluded from the family and with a greater resolution among lineages within the subfamily Solanoideae (*10*).

Among the nearly 100 genera included in Solanaceae (*10*), the occurrence of withanolides is restricted to the subfamily Solanoideae. Table 1 summarizes all genera and species known to contain withanolides to date. The four major contributors of withanolide structures are the genera *Jaborosa* Juss., *Datura* L., and *Physalis* L. from the North and South American continents, and *Withania* Pauq., native to the Old World. Up to the present, *ca*. 50% of the species in these genera have been investigated. *Jaborosa* is an interesting South American genus with a much varied corolla odor, color, and morphology as an adaptation to different pollinators growing from southern Peru to Argentina in very diverse habitats. *Datura* comprises annual or short-lived perennial herbs, mostly with erect large flowers, common in semiarid habitats in Mexico and the southwest of the United States, but introduced in many countries. *Physalis* includes mostly American herbs (Central America, Mexico and United States, except for the Euroasian *P. alkekengi*), with solitary pendant yellow or white flowers, and fruiting calyxes that become enlarged and inflated. Finally, *Withania* is a well-known genus

Table 1. Genera and species of the Solanaceae containing withanolides

Genera[a]	Species	Previous names[b]
Acnistus (1/1)	*arborescens* (L.) Schltdl.[c]	*Acnistus ramiflorus* Miers
Brachistus (2/4)	*stramoniifolius* (Kunth) Miers[c]	
	hunzikeri (D'Arcy) Sousa-Peña[c]	*Witheringia hunzikeri*
Datura (6/*ca*. 11)	*ferox* L.[c]	
	inoxia Mill.[c]	
	metel L.[c]	
	metel var. *fastuosa* (L.) Saff.[c]	*Datura fastuosa* L.
	quercifolia Kunth[c]	
	stramonium L.	
	stramonium var. *tatula* (L.) Torr.[c]	*Datura tatula* L.
Deprea (1/7)	*orinocensis* (Kunth) Raf.[c]	
Discopodium (1/1)	*penninervium* Hochst.[c]	
Dunalia (2/5)	*brachyacantha* Miers[c]	
	solanacea Kunth[c]	
Eriolarynx (1/3)	*lorentzii* (Dammer) Hunz.[c]	*Vassobia lorentzii* Dammer; *Acnistus lorentzii* (Dammer) Hunz.
Exodeconus (1/6)	*maritimus* (Benth.) D'Arcy[c]	
Hyoscyamus (1/17)	*niger* L.[c]	
Iochroma (4/*ca*. 25)	*australe* Griseb.[c]	*Acnistus australis* (Griseb.) Griseb.; *Dunalia australis* (Griseb.) Sleumer
	coccineum Scheid.	
	fuchsioides Miers	
	gesneroides Miers[c]	
Jaborosa (13/23)	*araucana* Phil.[c]	
	bergii Hieron.[c]	
	caulescens var. *bipinnatifida* (Dunal) Reiche[c]	
	caulescens Gillies & Hook. var. *caulescens*[c]	
	integrifolia Lam.	
	kurtzii Hunz. & Barboza[c]	
	laciniata (Miers) Hunz. & Barboza[c]	*Trechonaetes laciniata* Miers
	lanigera (Phil.) Hunz. & Barboza[c]	
	leucotricha (Speg.) Hunz. [c]	
	magellanica (Griseb.) Dusén	
	odonelliana Hunz.[c]	
	rotacea (Lillo) Hunz. & Barboza[c]	
	runcinata Lam.[c]	
	sativa (Miers) Hunz. & Barboza[c]	
Larnax (2/*ca*. 30)	*glabra* (Standl.) Sawyer[c]	
	subtriflora (Ruiz & Pav.) Miers[c]	*Deprea subtriflora* Ruiz & Pav.
Lycium (2/*ca*. 80)	*chinense* Mill.	
	barbarum L.	*Lycium halimifolium* Mill.

(continued)

Table 1. (continued)

Genera[a]	Species	Previous names[b]
Nicandra (1/2)	*physalodes* (L.) Gaertn.	
Margaranthus (1/1)	*solanaceous* Schltdl.[c]	*Physalis solanaceous* (Schltdl.) Axelius
Physalis (15/*ca*. 90)	*alkenkegi* L.[c]	
	alkenkegi var. *franchetii* (Mast.) Makino[c]	
	angulata L.[c]	
	chenopodifolia Lam.[c]	
	cinerascens (Dunal) Hitchc.[c]	
	coztomatl Dunal[c]	
	divaricata D. Don[c]	
	lanceifolia Nees	
	minima L.[c]	
	peruviana L.[c]	
	philadelphica Lam.[c]	*Physalis ixocarpa* Brot. ex Hornem.
	pruinosa L.	
	pubescens L.	
	virginiana Mill.[c]	
	viscosa L.	*Physalis curassavica* L.
Salpichroa (1/16)	*origanifolia* (Lam.) Thell.[c]	
Schraderanthus (1/1)	*viscosus* (Schrad.) Averett[c]	*Saracha viscosa* Schrad. *Leucophysalis viscosa* (Schrad.) Hunz.
Solanum (2/*ca*. 1,500)	*ciliatum* Lam.[c]	*Solanum cilistum* Lam.
	sisymbriifolium Lam.[c]	
Tubocapsicum (1/2)	*anomalum* (Franch. & Sav.) Makino[c]	
Vassobia (1/2)	*breviflora* (Sendtn.) Hunz.[c]	*Acnistus breviflorus* Sendtn.
Withania (6/20)	*adpressa* Cors.[c]	
	aristata (Aiton) Pauq.[c]	
	coagulans (Stocks) Dunal[c]	*Withania coagulance*
	frutescens (L.) Pauq.	
	obtusifolia V. Tackh.	
	somnifera (L.) Dunal[c]	
Witheringia (2/12)	*coccoloboides* (Dammer) Hunz.[c]	
	solanacea L´Hér.[c]	

[a]In parenthesis are the number of species with withanolides/number of total species. [b]Previous names cited in literature. [c]Species included in this chapter

of perennial herbs or shrubs with flowers that are perfect or functionally imperfect, occurring in Europe and Asia.

Table 1 also includes four monotypic genera, *Acnistus* Schott (Southern Mexico to Eastern Brazil and Paraguay), *Margaranthus* Schltdl. (Southern United States to the Antilles), *Schraderanthus* Averett (Mexico to Guatemala), and *Discopodium* Hochst. (tropical Africa). In the remaining genera containing withanolides, only isolated species have been characterized phytochemically.

2.2. Non-Solanaceous Genera Containing Withanolides

Withanolides have been detected in six species belonging to different families (Table 2), including the rhizomes of species of *Tacca* J.R. Forst. & G. Forst. (family Dioscoreaceae, formerly the family Taccaceae), in the aerial parts of *Senna siamea* (family Leguminosae), in the bark of *Eucalyptus globulus* (family Myrtaceae), and in species of *Ajuga* L. (family Lamiaceae).

3. Classification of Withanolides

The withanolides are polyoxygenated steroids with a C_{28} ergostane skeleton. A common feature is the presence of oxygen atoms at C-1, C-22, and C-26 although a few exceptions with a non-functionalized C22 are included. They may be classified into two major groups depending on the arrangement of the side chain, those with a δ-lactone or δ-lactol comprising C-22 and C-26 and those with a γ-lactone usually involving C-23 and C-26.

3.1. Withanolides with a δ-Lactone or δ-Lactol Side Chain

Most of the known withanolides belong to this group, which may be further divided into 13 subgroups: withanolides with the parent skeleton of withaferin A (**1**), withaphysalins, physalins, acnistins, withajardins, withametelins, sativolides, subtriflora-δ-lactones, spiranoid-δ-lactones, norbornane-type withanolides, ring-D aromatic withanolides, ring-A aromatic withanolides, and taccalonolide-δ-lactones (Fig. 2). The δ-lactone formed between a carboxyl group at C-26 and a hydroxy at

Table 2. Genera containing withanolides from outside the Solanaceae

Family and genera	Species	Name cited[a]
Monocotyledoneae	*chantrieri* André[b]	
Fam. Dioscoreaceae		
Tacca	*paxiana* H. Limpr.[b]	
	plantaginea (Hance) Drenth[b]	
	subflabellata P.P. Ling & C.T. Ting[b]	*Tacca subflaellata*
Dicotyledoneae	*siamea* (Lam.) Irwin & Barneby	*Cassia siamea* Lam.
Fam. Leguminosae		
Senna		
Fam. Myrtaceae	*globulus* Labill.[b]	
Eucalyptus		
Fam. Lamiaceae	*bracteosa* Wall. ex Benth.[b]	
Ajuga	*parviflora* Benth.[b]	

[a]Names cited in literature. [b]Species included in this chapter

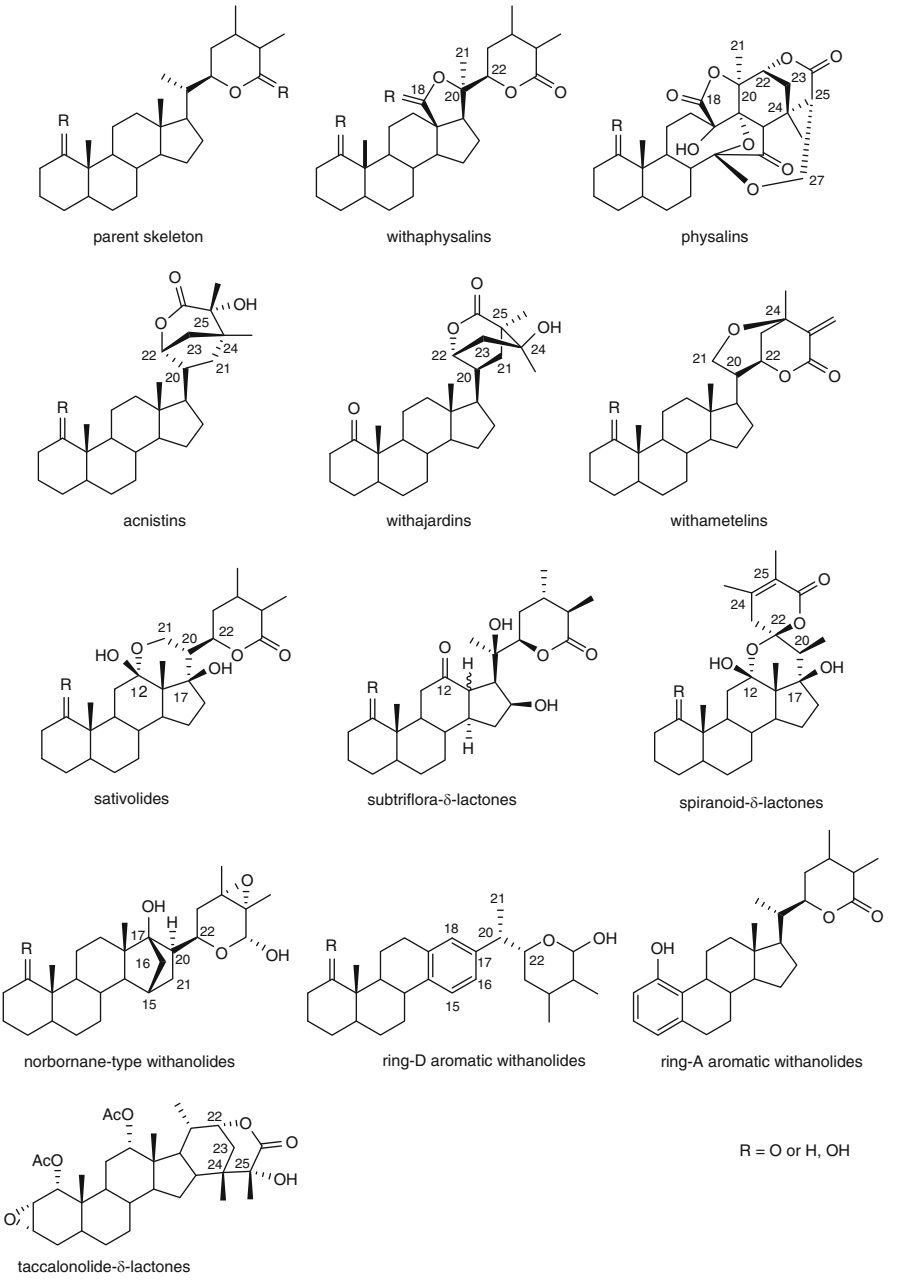

Fig. 2. General structures of withanolides with a δ-lactone or δ-lactol side chain. Numbering of relevant positions has been added for clarity in some structures

C-22 is the most common arrangement; other types include lactone formation with a hydrated carbonyl at C-22 and δ-lactols between an aldehyde at C-26 and a hydroxy at C-22. All known withanolides have the same stereochemistry at C-22, which corresponds to (22*R*) except when substituents at C-23 or C-22 change the relative priorities of groups around the asymmetric center.

Withanolides with an unmodified skeleton are the most abundant and are regarded as possible precursors of most of the other compounds in this group. A further subdivision of the withanolides is usually made according to the orientation of the side chain; those with the "normal" 17β-oriented side chain as well as those with the less usual 17α-oriented side chain are known. In the latter case a 17β-hydroxy (either free or involved in a cyclic ether) is generally present although several exceptions are known.

3.2. Withanolides with a γ-Lactone Side Chain

The presence of an oxygenated function at C-23 allows the formation of a γ-lactone with a carboxyl group at C-26; these withanolides may be divided in five subgroups, spiranoid withanolides, trechonolides, subtriflora-γ-lactones, ixocarpalactones, and taccalonolide-γ-lactones. A sixth subgroup with a γ-lactone side chain involving C-26 and C-28 corresponds to the perulactones (Fig. 3).

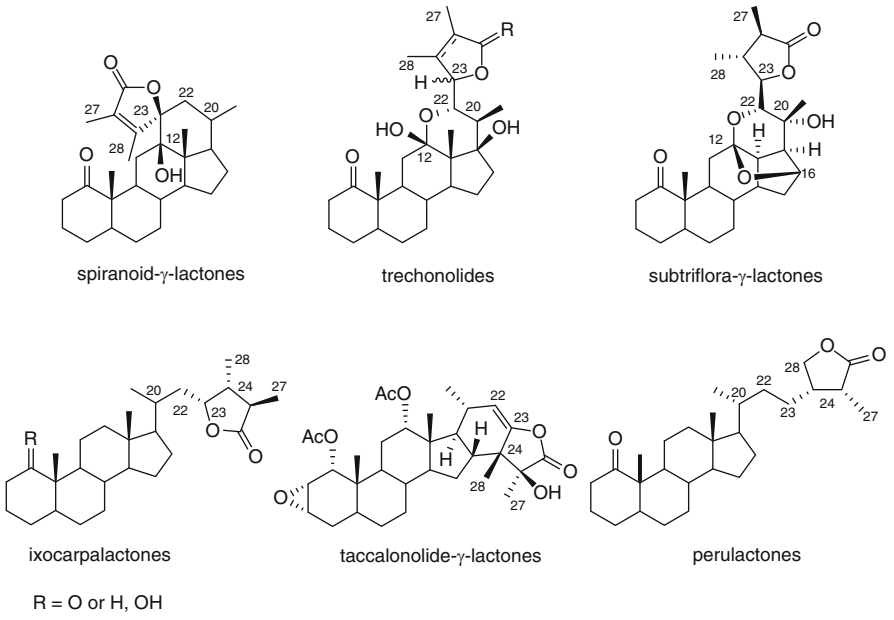

Fig. 3. General structures of withanolides with a γ-lactone side chain. Numbering of relevant positions has been added for clarity

4. Withanolides with an Unmodified Skeleton

Despite the large number of withanolides with the parent skeleton of withaferin A (**1**) that are already known, many new entities have been described with minor variations. These correspond mostly to different combinations of hydroxylated substituents and the occurrence of glycosidated derivatives. Among the many structures that fall within this group, the *Withania* withanolides comprise a major subgroup and are presented separately. Then, other representative substitutions on the parent skeleton will be described.

4.1. The Withania *Withanolides*

The *Withania* genus, although studied extensively in the past, has continued to provide new withanolide structures. Leaves, roots, and fruits of *W. somnifera* and *W. coagulans* have been investigated, with a total of 45 and 29 new structures reported, respectively. New withanolides have also been isolated from *W. adpressa* and *W. aristata*. Unfortunately, with several groups working simultaneously on the same plant, some structures have been reported as new more than once. As mentioned above, all of them conform to the classical withanolide skeleton with few unusual features.

4.1.1. 5*β*,6*β*-Epoxywithanolides and Related Compounds

The basic structure of withaferin A (**1**) may be found in several new structures isolated from *W. somnifera*, and simple variations are the 17α-hydroxy derivative **2** (*11*) and the Δ^{16} analogues **3** (*12*) and witharistatin (**4**) (*13*), with the latter isolated from *W. aristata*. The same basic structure may be found in **5** where the 2,3-double bond has been hydrated (*14*) and in **6** in which the double bond is reduced (*15*). The latter compound also has an unusual fragment etherifying the 4*β*-hydroxy group. One of the most common variations in the withaferin A substitution pattern is the hydrolytic cleavage of the 5,6-epoxide according to the *Fürst-Plattner* rule (*16*), to give the *trans*-diaxial 5α,6*β*-diol as in coagulin H (**7**) and coagulin S (**8**) isolated from *W. coagulans* (*17, 18*). A less common cleavage is that occurring in a *trans*-diequatorial manner, as found in **9** and **10** (*14*), later reported as new by *Kuroyanagi et al.* (*19*), and in 4-deoxywithaperuvin (**11**) (*20*). Compound **12** represents an unusual variant of the above, with a 3α,6α-epoxy bridge (*21*), which could derive from the cyclization of **10** also present in the same extract. While *Michael*-type addition of alcohols to the Δ^2-1-keto system of withanolides is well known, intramolecular addition is rare. Nevertheless, the same arrangement has been found previously in withaperuvins D (*22*) and F (*23*), although the authors did not directly compare the spectroscopic data of these substances.

Compounds **13** and **14** are two glycosides closely related to withaferin A (**1**). In the case of **13** the configuration of the hydroxy group at C-16 was not determined (*15*).

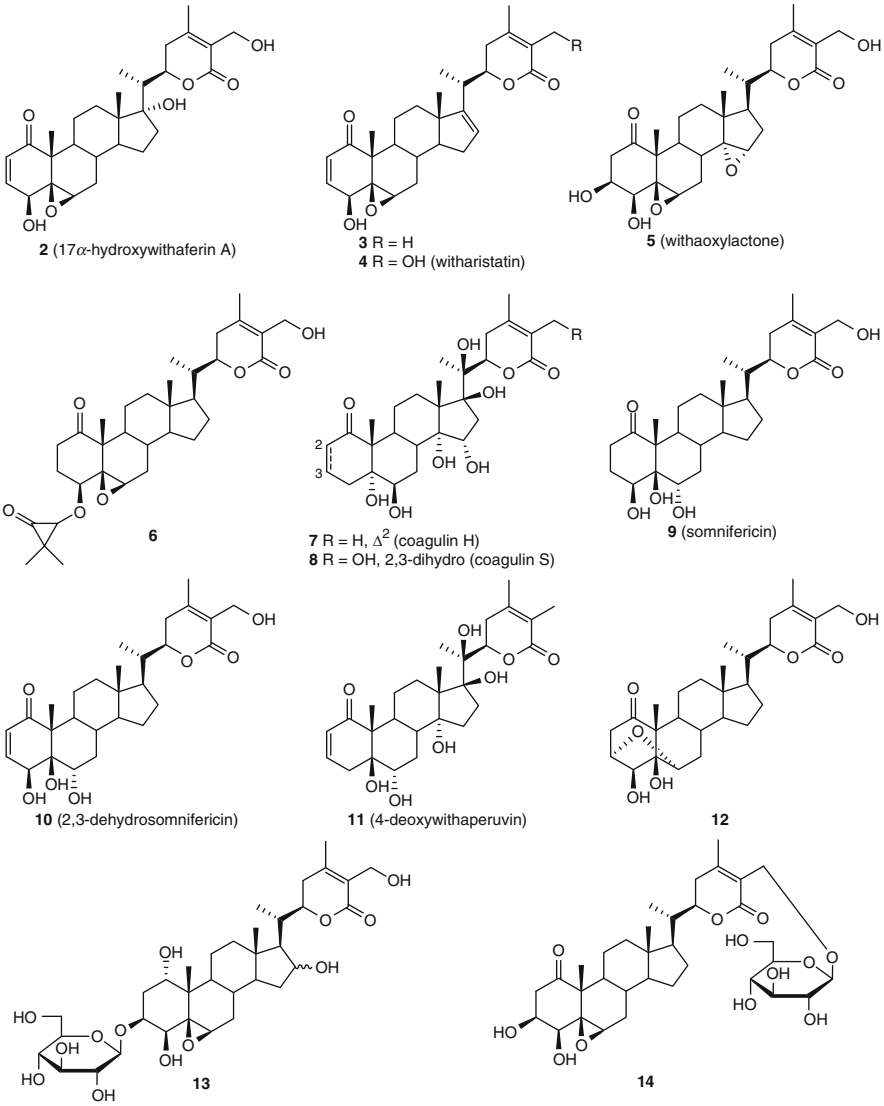

4.1.2. 5α-Hydroxy-6α,7α-Epoxywithanolides and Related Compounds

The 5α-hydroxy-6α,7α-epoxy substitution pattern is also a common arrangement found in *W. somnifera* withanolides. Simple variations arising from the

combination of hydroxy substituents at both typical positions (C-14, C-17, C-20) and some less common ones such as C-16 or C-23 are observed in withasomniferols A (**15**) and B (**16**) (*24*), 14α,17α-dihydroxywithanolide R (**17**) (*20*), isowithanone (**18**) (*25*), and the 16β-acetate **19** (*26*). Withasomniferol B (**16**) is a stereoisomer of the known ixocarpanolide, although the configurations at positions 24 and 25 were not specified. Hydration of the 2,3-double bond was found in compounds **20** (*11*), **21**, and **22** (*12*), and the latter was isolated as the 3-sulfate, an unusual feature in withanolides (see Sect. 4.2.5.). Other variations found were the reduced 1α-alcohol **23** (*25*) and the related glycosides withanoside II (**24**), withanoside I (**25**), and withanoside III (**26**) (*27*), with the 1α,3β-dihydroxy arrangement being fairly common among withanolides (see next section). Also, the chlorinated withanolide Z (**27**) (*28*), arising from *trans*-diaxial cleavage of the 6,7-epoxide and the Δ^7-withanolide **28** (*24*) are known. Compound **29** contains an unusual 5α,7α-epoxy bridge that would result from rearrangement of the 5α-hydroxy-6α,7α-epoxide (*26*).

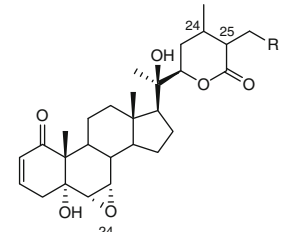

15 R = OH, Δ^{24} (withasomniferol A)
16 R = H (withasomniferol B)

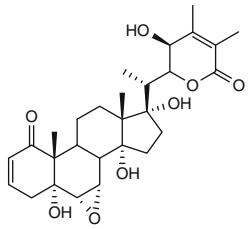

17 (14α,17α-dihydroxywithanolide R)

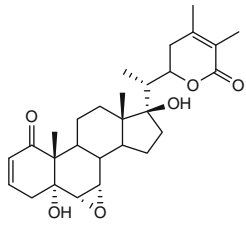

18 (iso-withanone)

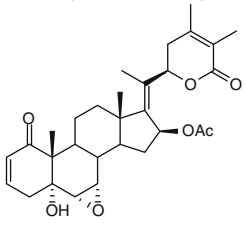

19

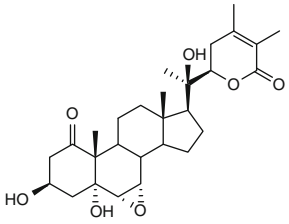

20

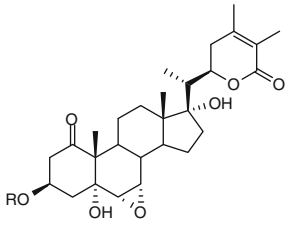

21 R = H
22 R = SO_3H

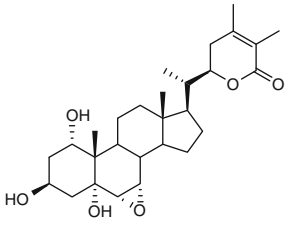

23

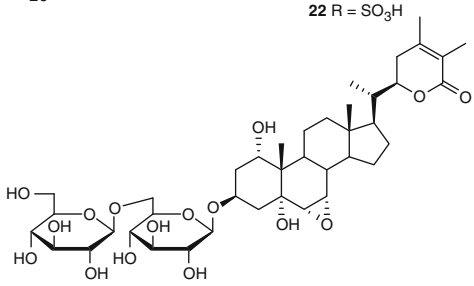

24 (withanoside II)

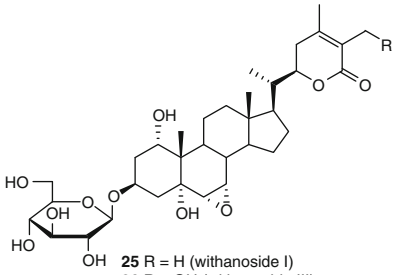

25 R = H (withanoside I)
26 R = OH (withanoside III)

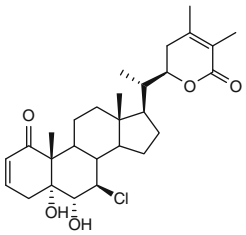

27 (withanolide Z)

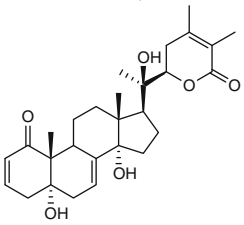

28 (withasomniferol C)

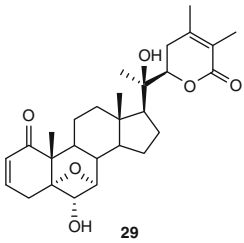

29

4.1.3. 1α,3β-Dihydroxy-Δ^5-Withanolides and Related Compounds

As mentioned above, the 1α,3β-dihydroxy arrangement is a well-known structural variation among the withanolides and several examples have been shown in combination with 5β,6β- or 6α,7α-epoxides. Eleven 3β-*O*-glycosides isolated from *W. somnifera* contained the 1α,3β-dihydroxy arrangement combined with a 5,6-double bond in ring B. These include compound **30**, later reported as withanoside V (*19, 27*), withanosides IV (**31**), VI (**32**) and VII (**33**) (*27*), and 24,25-dihydrowithanoside VI (**34**) containing a disacharide at position 3 (*29*). The configurations at positions 24 and 25 of the latter compound were not elucidated. Also within this group are three withanolides with an additional sugar moiety at C-27 (*21*), withanosides VIII (**35**), IX (**36**), and X (**37**) (this structure was reported again as new, one year later (*15*)), an analogue of withanoside VI with a monosacharide at C-3 named withanoside XI (**38**) (*21*), and an analogue of withanoside IV with a trisacharide moiety at C-3 (**39**) (*15*). Coagulin Q (**40**) isolated from *W. coagulans* (*30*), has the same aglycone as withanoside VI (**32**), but with a monosacharide unit at C-3. In all cases the carbohydrate units are β-D-glucose.

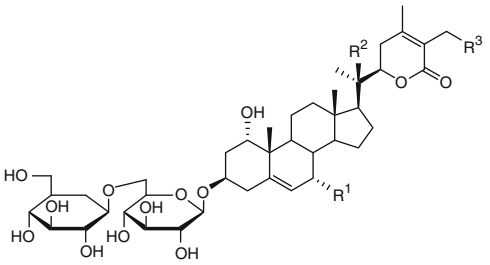

30 $R^1 = R^2 = R^3 = H$ (withanoside V)
31 $R^1 = R^2 = H$, $R^3 = OH$ (withanoside IV)
32 $R^1 = R^3 = H$, $R^2 = OH$ (withanoside VI)
33 $R^1 = OH$, $R^2 = R^3 = H$ (withanoside VII)
35 $R^1 = R^2 = H$, $R^3 = O$-β-gluc (withanoside VIII)
36 $R^1 = R^2 = H$, $R^3 = O$-β-gluc(1-6)-β-gluc (withanoside IX)

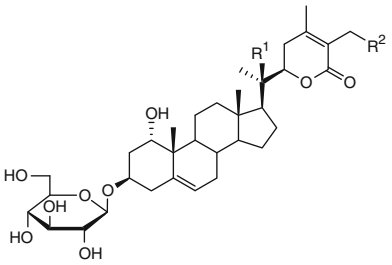

37 $R^1 = H$, $R^2 = O$-β-gluc (withanoside X)
38 $R^1 = R^2 = OH$ (withanoside XI)
40 $R^1 = OH$, $R^2 = H$ (coagulin Q)

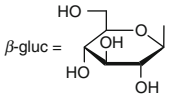

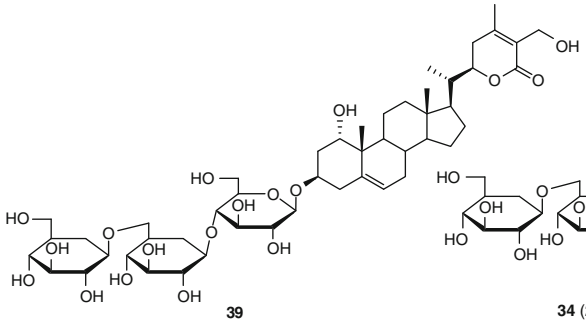

39

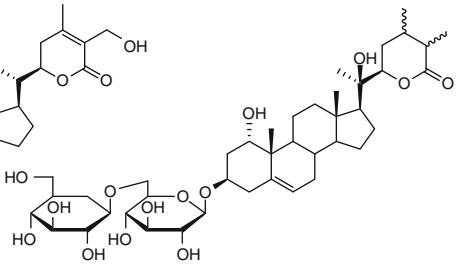

34 (24,25-dihydrowithanoside VI)

4.1.4. Other Δ^5-Withanolides

Withanolides containing a 5,6-double bond in combination with either a Δ^2- or Δ^3-1-ketone or a 3β-hydroxy-1-ketone are quite common and are the biosynthetic precursors of the 5β,6β-epoxywithanolides. Several new withanolides with these arrangements have been isolated from *Withania* species, mostly from *W. coagulans*. Compound **41** was isolated originally from *W. adpressa* (*31*) and later reported as new from *W. coagulans* (*32*). Compound **42** had been synthesized by *Lavie* and coworkers (*33*) but was isolated for the first time as a natural product by *Atta-ur-Rahman et al.* from *W. coagulans* (*34*). Ten withanolides with closely related structures were also isolated from this plant, withacoagulin (**43**) (*34*), withacoagulins A–F (**44**–**49**) (*35*), the 14β,15β-epoxide **50**, the 14α-alcohol **51** (*36*), and the 17-epimer of withacoagulin D, coagulansin A (**52**) (*37*). The 3β-hydroxy-Δ^5 arrangement is present in coagulansin B (**53**) (*37*) and in the three 3β-*O*-glycosides, coagulin L (**54**) (*17*), coagulin O (**55**) (*38*), and coagulin P (**56**) (*30*).

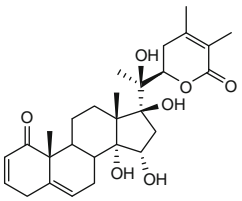

41

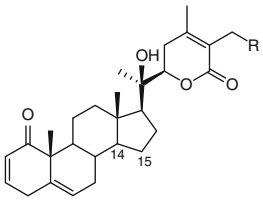

42 R = H
43 R = OH, Δ^{14} (withacoagulin)

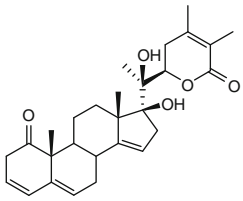

44 (withacoagulin A)

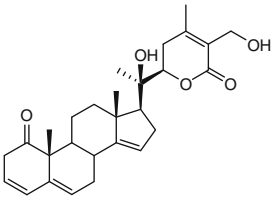

45 (withacoagulin B)

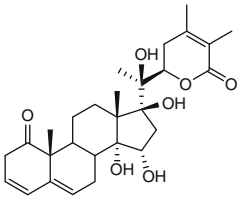

46 (withacoagulin C)

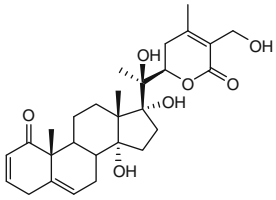

47 (withacoagulin D)

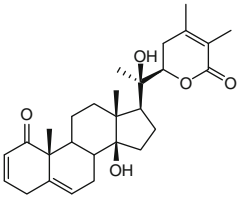

48 (withacoagulin E)

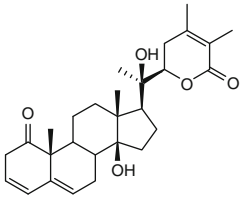

49 (withacoagulin F)

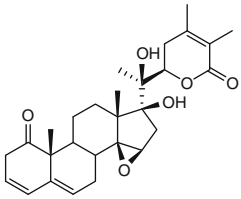

50 (14,15β-epoxywithanolide I)

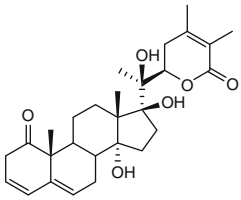

51 (17β-hydroxywithanolide K)

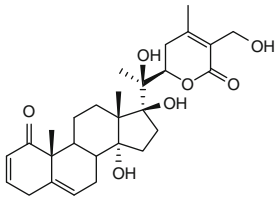

52 (coagulansin A)

Glucosomniferanolide (**57**), isolated from *W. somnifera*, contains a glucose unit at the tertiary hydroxy group at C-20 (*39*). This compound was described as having a (22*S*) configuration, opposite to that found in all withanolides with a δ-lactone side chain. However, spectroscopic observations supporting this assumption only indicate that H-22 is equatorial instead of axial (broad signal with $W_{1/2} = 5$ Hz), an orientation that can result from a simple conformational inversion of the lactone ring half chair, probably due to the presence of the bulky substituent at C-20. Thus, this structure should be revised.

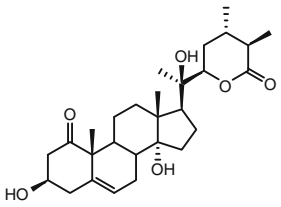

53 (coagulansin B)

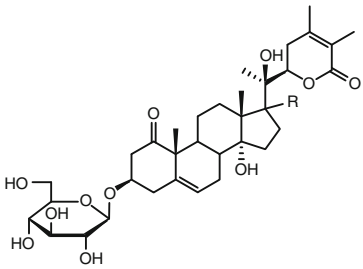

54 R = β-OH (coagulin L)
55 R = α-H (coagulin O)

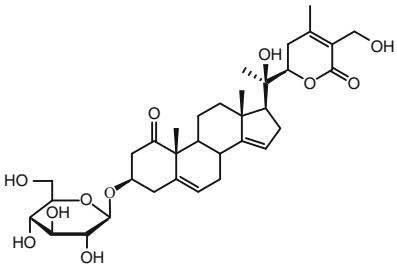

56 (coagulin P)

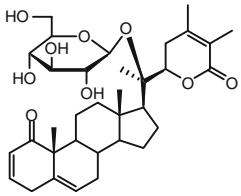

57 (glucosomniferanolide)

Several 14α,20-epoxywithanolides closely related to the known coagulin (**58**) (*40*), were isolated from *W. coagulans*. These included coagulins B–E (**59**–**62**) (*41*), coagulins F and G (**63**, **64**) (*42*), coagulin R (**65**) (*30*), the diol coagulin M (**66**) and the glycoside coagulin N (**67**) (*38*), coagulin J (**68**), the diol coagulin I (**69**) and the glycoside coagulin K (**70**) (*17*), and compound **71** (*34*). *Malik* and coworkers had previously reported the isolation of **71** and the 3-*O*-glycoside of coagulin R from *Physalis peruviana* (*43*, *44*) and of ajugin, identical to coagulin R from *Ajuga parviflora* (see Sect. 4.2.) (*45*).

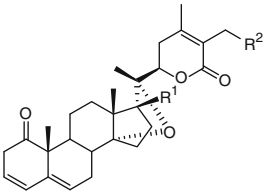

58 R^1 = OH, R^2= OH (coagulin)
62 R^1 = R^2 = H (coagulin E)
63 R^1 = H, R^2 = OH (coagulin F)
71 R^1 = OH, R^2 = H

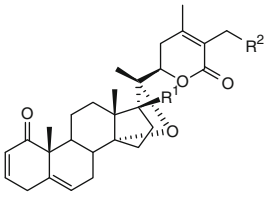

59 R^1 = H, R^2 = OH (coagulin B)
60 R^1 = OH R^2 = H (coagulin C)
61 R^1 = R^2 = H (coagulin D)
64 R^1 = R^2 = OH (coagulin G)

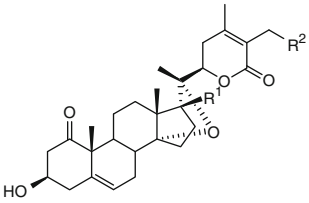

65 R^1 = OH R^2 = H (coagulin R)
68 R^1 = H R^2 = OH (coagulin J)

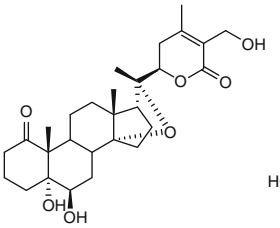

66 (coagulin M)

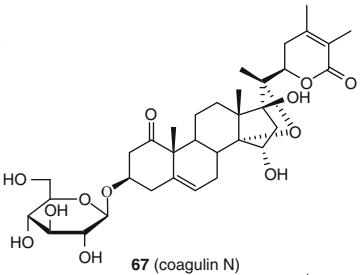

67 (coagulin N)

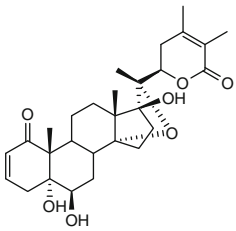

69 (coagulin I)

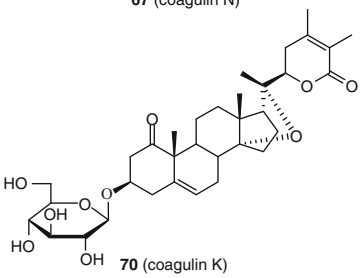

70 (coagulin K)

4.1.5. Other Substitution Patterns

Some less common substitution patterns isolated from *W. somnifera* include a $\Delta^{1,4}$-3-keto withanolide (**72**) (*12*), a series of four 8β-hydroxywithanolides (**73**–**76**), a 7β-hydroxywithanolide with a $\Delta^{2,4}$-1-keto arrangement in ring A (**77**) (*46*), and two dimeric withanolides bound by a thioether linkage (**78**) (*47*) or a sulfoxide (**79**) (*48*). Other less common features found in these compounds are the presence of an 11β-hydroxy (**74**, **76**) or an 18-hydroxy group (**75**, **77**) (*46*). The 3β-*O*-sulfate of 2,3-dihydrowithaferin A (**80**) was isolated from aeroponically grown *W. somnifera* plants (*49*).

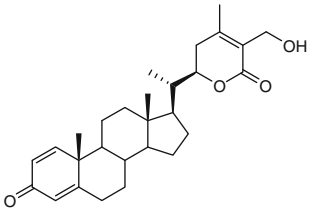

72

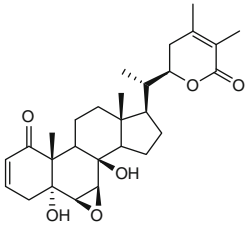

73 (withasomnilide)

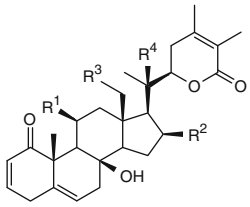

74 $R^1 = R^2 = OH$, $R^3 = R^4 = H$ (withasomniferanolide)
75 $R^1 = R^2 = H$, $R^3 = R^4 = OH$ (somniferawithanolide)

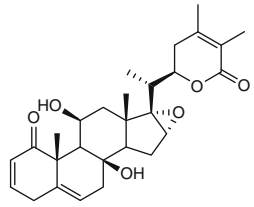

76 (somniferanolide)

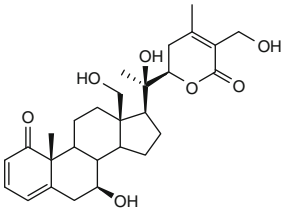

77 (somniwithanolide)

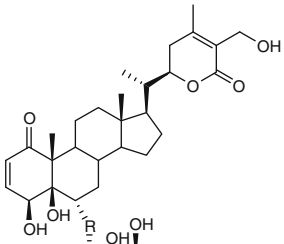

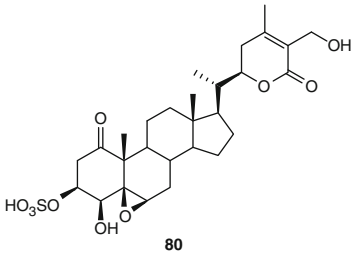

80

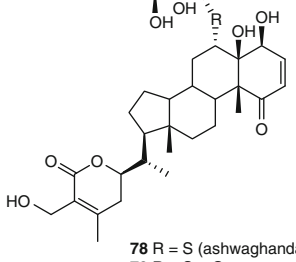

78 R = S (ashwaghandanolide)
79 R = S = O

4.2. Other Withanolides with an Unmodified Skeleton

As mentioned above, a considerable number of withanolides with the parent skeleton of withaferin A (**1**) have been isolated. With few exceptions, in new withanolides the substitution patterns of rings A and B correspond to those described in the previous section for the *Withania* withanolides. Structural variations consist mainly of combinations of oxygenated functions (hydroxy or carbonyl groups) at different positions of the steroid nucleus (most commonly at positions 12, 14, 16, 17, and 18) and the side chain (mostly at C-20, C-21, and C-27). These functionalities may also be involved in cyclic entities as lactones, lactols, or cyclic ethers. These withanolides are presented in Sect. 5., with the exception of 14α,20-epoxywithanolides that are included in Sect. 4.2.1.

4.2.1. C-14, C-17, and C-20 Hydroxylated Withanolides and Related Compounds

Hydroxylation at C-14, C-17 and C-20 is common in many withanolides. Usually the 14-hydroxy group has the α-orientation (see Sect. 4.1.), although there is a growing number of 14β-hydroxywithanolides. As already mentioned, hydroxy substitution at C-17 occurs with either the α− or β−orientation, of which the former is more common. New structures with different combinations of hydroxy groups at the above-mentioned positions have been reported, occasionally combined with hydroxy groups at positions 15, 16, and 18. The genus *Physalis* is particularly rich in 14-hydroxywithanolides, with these probably being the biosynthetic precursors

of polyoxyfunctional structures such as the physalins, present in many *Physalis* species (see Sect. 5.2.). Both 14α- and 14*β*-hydroxywithanolides are present in *Physalis* plants. A series of 14α,17*β*,20-trihydroxywithanolides was isolated from *P. peruviana* (**81**–**85**) (*50*). Phyperunolides B (**81**) and C (**82**) have the unusual feature of a free hydroxy group at C-28; another 28-hydroxywithanolide, **86**, was reported by *Dinan et al.* from the same plant (*51*). Hydroxylation at C-28 is a prerequisite in the formation of perulactones (Fig. 3), common components of *P. peruviana*. The 3-ethoxy withanolide **85** is probably an artifact formed during isolation. Also from *P. peruviana*, *Ahmad* and coworkers isolated the closely related **87** (*52*), the glycosides **88**–**91** (*53*), and a glycoside of coagulin R (**92**) (*44*). As already mentioned (Sect. 4.1.4.), another withanolide with a 14α,20-ether bridge (**71**), was also isolated from this plant (*43*). From *P. cinerascens* collected in Mexico, *Maldonado et al.* isolated 24,25-dihydrowithanolide S (**93**) with a saturated lactone side chain, together with the known withanolide S (*54*).

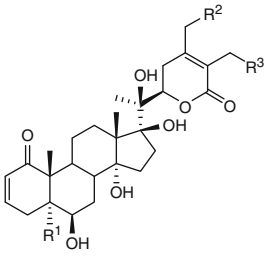

81 $R^1 = R^2 = OH$, $R^3 = H$ (phyperunolide B)
82 $R^1 = Cl$, $R^2 = OH$, $R^3 = H$ (phyperunolide C)
83 $R^1 = R^3 = OH$, $R^2 = H$ (phyperunolide D)

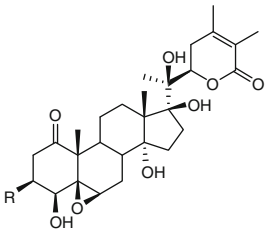

84 R = OH (phyperunolide E)
85 R = OCH_2CH_3 (phyperunolide F)

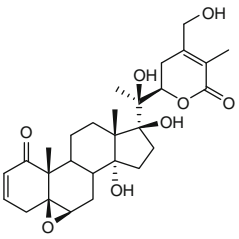

86 (28-hydroxywithanolide E)

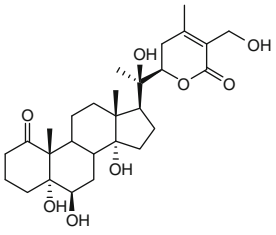

87

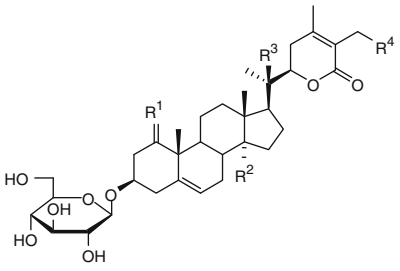

88 $R^1 = H$, α-OAc, $R^2 = R^3 = OH$, $R^4 = H$
89 $R^1 = H$, α-OAc, $R^2 = R^3 = H$, $R^4 = OH$
90 $R^1 = O$, $R^2 = H$, $R^3 = R^4 = OH$
91 $R^1 = O$, $R^2 = R^3 = R^4 = OH$

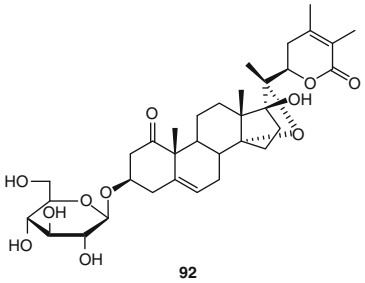

92

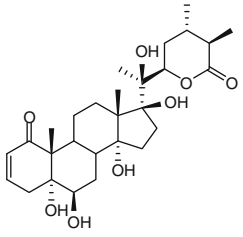

93 (24,25-dihydrowithanolide S)

An investigation of *P. angulata* growing in Taiwan gave the 15-oxygenated withangulatins B–D (**94–96**) and the 16-hydroxylated withangulatins G (**97**) and H (**98**) together with withangulatin E (**99**) and a Δ^{16} 14α-hydroxywithanolide, withangulatin F (**100**) (*55*). Several other Δ^{16} 14α-hydroxywithanolides have been reported from *Physalis* species. These include phyperunolide A (**101**) isolated from *P. peruviana* (*50*) and four 15-acetyloxy withanolides isolated from *P. angulata*, withangulatin I (**102**) (*56*), physagulin M (**103**) with the unusual feature of a free hydroxy group at C-23 (*57*), physagulin O (**104**), and compound **105** (*58*). The latter withanolide was incorrectly named physagulin L, as this name had already been assigned (see below). Physagulin N (**106**), the methanol addition product of physagulin A, was probably formed during its isolation (*57*). Δ^{16}-Withanolides with oxygen substituents at C-14 and C-15 have the appropriate functionalities for cleavage of the 13,14-bond, and the occurrence of such withanolides in physalin-rich plants strongly suggests that they are either precursors or shunt products in the biosynthesis of physalins (*59*). A Δ^{14}-withanolide, **107**, was also reported from *P. minima* collected in Pakistan (*60*).

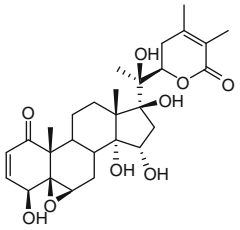

94 (withangulatin B)

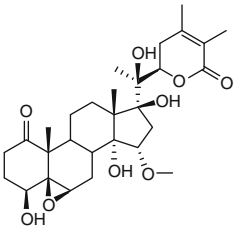

95 (withangulatin C)

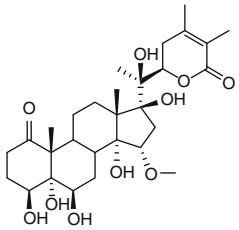

96 (withangulatin D)

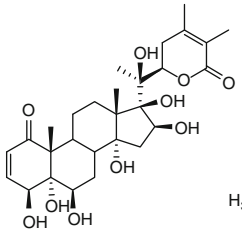

97 (withangulatin G)

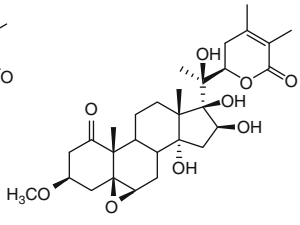

98 (withangulatin H)

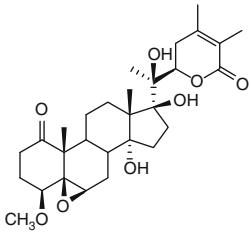

99 (withangulatin E)

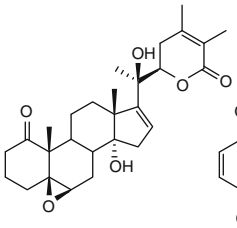

100 (withangulatin F)

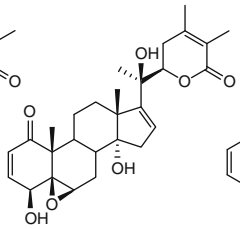

101 (phyperunolide A)

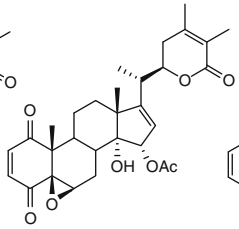

102 (withangulatin I)

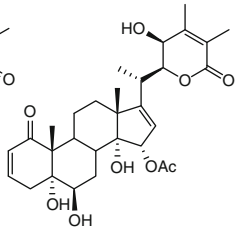

103 (physagulin M)

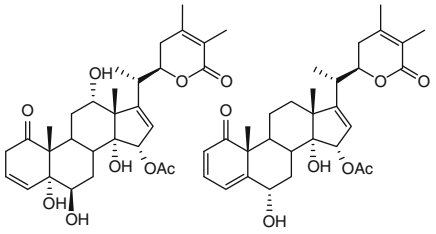

104 (physagulin O) **105**

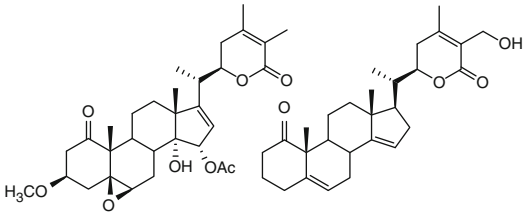

106 (physagulin N) **107**

Ajuga (Lamiaceae) is one of the few genera outside the Solanaceae that contains withanolides, most of which are closely related to the coagulins (Sect. 4.1.). From *A. parviflora*, *Malik* and coworkers have reported seven 14α-hydroxywithanolides, compound **108** (isolated together with coagulin J) (*61*), ajugins A (**109**), B (**110**) (*62*), C (**111**), D (**112**) (*63*), E (**113**), and F (**114**) (*64*), a Δ^{14} withanolide (**115**), and a 14α,20-epoxywithanolide (**116**) (*65*). As already mentioned, ajugin, identical to coagulin R (**65**), was first isolated from this plant (*45*).

Several 14*β*-hydroxywithanolides have been isolated from *Physalis* species, and all of them also have an α−oxygenated function (hydroxy or acetate) at position 15. These include physagulins H–K (**117–120**) (*66*), physagulin L (**121**) (*57*), and compounds **122** and **123** (*58*) from *P. angulata*. The latter two compounds were

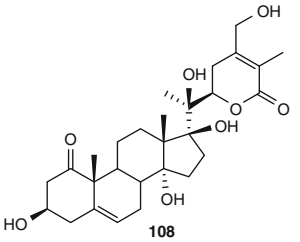

108

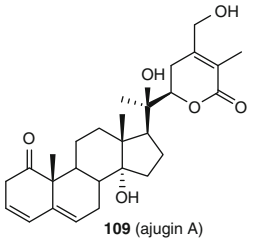

109 (ajugin A)

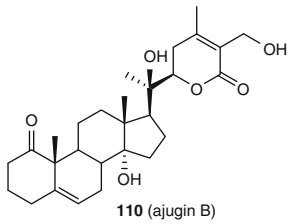

110 (ajugin B)

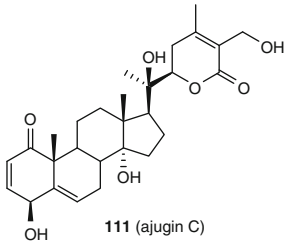

111 (ajugin C)

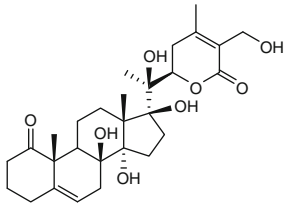

112 (ajugin D)

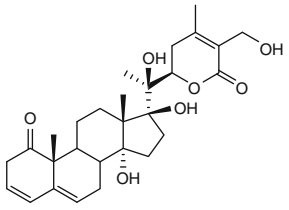

113 (ajugin E)

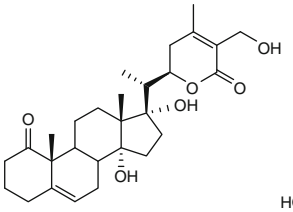

114 (ajugin F)

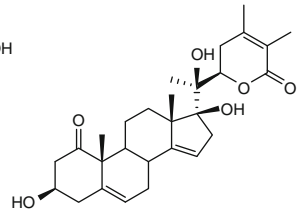

115

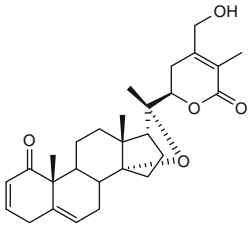

116

incorrectly named physagulins M and N, as these names had already been assigned (see above). The chlorohydrin **124** was reported from *P. alkekengi* var. *franchetii* (*67*) and the deacetylated analogue of physapubenolide (**125**) from *P. peruviana* (*52*). Outside the *Physalis* genus, new 14*β*-hydroxywithanolides have been isolated from *Jaborosa leucotricha* (jaborosalactone 8 (**126**)) (*68*) and *J. bergii* (jaborosalactol 23 (**127**)) (*69*).

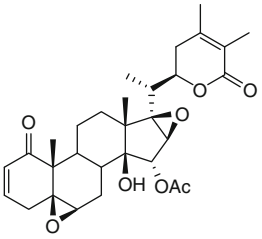

117 (physagulin H)

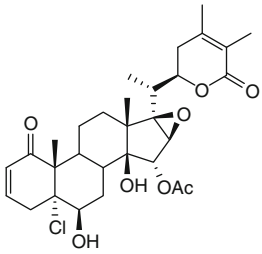

118 (physagulin I)

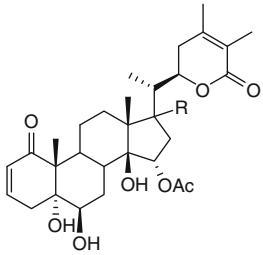

119 R = *α*-H (physagulin J)
120 R = *β*-OH (physagulin K)

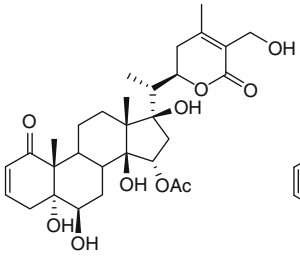

121 (physagulin L)

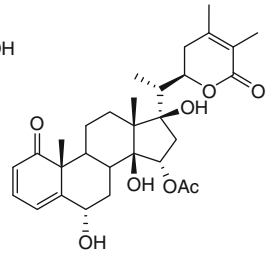

122

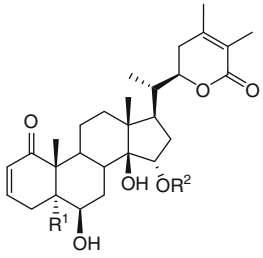

123 R^1 = OH, R^2 = H
124 R^1 = Cl, R^2 = Ac

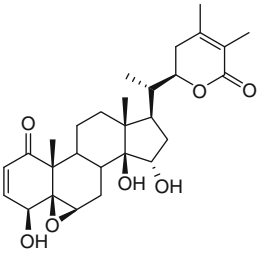

125 (deacetylphysapubenolide)

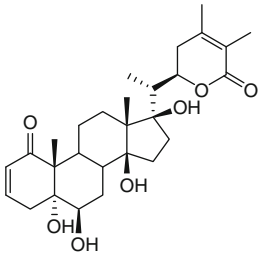

126 (jaborosalactone 8)

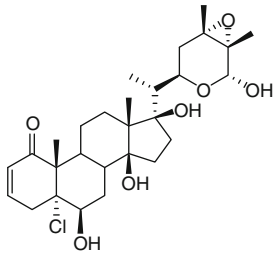

127 (jaborosalactone 23)

4.2.2. C-18 Hydroxylated Withanolides

Withanolides with a functionalized C-18 at various oxidation levels (alcohol, aldehyde, and lactone carbonyl) have been isolated from plants of the genera *Withania* (see Sect. 4.1.5.), *Acnistus, Dunalia*, *Eriolarynx*, *Iochroma*, and *Physalis* (*4*, *5*). Hydroxylation at C-18 is usually combined with hydroxy groups occurring at positions 14, 17, or 20. Thus, 18-hydroxywithanolide D (**128**) was isolated from *Eriolarynx lorentzii* (synonym *Vassobia lorentzii*) (*70*), and the related 18-hydroxywithanolide **129** and the corresponding 18-aldehyde **130** were isolated from *Dunalia brachyacantha* (*71*) (both plants collected in Argentina), while the 18-acetoxywithanolide **131** was reported from *Iochroma gesneroides* together with several 3-methoxylated derivatives formed during the extraction procedure (*72*). As part of a systematic study of Mexican *Physalis* species, five 18-acetoxywithanolides, the physachenolides A–E (**132–136**) were isolated from the leaves, flowers, and stems of *Physalis chenopodifolia* (*73*). Physachenolide B (**133**) has a 28-hydroxy group while physachenolide E (**136**) is a Δ^{14}-withanolide. The aerial parts of *Physalis coztomatl*, also collected in Mexico,

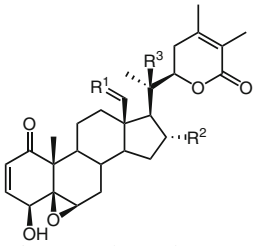

128 R^1 = H,OH, R^2 = H, R^3 = OH (18-hydroxywithanolide D)
129 R^1 = H,OH, R^2 = R^3 = H
130 R^1= O, R^2 = OH
131 R^1 = H,OAc, R^2 = OAc, R^3 = H

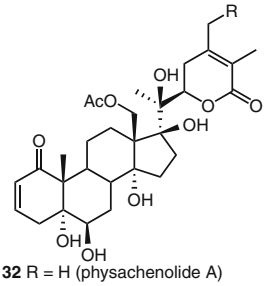

132 R = H (physachenolide A)
133 R = OH (physachenolide B)

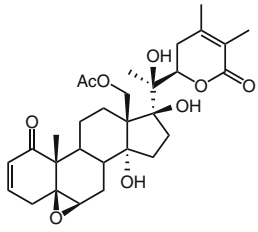

134 (physachenolide C)

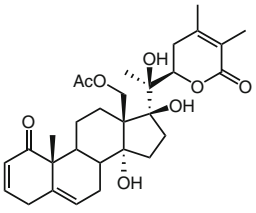

135 (physachenolide D)

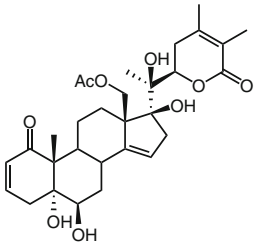

136 (physachenolide E)

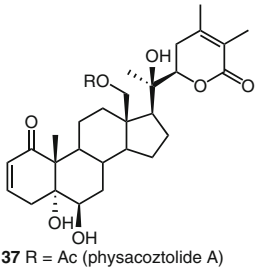

137 R = Ac (physacoztolide A)
138 R = H (physacoztolide B)

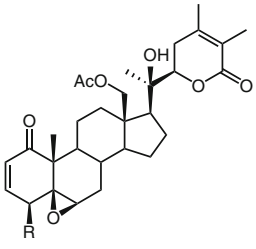

139 R = H (physacoztolide C)
142 R = OH (18-acetoxywithanolide D)

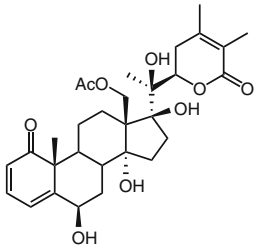

140 (physacoztolide D)

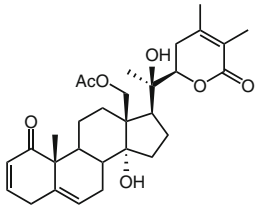

141 (physacoztolide E)

rendered five new withanolides functionalized at C-18, physacoztolides A–E (**137**–**141**), together with physachenolide C (**134**), 18-acetoxywithanolide D (**142**), and 18-hydroxywithanolide D (**128**) (*74*).

4.2.3. C-12 and C-21 Oxygenated Withanolides

Withanolides with a free hydroxy or keto group at C-12 are mostly restricted to the *Datura* genus. In the genus *Jaborosa*, 12-ketowithanolides are most probably involved as precursors in the formation of additional rings with the side chain, giving rise to several modified skeletons (see Sect. 5.9.). However, only two withanolides with unmodified skeletons containing a free ketone at C-12 have been reported from these plants, (−)-jaboromagellonine (**143**) from *J. magellanica* (*75*) and jaborosalactone 44 (**144**) from *J. kurtzii* (*76*). Four new 12-oxygenated withanolides were isolated from plants of *Datura ferox* collected in Argentina, together with other known daturalactones. 15*β*-Hydroxynicandrin B (**145**) was found to have the common 5α-hydroxy-6α,7α-epoxy substitution pattern in ring B (see Sect. 4.1.2.) (*77*), while daturalactones 5–7 (**146**–**148**) exhibit related arrangements resulting from hydrolytic cleavage of the epoxide or rearrangement of the epoxyalcohol (*78*). The 12*β*-epimer of **145**, baimantuololine A (**149**) (*79*) and the closely related glycosides baimantuoluosides A–C (**150**–**152**) (*80*), were isolated from the dry flowers of *Datura metel* (used in Chinese medicine). The 1*β*-alcohol **153** from *Datura quercifolia* collected in India is closely related to the compounds mentioned above (*81*). 12-Oxygenated withanolides have also been reported from the stem bark of the Ethiopian shrub *Discopodium penninervium* (**154**) (*82*), from *Iochroma gesneroides* (**155**) (*72*), and from *Acnistus arborescens* (**156**) (*83*), with the latter two compounds bearing a 12*β*-acetoxy group.

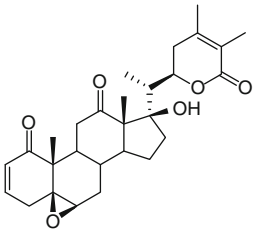

143 ((-)jaboromagellonine)

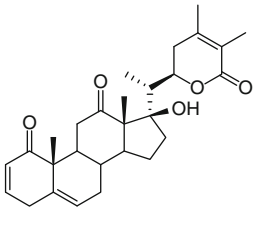

144 (jaborosalactone 44)

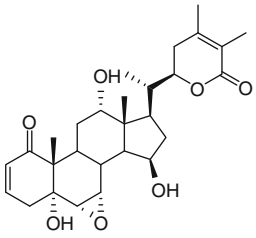

145 (15*β*-hydroxynicandrin B)

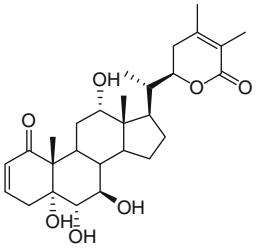

146 (daturolactone 5)

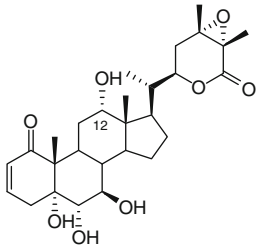

147 (daturolactone 6)

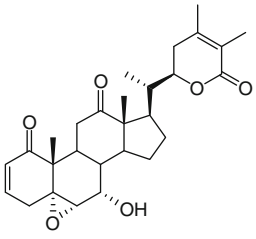

148 (daturolactone 7)

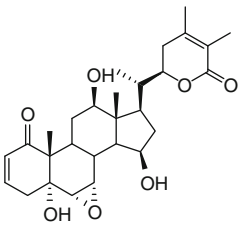

149 (baimantuoluoline A)

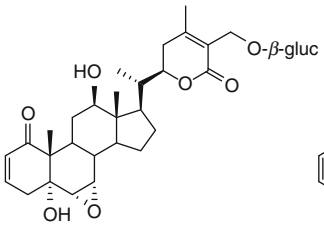

150 (baimantuoluoside A)

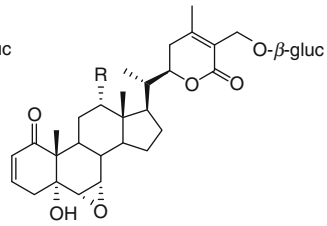

151 R = OH (baimantuoluoside B)
152 R = H (baimantuoluoside C)

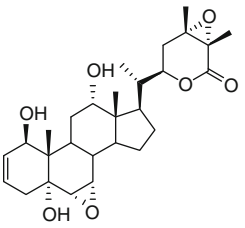

153

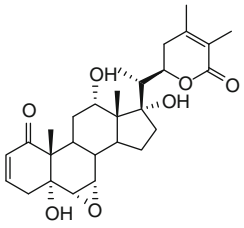

154

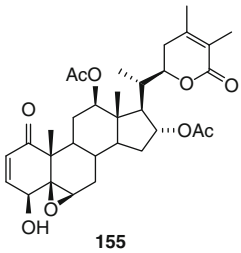

155

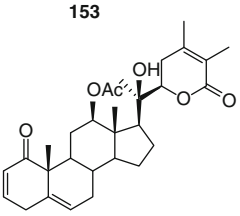

156

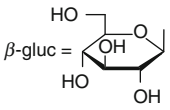

From *Dunalia brachyacantha* collected in Bolivia, *Bravo et al.* isolated the glycosides dunawithanine G (**157**) and dunawithanine H (**158**) (*84*), closely related to the known dunawithanine F (**159**) (*85*).

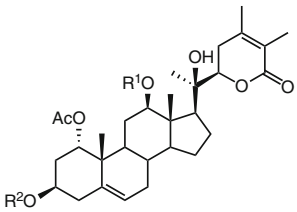

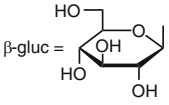

157 R^1 = Ac, R^2 = (dunawithanine G)

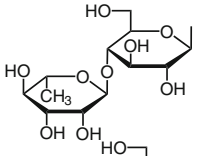

158 R^1 = H, R^2 = (dunawithanine H)

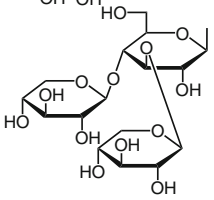

159 R^1 = H, R^2 = β-gluc(1-3)-[β-gluc(1-4)]-β-gluc- (dunawithanine F)

Outside the Solanaceae, most withanolides from *Tacca* species bear a 12α-acetoxy group. *Tacca* species originate in the tropical and subtropical regions, mostly in Asia and Africa. They contain highly oxygenated withanolides, usually with modified skeletons (see Sect. 5.4.4.) characterized by a 1α-acetoxy group and a 2α,3α-epoxide in ring A, although several have been reported with the unmodified parent skeleton. From the rhizomes of *Tacca chantrieri*, *Yokosuka et al.* isolated two glycosides, chantriolides A (**160**) and B (**161**), with a glucose unit at C-27 (*86*). From *Tacca plantaginea*, *Liu et al.* isolated plantagiolides A–E (**162–166**) (*87*). *Tacca* species are also rich in glycosidated sterols not included in this review; the withanolide **167** with a steroid nucleus that resembles a sterol was also isolated from the rhizomes of *T. chantrieri* (*88*).

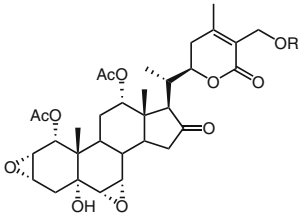

160 R = β-gluc (chantriolide A)
162 R = H (plantagiolide A)

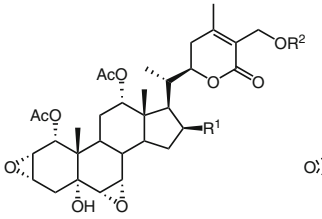

161 R^1 = OH, R^2 = β-gluc (chantriolide B)
163 R^1 = OH, R^2 = H (plantagiolide B)
164 R^1 = R^2 = H (plantagiolide C)

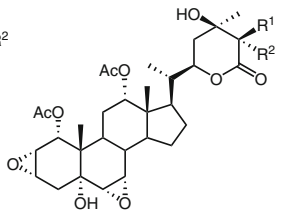

165 R^1 = CH_3, R^2 = H (plantagiolide D)
166 R^1 = OH, R^2 = CH_3 (plantagiolide E)

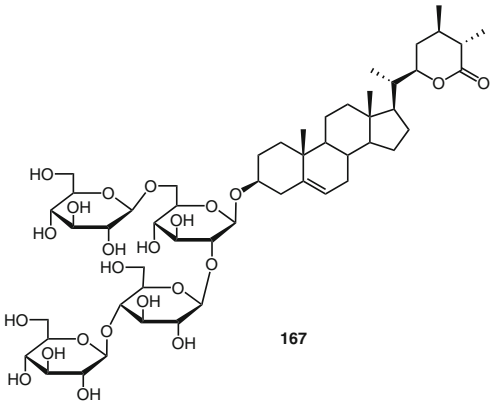

167

Although 21-oxygenated withanolides are present in *Datura*, *Jaborosa*, and *Tacca* species, 21-hydroxywithanolides with an unmodified skeleton have only been reported in the genus *Datura*, in many cases combined with a 12β-hydroxy group. Withafastuosin D (**168**) is the major withanolide of *D. metel* var. *fastuosa* (synonym *D. fastuosa*), and was isolated from the leaves together with withafastuosin E (**169**) (*89*); withafastuosin F (**170**) was isolated from the flowers of the plant (*90*). Withametelin H (**171**) isolated from the leaves of *D. metel* has the unusual feature of a methoxy group at C-27 (*91*). From flowers of *D. metel*, *Pan et al.* isolated the 27-glycoside withametelin P (**172**) (*92*) and *Yang et al.*

isolated baimantuoluolines C, B, and F (**173–175**), with the former also having a 27-methoxy group (*79*, *93*). It should be noted that the name "withametelin" is usually reserved for withanolides possessing an oxygen bridge between C-21 and C-24 (see Sect. 5.1.1.), and 21-hydroxywithanolides are the most probable biosynthetic precursors of these compounds. Another five 21-hydroxywithanolides, withatatulin (**176**) (*94*) and withatulins B–E (**177–180**), were isolated by *Ray* and coworkers from *D. stramonium* var. *tatula* (synonym *D. tatula*), which grows in the sub-Himalayan tracts of India and is often cultivated as an ornamental plant (*95*, *96*).

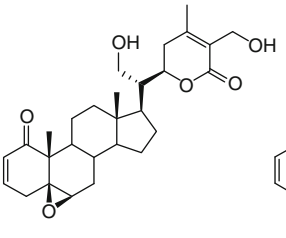

168 (withafastuosin D)

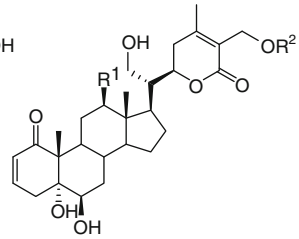

169 R^1 = H, R^2 = H (withafastuosin E)
170 R^1 = OH, R^2 = H (withafastuosin F)
171 R^1 = H, R^2 = CH_3 (withametelin H)
172 R^1 = H, R^2 = β-gluc (withametelin P)
173 R^1 = OH, R^2 = CH_3 (baimantuoluoline C)

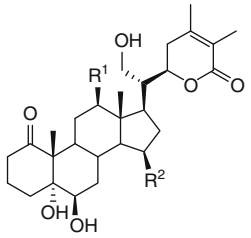

174 R^1 = H, R^2 = OH (baimantuoluoline B)
175 R^1 = OH, R^2 = H (baimantuoluoline F)

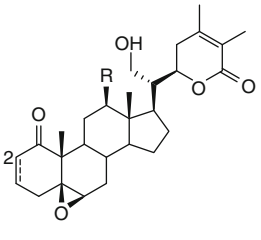

176 R = H (withatatulin)
177 R = OH, Δ^2 (withatatulin B)
180 R = H, Δ^2 (withatatulin E)

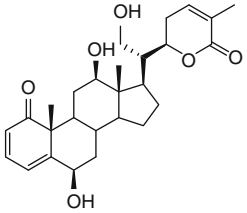

178 (withatatulin C)

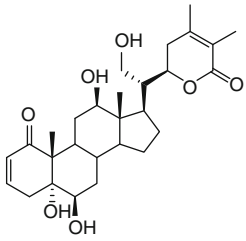

179 (withatatulin D)

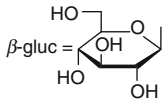

β-gluc =

4.2.4. Other Hydroxylated Withanolides

Besides those already mentioned above, several other 16-oxygenated withanolides have been reported. Exodeconolides A–C (**181–183**) were isolated from *Exodeconus maritimus* collected in Peru (*97*), the 16-acetates **184** and **185** were reported from *Acnistus arborescens* collected in Brazil (*98*), 16α-acetoxyhyoscyamilactol (**186**) from the seeds of *Hyoscyamus niger* used in

Chinese medicine (*99*), **187** from *Dunalia brachyacantha* collected in Argentina (*71*), **188–190** from the leaves of *Discopodium penninervium* (*100*), and virginols A (**191**) and C (**192**) from *Physalis virginiana* (*101*). Virginol B (**193**) was also reported from *P. virginiana* (*101*) and **194** was isolated from the roots of *D. penninervium* (*102*). The known withaphysacarpin (**195**) and its 3-methoxy derivative, **196**, with a 16*β*-hydroxy group, were isolated from the fruits of *Physalis philadelphica* and the configuration of the lactone methyl groups was established as shown, for both compounds (*103*). LC-MS analysis of an ethyl acetate extract of the plant suggested that **196** may occur naturally although in minor amounts, being generated to a larger extent as a result of the extraction procedure. From leaves and stems of *P. philadelphica*, *Kinghorn* and coworkers isolated philadelphicalactones A and B (**197**, **198**) and compound **199**, all of them with a saturated δ-lactone side chain (*104*, *105*).

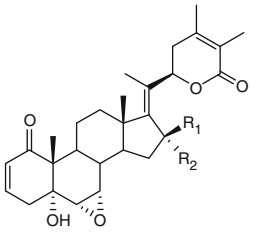

181 R^1 = OH, R^2 = H (exodeconolide A)
182 R^1 = H; R^2 = OH (exodeconolide B)

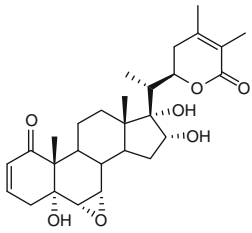

183 (exodeconolide C)

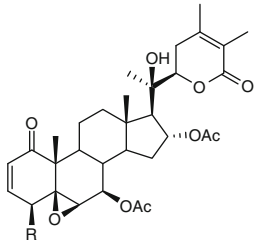

184 R = OH
185 R = H

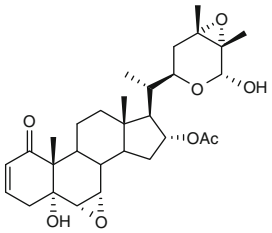

186 (16*α*-acetoxyhyoscyamilactol)

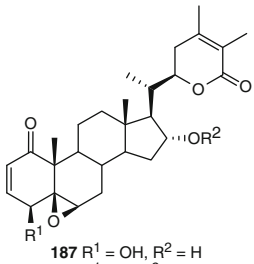

187 R^1 = OH, R^2 = H
188 R^1 = H, R^2 = Ac

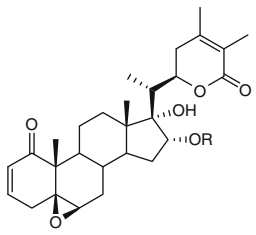

189 R = Ac
190 R = H

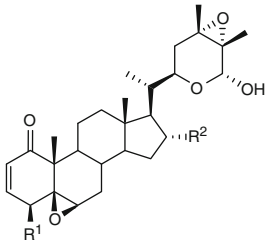

191 R^1 = OH, R^2 = OAc (virginol A)
192 R^1 = H, R^2 = OAc (virginol C)
193 R^1 = OH, R^2 = H (virginol B)

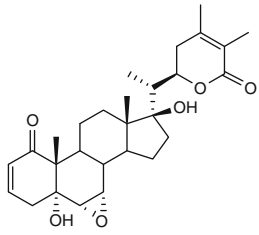

194

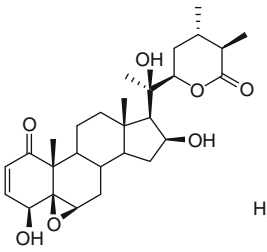

195 (withaphysacarpin)

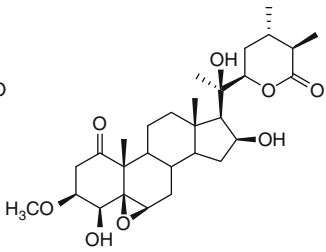

196

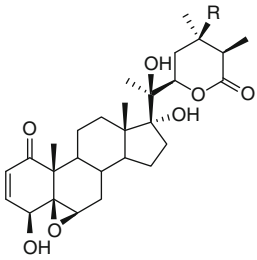

197 R = H (philadelphicalactone A)
198 R = OH (philadelphicalactone B)

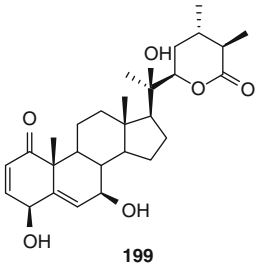

199

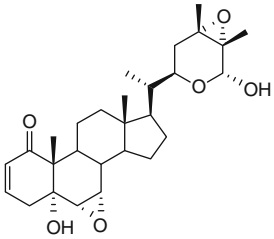

200 (Nic-3)

A 24,25-diol related to Nic-3 was reported from *Larnax glabra* (*106*), but, however, comparison of the NMR data indicates that this compound (larnaxolida A) is actually Nic-3 (**200**) (*3*). An epimer at C-5 was also reported (larnaxolida B), but the spectroscopic data do not correspond to the proposed structure.

Tubocapsanolides A (**201**), D (**202**), and F (**203**) and the 20-hydroxy and the 23-hydroxy derivatives of tubocapsanolide A **204** and **205** were isolated from *Tubocapsicum anomalum* (*107*). From *Ajuga bracteosa* collected in the north of Pakistan, *Malik* and coworkers isolated two 28-hydroxywithanolides, bracteosins A (**206**) and B (**207**), with C-19 in the latter compound oxidized to a carboxylic acid, and bracteosin C (**208**) (*108*). As in previous cases, these compounds probably derive from the corresponding Δ^2-1-ketones, upon reaction with methanol during their isolation.

From the aerial parts of *Datura metel* collected in China, *Ma et al*. isolated three new 27-glycosides, daturametelins H, I, and J (**209–211**), together with the known daturataturin A (**212**) and the aglycone **213** (*109*). The closely related 7-acetate **214** was isolated from *Iochroma gesneroides* (*72*).

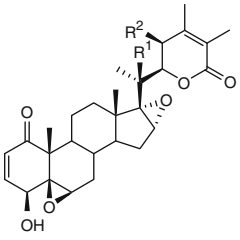

201 $R^1 = R^2 = H$ (tubocapsanolide A)
204 $R^1 = OH$, $R^2 = H$
205 $R^1 = H$, $R^2 = OH$

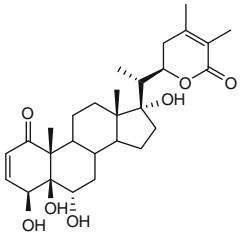

202 (tubocapsanolide D)

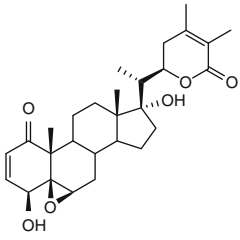

203 (tubocapsanolide F)

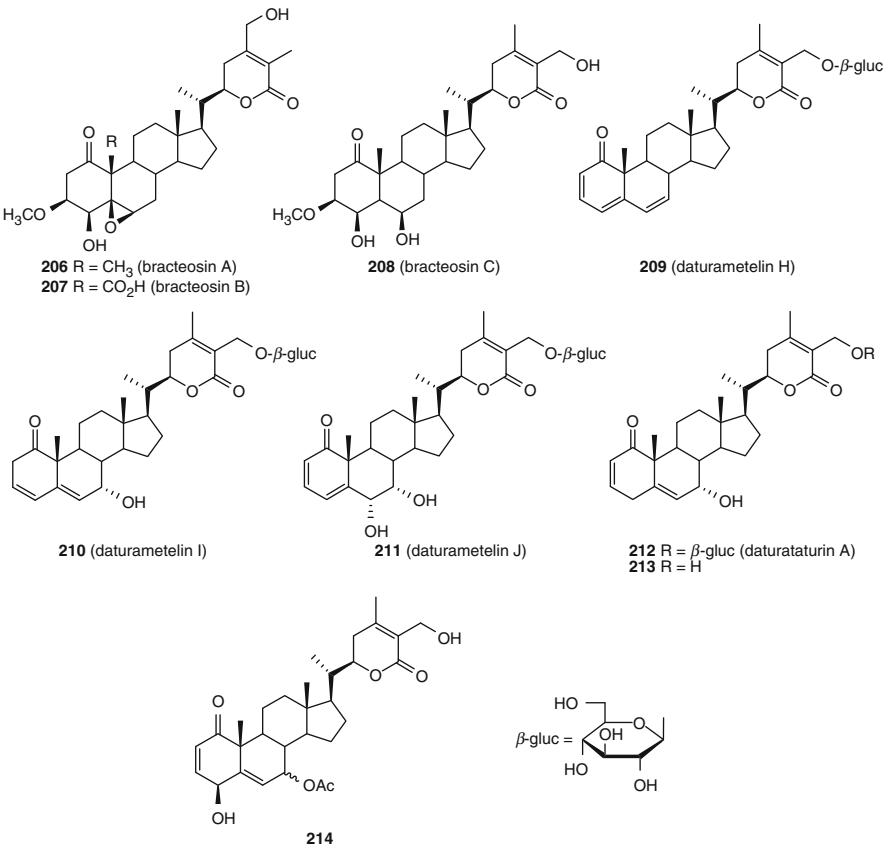

4.2.5. Cilistols and Related Withanolides

Nohara and coworkers investigated *Solanum ciliatum* (synonym *Solanum cilistum*) and isolated a series of withanolides with a δ-lactol side chain, which included several Δ^5-3β-*O*-sulfates and 6-substituted 3,5-cyclowithanolides. Variations at the side chain comprise a 24,25-epoxide or the corresponding 24,25-diol from hydrolytic cleavage, 26-*O*-glycosides, or reaction products of the epoxide or the hemiketal with methanol. Cilistols a, b, d, q, g, and f (**215–220**) contain a $\Delta^{2,5}$-1-ketone in rings A/B, and the latter two compounds (with the cleaved epoxide) exist as equilibrium mixtures of the epimeric C-26 hemiketals (*110*). The C-26 glycosides, cilistols t, i, and j (**221–223**) present a Δ^5-1α,3β-diol arrangement in rings A/B and cilistols y (**224**) and w (**225**) have the unusual feature of a 3β-*O*-sulfate group (*111*). The 3,5-cyclosteroid moiety found in cilistols u, p, pm, and p1 (**226–229**) (*112*) has no precedent among natural products but is easily formed from Δ^5-steroids with a good leaving group at C-3

(*e.g.* a sulfate); this rearrangement occurs even under very mild conditions (traces of methanol or water in the extraction or purification solvents may be enough), thus the assumption that these compounds are natural products should be taken with caution. The ergostane glycoside, cilistol v (**230**), or a closely related sterol, is probably the biosynthetic precursor of cilistols in this plant (*111*). Cilistepoxide (**231**) and cilistediol (**232**) are two closely related withanolides isolated from *Solanum sisymbriifolium* collected in Brazil (*113*).

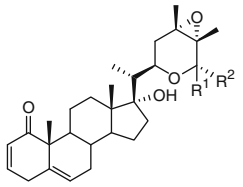

215 R^1 = H, R^2 = OH (cilistol a)
216 R^1 = OCH_3, R^2 = H (cilistol b)
217 R^1 = H, R^2 = OCH_3 (cilistol d)
218 R^1 = H, R^2 = O-*β*-gluc (cilistol q)

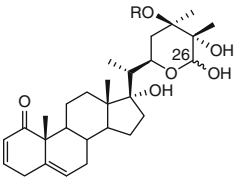

219 R = H, (26*R*/*S*) (cilistol g)
220 R = CH_3, (26*R*/*S*) (cilistol f)

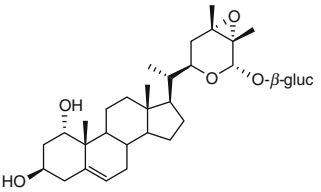

221 (cilistol t)

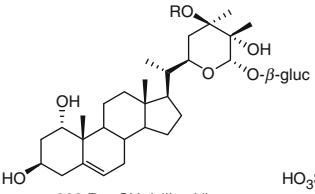

222 R = CH_3(cilistol i)
223 R = H (cilistol j)

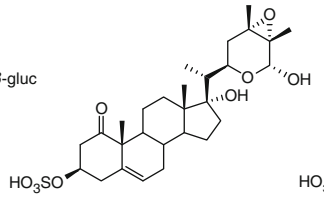

224 (cilistol y)

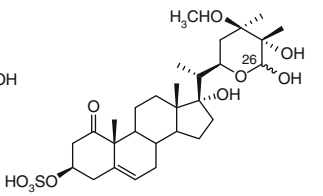

225 (26*R*/*S*) (cilistol w)

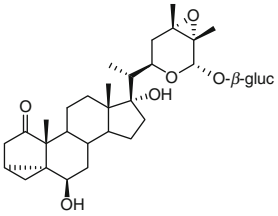

226 (cilistol u)

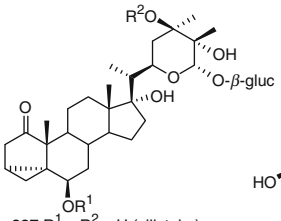

227 R^1 = R^2 = H (cilistol p)
228 R^1 = CH_3, R^2 = H (cilistol pm)
229 R^1 = R^2 = CH_3 (cilistol p1)

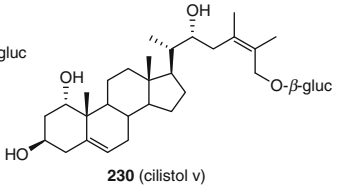

230 (cilistol v)

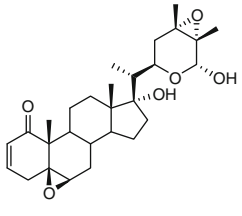

231(cilistepoxide)

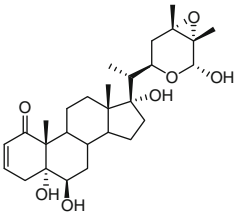

232 (cilistediol)

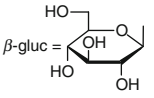

5. Withanolides with Modified Skeletons

A large number of withanolides with structures that depart from the classical withaferin A (**1**) parent structure are known nowadays. Modifications usually found are additional rings formed by direct C–C bonds, cyclic ethers and hemiketals, or lactones that may involve carbons from the steroid nucleus or from the side chain. Other modifications include formation of *seco*-steroids (as in physalins), a rearranged steroid nucleus, aromatic rings, and lack of an angular methyl as among the most important. One particularly interesting example is that present in a C_{29} withanolide from the bark of *Eucalyptus globulus* (**233**) that has an ethyl substituent at C-25 instead of the usual methyl group (*114*).

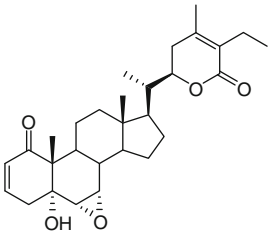

233

5.1. Withanolides with Additional Rings Involving C-21

Carbon-21 may participate in additional rings by forming either direct C–C bonds or ether bridges with other carbons in the side chain or in the steroid nucleus. Several new withanolide types with these arrangements have been reported.

5.1.1. Withametelins and Sativolides

Withametelin (**234**) exhibits an oxygen bridge between C-21 and C-24 resulting in a bicyclic side chain; it was isolated by *Ray* and coworkers from the dried leaves of *Datura metel* (*3*). Several withanolides with this functionality were subsequently isolated; some have also been named as withafastuosins, daturametelins, and baimantuoluolines on different occasions. The flowers of *D. metel*, used for centuries in traditional Chinese medicine, have been shown to contain several withametelins. *Pan et al*. isolated the 12β-hydroxylated derivatives withametelins I–M (**235**–**239**), together with withametelins N (**240**) and O (**241**), and the *seco*-withametelins **242** and **243** (*92*). Also from the dry flowers, *Yang et al*. isolated baimantuoluolines D (**244**) and E (**245**) (*93*). The closely related structures withametelinone (**246**), withametelinol (**247**), withametelinols A (**248**) and B (**249**), witharifeen (**250**), and daturalicin (**251**) were isolated by *Siddiqui et al*.

from the aerial parts of *Datura inoxia* collected in Pakistan (*115*–*117*). Daturacin (**252**) was reported also from *D. inoxia* as the first withanolide with a (22*S*) configuration based on a negative *Cotton* effect at 249.4 nm (*118*). The proposed configuration inversion at C-22 and C-24 compared to other withametelins (*92*), would require H-20 to occupy an *axial* instead of *equatorial* position. However, the almost perfect coincidence of the ^{1}H and ^{13}C NMR data of the side chain with those of other "normal" withametelins and the assignment of the configuration at C-5 based exclusively on CD data, suggest that this structure should be extensively revised.

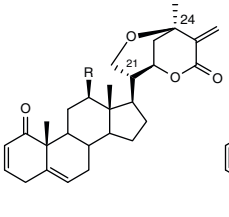

234 R = H (withametelin)
238 R = OH (withametelin L)

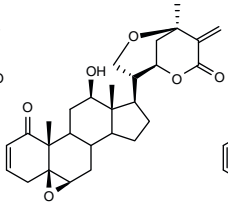

235 (withametelin I)

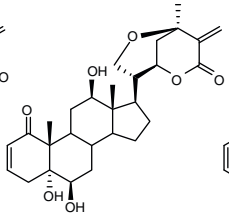

236 (withametelin J)

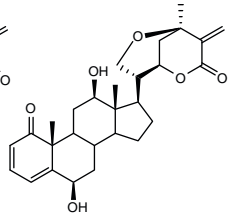

237 (withametelin K)

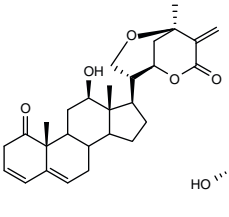

239 (withametelin M)

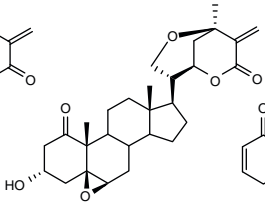

240 (withametelin N)

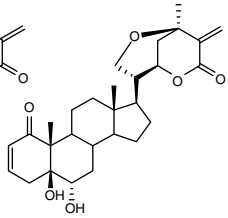

241 (withametelin O)

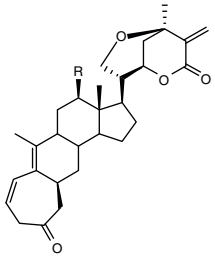

242 R = H
243 R = OH

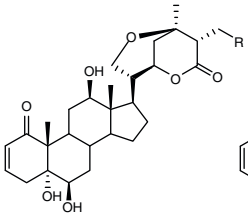

244 R = OCH_3 (baimantuoluoline D)
245 R = OH (baimantuoluoline E)

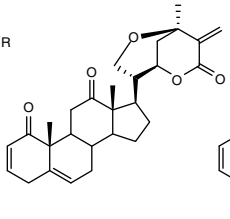

246 (withametelinone)

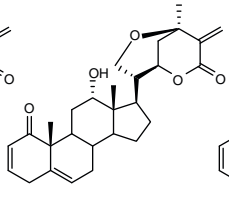

247 (withametelinol)

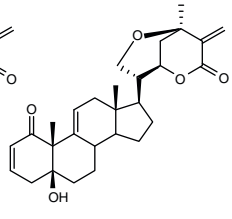

248 (withametelinol A)

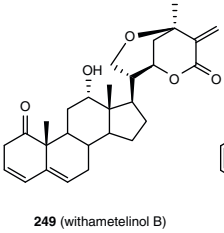

249 (withametelinol B)

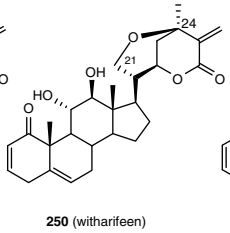

250 (witharifeen)

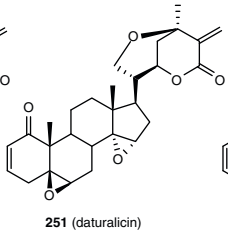

251 (daturalicin)

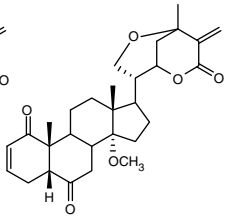

252 (daturacin)

At variance with the above, sativolides have an oxygen bridge between C-21 and C-12 in the steroid nucleus. The additional six-membered hemiketal (or ketal) ring, results from what must have been originally a C-12 ketone and a C-21 hydroxy group. Jaborosalactones R (**253**), S (**254**), and T (**255**), were isolated from *Jaborosa sativa* (synonym *Trechonaetes sativa*) collected in Argentina (*119*). C-12-Hemiketals are highly reactive towards simple alcohols (see Sect. 5.4.2.), thus the methyl ketal **255** is probably formed during isolation. *Nicotra et al.* reported the isomeric clorohydrin, jaborosalactone 37 (**256**), from *Jaborosa rotacea* (*120*). Interestingly, the Δ^2-withanolide **257** was present in *Jaborosa caulescens* var. *caulescens* (isolated together with the 12-*O*-methyl derivative) while its 2,3-dihydro derivative **258** was present in *J. caulescens* var. *bipinnatifida* (*121*).

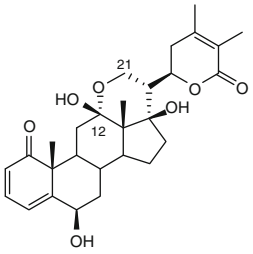

253 (jaborosalactone R)

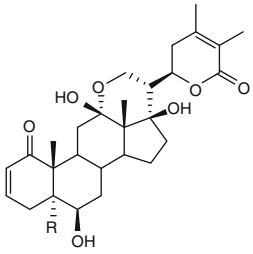

254 R = OH (jaborosalactone S)
256 R = Cl (jaborosalactone 37)

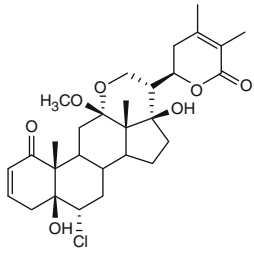

255 (jaborosalactone T)

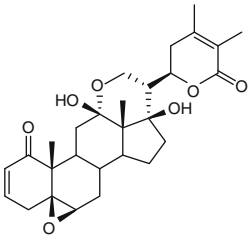

257 (jaborosalactone 38)

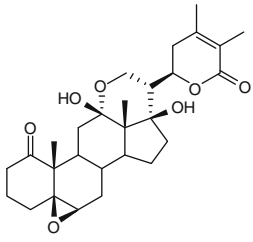

258 (jaborosalactone 39)

5.1.2. Acnistins

The acnistins also exhibit a bicyclic side chain involving C-21 and the lactone ring but, at variance with withametelins, C-21 is directly bonded to C-24 via a C–C bond instead of an ether bond (*3*, *4*). It has been proposed that the 21,24 bond is probably formed via a SN_2 type reaction in withanolides having a good leaving group at C-21. The first examples of this family, acnistins A (**259**) and E (**260**), were isolated by *Usubillaga et al.* from plants of *Acnistus arborescens* (synonym *Acnistus ramiflorus*) collected in Venezuela, with their stereochemical and spectroscopic assignments later revised by *Luis et al.* (*122*, *123*). Withanolides with this bicyclic side chain have been reported also from *Tubocapsicum anomalum* (*3*). *Luis* and coworkers isolated acnistins A and E, together with the new acnistins B (**261**),

C (**262**), D (**263**), F (**264**), G (**265**), and H (**266**), from the leaves of *Dunalia solanacea* collected in Medellin (Colombia) (*124–126*).

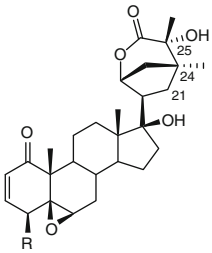

259 R = H (acnistin A)
260 R = OH (acnistin E)

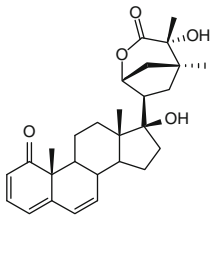

261 (acnistin B)

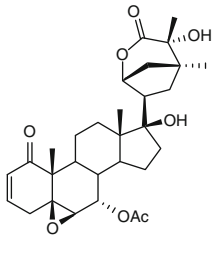

262 (acnistin C)

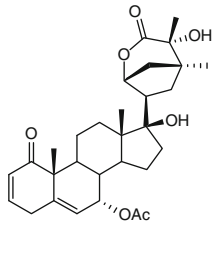

263 (acnistin D)

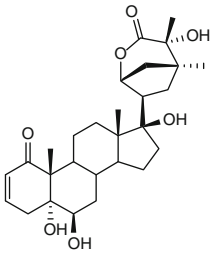

264 (acnistin F)

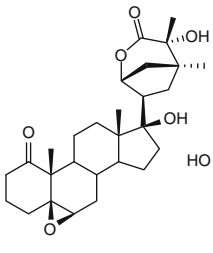

265 (acnistin G)

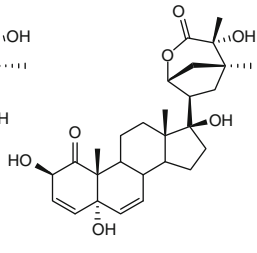

266 (acnistin H)

An epimer of acnistin A, 17-epiacnistin A (**267**) was isolated from *Discopodium penninervium* collected in Ethiopia (*127*). Recently, using bioassay-directed fractionation, six new 17-epiacnistins were isolated from *Tubocapsicum anomalum* collected in Taiwan (*107*). Anomanolides A (**268**) and B (**269**) were identified as the 17-epimer of acnistin E and the ring B diol resulting from diequatorial cleavage of the epoxide. Anomanolides C–F (**270**–**273**) had an additional 16α-hydroxy substituent. From fruits of *T. anomalum* collected in Japan, *Kiyota et al.* isolated three acnistin glycosides, isotubocaposides A–C (**274–276**) with a 1α,3β-dihydroxy substitution pattern in ring A (*128*). The distinctive feature of these acnistins was an inverted configuration at C-25 as determined by X-ray crystallography.

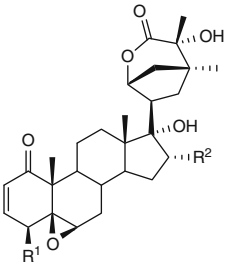

267 $R^1 = R^2 = H$ (17-epiacnistin A)
268 $R^1 = OH$, $R^2 = H$ (anomanolide A)
270 $R^1 = R^2 = OH$ (anomanolide C)

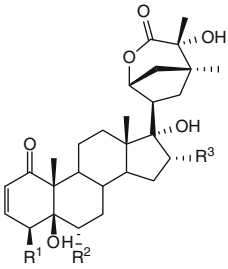

269 $R^1 = R^2 = OH$, $R^3 = H$ (anomanolide B)
271 $R^1 = R^3 = OH$, $R^2 = Cl$ (anomanolide D)
272 $R^1 = H$, $R^2 = R^3 = OH$ (anomanolide E)
273 $R^1 = R^3 = OH$, $R^2 = H$ (anomanolide F)

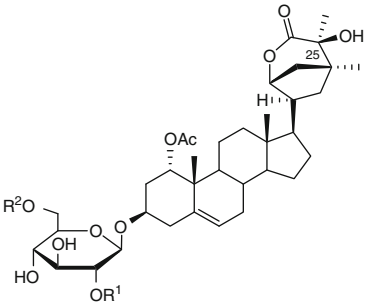

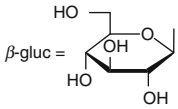

274 $R^1 = R^2 = \beta$–gluc (isotubocaposide A)
275 R^1 = H, $R^2 = \beta$–gluc (isotubocaposide B)
276 $R^1 = \beta$–gluc, R^2 = H (isotubocaposide C)

5.1.3. Withajardins

In the withajardins, C-21 is directly bonded to C-25 resulting in a bicyclic lactone side chain with a six-membered homocycle. Withajardins A–E (**277**–**281**) were isolated from plants of *Deprea orinocensis* collected in Colombia (*129*, *130*). A 16,17-dihydroxylated withajardin, tubonolide A (**282**), was isolated from the stems and leaves of *T. anomalum* (*107*) and the glycosides tuboanosides A and B (**283** and **284**) from the fruits of this same plant (*131*). The latter three compounds have an inverted configuration at C-24 compared to the other withajardins, and this was confirmed by X-ray diffraction in the case of tuboanosides A and B (Fig. 4). (It should be noted that in the original publication, the configuration at C-20 in the structure drawing of these compounds is incorrect; the structure shown here was taken from the X-ray data deposited at the Cambridge Crystallographic Data Centre, CCDC). A common precursor has been proposed in the biogenetic routes to acnistins, withajardins, and withametelins; the simultaneous finding of acnistins and withajardins in *T. anomalum* supports this proposal.

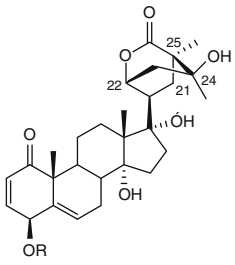

277 R = H (withajardin A)
280 R = Ac (withajardin D)

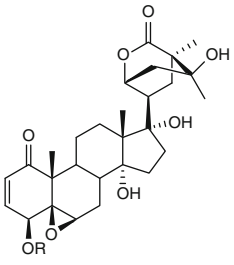

278 R = H (withajardin B)
279 R = Ac (withajardin C)

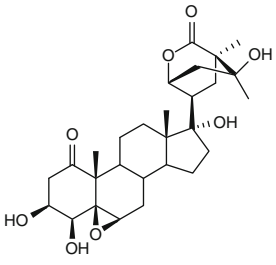

281 (withajardin E)

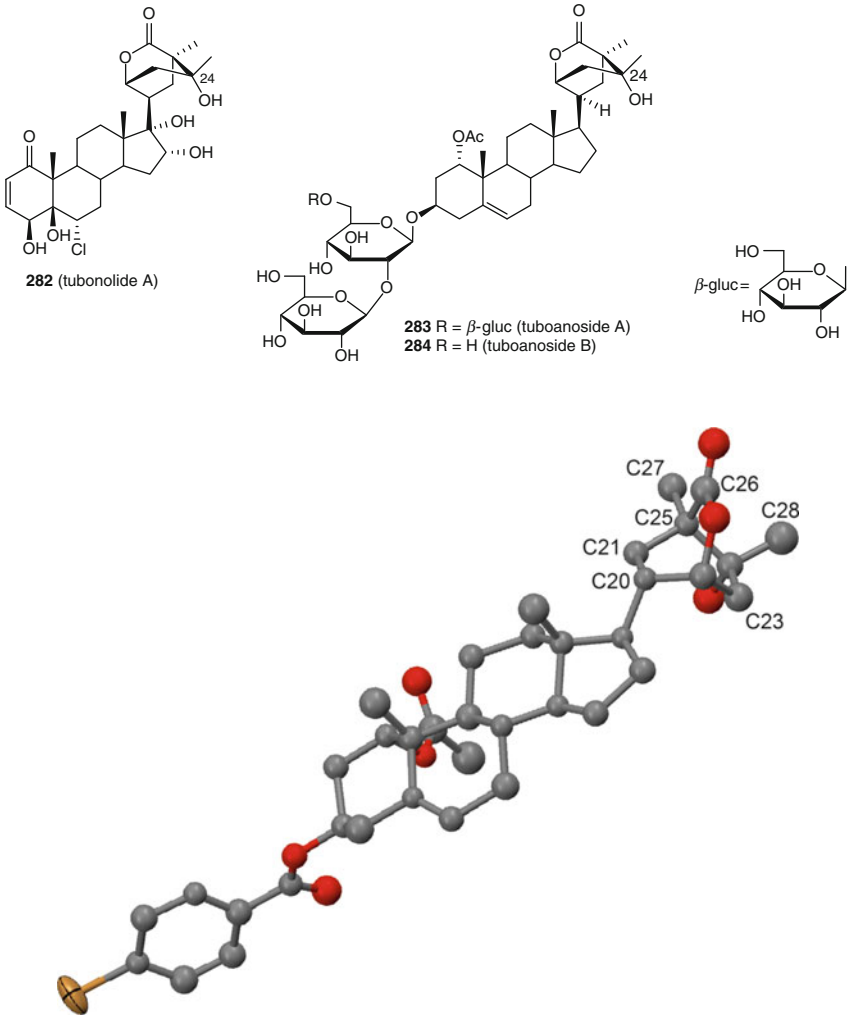

Fig. 4. X-ray crystal structure of the *p*-bromobenzoate of tuboanosigenin (CCDC 680092), aglycone of tuboanosides A (**283**) and B (**284**) (*131*). Structure drawing generated with Mercury 2.3

5.1.4. 15,21-Cyclowithanolides (Norbornane Type)

Nicotra et al. reinvestigated *Jaborosa bergii* and isolated five new withanolides with a carbon-carbon bond between C-15 and C-21, resulting in a novel norbornane-type structure in ring D (*69*). Jaborosalactols 18 (**285**) and 22 (**286**) have a 14α-hydroxy group while jaborosalactols 19–21 (**287–289**) contain a 8,14 double bond. 14α-Hydroxywithanolides are known to dehydrate easily giving a mixture of $\Delta^{8,14}$ and Δ^{14} unsaturated derivatives (*132*), and the finding

that jaborosalactone 22 (**286**) spontaneously gave **289** strongly suggests that, in this case, the $\Delta^{8,14}$ unsaturated compounds are artifacts formed during isolation. The bridgehead nature of C-15 would prevent the formation of Δ^{14} derivatives (*69*).

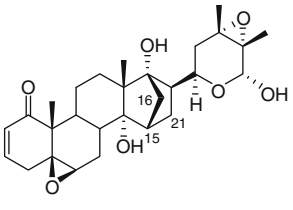

285 (jaborosalactol 18)

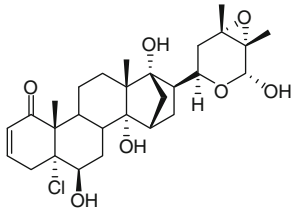

286 (jaborosalactol 22)

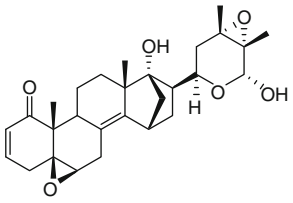

287 (jaborosalactol 19)

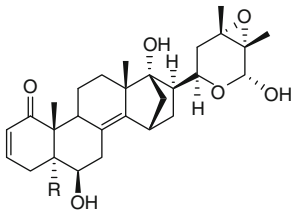

288 R = OH (jaborosalactol 20)
289 R = Cl (jaborosalactol 21)

5.2. Physalins and Withaphysalins

The physalins are a group of 13,14-*seco*-16,24-cycloergostane constituents of certain *Physalis* species (*3*, *133*). In recent years, some known physalins have been found in *Brachistus stramoniifolius* (physalins B, F, and H) (*134*), *B. hunzikeri* (*sub nom. Witheringia hunzikeri*) (physalin B) (*135*), *Margaranthus solanaceous* (*sub nom. Physalis solanaceous*) (physalins A, B, D, and F) (*136*), *Schraderanthus viscosus* (*sub nom. Saracha viscosa*) (physalins D, F, and H) (*137*), and *Witheringia solanacea* (physalins B, D, and F) (*138*). A total of 22 new physalins have been reported from *Physalis* species and several structures described previously have been revised. Withaphysalins, with an oxidized C-18 involved in a lactone or lactol ring with C-20 (see Fig. 2), are believed to be the biosynthetic precursors of physalins.

5.2.1. Normal Physalins

Fifteen new withanolides with the normal physalin skeleton were isolated from *Physalis* species, differing in the substitution pattern of rings A and B. From the

calyces of *P. alkekengi* var. *franchetii*, *Qiu et al.* isolated three 3-hydroxy-1-ketophysalins (*139*), the new physalins Y (**290**) and Z (**291**) with a 3α-oriented hydroxy group, and compound **292** that had NMR data coincident with isophysalin G previously isolated from the same plant by *Sunayama et al.*, but was not fully characterized (*140*). N*O*E correlations of **292** established the *β*-orientation for the 3-hydroxy group of isophysalin G. The 3-methoxy analogues **293** and **294** had been isolated previously by the same authors (*141*). Physalin S (**295**) isolated from the same plant, had a 6*β*-hydroxy-3,5-cyclo arrangement, a common acid rearrangement product of 3-hydroxy-Δ^5 steroids (see Sect. 4.2.5.) (*142*).

Two other physalins from *P. alkekengi* var. *franchetii* corresponded to the 5α,6*β*-diol, physalin T (**296**) (as already mentioned derived from hydrolytic opening of a 5,6-epoxide) (*143*), and the less common 2,5-endoperoxy-Δ^3 arrangement of physalin Q (**297**) (*144*). *Choudhary et al.* isolated the four physalins **298**, **299** (*60*), **300**, and **301** (*145*) from *P. minima*, the latter three containing a 11*β*-hydroxy group. A reduced derivative at C-1, physalin V (**302**), was also isolated from *P. angulata* (*146*).

Several 3-alkoxy derivatives besides those mentioned above have been reported, but most probably all of these are artifacts formed by reaction of a Δ^2-1-ketone with ethanol or methanol during isolation. Thus, the 3-ethoxy derivative **303** isolated from *P. alkekengi*, was found only in trace amounts in the original extract when analyzed by HPLC (*67*). The 3-methoxy derivative **304** (physalin U) was initially isolated from *P. minima* (*60*) and later from *P. angulata* (*146*), while the 3-methoxy derivative **305** was isolated from *P. angulata* (*55*). The latter compound was named physalin W although this name had already been assigned to another physalin (see below).

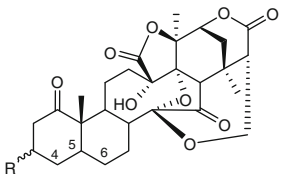

290 R = α-OH, Δ^5 (physalin Y)
291 R = α-OH, $\Delta^{4,6}$ (physalin Z)
292 R = β-OH, $\Delta^{4,6}$ (isophysalin G)
293 R = α-OCH_3, $\Delta^{4,6}$
294 R = β-OCH_3,$\Delta^{4,6}$

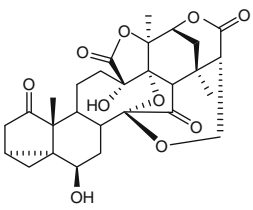

295 (physalin S)

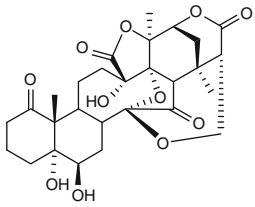

296 (physalin T)

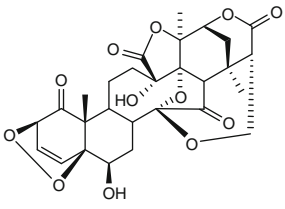

297 physalin Q

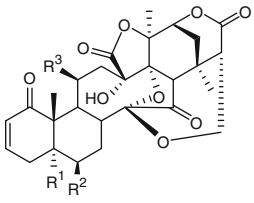

298 R^1 = OH, R^2 = R^3 = H
299 R^1 = R^2 = R^3 = OH
300 R^1 = OCH_3, R^2 = H, R^3 = OH

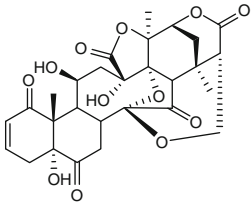

301

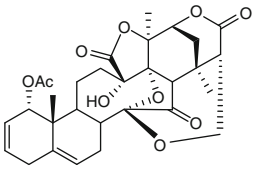

302 (physalin V)

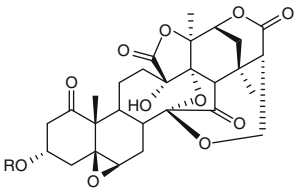

303 R = CH_2CH_3
304 R = CH_3 (physalin U)

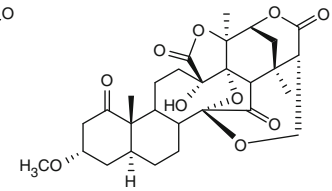

305

5.2.2. Neophysalins and Cyclophysalins

Neophysalins have a rearranged skeleton in which C-14 is directly bound to C-16 and the C-15 carbonyl forms a lactone with the oxygen atom at C-17. Four new neophysalins and a 11,16-cyclophysalin were isolated from *P. alkekengi* var. *franchetii*. Physalins W (**306**) and X (**307**) were initially isolated by *Chen et al.* (*147*) and their structures revised by *Qiu* and coworkers (*139*). The latter authors also reported the isolation of the 3-methoxy analogues physalin I (**308**) and physalin II (**309**). Physalin R (**310**) is a normal physalin with an additional bond between C-11 and C-16 (*142*). The authors showed that this cyclophysalin skeleton could be obtained from normal physalins upon irradiation with an halogen-tungsten lamp under argon.

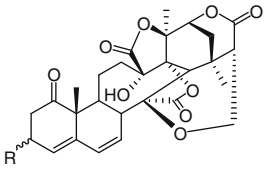

306 R = α-OH (physalin W)
307 R = β-OH (physalin X)

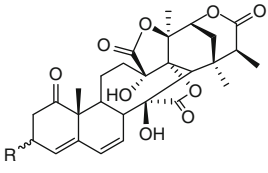

308 R = α-OCH_3 (physalin I)
309 R = β-OCH_3 (physalin II)

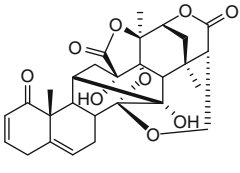

310 (physalin R)

5.2.3. Revised Physalin Structures

The structures of several physalins have been revised. Spectroscopic studies and chemical correlations revealed that the reported structure of physalin K containing a 4α,5α-epoxy-6α-hydroxy-2-en-1-one arrangement in rings A/B was incorrect, and the revised structure corresponds to a 2α,5α-epidioxy-6β-hydroxy-3-en-1-one (**311**), an isomer of physalin Q (**297**) (*144*).

Makino et al. have revised the structure of physalin H, originally reported as having a Δ^5-7β-hydroxy arrangement in ring B. The correct structure corresponded to the clorohydrin **312** (*148*). The authors also demonstrated that physalin E originally reported as a 5α,7α-dihydroxy-2-en-1-one is identical to the 5,6-diol

physalin D (**313**). The acetate of physalin E also corresponds to the 6-acetate of physalin D. *Chen et al.* revised the structure of physalin G (**314**), and the NMR resonances were assigned using 2D NMR and the configuration at C-6 established as (*R*) based on N*O*E data and the coupling constants of H-6 with H-7α and H-7β (*149*).

Sen and *Pathak* reported a constituent of *P. minima* as "physalin L" but the proposed structure **315** (*150*) was different from that reported previously for this compound and was also inconsistent with the spectroscopic data given as shown by *Kawai et al.*, who synthesized compound **315** (*151*). The true structure of the compound isolated by *Sen* and *Pathak* has not been established although its ^{1}H NMR spectrum was comparable to the 2,3-dihydro derivative of **315**.

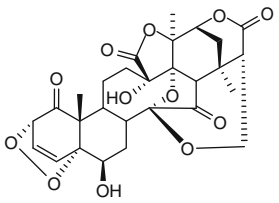

311 (physalin K)

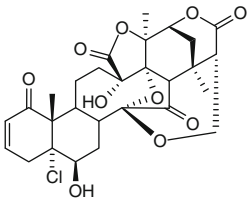

312 (physalin H)

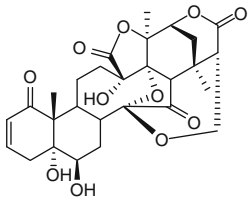

313 (physalin D and E)

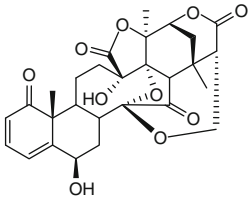

314 (physalin G)

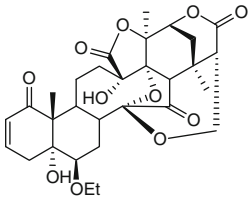

315

5.2.4. Withaphysalins and Related Withanolides

Withaphysalins comprise a group presenting an oxygen bridge between C-18 and C-20; depending on the oxidation state of C-18, a lactol or lactone ring may result (see Fig. 2). Hemiketals at C-18 are highly reactive towards simple alcohols and usually the methyl ketals are formed when methanol is used for extraction or purification. When the free hemiketals are isolated, they exist as an equilibrium mixture of both epimers at C-18; epimeric methyl ketals on the other hand may be separated.

Withaphysalins F–L (**316–322**) were isolated from *Eriolarynx lorentzii* (*sub nom. Vassobia lorentzii*) collected in Argentina (*70*). Compounds **318** and **319**

are the corresponding methyl ketals of withaphysalin G (**317**) and most probably artifacts. The hemiketal corresponding to withaphysalins K and L was not isolated. *Veras et al*. isolated withaphysalins M (**323**), N (**324**), O (**325**), 2,3-dihydrowithaphysalin F (**326**), and withaphysalin F (**316**) from *Acnistus arborescens* collected in northeastern Brazil (*152*, *153*). The ethyl ketal **325** is most probably an artifact from reaction of **316** with ethanol used for extraction. The 4-acetate of withaphysalin F (**327**) and the saturated lactone derivative **328** were isolated from *Dunalia brachyacantha* (*71*).

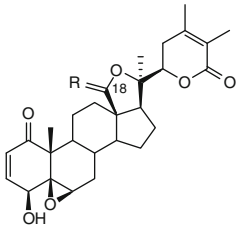

316 R = H,OH, (18 *R*/ *S*) (withaphysalin F)
323 R = O (withaphysalin M)
325 R = H,OEt (withaphysalin O)

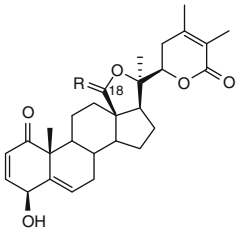

317 R = H,OH, (18 *R*/ *S*) (withaphysalin G)
318 R = H,OCH_3,(18 *R*)(withaphysalin H)
319 R= H,OCH_3, (18 *S*) (withaphysalin I)
320 R = O (withaphysalin J)

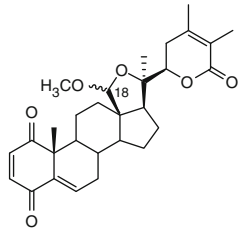

321 (18*R*) (withaphysalin K)
322 (18*S*) (withaphysalin L)

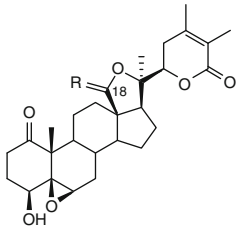

324 R = O (withaphysalin N)
326 R = H,OH, (18*R*/*S*)

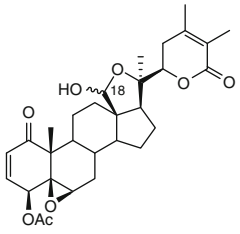

327 (18*R*/*S*)

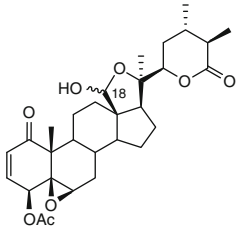

328 (18*R*/*S*)

From *Physalis minima*, *Ma et al*. reported seven new withaphysalins (*154*). Withaphysalins Q–S (**329**–**331**) and the 5-*O*-methyl derivative **332** were isolated as the methyl ketals at C-18; as hemiketals are highly reactive and methanol was extensively used during isolation and purification, it is possible that the actual natural products are the free hemiketals. The 3-methoxy group in **329** probably derives from the Δ^2-1-ketone and the 5-methoxy group in **332** could result from addition of methanol to a 5β,6β-epoxide, thus both compounds might be artifacts derived from the known withaphysalin B (**333**). Withaphysalin P (**334**) and the acetylated derivatives of the known withaphysalin C, **335** and **336**, appear to be biosynthetic intermediates in the conversion of withaphysalins to physalins. The authors also mention the isolation of the known 5α,6α-epoxywithaphysalin A (**337**), but this compound has been described only as a synthetic product (*155*). 5α,6α-Withanolides are rare and this would be the first report of **337** as a natural product.

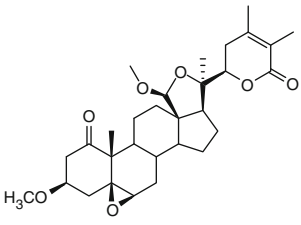

329 (withaphysalin Q)

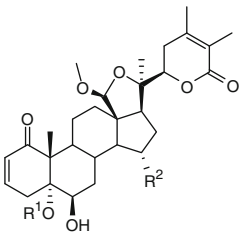

330 R^1 = H, R^2 = H (withaphysalin R)
331 R^1 = H, R^2 = OH (withaphysalin S)
332 R^1 = CH_3, R^2 = H

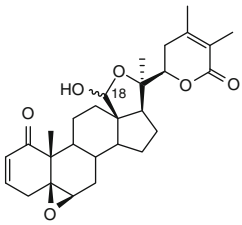

333 (18*R/S*) (withaphysalin B)

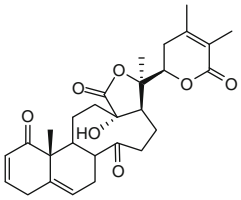

334 (withaphysalin P)

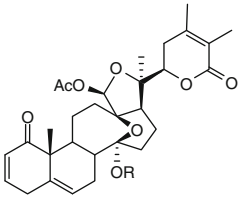

335 R = H
336 R = Ac

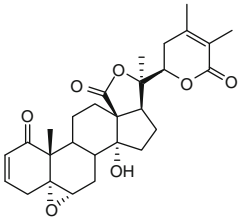

337 (5α,6α-epoxywithaphysalin A)

5.3. *Withanolides Containing an Aromatic Ring and Related Steroids*

Two distinct groups of withanolides containing aromatic rings in the steroid nucleus have been found. One of them corresponds to an *abeo*-ergostane skeleton with an expanded 6-membered ring D that incorporates C-18 (see Fig. 2) (*3*). The other group presents an aromatic A ring with loss of the angular methyl at C-10. In the discussion that follows, closely related withanolides from a biosynthesis standpoint are also included.

5.3.1. Aromatic Ring-D Withanolides and Related Steroids

A small group of withanolides and related steroids with a six-membered aromatic ring D, the nicandrenoids, were isolated in the early 1970s from the Peruvian "shoofly" plant *Nicandra physalodes* (*e.g.* Nic-1, **338**) (*59*). These compounds remained a curiosity within the withanolides for almost 20 years, until *Veleiro et al.* isolated salpichrolide A (**339**) from *Salpichroa origanifolia* (*156*). Compound **339** was also the first withanolide having a 5,6-epoxide with α-configuration, a feature that proved to be characteristic of several salpichrolides. Further studies on this plant showed that the withanolides present and the relative amounts were strongly dependent on the time of the year in which plants were collected and

also on their geographical origin. The major components in *S. origanifolia* plants collected in Buenos Aires and Córdoba provinces (Argentina), were salpichrolides A (**339**) and G (**340**), with salpichrolides B (**341**) and C (**342**) being isolated as minor components (*157*, *158*).

At variance with other withanolide families, salpichrolides present limited modifications in the substitution pattern of rings A and B. On the other hand, a higher variability was observed for the side chain. Salpichrolides H (**343**) and I (**344**) were isolated from plants collected in Buenos Aires in the winter (*158*), and salpichrolides J (**345**), K (**346**), and M (**347**) from plants collected in Salta province (Argentina) in the summer (*159*). Salpichrolides H (**343**) and M (**347**) correspond to the two possible products resulting from hydrolytic (*trans*) cleavage of the side-chain epoxide. Salpichrolides J (**345**) and K (**346**) are the first examples of withanolides with a side chain in which the oxidation levels at C-22 and C-26 are reversed; salpichrolide K (**346**) slowly cyclized to salpichrolide J (**345**) in solution. Figure 5 shows a possible biosynthesis pathway for these compounds.

Plants collected in Buenos Aires in winter also contained two ergostane derivatives, salpichrolides E (**348**) and F (**349**), probably resulting from degradation of the lactone side chain of salpichrolides A and C (*160*). The configuration at C-22 was assumed to be the same as that in the salpichrolides with an intact side chain (*i.e.* (22*R*)), but the orientation of the C-24 methyl could not be determined. It is noteworthy that similar degradation products are present in *N. physalodes*, the other plant known to contain withanolides with an aromatic ring D (*59*).

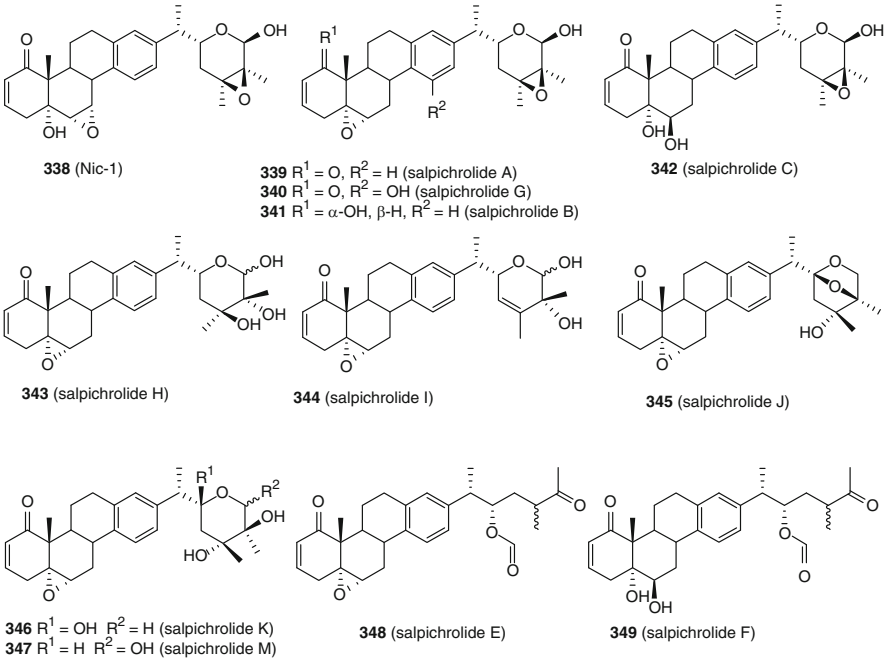

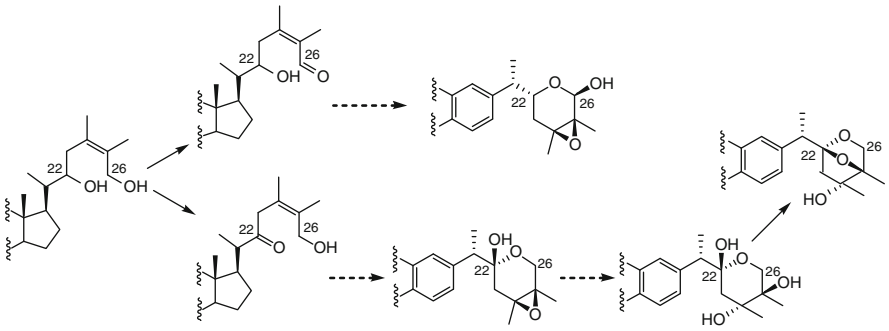

Fig. 5. Proposed biosynthetic pathway for the formation of the side chain in normal salpichrolides and in salpichrolides J (**345**) and K (**346**)

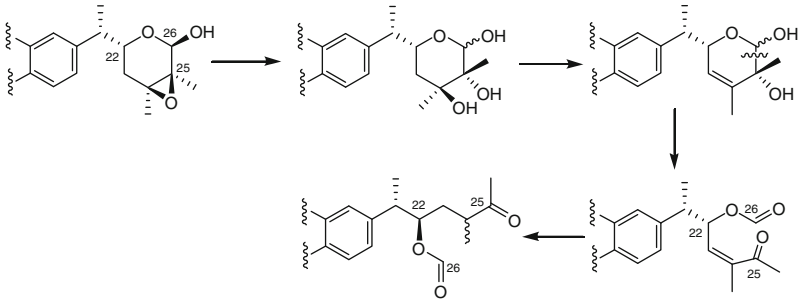

Fig. 6. Proposed degradative pathway for the formation of the side chain in salpichrolides E (**348**) and F (**349**). Starting from salpichrolide A (**339**) the first two intermediates correspond to compounds **343** and **344**

Salpichrolides H (**343**) and I (**344**) could be intermediates in the degradation pathway leading from salpichrolide A (**339**) to salpichrolide E (**348**). Oxidative cleavage of the C-25–C-26 bond would give rise to the formyloxy group (C-26) and the methyl ketone (Fig. 6).

Besides the withanolides with an aromatic D ring, salpichrolides D (**350**), (*157*) L (**351**), and N (**352**) (*159*), with a normal (5-membered) D ring were isolated from *S. origanifolia*. All of these have a characteristic 5α,6α-epoxide moiety, unique to *S. origanifolia*. A possible pathway for ring D aromatization proposed by *Whiting* involves the oxidation of C-18 followed by a 1,2-shift of C-17 to form a new six-membered ring via a cyclopropyl fused intermediate (*161*). Salpichrolide L (**351**) may be the precursor of the putative 14,16-diene intermediate; cleavage of the C-13–C-17 bond would lead to salpichrolide A and related compounds (Fig. 7, route *a*). An alternative cleavage of the cyclopropyl intermediate through the C-13–C-18 bond would result in migration of the angular methyl to give salpichrolide N (**352**) (Fig. 7, route *b*).

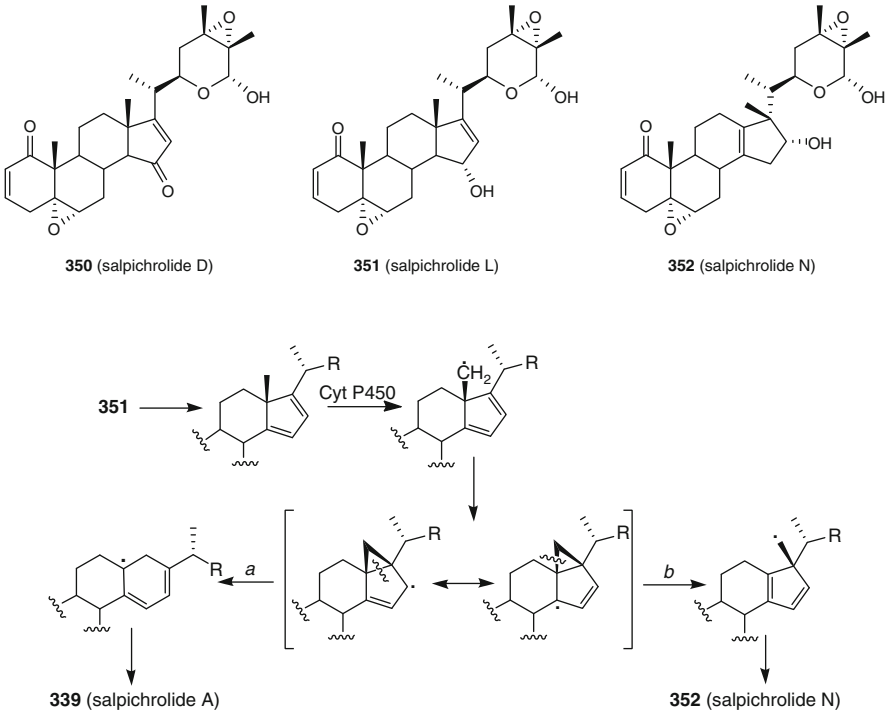

Fig. 7. Proposed biosynthesis pathways for the formation of withanolides with an aromatic D ring (*e.g.* salpichrolide A (**339**), pathway *a*) and for the rearranged skeleton in salpichrolide N (**352**) (pathway *b*)

5.3.2. Aromatic Ring-A Withanolides and 19-Hydroxywithanolides

The first 19-hydroxylated withanolide, jaborosalactone O (**353**), was isolated from *Jaborosa leucotricha* collected in late spring in Argentina (*162*). Another three 19-hydroxywithanolides, jaborosalactones V (**354**), W (**355**), and X (**356**) were isolated from plants collected in the autumn together with jaborosalactone Q (**357**) (*163*) and jaborosalactone 7 (**358**) (*68*), with the latter two containing an aromatic A ring. Compound **357** had been previously found in plants of *J. leucotricha* collected at a different location (*164*). Cinerolide (**359**), isolated from *Physalis cinerascens* collected in Mexico is the only 19-hydroxywithanolide outside the *Jaborosa* genus (*54*). The coexistence of 19-hydroxywithanolides and A-ring aromatic 19-norwithanolides in *J. leucotricha* is indicative of an oxidative degradation pathway for the loss of C-19 and aromatization. (+)-Jaborol and jaborosalactone 45 (see Sect. 5.4.2.) are the only other known withanolides with an aromatic A ring.

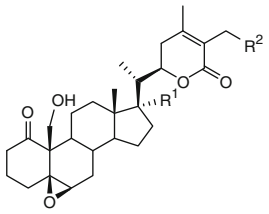

353 R^1 = OH, R^2 = H (jaborosalactone O)
355 R^1 = H, R^2 = OH (jaborosalactone W)

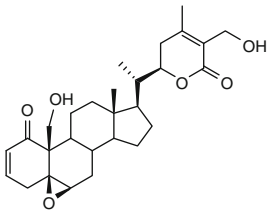

354 (jaborosalactone V)

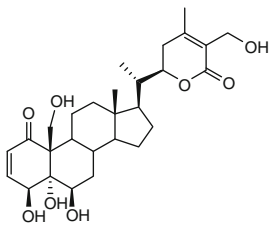

356 (jaborosalactone X)

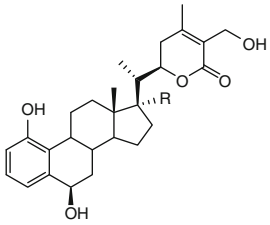

357 R = H (jaborosalactone Q)
358 R = OH (jaborosalactone 7)

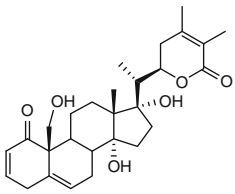

359 (cinerolide)

5.4. *Withanolides with a γ-Lactone Side Chain*

Ixocarpalactone A (**360**) was the first withanolide isolated with a γ-lactone side chain. It is the major withanolide of *Physalis philadelphica* (*sub nom. Physalis ixocarpa*), a plant with edible fruits (tomatillos) cultivated in Mexico and Guatemala (*165*). Nowadays several groups of withanolides containing variations of this γ-lactone moiety are known (see Fig. 3).

5.4.1. Ixocarpalactones and Perulactones

Kinghorn and coworkers reinvestigated *Physalis philadelphica* and isolated two new withanolides with a γ-lactone side chain of the ixocarpalactone type (**361**, **362**), also the configuration of ixocarpalactone A was confirmed by X-ray crystallography (*104*, *105*) (Fig. 8). The 3-methoxy derivatives of ixocarpalactones A and B, resulting from the addition of methanol were also isolated and shown to be artifacts of the isolation procedure. The 4-acetate of **361** had been reported previously from fruits of the same plant (*165*). *Huang et al.* isolated two perulactones, taccalonolides O (**363**) and P (**364**), from rhizomes and tubers of *Tacca*

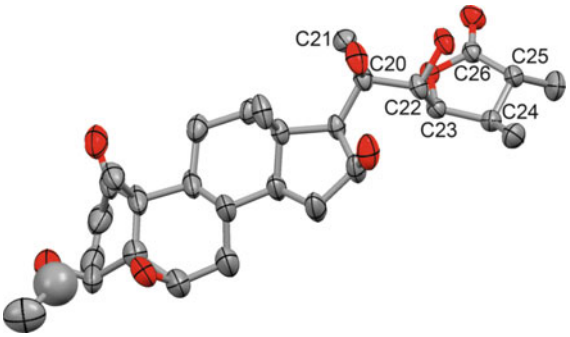

Fig. 8. X-ray crystal structure of ixocarpalactone A (**360**, CCDC 171420) (*104*). The two atoms close to the 4-hydroxy group probably correspond to a solvent molecule. Structure drawing generated with Mercury 2.3

subflabellata (*166*, *167*). Recently, perulactones C (**365**) and D (**366**) were reported from *Physalis peruviana* (*168*).

Physanolide A (**367**) was isolated from *Physalis angulata* by *Kuo et al.* (*146*). This withanolide has a novel skeleton related to the perulactones (γ-lactone between C-26 and C-28) with a carbon-carbon bond between C-16 and C-25 that results in a seven-membered ring.

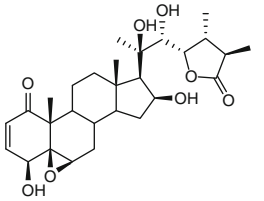

360 (ixocarpalactone A)

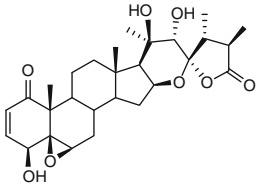

361 (ixocarpalactone B)

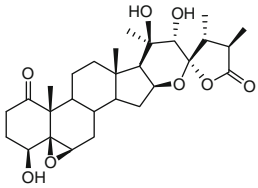

362

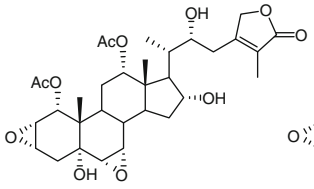

363 (taccalonolide O)

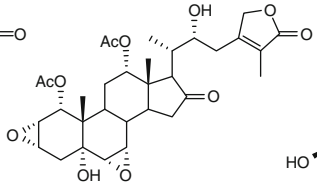

364 (taccalonolide P)

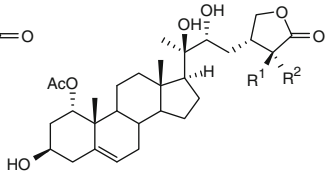

365 $R^1 = CH_3$, $R^2 = OH$ (perulactone C)
366 $R^1 = OH$, $R^2 = CH_3$ (perulactone D)

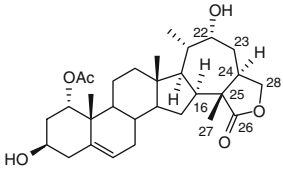

367 (physanolide A)

5.4.2. Trechonolides

The first member of this group of withanolides was trechonolide A (**368**), isolated by *Lavie et al*. from *Jaborosa laciniata* (*sub nom. Trechonaetes laciniata*) collected in Argentina (*169*). Closely related to the ixocarpalactones, an unusual characteristic feature of this compound was a hemiketal bridge formed by the 22-hydroxy group and a ketone at C-12, resulting in a six-membered ring with a β-oriented hydroxy at C-12. The same compound was later isolated by *Parvez et al*. from the Chilean *J. magellanica* (*170*). Curiously, although in both cases the structure was elucidated by X-ray crystallography, the configuration at C-23 was incorrectly assigned as (*R*). In 2006 *Nicotra et al*. reported the isolation of the C-23 epimer of trechonolide A (jaborosalactone 32, **369**) from *J. rotacea* (*120*). The configuration at C-23 was established by X-ray crystallography and shown to be (*R*) (Fig. 9). Careful inspection of the original X-ray data for trechonolide A (*169*, *170*) confirmed the (23*S*) configuration. The C-23 epimers of jaborotetrol and jaborochlorotriol (**370** and **371**) were also isolated from *J. rotacea* and shown to be (23*R*) (*120*). The chemical shift of C-23 and the sign of the *Cotton* effect at 218 nm may be used as direct indicators of the configuration at this position of trechonolides, thus the (23*S*) epimers have a negative *Cotton* effect and the C-23 resonance at δ 82.0–82.5 ppm, while the (23*R*) epimers exhibited a positive *Cotton* effect and a downfield shift for C-23 to δ 85.5–86.0 ppm. According to this, the structures of all previously known trechonolides that have been assigned the (23*R*) configuration upon comparison with trechonolide A should now be revised. For the above structures and in those that follow, the configuration at C-23 has been corrected according to *Nicotra et al*. when appropriate.

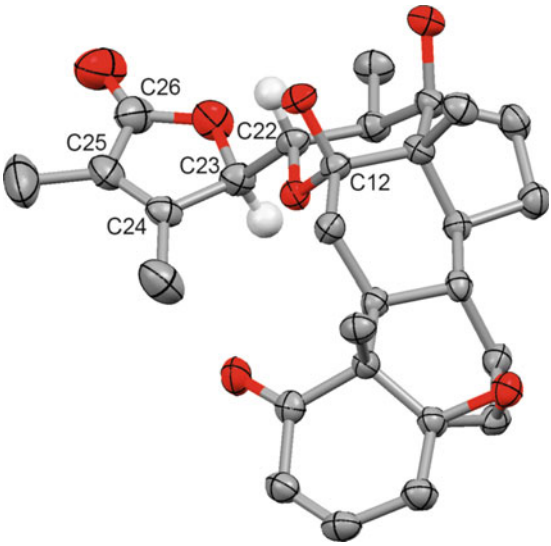

Fig. 9. X-ray crystal structure of jaborosalactone 32 (**369**, CCDC 255337), the C-23 epimer of trechonolide A showing the (23*R*) configuration (*120*). Hydrogens at positions 22 and 23 are included for clarity. Structure drawing generated with Mercury 2.3

Several withanolides structurally related to trechonolide A with the classical variations in the substitution pattern of rings A and B, have been subsequently isolated from different species of *Jaborosa*. Jaborotetrol (**372**), previously isolated from *J. magellanica*, and trechonolide A (**368**) are the most commonly found. As already observed with the sativolides, the C-12 hemiketal of the trechonolides is highly reactive towards alcohols and even small amounts of methanol or ethanol used during the isolation procedure will give the 12-*O*-methyl or ethyl derivatives. For example, when **370** was dissolved in deuterochloroform containing a few drops of deuteromethanol (to enhance solubility), the 12-*O*-trideuteromethyl derivative was formed (*120*). The clorohydrins jaborosalactone 42 (**373**) and jaborosalactone 49 (**374**) were isolated from *J. caulescens* var. *bipinnatifida* (*121*) and *J. laciniata* (*171*). Also from *J. caulescens* var. *bipinnatifida* were isolated two 21-hydroxytrechonolides epimeric at C-23, **375** and **376** (*121*). The 19-oxygenated trechonolides **377**–**379** were isolated from *J. laciniata* together with **380** (and its 12-*O*-methyl derivative) containing an aromatic ring A (*171*). Again, the 19-hydroxy withanolides appear as intermediates in an oxidative degradation pathway leading to the loss of the C-10 methyl and aromatization of ring A (see Sect. 5.3.2.). As already mentioned, the 12-*O*-methyl derivatives are most probably formed during the isolation procedure, with the 12-hydroxy compounds being the actual natural

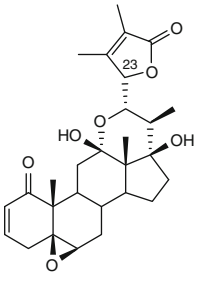

368 (23*S*) (trechonolide A)
369 (23*R*) (jaborosalactone 32)

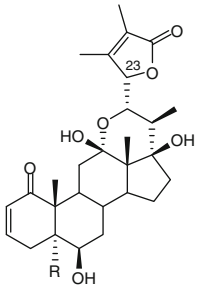

370 (23*R*), R = OH (jaborosalactone 33)
372 (23*S*), R = OH (jaborotetrol)
373 (23*R*), R = Cl (jaborosalactone 42)
374 (23*S*), R = Cl (jaborosalactone 49)

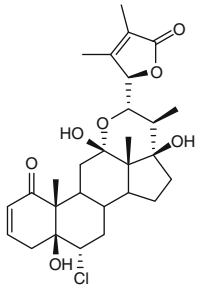

371 (jaborosalactone 34)

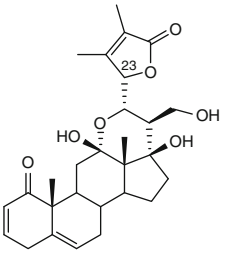

375 (23*R*) (jaborosalactone 40)
376 (23*S*) (jaborosalactone 41)

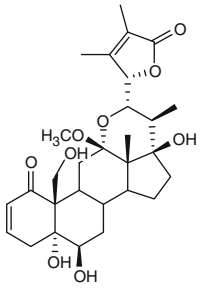

377 (jaborosalactone 46)

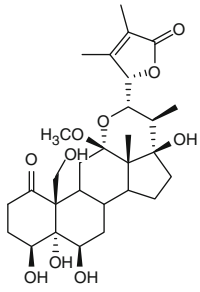

378 (jaborosalactone 47)

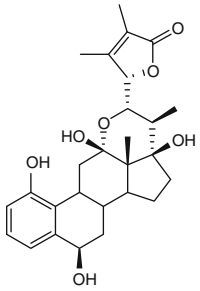

380 (jaborosalactone 45)

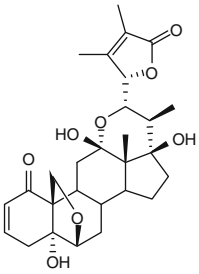

379 (jaborosalactone 48)

products. The 6,19-oxygen bridge present in **379** is an unusual functionality for a natural product. Interestingly, synthetic steroids with this moiety exhibit remarkable biological properties as selective glucocorticoid receptor modulators (*172*).

Although epoxy-δ-lactones and lactols are quite common among the withanolides, this did not appear to be the case for the γ-lactone side chains. Jaborosalactone U (**381**) isolated from *J. sativa* (Argentina), is the only known example of a 24,25-epoxy-γ-lactone (*119*). The (23*R*) configuration was originally proposed for this compound based on N*O*E data, however, more recently X-ray crystallography showed that the configuration is (23*S*) (Fig. 10) (*173*). Recently, several 24,25-epoxy-γ-lactols were isolated from plants of *J. parviflora* (**382**–**385**); some 12-*O*-ethyl derivatives were also reported (*174*). The authors used powder

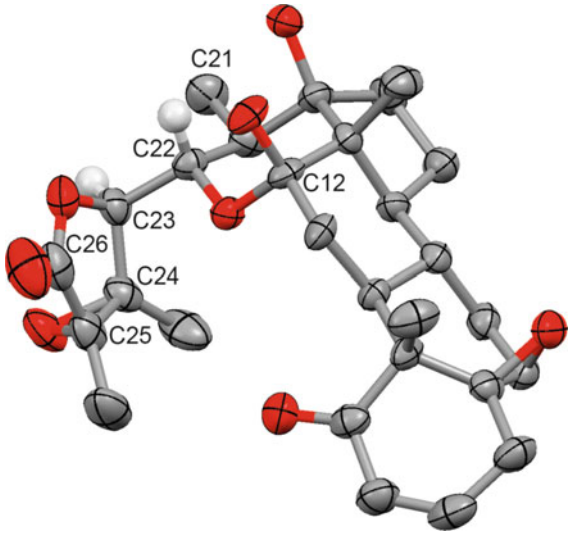

Fig. 10. X-ray crystal structure of jaborosalactone U (**381**) showing the configuration of the side chain epoxylactone (*173*). Hydrogens at positions 22 and 23 are included for clarity. Structure drawing generated with Mercury 2.3

X-ray diffraction analysis and NMR spectroscopy residual dipolar couplings to establish the absolute configuration of the epoxy-lactol side chain of **382**, confirming it was (23*S*). Both methodologies proved to be valid alternatives to single crystal X-ray diffraction. For the other compounds the same configuration was established by comparison of their ^{13}C NMR spectra.

Tettamanzi et al. had reported the isolation of a closely related epoxy-γ-lactol from *J. lanigera* for which the (23*R*) configuration was proposed (*175*); this compound had ^{13}C NMR data identical to **382** for C-12–C-18 and C-20–C-28 indicating that both compounds should have the same configuration in the side chain, hence the revised structure **386** is proposed. Thus so far, all known epoxy-γ-lactones and lactols have the same configuration at C-23, opposite to that of trechonolide A. Jaborosalactones 35 (**387**) and 36 (**388**) isolated from *J. rotacea* would result from cyclization of a 21-hydroxy-epoxy-γ-lactone (*120*). It should be noted that to date, trechonolides have been reported in nine of the thirteen *Jaborosa* species studied. A group of closely related γ-lactones isolated from *Larnax subtriflora* (*sub nom. Deprea subtriflora*) is discussed in Sect. 5.5.2.

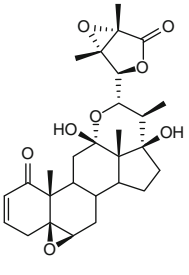

381 (jaborosalactone U)

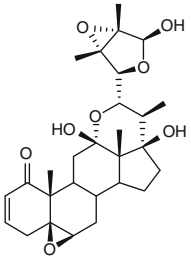

382 (jaborosalactol 24)

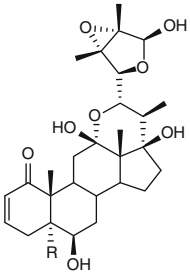

383 R = Cl (jaborosalactol 25)
385 R = OH (jaborosalactol 27)

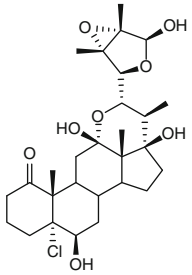

384 (jaborosalactol 26)

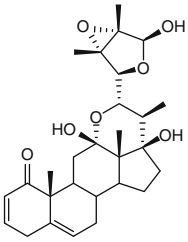

386

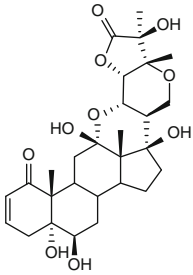

387 (jaborosalactone 35)

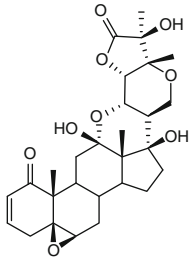

388 (jaborosalactone 36)

5.4.3. Spiranoid-γ-Lactones

The first withanolide with a spiranoid γ-lactone side chain, jaborosalactone P (**389**), was isolated by *Monteagudo et al.* from plants of *Jaborosa odonelliana* collected in Argentina (*176*). *Cirigliano et al.* reinvestigated this plant collected at different times of the year. Jaborosalactones 10 (**390**), 14 (**391**), and 15 (**392**) were found in plants collected in the summer while jaborosalactones 11 (**393**), 12 (**394**), 13 (**395**), and 14 (**391**) were present in plants collected in the autumn (*177*). Jaborosalactone P was the major component in both cases. The C-23 epimer of jaborosalactone P, jaborosalactone 24 (**396**), was isolated as a minor component from plants collected in April and December (*178*). This is the only spiranoid withanolide with a (23*R*) configuration isolated so far.

A group of six spiranoid withanolides with a 17(*20*)-ene-22-keto system, jaborosalactones 1–6 (**397**–**402**) was isolated from *Jaborosa runcinata* collected in Argentina. Jaborosalactone 2 (**398**) was also isolated from *Jaborosa araucana* (*179*). More recently, jaborosalactone 25 (**403**) was isolated as a minor component of *J. runcinata* (*178*).

The structural similarity of jaborosalactone 2 (**398**) and trechonolide A (**368**), both present in *J. araucana*, suggests that these compounds may have a common biosynthetic precursor. In trechonolide A, ring closure on C-12 has occurred with a C-22 hydroxy group as shown in Fig. 11 pathway *a*. Oxidation of the intermediate or a related compound to the 22-ketone would allow cyclization between C-23 and the C-12 ketone to give the 22-keto-spiranoid withanolides (Fig. 11 pathway *b*).

Jaborosalactone 31 (**404**), isolated from *J. rotacea,* is closely related to the spiranoid withanolides isolated from *J. odonelliana*, *J. runcinata*, and

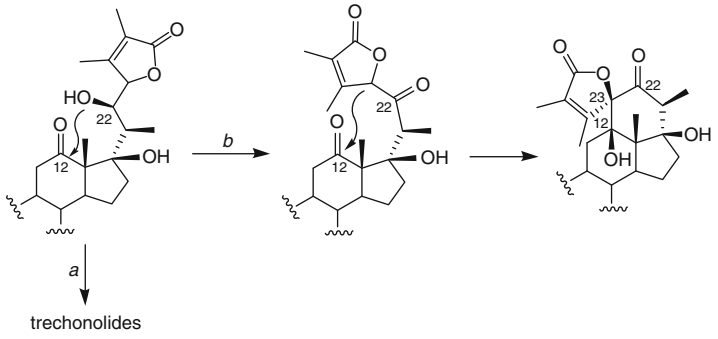

Fig. 11. Proposed biosynthesis routes to trechonolides (pathway *a*) and spiranoid withanolides (pathway *b*) via a common precursor

J. araucana. In this case, the C-12–C-23 bond is still present but instead of the spiranoid-γ-lactone arrangement (there is no oxygenated function at C-23), a δ-lactone is formed between the C-26 carboxyl and the C-12 hydroxy group (*120*).

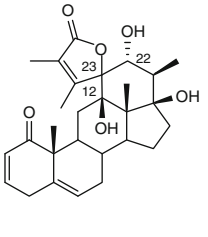

389 (23*S*) (jaborosalactone P)
396 (23*R*) (jaborosalactone 24)

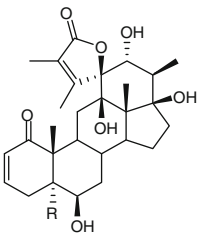

390 R = Cl (jaborosalactone 10)
391 R = OCH_3 (jaborosalactone 14)
395 R = OH (jaborosalactone 13)

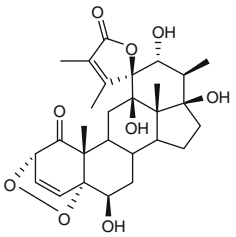

392 (jaborosalactone 15)

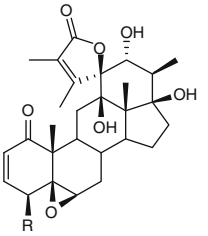

393 R = H (jaborosalactone 11)
394 R = OH (jaborosalactone 12)

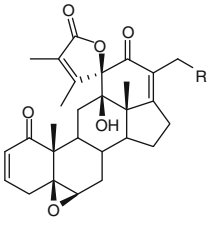

397 R =H (jaborosalactone 1)
400 R = OH (jaborosalactone 4)

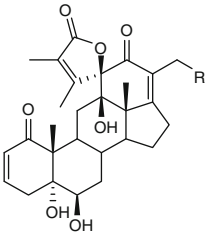

398 R = H (jaborosalactone 2)
403 R = OH (jaborosalactone 25)

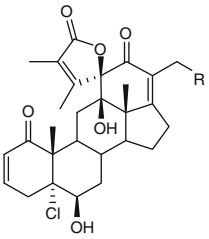

399 R = H (jaborosalactone 3)
402 R = OH (jaborosalactone 6)

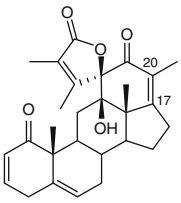

401 (jaborosalactone 5)

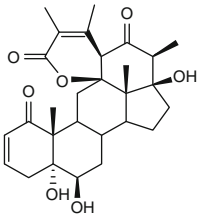

404 (jaborosalactone 31)

5.4.4. Taccalonolides

Tacca species contain highly oxygenated ixocarpalactone-type withanolides having an additional ring formed by a carbon-carbon bond between C-16 and C-24, with taccalonolide A (**405**) being the first example of these compounds (*3*). Eight

new withanolides related to taccalonolide A were isolated from *Tacca plantaginea*, taccalonolides L (**406**), M (**407**) (*180*), G, H, I, J, K (**408–412**) (*181*), and W (**413**) (*182*). Taccalonolides R, S, T, U, and V (**414–418**) were isolated from the Vietnamese plant *Tacca paxiana* together with the known taccalonolides A (**405**), K (**412**), B, E, and N (**419–421**) (*183*). A distinctive feature of most taccalonolides is the absence of a hydroxy group at C-22. Taccalonolide Q (**422**) (*167*) and Y (**423**) (*182*) containing a δ-lactone side chain with a C–C bond between C-16 and C-24 were isolated from *T. subflabellata* and *T. plantaginea*.

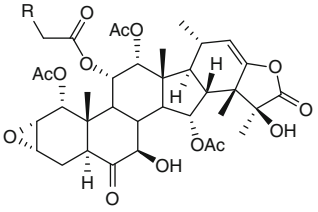

405 R = H (taccalonolide A)
406 R = OH (taccalonolide L)

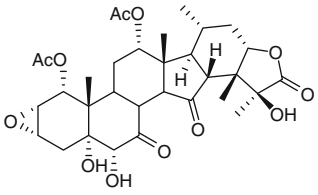

407 (taccalonolide M)

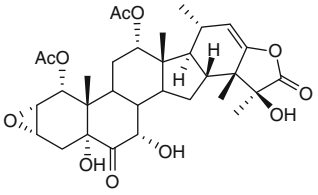

408 (taccalonolide G)

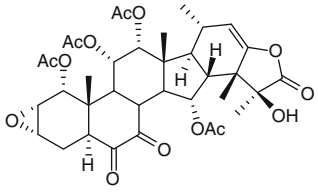

409 (taccalonolide H)

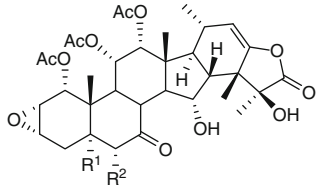

410 R^1 = H, R^2 = OH (taccalonolide I)
411 R^1 = H, R^2 = OAc (taccalonolide J)
412 R^1 = R^2 = OH (taccalonolide K)

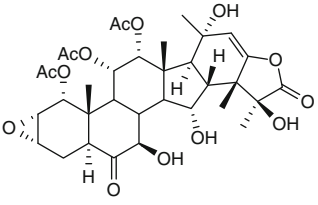

413 (taccalonolide W)

A sizeable number of steroids partially resembling withanolides have been isolated from *Tacca* species and some also dubbed taccalonolides, *e.g.* taccalonolide X (**424**) (*182*), but they are not included in this chapter. Other taccalonolides structurally related to the perulactones have been presented previously (see Sect. 5.4.1.).

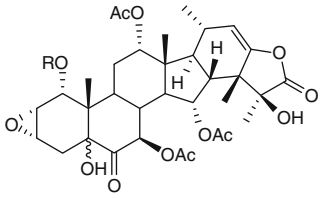

414 R = Ac (taccalonolide R)
416 R = isovaleryloxy (taccalonolide T)
417 R = H (taccalonolide U)

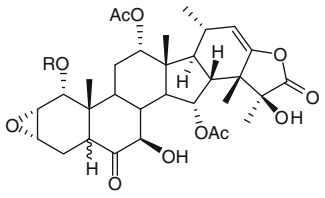

415 R = isobutyryloxy (taccalonolide S)

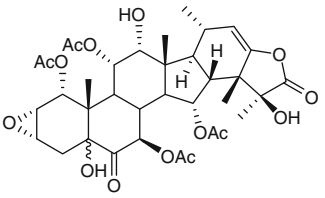

418 (taccalonolide V)

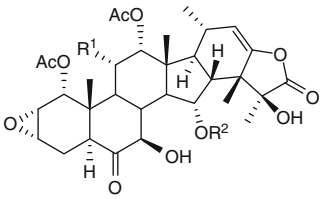

419 R^1 = OAc, R^2 = H (taccalonolide B)
420 R^1 = H, R^2 = Ac (taccalonolide E)
421 R^1 = R^2 = H (taccalonolide N)

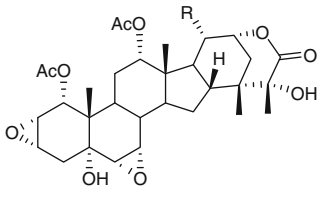

422 R = CO_2H (taccalonolide Q)
423 R = CH_2OH (taccalonolide Y)

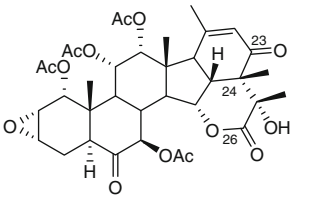

424 (taccalonolide X)

5.5. *18-Norwithanolides*

Kinghorn and coworkers used a quinone reductase induction assay for the activity-monitored fractionation of an extract of *Larnax subtriflora* (*sub nom. Deprea subtriflora*) collected in Peru. This led to the isolation of a novel group of highly oxygenated C_{27} 18-norwithanolides, dubbed subtrifloralactones. All subtrifloralactones found so far, have oxygenated functions at positions 12, 16, and 20 and a saturated lactone (γ or δ) side chain (see Figs. 2 and 3) (*184*, *185*). Another C_{27} 18-norwithanolide related to the physalins, has been reported recently from a *Physalis* species. A small group of C_{28} 17-methyl-18-norwithanolides is also included in this section.

5.5.1. Subtriflora-δ-Lactones and Related Withanolides

Subtrifloralactones D (**425**) and E (**426**) resemble the classic withanolide structure except for the lack of C-18. On the other hand, subtrifloralactones H, I, and J (**427–429**) have rings C and D *cis* fused, due to epimerization at position 13 (probably favored by the presence of the neighboring 12-ketone), allowing formation of a ketal bridge between a 20-hydroxy group and a 12-ketone (*184*). Due to the high reactivity of C-12 hemiketals towards even traces of small alcohols (see Sect. 5.4.2.), the formation of the methyl and ethyl ketals in the latter compounds probably took place during isolation. Another distinctive feature of subtrifloralactones H, I, and J is the presence of a formate group esterifying the 16-hydroxy group. The isolation of 13*β*-hydroxymethylsubtrifloralactone E (**430**) from the same plant (*185*) indicates an oxidative pathway for the loss of C-18 that could end as the 16-formate group via rearrangement of a 16,18-hemiketal (Fig. 12).

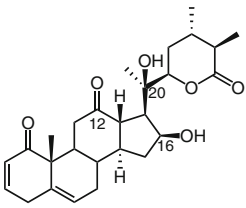

425 (subtrifloralactone D)

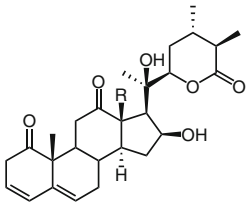

426 R = H (subtrifloralactone E)
430 R = CH_2OH

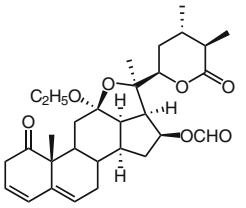

427 (subtrifloralactone H)

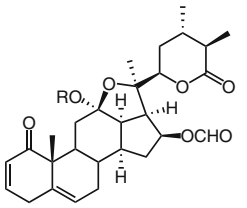

428 R = C_2H_5 (subtrifloralactone I)
429 R = CH_3 (subtrifloralactone J)

5.5.2. Subtriflora-γ-Lactones

Subtrifloralactones A (**431**), B (**432**), C (**433**), K (**434**), and L (**435**) present a side chain arrangement closely related to that observed in the trechonolides, with a γ-lactone between C-26 and C-23 and a ketal bridge between a 22-hydroxy and a 12-ketone (*184*, *185*). However, the *cis* fusion of rings C and D and the presence of a 16-hydroxy group allow an additional ketal bridge involving this hydroxy and

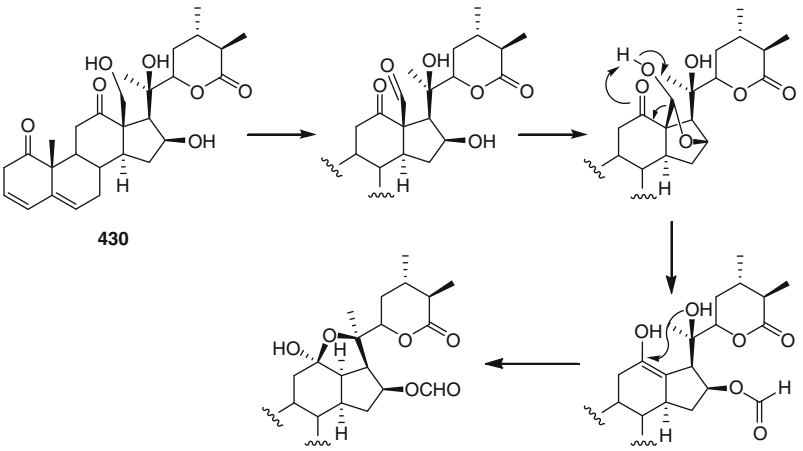

Fig. 12. Proposed biosynthetic pathway for the conversion of 13β-hydroxymethylsubtriflor-alactone E (**430**) to subtriflora-δ-lactones

C-12. In subtrifloralactones F (**436**) and G (**437**) the *trans* fusion of rings C and D results in an ixocarpalactone-type structure (*184*).

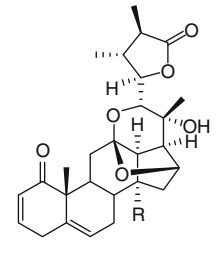

431 R = H (subtrifloralactone A)
433 R = OH (subtrifloractone C)

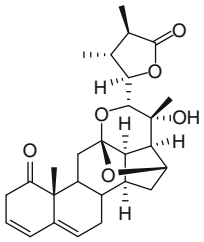

432 (subtrifloralactone B)

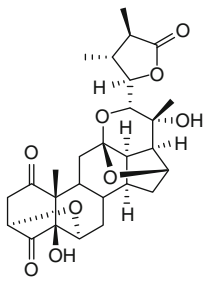

434 (subtrifloralactone K)

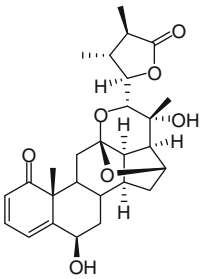

435 (subtrifloralactone L)

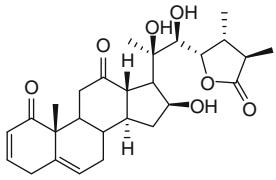

436 (subtrifloralactone F)

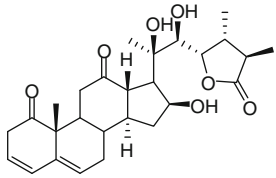

437 (subtrifloralactone G)

5.5.3. Other 18-Norwithanolides

Recently, *Ma et al*. reported the isolation of another 18-norwithanolide structurally related to the physalins, withaphysanolide A (**438**), together with several known physalins and withaphysalins from *Physalis divaricata* collected in Pakistan (*186*). The structure and configuration of withaphysanolide A was confirmed by X-ray crystallography.

TH-6 (**439**) and TH-12 (**440**) are two 17-methyl-18-nor-ergostanes isolated in 1990 by *Shingu et al*. from the acid hydrolysate of a methanolic extract of *Tubocapsicum anomalum* (*187*). The authors related these compounds to a putative precursor with a withanolide side chain that would rearrange in acid media. Recently *Hsieh et al*. isolated from the same plant three withanolides with the rearranged skeleton of TH-6 and TH-12 named tubocapsenolides A, F, and G (**441–443**) (*107*). Salpichrolide N (**352**) isolated from *Salpichroa origanifolia* (see Sect. 5.3.1.), was the first withanolide reported with this rearranged skeleton (*159*).

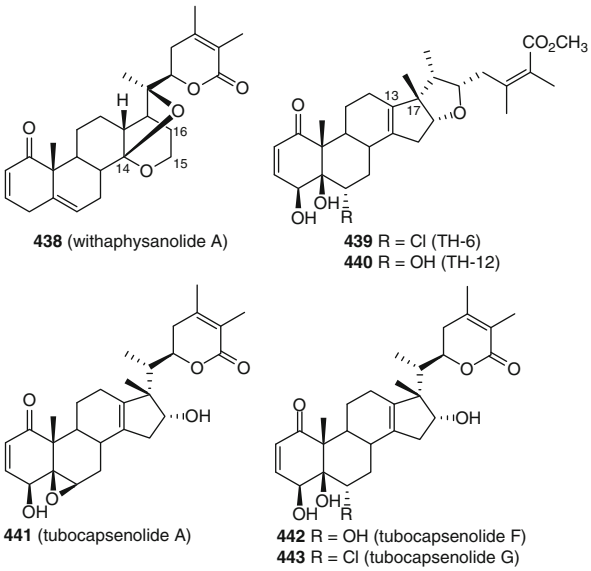

438 (withaphysanolide A)

439 R = Cl (TH-6)
440 R = OH (TH-12)

441 (tubocapsenolide A)

442 R = OH (tubocapsenolide F)
443 R = Cl (tubocapsenolide G)

5.6. *Spiranoid Withanolides at C-22*

This group of withanolides has a hemiketal bridge between what must have originally been ketone functions at C-12 and C-22. This gives rise to a new

six-membered ring with a β-oriented hydroxy group at C-12 and a spiroketal at C-22 upon formation of the δ-lactone. Jaborosalactones 26–30 (**444–448**) were isolated from *Jaborosa rotacea* (*120*) and jaborosalactone 43 (**449**) was isolated from *J. kurtzii* (*76*) both collected in Mendoza, Argentina. The 12-ketowithanolide jaborosalactone 44 (**144**) also present in *J. kurtzii* (see Sect. 4.2.3.) has been proposed as the biogenetic precursor of **449**.

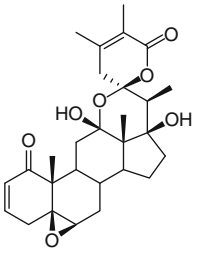

444 (jaborosalactone 26)

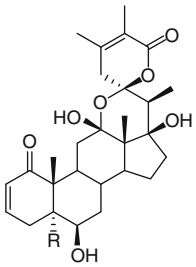

445 R = OH (jaborosalactone 27)
446 R = Cl (jaborosalactone 28)

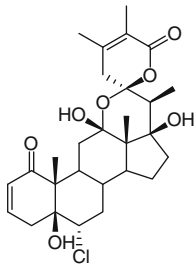

447 (jaborosalactone 29)

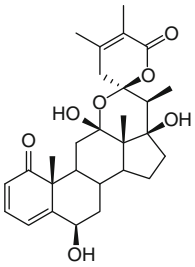

448 (jaborosalactone 30)

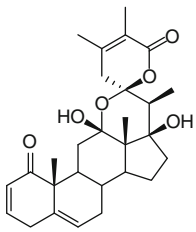

449 (jaborosalactone 43)

6. Chemical and Bio-transformations of Withanolides

The early synthesis work carried out on withanolides has been reviewed by *Glotter* (*59*), *Ray* and *Gupta* (*3*), and more recently by *Kovganko* and *Kashkan* (*188*). No new attempts on total or partial syntheses of withanolides have been reported in the last two decades. On the other hand, transformations usually involving interconversions of functional groups, of one withanolide into another or synthesis of simple derivatives, are fairly common and mostly used for structure confirmation or to study biological activities.

6.1. Chemical Transformations

Reactivity of the Δ^2-1-keto system of withanolides towards *Michael* addition (mostly of simple alcohols) has been discussed in the previous sections and several examples shown. As already mentioned, 5*β*,6*β*-epoxides are fairly common among the withanolides and also constitute a highly reactive center. Many chemical transformations involve the cleavage of the epoxide moiety to give the corresponding diols, chlorohydrins or alcohol addition products, with their configuration according to the *Fürst-Plattner* rule (*16*).

For the structure assignment of physalin H (**312**), *Makino et al.* treated physalin F (**450**) with aqueous hydrochloric acid to give a mixture of the diol **313** (physalin D) and the 5α,6*β*-clorohydrin **312** (physalin H) (Chart 1). When concentrated hydrobromic acid in THF was used the brominated analog of physalin H (**451**) was obtained. Reaction of physalin D (**313**) with phosphorus oxychloride in dry pyridine gave the isomeric chlorohydrin **452** (*148*). Cleavage of the epoxide of physalin F (**450**) with concentrated hydrochloric acid in ethanol gave the 5α-ethoxy-6*β*-hydroxy withanolide **453** (*151*).

The 5α,6α-epoxide present in the salpichrolides and a few other withanolides, reacts in a similar way. Thus, treatment of salpichrolide A (**339**) with THF containing 0.75% of 1.5 *N* sulphuric acid gave the corresponding diol **342** (salpichrolide C)

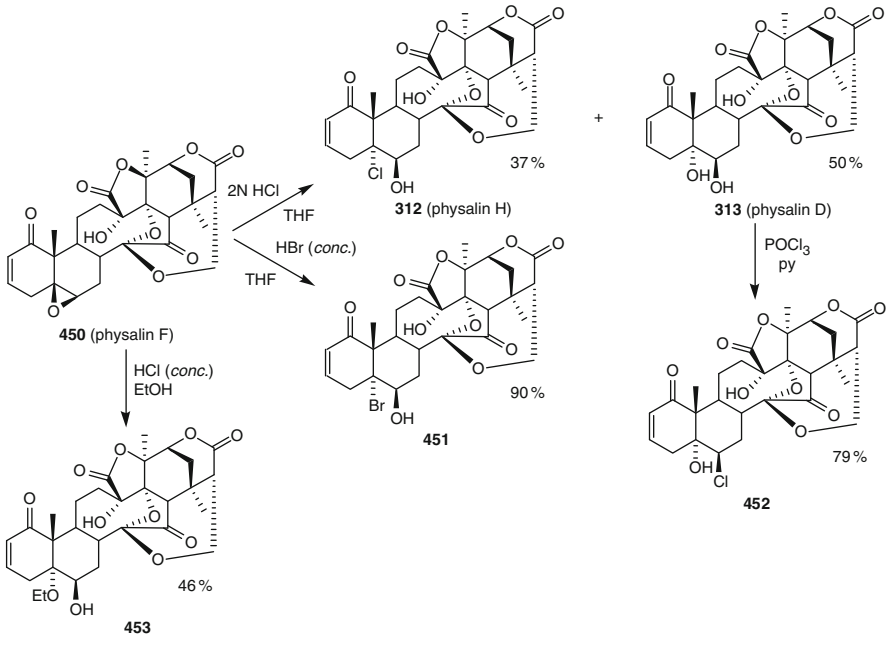

Chart 1 Cleavage reactions of the 5*β*,6*β*-epoxide of physalin F (**450**)

(*157*); increasing the amount of acid 10-fold, resulted in the concomitant cleavage of the 24,25-epoxide (compound **454**) (*159*). Reaction of salpichrolide A (**339**) with *Jones* reagent in acetone for 3 h gave the hydroxyketone **455** where oxidation of the side chain lactol to the lactone also occurred (*189*). On the other hand, cleavage of the epoxide with potassium bicarbonate in methanol gave the $\Delta^{2,4}$-6α-hydroxy withanolide **456** (Chart 2) (*190*). Reaction of physalin J (**457**) with sulfuric acid in ethanol gave the 5α-hydroxy-6*β*-ethoxy physalin **315** (*151*).

Misra et al. studied the reaction of 2-mercaptoethanol with several withanolides from *W. somnifera*. Withaferin A (**1**) and other 5*β*,6*β*-epoxywithanolides reacted readily under mild acid catalysis to give the 5*β*,6α-oxyethylenethio derivatives (Chart 3) in 47–60% yield. The additional ring would result from nucleophilic attack of the thiol at position 6, followed by acid-catalyzed condensation of the 6α-hydroxyethylthio intermediate. Withanolides with a 6α,7α-epoxide did not react

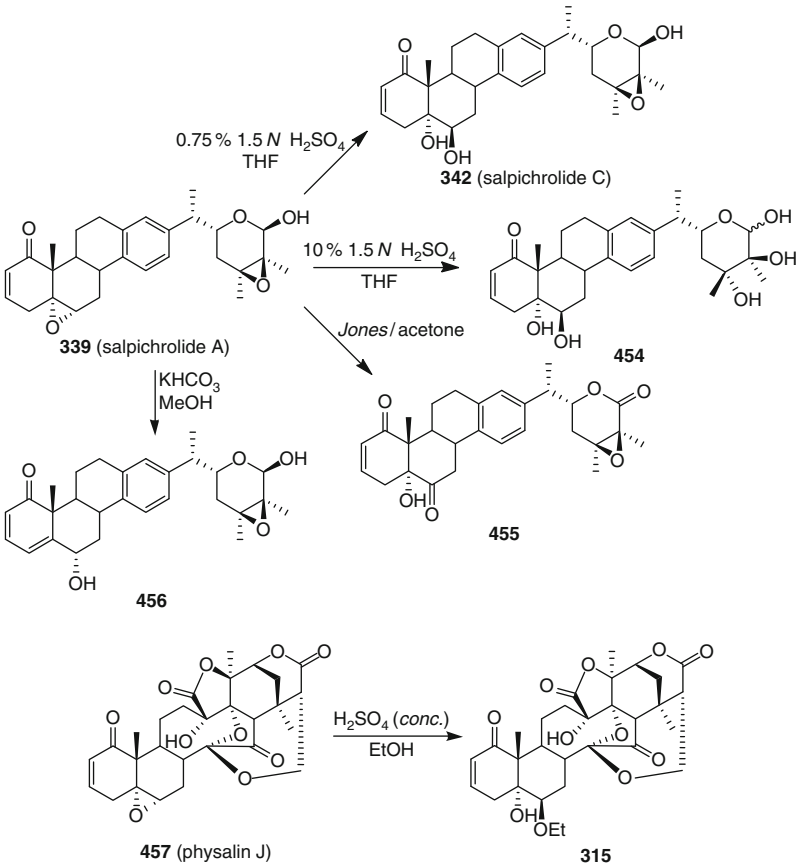

Chart 2 Cleavage reactions of 5α,6α-epoxy withanolides

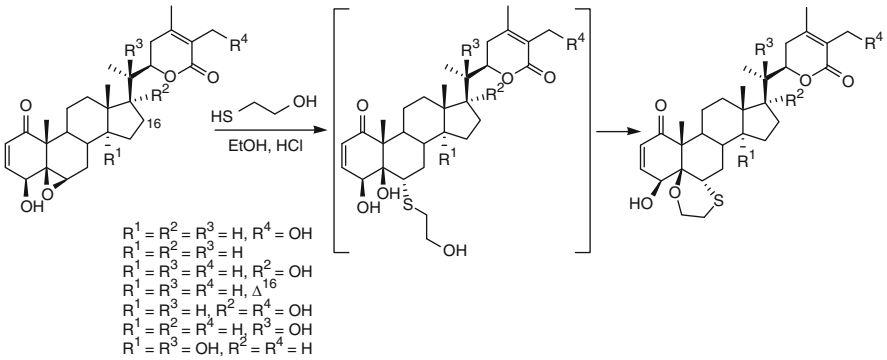

Chart 3 Reaction of withaferin A ($R^1 = R^2 = R^3 = H$, $R^4 = OH$) and related 5β,6β-epoxy withanolides with mercaptoethanol

under the same reaction conditions; attempts to force the reaction using a higher temperature and a lower pH resulted in complex mixtures (*191*).

Salpichrolide B (**341**), a minor constituent of *S. origanifolia* (see Sect. 5.3.1.), was obtained from the abundant salpichrolide A (**339**) by acetylation of the side chain hemiketal followed by stereoselective reduction of the C-1 ketone with sodium borohydride; deacetylation of the side chain occurred during workup. Following a similar protection/deprotection sequence, salpichrolide C (**342**) was oxidized to the 6-ketone **458** (Chart 4) (*190*).

Modifications at the side chain are less common, and one interesting example by *Mohan* and coworkers is the synthesis of a biotinylated analog of withaferin A (**459**) (Chart 5) for use as a probe to study angiogenesis (see Sect. 7.6.3.) (*192*).

6.2. *Photochemical Transformations*

Physalins containing an endoperoxy moiety in ring A were prepared from the corresponding $\Delta^{2,4}$-6-hydroxy physalin by photosensitized oxygenation. Thus, a *ca.* 1:1 mixture of physalins K (**311**) and Q (**297**) was obtained in 65% yield, by bubbling oxygen through a solution of physalin G (**314**) containing Rose Bengal and irradiated at 480 nm (Chart 6) (*144*). The same reaction carried out on 6-epiphysalin G (**460**) gave the 2β,5β-endoperoxide **461** as the major product (76% yield) and a trace amount (2%) of the 2α,5α-isomer **462**. (Note that names of physalin G and its 6-epimer have been assigned according to the revised structure of the former; see Sect. 5.2.3.). Photosensitized oxygenation of physalin B (**463**) gave a mixture of physalin K (**311**), the isomeric endoperoxide **461**, the 5α-hydroperoxide **464** and the corresponding alcohol **465** (Chart 6) (*144*).

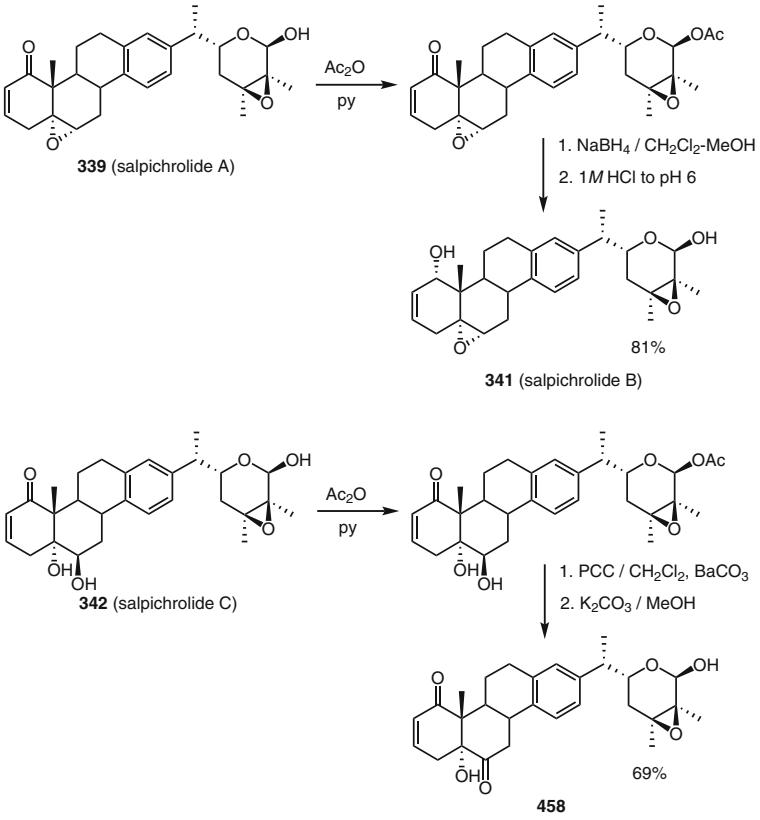

Chart 4 Chemical modification of salpichrolides A (**339**) and C (**342**)

Irradiation of an acetone solution of physalin B (**463**) with a tungsten-halogen lamp under argon, gave physalin R (**310**) in 49% yield. Irradiation of physalin F (**450**) under similar conditions gave the corresponding cyclophysalin (**466**). The 7α-hydroxy physalins, physalin N (**467**), A (**468**), and O (**469**), the latter two lacking the C-14–C-27 oxygen bridge, also gave the cyclophysalins (**470**–**472**) but required irradiation with a high-pressure mercury lamp (Chart 7) (*142*). The Δ^2-1-ketone system of the physalins would be involved in a self-sensitizing mechanism, as 2,3-dihydrophysalins failed to give the cyclized product.

6.3. Biotransformations

The modification of natural products by microorganisms may lead to new structures with potential biological activities. Application of this strategy to withanolides has been reviewed by *Anjaneyulu et al.* (*4*). Biotransformation of physalin H (**312**) by the fungus *Rhizopus stolonifer* gave the elimination product **473** in 2.1%

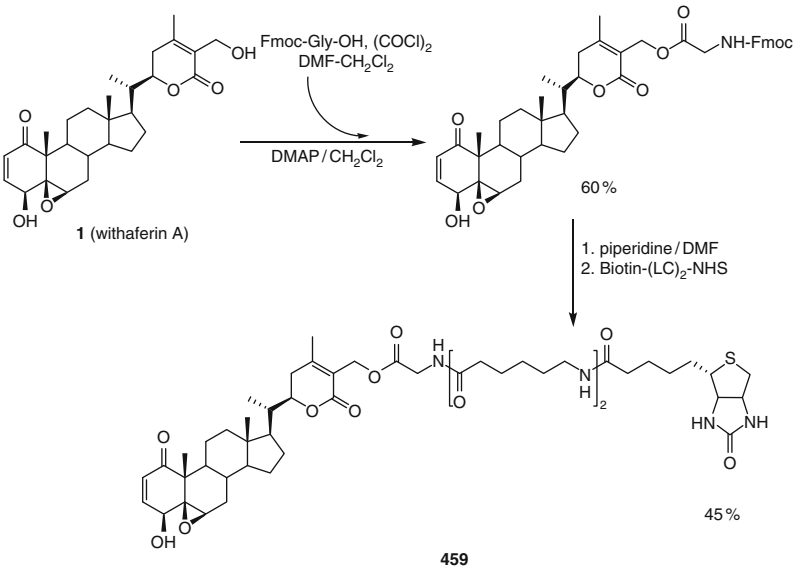

Chart 5 Synthesis of a biotinylated analog of withaferin A (**1**)

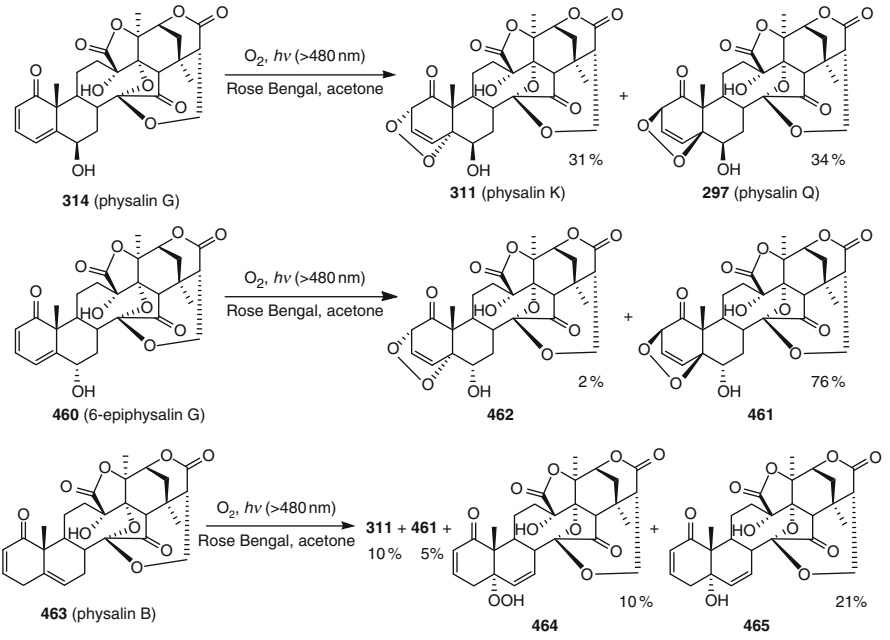

Chart 6 Photooxygenation of physalin G (**314**), 6-epiphysalin G (**460**) and physalin B (**463**)

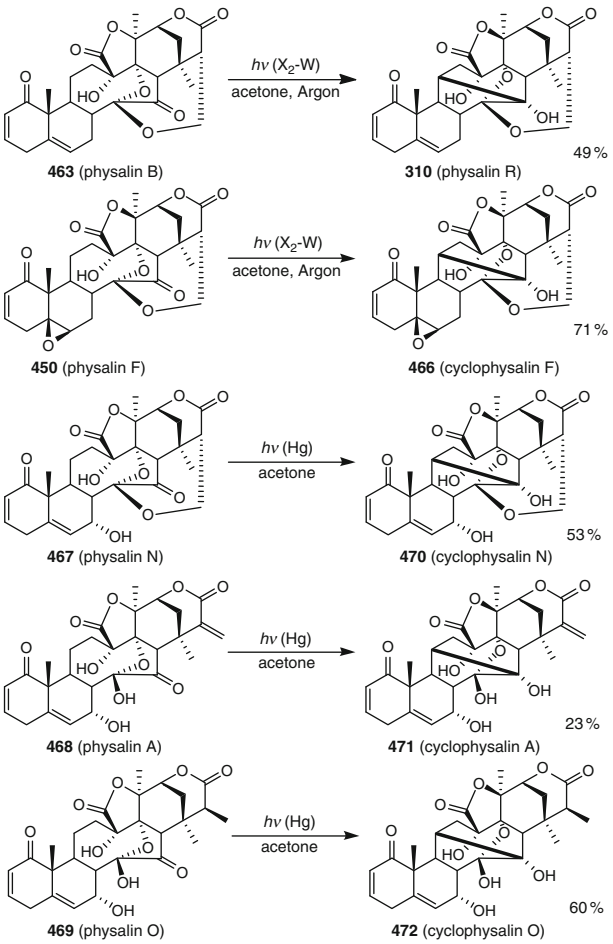

Chart 7 Photocyclization of physalins to cyclophysalins. *X_2-W* halogen-tungsten lamp; *Hg* high pressure mercury lamp

yield, while incubation with *Cunninghamella elegans* gave isophysalin B (**474**) and 6-deoxyphysalin H (**475**) in 9.4% overall yield (Chart 8) (*193*). Both **473** and **475** are new compounds. Incubation of withaferin A (**1**) with *Cunninghamella echinulata* gave 12β-hydroxywithaferin A (**476**) and 15β-hydroxywithaferin A (**477**) (*194*); the same hydroxylated products have been obtained upon incubation with *Cunninghamella elegans* (*4*). Several reports also describe the production of withanolides (mostly withaferin A) by shoot cultures of *Withania somnifera* (*195–198*).

Tuli and coworkers isolated two specific glucosyltransferases from *W. somnifera*. The cytosolic 3β-hydroxy sterol glucosyltransferase was most active on 24-methylene-cholesterol, and showed moderate activity for the 3β-*O*-monoglucosylation of the

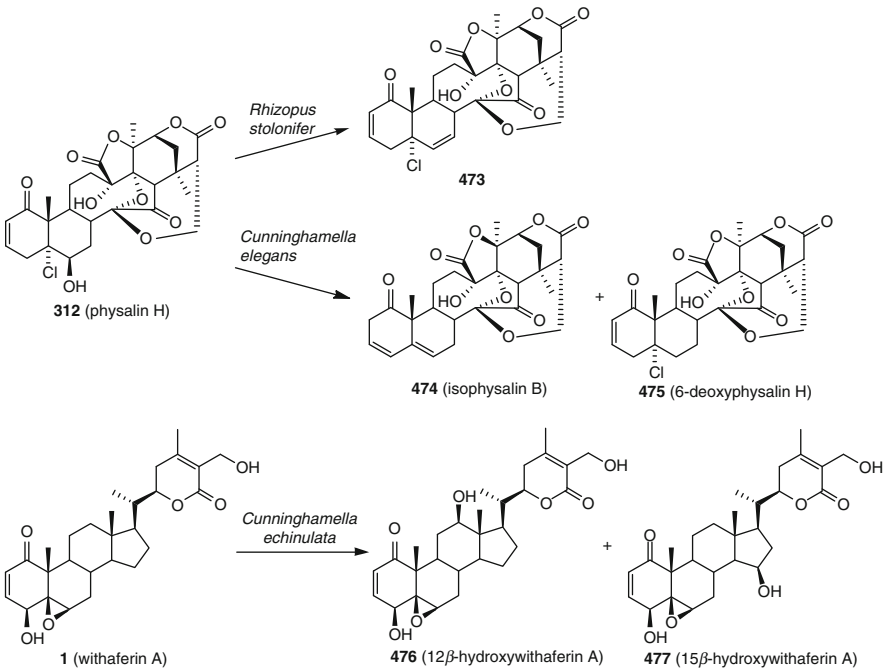

Chart 8 Biotransformations of physalin H (**312**) and withaferin A (**1**) with microorganisms

aglycone of withanoside V (**478**) (*199*). On the other hand the 27-hydroxy glucosyltransferase monoglucosylated several 27-hydroxywithanolides, provided a hydroxy group was also present at C-17 (Chart 9) (*200*).

7. Biological Activities of the Withanolides

As already mentioned, several withanolide-containing plants are used in traditional folk medicine throughout the world and many of the verified activities can be traced to their withanolide constituents. *Withania somnifera* used in Ayurvedic medicine in India since ancient times is the prototypical example, but similar uses have been accorded to *Datura metel* in traditional Chinese medicine and to several *Physalis* species in Asia and the Americas. Withanolides have proven active not only in a wide variety of assays related to human ailments, but also in potential applications as natural agrochemicals for pest and weed control. Despite the structural variety of withanolides and the many different activities they present, it is noteworthy, as will become evident in the following sections, that some structural characteristics are usually associated with biological activity (or the lack of it). One such feature is, with few exceptions, the lack of activity of 5α,6β-diols as compared to the corresponding epoxides (or the Δ^5 analogues) that are usually active.

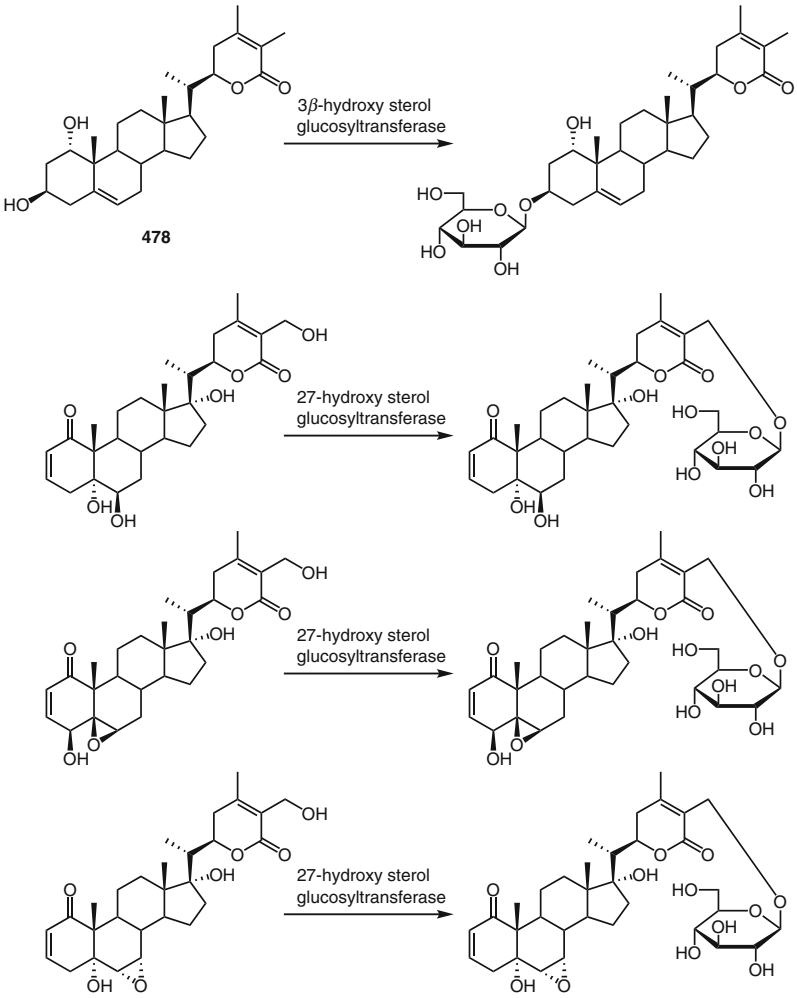

Chart 9 Enzymatic glucosylation of 3β- and 27-hydroxy withanolides

7.1. Insecticidal Activities

Insecticidal properties of withanolides were first noted for components isolated from the Peruvian plant *Nicandra physalodes* in the early 1960s. The major component of this plant, nicandrenone or Nic-1 (**338**), was later shown to be responsible for the insecticidal properties (*59*). Since then, several withanolides have been shown to exhibit insecticidal activity.

7.1.1. Antifeedant and Growth Inhibition

Antifeedant effects and species-specific activity were initially shown for the cotton leafworm *Spodoptera littoralis* (Boisd.) (Lepidoptera), the Mexican bean beetle, *Epilachna varivestis* Muls. (Coleoptera), and the red flour beetle, *Tribolium castaneum* (Herbst) (*59*). *Elliger* and coworkers found that some chromatographic fractions of an extract of *Physalis peruviana* leaves had a strong inhibitory effect on the development of larvae of the corn earworm *Helicoverpa zea*, an economic pest of numerous crops including tobacco and tomato (*201*). Bioassay-directed fractionation led to the isolation of a series of saccharide esters structurally related to the withanolides, with the δ-lactone side chain open and the carboxyl group esterified by mono-, di-, or trisaccharides (*202*, *203*). The most active compound in inhibiting larval growth was the 11β-hydroxy diglucoside ester **479** (ED_{50} 5.4 ppm) and the least active was the closely related monoglucoside ester **480** (ED_{50} 110 ppm). No clear structure-activity relationships could be established, but the lack of toxicity of the compounds led the authors to conclude that growth inhibition was a consequence of feeding deterrence resulting in semi-starvation of the animals. Previously, the feeding deterrent withanolides 4β-hydroxywithanolide E (**481**) and withanolide E (**482**) had been found in very high concentrations in the leaves and berries of *P. peruviana* (*204*).

The antifeedant activities of the major withanolides of *Salpichroa origanifolia*, salpichrolides A (**339**), C (**342**), and G (**340**), and some synthetic derivatives, were investigated on larvae of the common fly *Musca domestica* (*189*), the stored grain pest *Tribolium castaneum* (*205*), and the Mediterranean fly *Ceratitis capitata* (*190*). Salpichrolide A (**339**) was the most active in all cases producing a significant development delay in surviving larvae, when added to the diet at 500 ppm concentration. Similar delays were observed when medium and low nutrition diets (without withanolides) were offered as food, supporting the idea that these compounds act as feeding deterrents. The effects of salpichrolides C (**342**) and G (**340**) differed from one insect species to the other, thus both compounds produced development delays only at high concentrations (2,000 ppm) in *M. domestica* and *C. capitata*, but salpichrolide G was almost as effective as salpichrolide A in *T. castaneum*. Regarding toxicity, the three salpichrolides produced significant mortality for *M. domestica* larvae (EC_{50} 200–300 ppm), but only salpichrolides A and G had this effect on *C. capitata*. The authors proposed that differences could be related to different detoxifying mechanisms.

Oxidation of the hemiketal in the side chain to give the δ-lactone **483** eliminated the activity both for *M. domestica* and *T. castaneum*. However, acetylation to give **484** drastically reduced the activity only for the latter insect. Reduction of the Δ^2 double bond had only a minor negative effect on activity (*189*, *205*). The effect of functional group modifications in rings A and B on the resultant activity was evaluated on *C. capitata* larvae (*190*). Salpichrolide B (**341**), a minor component of *S. origanifolia*, was prepared from salpichrolide A in sufficient amounts for testing (see Sect. 6.1.). This compound was the most active of all salpichrolides tested, producing significant mortality when incorporated to the diet even at low doses (EC_{50} 83 ppm). It also produced clearly observed development delays in surviving

larvae at 25 ppm. Reduction of the Δ^2 double bond (**485** and **486**) produced a significant decrease in activity. Oxidation of salpichrolide C to the 6-ketone (**458**) or rearrangement of the 5,6-epoxide in salpichrolide A to the $\Delta^{2,4}$-6α-alcohol **456** resulted in inactive compounds.

The content of the salpichrolides in *S. origanifolia* was monitored during plant development, reaching a maximum during summer when insect populations are higher. These results, in conjunction with the observed toxic and feeding deterrent activities, suggest that these compounds may act as a chemical defense providing protection to the plant against phytophagous insects (*189*).

Feeding-deterrent activity of the major components of *Jaborosa odonelliana*, the spiranoid withanolides jaborosalactone P (**389**) and jaborosalactone 10 (**390**), was studied against *T. castaneum* (*177*). In this case, only jaborosalactone P (**389**) produced a significant delay in the development of neonate larvae. In the case of *J. integrifolia*, only jaborosalactone A (**487**) exhibited antifeedant activity on larvae of *Spodoptera littoralis* (*206*). Rearrangement of the epoxide to the allylic alcohol as in jaborosalactone B (**488**) or cleavage to the diol as in jaborosalactone D (**489**) resulted in complete loss of the activity. Jaborosalactone S (**254**) from *J. sativa* was a feeding deterrent for *Tenebrio molitor* (*207*) and the trechonolide-type withanolide **386** isolated from *J. lanigera* produced significant development delays in *C. capitata* larvae (*175*).

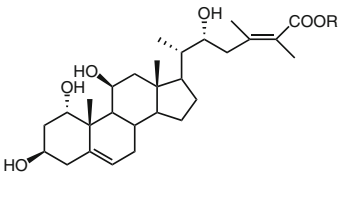

479 R = gluc-(1-2)-gluc-6'-Ac
480 R = gluc

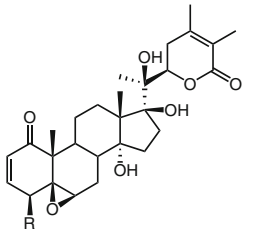

481 R = OH (4β-hydroxywithanolide E)
482 R = H (withanolide E)

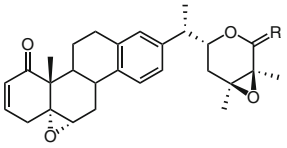

483 R = O
484 R = α-H, β-OAc

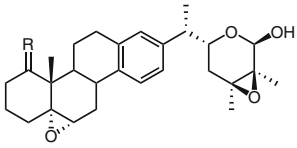

485 R = O
486 R = α-OH, β-H

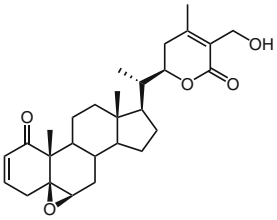

487 (jaborosalactone A)

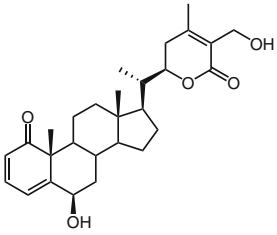

488 (jaborosalactone B)

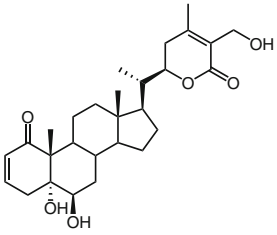

489 (jaborosalactone D)

Azambuja and coworkers studied the effect of several physalins from *Physalis angulata* on the blood-sucking insect *Rhodnius prolixus*, vector of *Trypanosoma rangeli*. Physalins B (**463**), D (**313**), F (**450**), and G (**314**) produced immune depression in *R. prolixus*, although apparently by different mechanisms. Without their defense system, insects infected with *T. rangeli* die (*208–210*).

7.1.2. Ecdysteroid Agonists and Antagonists

The ecdysteroid endocrine system is vital for insect development and a variety of secondary metabolites from plants have been shown to interfere with ecdysteroids, probably as a chemical defense mechanism. *Dinan* and coworkers developed a microplate-based bioassay with the ecdysteroid-responsive *Drosophila melanogaster* B_{11} cell line and used it to evaluate 16 withanolides isolated from *Iochroma gesneriodes*, for agonistic/antagonistic activity (*211*). Only withanolides containing an oxygenated functionality at C-3 (hydroxy or methoxy) and an α,β-unsaturated lactone in the side chain showed antagonistic activity, with 2,3-dihydro-3*β*-hydroxywithacnistine (**490**) being the most active (ED_{50} 2.5 μ*M* versus 0.05 μ*M* for 20-hydroxyecdysone). In a systematic study of 128 species of solanaceous plants including those known to contain high levels of withanolides, only a few of the methanolic extracts showed weak ecdysteroid antagonist activity (*212*). The high reactivity of the Δ^2-1-keto system present in many withanolides, raises the possibility that, even though inactive *in vitro*, they could be activated by conversion to the 2,3-dihydro-3*β*-hydroxywithanolides upon ingestion by insects (*213*). Further studies on 21 withanolides from different sources showed that withaperuvin D (**491**), with a C-3, C-6 oxygen bridge, had moderate agonistic activity (EC_{50} 25 μ*M*) (*214*).

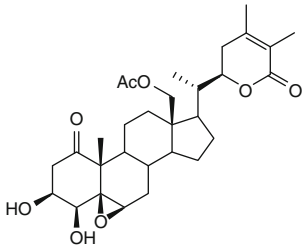

490 (2,3-dihydro-3*β*-hydroxywithacnistine)

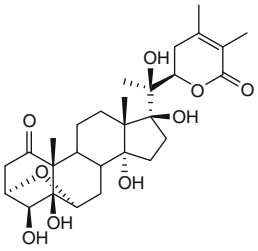

491 (withaperuvin D)

7.2. *Phytotoxic Activities*

Selective phytotoxicity has been reported for several withanolides. Three 7-oxygenated withanolides, **492–494**, isolated from *Iochroma australe*, reduced

radicle growth of the weeds *Sorghum halepense* (L.) Pers. (Monocot.) and *Chenopodium album* L. (Dicot.). Compound **493** inhibited radicle growth of *Lactuca sativa* L. (lettuce) but only at high concentration (1,000 ppm) (*215*). Jaborosalactol 18 (**285**) a major constituent of *J. bergii* (see Sect. 5.1.4.) showed significant inhibition of radicle growth at 2 m*M* on the dicotyledoneous species *C. album*, *Ipomoea purpurea* (L.) Roth and *L. sativa* (phytogrowth inhibitory activity $>$ 49%). On the other hand, **285** had a strong stimulatory effect for the monocotyledoneous species tested (*Zea mays* L. and *Sorghum halepense*) (*69*). Several withanolides isolated from *J. rotacea* also exhibited different activities towards mono- and dicotyledoneous species. Thus, jaborosalactones 29 (**447**), 30 (**448**), 31 (**404**), and 33 (**370**) had opposite effects on the dicotyledon *L. sativa* and the monocotyledon *Phalaris canariensis* L. Jaborosalactone 29 (**447**) was the most active, selectively inhibiting radicle growth, germination and the emergence rate index of *L. sativa* but with no effect on *P. canariensis*. Jaborosalactones 30 and 31 (**448**, **404**) had a strong stimulatory effect on radicle growth of *P. canariensis*. The chlorohydrin jaborosalactone 28 (**446**) was the only withanolide that inhibited the radicle growth of *P. canariensis* (*120*). A similar selectivity was exhibited by the major component of *J. kurtzii*, jaborosalactone 43 (**449**) (spiranoid type), and by withanolides of *J. caulescens*, the 12-*O*-ethyl derivative of jaborosalactone 42 (12-*O*-ethyl-**373**) (trechonolide type) and the sativolides **258**, and 12-*O*-methyl-**258**. All these compounds strongly inhibited radicle growth of *L. sativa* but exhibited a marginal effect on the monocotyledoneous *Avena sativa* L. (*76*, *121*).

7.3. Antiparasitic Activities

The first withanolides with antileishmanial and antitrypanosomial activities were isolated from *Dunalia brachyacantha* when screening extracts of Bolivian plants against *Trypanosoma cruzi* (Chagas disease), and several *Leishmania* species. Bioassay-guided fractionation of the leaf extract gave the known 18-acetoxywithanolide D (**142**) and its Δ^5 analogue **495**, with the latter compound being the most active against epimastigote forms of *T. cruzi* and promastigote cultures of *L. amazonensis*, *L. braziliensis*, and *L. donovani* (*84*).

7.3.1. Trypanocidal Activity

In a systematic study of the trypanocidal activity of secondary metabolites isolated from plants from northeastern Brazil, *Vieira et al.* found withaphysalins M and O (**323**, **325**) from *Acnistus arborescens* (see Sect. 5.2.4.) to be the most active compounds against epimastigotes of *T. cruzi*, with IC_{50} values of 100-fold less than the reference compound benznidazole (*216*). Reduction of the 2,3 double bond as in withaphysalin N (**324**) reduced the activity by an order of magnitude. Most

interestingly, these withaphysalins had no cytotoxic activity against dividing normal cells. Physalin F (**450**) from *Physalis angulata* was shown to be moderately active. *Abe* and coworkers investigated the trypanocidal activity of ten withanolides from *P. angulata* growing in Japan, against *T. cruzi* epimastigotes and trypomastigotes (the infectious form of the parasite) (*57*, *66*). Physagulins A–C (**496–498**), H (**117**) and I (**118**), and withangulatin A (**499**) had activity against both forms of *T. cruzi* similar to their cytotoxicity; activity against trypomastigotes was higher for these withanolides. Physagulins F (**500**), J (**119**), K (**120**), L (**121**), and M (**103**) and withaminimin (**501**) containing the 5α,6β-diol moiety were weakly active against epimastigotes, but the first two of these compounds were moderately active against the infectious trypomastigote form. Physagulin N (**106**), the methoxy derivative of physagulin A, was also marginally active confirming that the A ring enone is required for activity.

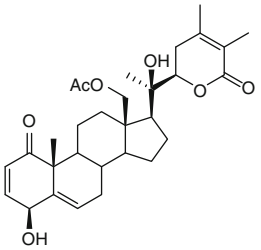

495

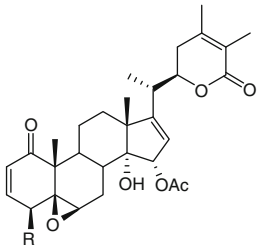

496 R = H (physagulin A)
499 R = OH (withangulatin A)

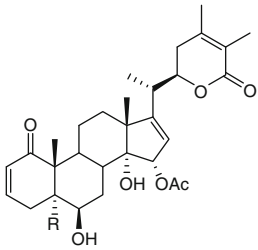

497 R = Cl (physagulin B)
501 R = OH (withaminimin)

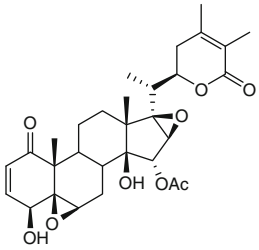

498 (physagulin C)

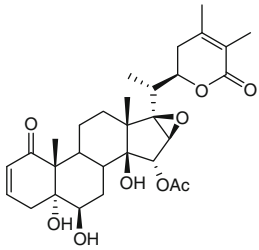

500 (physagulin F)

7.3.2. Leishmanicidal Activity

Atta-ur-Rahman and coworkers have reviewed the antileishmanial activity of withanolides from *Physalis minima* as well as some of their biotransformation products (*217*). Physalin **299** was the most active substance against *Leishmania major* promastigotes, (see Sect. 5.2.1.) while physalins **298**, **300**, **301**, physalin H (**312**), isophysalin B (**474**), and 5β,6β-epoxyphysalin B (**502**) also had significant activity.

The 3-methoxy derivative physalin U (**304**) and withanolide **107** with an unmodified skeleton were only marginally active (*60*, *145*). Removal of the C-6 hydroxy group of physalin H (**312**) to give either the dehydration product **473** or the deoxygenated physalin **475** (see Sect. 6.3.) did not affect the antileishmanial activity (*193*).

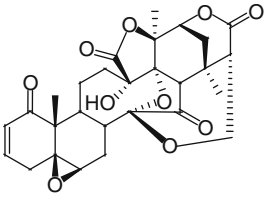

502 (5β,6β-epoxyphysalin B)

Echeverri and coworkers investigated the leishmanicidal activity of several acnistins (A, B, C, E, F, and G) and withajardins (A, B, and C) isolated from *Dunalia solanacea* and *Deprea orinocensis*, respectively (see Sects. 5.1.2. and 5.1.3.). Efficacy was evaluated using intracellular amastigotes of *Leishmania (V) panamensis* (*218*). Withajardin B (**278**) and acnistins A (**259**), C (**262**), and E (**260**) were the most active; withajardin A (**277**), and acnistins B (**261**), and F (**264**) were the least active. The 3-methoxy derivative of withajardin A was inactive. All compounds had poor selectivity, with antileishmanial activity closely paralleling cytotoxicity in all cases. The authors did a 3D-QSAR study and concluded that differences in bioactivity could be explained by the influence of steric and electrostatic fields in the vicinity of ring A. According to the model, bending of the steroid nucleus at the A/B ring junction, an increase of positive charge near positions 2, 3, and 4, or of a negative change near positions 5 and 6, increased the bioactivity.

Withaferin A (**1**) inhibited growth of *L. donovani* promastigotes. *In vitro* studies showed that withaferin A inhibits protein kinase C in the parasite, leading to apoptosis (*219*). Withanolide Z (**27**), but not withaferin A, partially inhibited *L. donovani* topoisomerase I (*28*).

7.4. Antimicrobial Activities

The antibacterial and antifungal properties of withaferin A (**1**) have been known for a long time and many other withanolides are known to display these activities (*3*, *4*). However, data are scattered throughout the literature involving the action of different compounds on different microorganisms thus making it difficult to rationalize the results. Withaferin A has been shown to be strongly active against *Bacillus subtilis* and moderately active for *Escherichia coli* and *Staphylococcus aureus*, but inactive against *Pseudomonas aeruginosa*. As an antifungal it exhibited

strong activity against *Aspergillus niger*, but was inactive against *Rhizopus oryzae* and *Candida albicans* (*220*). 4-Deoxywithaperuvin (**11**) was moderately active against several *Gram*-positive (*B. cereus*, *B. subtilis*, *Streptomyces* spp.), and *Gram*-negative (*Pseudomonas fluorescens*, *Serratia marcescens*) bacteria, but inactive against *Micrococcus luteus*, *M. roseus* and *S. aureus*; antifungal activity was poor (*20*). On the other hand, the 18-oxygenated withanolides 18-acetoxywithanolide D (**142**) and its Δ^5 analogue **495** from *D. brachyacantha* were active against *S. aureus* and *B. subtilis* and inactive against *E. coli* and *Shigella flexneri* (*84*).

17β-Hydroxywithanolide K (**51**) and the closely related 14α,20-epoxywithanolide, **71** (see Sect. 4.1.4.) showed antifungal activity against the human pathogens (*MIC* 300 µg/cm^3) *Aspergillus niger*, *Stachybotrys atra*, *Allescheria boydii*, *Drechslera rostrata*, *Microsporum canis*, and *Curvularia lunata* (*36*, *43*).

Among the physalins, physalin B (**463**) was active against *S. aureus* (several strains) and *N. gonorrhoeae* but not active against *E. coli* and *P. aeruginosa* (*221*). Physalin D (**313**), but not physalin B, was moderately active against *Mycobacterium tuberculosis* (*222*).

7.5. *Anti-inflammatory and Glucocorticoid Related Activities*

7.5.1. Anti-inflammatory Activity

The antiinflammatory properties of several withanolides are well known (*3*). *Souza* and coworkers have shown that in the case of physalins B (**463**) and F (**450**), the anti-inflammatory activity parallels that of the synthetic glucocorticoid dexamethasone in preventing inflammatory injury and lethality after intestinal ischemia and reperfusion in mice (*223*). Furthermore, they found that the effect could be reversed by pretreatment with the glucocorticoid antagonist RU-486, indicating that the *in vivo* activity displayed by the physalins is mostly due to activation of the glucocorticoid receptor. As observed with dexamethasone, physalins also decreased TNF-α concentration and enhanced the anti-inflammatory interleukin IL-10 concentration in tissues. Physalins B (**463**) and F (**450**) have been shown to inhibit TNF-α induced activation of NF-κB and either a 5,6 double bond or a 5β,6β-epoxide are required for activity; the 5α,6β-diol physalin D (**313**) is inactive (*138*).

An ethanol extract of *W. somnifera* significantly suppressed lipopolysaccharide (LPS)-induced production of the pro-inflammatory cytokines TNF-α, IL-1β, and IL-12p40 in peripheral blood mononuclear cells of normal individuals and reumathoid arthritis patients, and inhibited nuclear translocation of the transcription factors NF-κB and AP-1 and phosphorylation of IκBα. The major component, withaferin A (**1**), inhibited NF-κB translocation and was associated with these effects (*224*). Withaferin A inhibited NF-κB activation by preventing the TNF-induced activation of IκB kinase via a thioalkylation-sensitive redox mechanism

(*225*). 12-Deoxywithastramonolide (**503**) and withanolide A (**504**) were much less effective. A more detailed study on the inhibition of NF-κB activation by various agents was conducted by *Ichikawa et al*. (*226*). The authors isolated a series of withanolides from a *W*. *somnifera* leaf extract, which included withaferin A (**1**), viscosalactone B (**505**), withanosides IV (**31**) and X (**37**), and related compounds. The 1α,3β-dihydroxy-Δ^5-withanolides and their glycosides did not inhibit NF-κB activation while withaferin A and its diacetate were strong inhibitors. Reduction of the 2,3-double bond of withaferin A rendered the compound inactive but addition of a 3-hydroxy substituent (as in viscosalactone B) restored activity. Acetylation of the hydroxy groups of the latter compound did not affect activity, but glycosylation at C-27 gave an inactive compound.

Nair and coworkers reported the selective cyclooxygenase-2 (COX-2) inhibitory activity of leaf extracts of *W*. *somnifera* and related such information to the use of this plant as an antiinflammatory. From the methanolic extract they isolated 12 withanolides and evaluated their abilities to inhibit COX-1 and -2. None of the withanolides inhibited COX-1 even at high doses but most of them exhibited some inhibitory activity on COX-2, with withaferin A (**1**) and viscosalactone B (**505**) being the most active (*15*). Molecular docking studies showed that most of the withanolides had more favorable binding to COX-2 than to COX-1 (*227*).

The 12-oxygenated withanolide **154** from *Discopodium penninervium* (see Sect. 4.2.3.) was a selective inhibitor of cyclooxygenase-2 and also of leukotriene formation; as both these pathways are involved in cell proliferation and angioneogenesis, the dual inhibition of COX-2 and leukotriene formation by **154** has been proposed as a starting point for the development of anti-inflammatory and cancer chemopreventive agents (*82*).

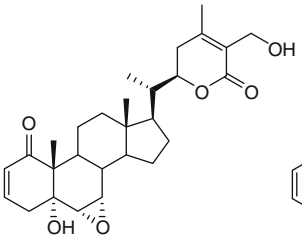

503 (12-deoxywithastramonolide)

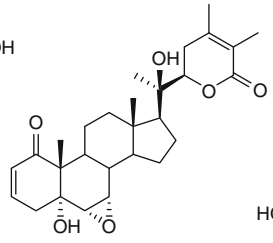

504 (withanolide A)

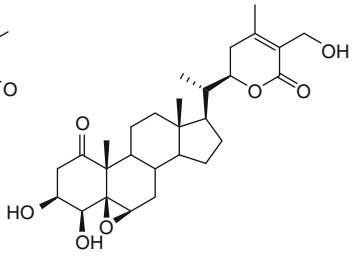

505 (viscosalactone B)

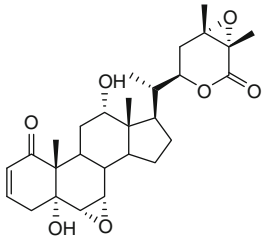

506 (daturalactone 1)

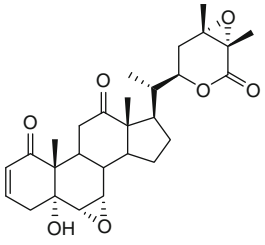

507 (daturalactone 2)

7.5.2. Antistress Activity

Withafastuosin D (**168**), the major withanolide in *Datura fastuosa* leaves, maintained corticosterone levels in male albino rats during experimental stress and exhibited antistress activity evidenced as an anxiolytic effect (*228*). Withafastuosin E (**169**) has also been found to increase the release of prostaglandins, which play an important role in the resistance to gastroduodenal mucosa to ulceration (*229*, *230*). On the other hand, the antistress activity of *W. somnifera* glycowithanolides (*e.g.* sitoindosides) has been linked to their antioxidant activity (*231*, *232*).

7.5.3. Immunosuppressive and Immunomodulatory Activity

The 16-oxygenated withanolides **188–190** isolated from *Discopodium penninervium* (see Sect. 4.2.4.) exhibited potent immunosuppresive activity; they inhibited the incorporation of [^{3}H]-thymidine in cultured rat spleen cells without being overtly toxic to the cells (*233*). Acnistins A (**259**), B (**261**), and E (**260**) from *Dunalia solanacea* significantly inhibited the incorporation of [^{3}H]-thymidine in human lymphocytes at doses as low as 0.1 μg/cm^3 (*124*). Coagulin H (**7**) isolated from *W. coagulans* also was a strong inhibitor of incorporation of [^{3}H]-thymidine in stimulated human mononuclear cells. It inhibited T-cell proliferation with an activity similar to that of the synthetic glucocorticoid, prednisolone. Like prednisolone, the T-cell suppression effect was correlated with a decrease in production of the cytokine IL-2. However, at variance with the glucocorticoid, coagulin H did not have any damaging effects on the cells (*234*).

Immunomodulatory effects of three daturalactones from *Datura quercifolia* were evaluated by observing their effects on antibody production, T-cell and B-cell activation, and cytokine production from splenocytes. The 1β-alcohol **153** was immunosuppressive at lower doses while daturalactones 1 (**506**) and 2 (**507**) were immunostimulators (*81*).

Physalins B (**463**), F (**450**), and G (**314**), but not D (**313**), inhibited nitric oxide production by activated macrophages. Addition of physalin B to lipopolysaccaride-stimulated peritoneal macrophage cultures induced decreases of TNF-α IL-6, and IL-12 production. Physalins B, F, and G also protected mice against administration of a lethal dose of lipopolysaccaride (*235*). The effects of the above-mentioned physalins were not blocked by the antiglucocorticoid, RU-486, suggesting that they act by a mechanism different from that of the glucocorticoids. Physalins B, F, and G also have potent suppressive activities *in vitro* on splenocyte cultures and *in vivo* on allogeneic transplants (*236*). The effects of physalins on transplant rejection could be explained by a direct effect of these withanolides on lymphocytes.

Several physalins isolated from *Physalis alkekengi* were found to be strong inhibitors of nitric oxide production induced by lipopolysaccaride, including the above-mentioned physalins B and F and also physalins A (**468**) and O (**469**). Compounds of the neophysalins class (see Sect. 5.2.2.) were inactive (*139*).

7.6. Cancer-Related Activities

Many studies have dealt with the potential antitumor activity of withanolides, and large amounts of data are available, mostly their cytotoxicity to cancer cell lines. However, other cancer-related activities specific to certain withanolide structural types have also been investigated in the last decade. Particularly interesting are those related to cancer chemoprevention, inhibition of angiogenesis, and microtubule stabilization.

7.6.1. Cytotoxicity

Most withanolides exhibit some level of cytotoxicity against different tumor cell lines, but usually this is non-selective and in the micromolar concentration range. Withaferin A (**1**) has been investigated extensively in this respect, with several recent studies also addressing its mechanism of action (*191*, *237–239*).

Nair and coworkers assayed several withanolides from *W. somnifera* against human lung, breast, CNS, and colon cancer cell lines. Withaferin A (**1**), its diacetate, viscosalactone B (**505**), compound **6**, and ashwagandhanolide (**78**) were the most active (IC_{50} range 0.5–1 μM) and comparable in potency to a reference compound, adriamycin (*47*, *240*). Compound **78** also inhibited lipid peroxidation and the activity of the enzyme cyclooxygenase-2 *in vitro*. Several withanolides from *Acnistus arborescens* were evaluated against panels of human cancer lines, including some 16-acetoxywithanolides and withaphysalins F (**316**), M (**323**), N (**324**), and O (**325**), with IC_{50} values in the 0.2–2 μM range (*98*, *152*, *153*, *241*). The 16-oxygenated withanolides **188–190** isolated from *Discopodium penninervium* (see Sect. 4.2.4.) exhibited significant cytotoxicity only against murine RAW 264.7 carcinoma cell lines (*233*). The 12β-acetoxywithanolide **156** did not show any cytotoxic activity up to 10 μM (*83*).

Bioassay of seventeen withanolides from *Tubocapsicum anomalum* showed significant cytotoxic activity (comparable to that of doxorubicin) against a panel of human cancer cell lines for eight of the compounds (*107*). From the 18-nor withanolides (see Sect. 5.5.3.), only tubocapsenolide A (**441**) exhibited potent cytotoxicity; this compound was shown to inhibit proliferation and induce apoptosis in MDA-MB-231 cells by thiol oxidation of heat shock proteins (*242*). Potent cytotoxicity was also exhibited by tubocapsanolide A (**201**) and

its 20-hydroxy (**204**) and 23-hydroxy (**205**) derivatives, tubocapsanolide F (**203**), and anomanolide B (**269**) (*107*, *243*). The other active withanolides isolated were the known withanolide D (**508**) and its 17α-hydroxy derivative (**509**). Withaferin A (**1**), also used as a reference compound, was *ca*. 10 times more active.

Withametelins I (**235**), K (**237**), L (**238**), and N (**240**), isolated from *Datura metel*, exhibited cytotoxicity against selected human cancer cell lines, namely, A549 (lung), BGC-823 (gastric), and K562 (leukemia), with IC_{50} values of 0.05–3.5 μ*M*. Withametelin J (**236**) was only moderately active for the last two cell lines (*92*).

Withanolides from *Physalis* species have also been studied extensively in terms of their cytotoxicity against human and murine cancer cells. Among the physalins, physalins B (**463**), D (**313**), F (**450**), and H (**312**) showed strong cytotoxicity against multiple tumor cell lines, while physalins G (**314**), I (**510**), and physanolide A (**367**) were inactive. Physalins J (**457**) and U (**304**) were marginally active (*55*, *134*, *146*, *244*, *245*). The 18-*nor*-physalin, withaphysanolide A (**438**), also was weakly active (*186*). For physalins B and D, the antineoplastic activity was confirmed *in vivo* by inhibition of tumor proliferation in mice bearing sarcoma 180 tumor cells (*245*). Both physalins B and F have been shown to inhibit hedgehog (Hh)/GLI-mediated transcriptional activation, which is involved directly in tumor formation and progression (*246*). Recently, *Magalhães et al*. reported different activities for physalins D and E isolated from *P*. *angulata*. However, as already mentioned in Sect. 5.2.3., the structure of physalin E was incorrectly assigned and later shown to be identical to physalin D (**313**) (*244*). Accordingly, these bioactivity results should be considered with caution. Among the *Physalis* withanolides with an unmodified skeleton, potent cytotoxic activity has been reported for withangulatins A (**511**), B (**94**), and I (**102**), physangulin B (**512**), phyperunolide A (**101**), withaphysacarpin (**195**), philadelphicalactones A (**197**) and B (**198**), 18-hydroxywithanolide D (**128**), and withanone (**513**) (*50*, *55*, *56*, *58*, *104*, *247*).

Ixocarpolactones A (**360**) and B (**361**), isolated from *P*. *philadelphica*, exhibited significant inhibition of murine epidermal JB6 cell transformation (*104*) and ixocarpolactone A (**360**) present in the edible fruit of the plant showed potent antiproliferative and apoptotic activity in SW480 human colon cancer cells (*247*). Evaluation of 12 withaphysalins from *P*. *minima* and *P*. *divaricata*, including **331–334**, showed only moderate cytotoxicity against the HCT-116 and H460 human cancer cell lines (*154*, *186*).

The potential antitumor activities of an alcoholic extract of *W*. *somnifera* roots and of withaferin A (**1**) have also been studied in conjunction with radiation therapy in experimental tumors *in vivo*. Both exhibited significant antitumor and radiosensitizing effects without systemic toxicity (*248–250*).

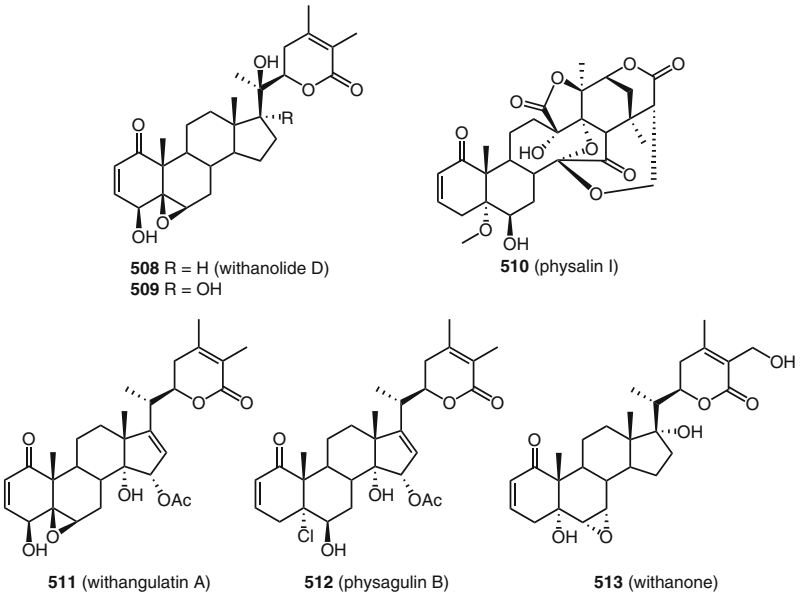

7.6.2. Cancer Chemopreventive Activity

Cancer chemoprevention by the ingestion of modulators of carcinogenesis from synthetic or natural origin has been proposed as a strategy to reduce cancer mortality in apparently healthy persons at risk of cancer (*6*, *251*). *Pezzuto*, *Kinghorn* and collaborators have used a battery of *in vitro* bioassays to monitor inhibition of tumorigenesis at the stages of initiation, promotion, and progression by plant extracts and pure compounds. One key bioassay used, is based on the induction of the phase II drug-metabolizing enzyme NAD(P)H:quinone reductase (QR), on Hepa 1c1c7 hepatoma cells; QR induction is indicative of potential cancer prevention at the initiation phase (*252*). A large number of compounds of plant origin have been evaluated as QR inducers, including many withanolides (*6*). Of particular interest are QR inducers that exhibit low cytotoxicity and thus a high selectivity measured as the chemopreventive index, the ratio between the concentration needed to double QR activity (CD) and the concentration that inhibits cell growth by 50% (IC_{50}).

Kinghorn and coworkers investigated QR induction by the withanolides in fruits and aerial parts of *Physalis philadelphica* (see Sect. 4.2.4.) (*103–105*). With the exception of withanone (**513**), all the withanolides were potent QR inducers with activity comparable to or better than the reference compound, sulforaphane, a known chemopreventive agent. Ixocarpalactone A (**360**), philadelphicalactone A (**197**), withaphysacarpin (**195**), and 4β,7β,(20*R*)-trihydroxy-1-oxowitha-2,5-dien-22,26-olide (**199**) exhibited the highest chemopreventive indexes. The fact

that ixocarpolactone A (**360**), is present in the edible fresh fruit of *P. philadelphica* (tomatillo) at a concentration level of 143 ppb (*105*), make these findings especially important.

In a broader study comprising withanolides from 13 Solanaceae species, 37 withanolides representative of a variety of structural types were evaluated for their potential to induce quinone reductase (*253*). Jaborosalactone 1 (**397**), jaborosalactone O (**353**), jaborosalactone P (**389**), trechonolide A (**368**), and withaphysalin J (**320**), were significant QR inducers with CD values in the range of 0.27–1.52 μ*M*. Results indicated that a functionalized methyl-18 plays an important role in improving QR induction while the presence of 5α-substituents is deleterious for the activity. Overall, spiranoid- and trechonolide-type withanolides exhibited good QR induction. Some of the active withanolides had low cytotoxicity, with chemopreventive indexes that compared favorably with the reference compound sulforaphane. One such compound, the spiranoid, jaborosalactone P (**389**), was selected to test its capacity to induce steady-state levels of quinone reductase in multiple organ sites of BALB/c mice. With jaborosalactone P-treated mice, a significant induction was observed in liver and colon, but not in lung, stomach, or mammary gland (*253*). This *in vivo* study confirmed the *in vitro* results, indicating that withanolides may function as potent phase II enzyme inducers.

Withanolides **184** and **185** from *A. arborescens*, bearing acetates at positions 7*β* and 16α, were also very potent QR inducers, but exhibited high cytotoxicity resulting in poor selectivity (*98*). From *Larnax subtriflora*, subtrifloralactones A (**431**), C (**433**), D (**425**), F (**436**), I (**428**), and J (**429**) containing an α,β-unsaturated ketone functionality in ring A (see Sect. 5.5.) had significant QR induction activity (*184*). Both δ- and γ-lactones were active, indicating that this part of the molecule was not critical for activity. Subtrifloralactone D was the most active, but subtrifloralactones A and F had the highest chemopreventive index (*ca*. 3 times that of sulforaphane). Subtrifloralactone L (**435**) with a doubly unsaturated ring A ketone, was inactive in the QR assay, while subtrifloralactone K (**434**) with the less common 3,6-epoxy arrangement, was active (*185*). The above data although limited, suggest that even though the presence of an α,β-unsaturated ketone unit in ring A of withanolides appears to be important for inducing QR, other structural features may compensate the lack of this functionality or block its beneficial effects.

Panjamurthy et al. have reported that pretreatment with withaferin A (**1**) significantly reduced *in vivo* 7,12-dimethylbenz[*a*]anthracene (DMBA)-induced genotoxicity, in the bone marrow of golden Syrian hamsters (*254*). This effect could also be related to the induction of phase II detoxifying enzymes.

7.6.3. Antiangiogenic Activity

Formation of new blood vessels from existing vasculature or "angiogenesis" is characteristic of all solid tumors allowing for nutrition, oxygenation, and

metastasis. Thus, angiogenesis inhibitors provide an alternative way of controlling the growth of tumor cells in both pre-invasive and invasive stages. Angiogenesis is also involved in the pathogenesis of several non-malignant inflammatory diseases (age-related macular degeneration, arthritis, endometriosis, *etc*.). *Mohan et al*. reported the antiangiogenic activity of extracts of *W. somnifera* containing non-cytotoxic levels of withanolides and also of withaferin A (**1**) (*255*). Thus, withaferin A inhibited cell proliferation in human umbilical vein endothelial cells (HUVECs) (IC_{50} 12 n*M*) through a process associated with inhibition of cyclin D1 expression. A potent antiangiogenic effect was also observed *in vivo*, at doses that are 500-fold lower than those previously reported to exert antitumor activity. The authors proposed that the inhibition of NF-κB by withaferin A in HUVECs occurs by interference with the ubiquitin-mediated proteasome pathway as suggested by the increased levels of poly-ubiquitinated proteins. The biotinylated derivative **459** was used to identify protein targets of withaferin A in HUVECs (see Sect. 6.1.). Preliminary results showed that withaferin A binds irreversibly with a 56 kDa protein target and a less abundant 180 kDa species but interacts reversibly with a 70 kDa protein species (*192*). Withaferin A and withanolide D (**508**) also displayed antiangiogenic activity in human choroidal endothelial cells (HCECs). These results may lead to novel treatments of choroidal neovascularization, the major contributor to age-related macular degeneration and one of the leading causes of irreversible blindness in the Western hemisphere (*256*). Physalin B (**463**) has been identified recently as an inhibitor of the ubiquitin-mediated proteasome pathway in the DLD-1 human colon cancer cell line, producing an accumulation of ubiquitinated proteins and inhibiting TNFα-induced NF-κB activation (*257*). The antiangiogenic activity of this compound remains to be tested.

7.6.4. Microtubule Stabilizing Activity

The microtubule stabilizing activity of taccalonolides A (**405**) and E (**420**) was reported by *Mooberry* and coworkers after bioassay-directed fractionation of an extract of *Tacca chantrieri* (*258*). Microtubule stabilizers are highly effective drugs used in the treatment of many types of cancers. The taccalonolides are particularly interesting as they appear to have a unique mechanism of action, which does not involve direct binding to tubulin. Special attention has been drawn to these compounds and also to their closely related analogues, taccalonolides B (**419**) and N (**421**), as they retain efficacy in taxane- and epothilone-resistant models (*259*). Although these taccalanolides are less potent than other microtubule stabilizers in drug-sensitive cell lines, they are effective at similar concentrations against taxane-resistant cell lines. The microtubule stabilizing activity of taccalonolides has been reviewed recently by *Risinger* and *Mooberry* (*260*).

7.7. *CNS-Related Activities*

Reports on activities affecting the CNS by withanolides are mostly based on properties attributed to "Ashwagandha" in ayurvedic medicine and are restricted to withanolides from *W. somnifera*.

7.7.1. Synaptogenesis and Neuritic Outgrowth

Facilitating synaptogenesis and reconstructing neuronal networks in the damaged brain is required for the therapeutic treatment of neurodegenerative diseases that produce neuronal degeneration and atrophy. Several withanolides isolated from the methanolic extract of *W. somnifera* roots as well as the extract itself, have been shown to possess neurite outgrowth activity (*21*, *261*). Withanoside IV (**31**) and VI (**32**) predominantly induced dendritic outgrowth in normal cortical neurons, while withanolide A (**504**) predominantly induced axon outgrowth (*262*). These withanolides also showed neuritic regeneration and synaptic reconstruction of damaged cortical neurons and prevented both dendritic and axonal atrophy induced by Aβ(25–35) (*261*, *263*). Oral administration of withanoside IV significantly improved memory deficit in Aβ(25–35) treated mice, and sominone, the aglycone of withanoside IV, was shown to be the major metabolite after administration. Sominone was more active than withanoside IV (*264*).

7.7.2. Cholinesterase Inhibition

Natural cholinesterase inhibitors are of special interest in drug development due to the involvement of cholinesterases in *Alzheimer*'s disease and other related dementias. Acetylcholinesterase (AChE) inhibitors activate central cholinergic function by increasing the acetylcholine levels in the brain. Bracteosins A (**206**), B (**207**), and C (**208**), isolated from *Ajuga bracteosa* (*108*), and withanolide A (**504**) and withaferin A (**1**) from *W. somnifera*, were moderate inhibitors of AChE and BChE (butyrylcholinesterase) (*11*). Molecular docking studies indicated that all compounds are imbedded in the aromatic gorge of AChE. All these withanolides also showed dose-dependent spasmolytic and Ca^{2+} antagonistic activities that may help in prolonging neuron survival and function (*265*). Withanoside VI (**32**) and withaferin A attenuated the desensitization to clonidine of smooth muscle, and this effect was related to the effect of *W. somnifera* on morphine tolerance and dependence (*27*). It should be noted that clonidine inhibits the release of acetylcholine by acting on α_2-adrenoceptors in these tissues.

8. Chemotaxonomic Considerations

As already mentioned, *ca*. 650 withanolides have been described, most of them from genera of the Solanaceae, subfamily Solanoideae. The absence so far of withanolides in members of the other subfamilies is curious. In Table 3, the genera of subfamily Solanoideae containing withanolides are arranged according to the most recent phylogenetic classification (*10*). As different groups of withanolides have been reported in 23 genera and *ca*. 70 species of the Solanoideae, some chemotaxonomic considerations can be made.

Withanolides with an unmodified skeleton (Fig. 2) are the most common, occurring in 14 genera of the different tribes (Physaleae, Datureae, Hyoscyameae, Lycieae, and Solaneae). Among the six genera still not assigned phylogenetically to

Table 3. Genera of the subfamily Solanoideae containing withanolides arranged according to a established phylogenetic system

Tribe (subtribe)	Genus (section)	Main withanolide types
Physaleae (Physalinae)	*Physalis*	Physalins, neophysalins, cyclophysalins, withaphysalins, unmodified skeleton
	Margaranthus	Physalins, unmodified skeleton
	Witheringia	Physalins
	Brachistus	Physalins
Physaleae (Iochrominae)	*Acnistus*	Acnistins, withaphysalins, unmodified skeleton
	Iochroma	Unmodified skeleton
	Eriolarynx	Withaphysalins, unmodified skeleton
	Vassobia	Unmodified skeleton
	Dunalia	Acnistins, withaphysalins, unmodified skeleton
Physaleae (Withaninae)	*Withania*	Unmodified skeleton
	Tubocapsicum	Acnistins
	Discopodium	Acnistins, unmodified skeleton
Physaleae[a]	*Larnax*	Subtrifloralactones, unmodified skeleton
Datureae	*Datura (Datura)*	Unmodified skeleton
	Datura (Dutra)	Withametelins, unmodified skeleton
Hyoscyameae	*Hyoscyamus*	Unmodified skeleton
Lycieae	*Lycium*	Unmodified skeleton
Solaneae	*Solanum*	Unmodified skeleton
Genera not assigned to a more inclusive clade	*Deprea*	Withajardins
	Exodeconus	Unmodified skeleton
	Jaborosa (Jaborosa)	Aromatic ring A, spiranoid-γ-lactones, unmodified skeleton
	Jaborosa (Lonchestigma)	15,21-cyclowithanolides, sativolides, spiranoid-γ-lactones, spiranoid at C-22, trechonolides, unmodified skeleton
	Nicandra	Aromatic ring D, unmodified skeleton
	Salpichroa	Aromatic ring D, unmodified skeleton
	Schraderanthus	Physalins

[a]Genus not assigned to a subtribe

a more inclusive clade but within the Solanoideae (Table 3), withanolides with an unmodified skeleton have now been reported only in the *Larnax* (*Deprea*) and *Schraderanthus* genera.

8.1. Tribe Physaleae

Different withanolides with modified skeletons are present within this tribe (Plates 1 and 2). Physalins and related withanolides (Fig. 2) are frequent in the subtribe Physalinae (Plate 1, a–f), particularly in *Physalis*, *Margaranthus*, *Witheringia*, and *Brachistus*. The occurrence of physalins and the non-occurrence of the unmodified skeletons in *Witheringia* and *Brachistus* support the close phylogenetic relationship between both genera, which appear together in a small clade and are sisters to one another (*10*). In addition, the presence of physalins in *Schraderanthus* is noteworthy, which is a monotypic genus recently segregated from *Leucophysalis* (tribe Physaleae, subtribe Physalinae). *Schraderanthus* still remains unassigned to any tribe due to the lack of molecular analysis; the chemical information would support the inclusion of *Schraderanthus* in the subtribe Physalinae, the only subtribe where physalins have been found.

In the subtribe Physalinae, withaphysalins (Fig. 2), ixocarpalactones, and perulactones (Fig. 3) have been reported in certain *Physalis* species (*P. minima, P. philadelphica*, and *P. peruviana*); since this genus comprises *ca.* 90 species, these metabolites may probably appear in other species. As more information emerges from research conducted in other *Physalis* species, it will be able to evaluate the potential chemotaxonomical value of these compounds, either as chemical generic markers or as an exception in the genus.

Withaphysalins are more frequent in the subtribe Iochrominae (Plate 2), a well-supported clade but with the relationships within this clade poorly resolved (*10*). The chemical data presented in this chapter, support some taxonomic changes proposed by morphological data (*9*) and confirmed by molecular evidence (*10*), as is the case for the segregation of *Eriolarynx* containing withaphysalins F-L (see Sect. 5.2.4.) from *Vassobia* (no withaphysalins).

Acnistins (Fig. 2) appear in the subtribes Iochrominae and Withaninae and are absent in all the remaining genera investigated so far. Within the latter subtribe, three small clades have been identified with unresolved relationships between them (*10*). One clade includes *Aureliana* and *Athenaea,* two South American genera not investigated phytochemically up to now. The second clade comprises a monotypic Asiatic genus (*Mellisia*) and *Withania*, the "parent genus" of the withanolides (Plate 1, g–j); finally, *Nothocestrum*, *Tubocapsicum* and *Discopodium* are included in the third clade. The chemical evidence is consistent with this proposal since *Withania* is characterized by the presence of a large number of withanolides with the unmodified parent skeleton of withaferin A (**1**). In contrast, *Discopodium* and *Tubocapsicum* produce withanolides with structural variations. The close affinity

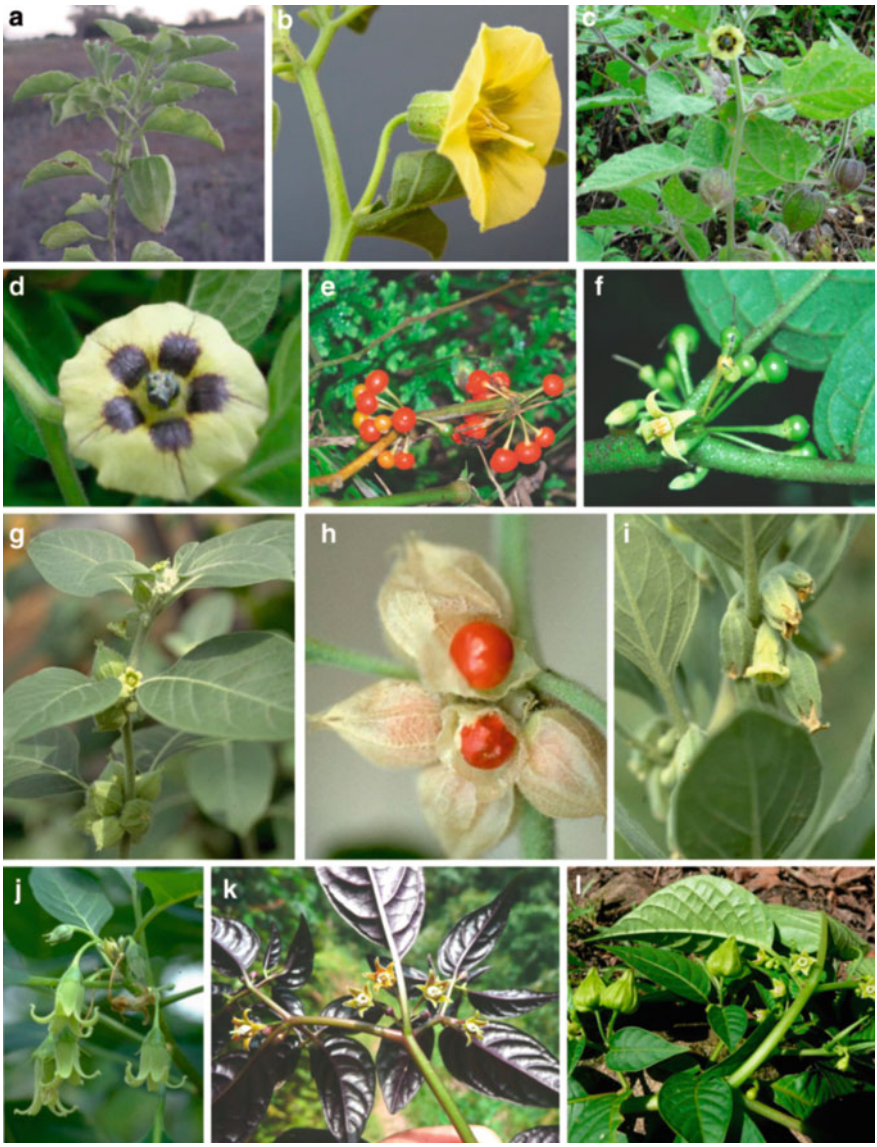

Plate 1. Solanaceae species of Tribe *Physaleae*. Subtribe *Physalinae*: (a) *Physalis viscosa*, branch with fruit; (b) *P. viscosa*, flower (photographs: J. Toledo and M.T. Cosa). (c) *P. pubescens*, plant with flower and fruits (photograph: G. Barboza); (d) *P. peruviana*, detail of corolla (photograph: J. Toledo); (e) *Witheringia solanacea*, stem with fruits; (f) *W. solanacea*, flower and immature fruits (photograph: G. Beltrán). Subtribe *Withaninae* (photographs with permission of the Experimental Garden and Genebank of the Radboud University of Nijmegen, The Netherlands): (g) *Withania somnifera*, flowering branch; (h) *W. somnifera*, fruits; (i) *W. adpressa*, flowers; (j) *W. aristata*, flowering branch. Genus not assigned to a subtribe: (k) *Larnax* sp., branch with flowers and fruits; (l) *Larnax* sp., flowering branch (photographs: S. Leiva)

Plate 2. Solanaceae species of Tribe *Physaleae* subtribe *Iochrominae*. (a) *Eriolarynx lorentzii*, flower; (b) *Vassobia breviflora*, branch with flowers and fruits; (c): *Acnistus arborescens*, flowering branch (photographs: F. Chiarini); (d) *Iochroma australe*, flowering branch; (e) *I. australe*, fruit (photographs: M. T. Cosa and G. Barboza); (f) *I. fuchsioides*, flowering branch and (g) *I. gesneroides*, flowering branch (photographs with permission of Experimental Garden and Genebank of the Radboud University of Nijmegen, The Netherlands)

between the latter two genera is evidenced by them both producing the 17-epiacnistins, which are absent in *Withania*.

8.2. Tribes Hyoscyameae, Lycieae, and Solaneae

In these tribes (Plate 3, d–i), only five species have been investigated (Tables 1 and 3), thus, only preliminary chemotaxonomic suggestions may be proposed. These species are consistent in always containing withanolides with an unmodified skeleton. Worth mentioning is the fact that in the largest genus of the family, *Solanum* (with *ca*. 1,500 species), withanolides have been reported in only two species (*S*. *ciliatum* and *S*. *sisymbriifolium*) (See Sect. 4.2.5.).

8.3. Tribe Datureae

The tribe comprises two genera, *Brugmansia* and *Datura*, but, however, no information is available on *Brugmansia*. In the conventional classification, the 14 species of *Datura* are included in three sections: sect. *Datura* (*D*. *quercifolia* and *D*. *stramonium*), sect. *Ceratocaula* (*D*. *ceratocaula*), and sect. *Dutra* (the remaining species) (Plate 3, a–c). Withanolides from seven taxa have been investigated extensively, and more than 70 different compounds have been reported. The withametelin skeleton (Fig. 2), occurring in *ca*. 30 compounds, is exclusive to *Datura*. Withametelins were reported in *D*. *inoxia* and *D*. *metel*. Genetic similarity and phylogenetic analysis both suggest that *D*. *metel* is related more closely to *D*. *inoxia* than to the other taxa of section *Dutra*, based upon the small genetic distance between them (*266*, *267*), which is supported by the available chemical information. Other chemical coincidence with conventional and phylogenetic proposals is represented by the close relationship between the two members of the section *Datura* (*266*), *i.e*. *D*. *quercifolia* and *D*. *stramonium*, which share the occurrence of 12α-hydroxylated unmodified withanolides.

8.4. Genera with Uncertain Positions in the Solanaceae Taxonomic System

Some genera (*Jaborosa*, *Nicandra*, *Salpichroa*) contain withanolides with exclusive arrangements, which can be considered as chemotaxonomic markers at the generic level. *Jaborosa* is a good example since more than 50% of its species have been studied (Plate 4). In this genus, several peculiar modified skeletons of the

Plate 3. Solanaceae species of Tribe *Datureae*: (a) *Datura ferox*, plant; (b) *D. ferox*, fruit (photograph: F. Chiarini); (c) *D. inoxia*, plant (photograph: M.T. Cosa). Species of Tribe *Lycieae*: (d) *Lycium chinense*, flower; (e) *L. chinense*, fruits (photograph: B. Liu); (f) *L. barbarum*, branches with fruits (photograph: M. Li). Species of Tribe *Solaneae*: (g) *Solanum sisymbriifolium*, fruits; (h) *S. sisymbriifolium*, flowers (photographs: M.T. Cosa). Species of Tribe *Hyoscyameae*: (i) *Hyoscyamus niger*, flowering branch (photograph: B. Liu). Species not assigned to a tribe: (j) *Deprea* sp., Flower (photograph: S. Leiva); (k) *Exodeconus maritimus*, plant (photograph: E. Rodríguez R.); (l) *Salpichroa origanifolia*, flowering branch (photograph: G. Barboza)

Plate 4. *Jaborosa* spp.: (a) *J. rotacea*, plant; (b) *J. rotacea*, flower (photographs: F. Chiarini); (c) *J. leucotricha*, plant; (d) *J. leucotricha*, flowers (photographs: G. Barboza). (e) *J. sativa*, flowering branch (photograph: F. Chiarini); (f) *J. laciniata*, plant and flowers in detail; (g) *J. odonelliana*, flower (photographs: G. Barboza); (h) *J. caulescens*, flower (photograph: A.A. Cocucci); (i) *J. kurtzii*, flowers (photograph: G. Barboza); (j) *J. reflexa*, plant; (k) *J. reflexa*, flowers (photographs: G. Barboza); (l) *J. bergii*, fruits; (m) *J. bergii*, flower (photographs: A.A. Cocucci); (n) *J. magellanica*, plant (photograph: G. Barboza)

withanolides appear repeatedly in different species, such as the sativolides, trechonolides, spiranoid withanolides at C-22, and spiranoid-γ-lactones (Figs. 2 and 3).

The trechonolides, sativolides, and spiranoid withanolides at C-22 are exclusive to species in *Jaborosa* section *Lonchestigma*. The trechonolides are the most widespread in the genus, being present in nine species (*J. araucana*, *J. caulescens*, *J. laciniata*, *J. lanigera*, *J. leucotricha*, *J. magellanica*, *J. parviflora*, *J. rotacea*, and *J. sativa*); sativolides appear in *J. caulescens*, *J. rotacea*, and *J. sativa*, while the spiranoid withanolides at C-22 are only present in *J. kurtzii* and *J. rotacea*.

Spiranoid-γ-lactones have been isolated from *J. odonelliana*, *J. runcinata* and *J.integrifolia* (unpublished data), all belonging to *Jaborosa* sect. *Jaborosa*. Only one spiranoid-γ-lactone, jaborosalactone 2, was obtained from *J. araucana* (section *Lonchestigma*). As was stated in Sect. 5.4.3., the structural similarity of jaborosalactone 2 with trechonolide A, both present in *J. araucana*, suggests that these compounds may have a common biosynthetic precursor, and probably this species could be a link between section *Jaborosa* and section *Lonchestigma*.

Other distinctive variations with modified skeletons are the withanolides and related steroids with an aromatic ring D, the nicandrenoids isolated from *Nicandra*, and the salpichrolides from *Salpichroa* (Plate 3, l). Moreover, both genera exhibit the same δ-lactol side chain at C-17. In spite of this chemical similarity, *Nicandra* and *Salpichroa* are not phylogenetically close (*10*).

Nicandra has been suggested as being close to *Exodeconus* (*10*) (Plate 3, k). Although the withanolides isolated from *Exodeconus* have an unmodified skeleton and the major components of *Nicandra* have an aromatic ring D, all the withanolides found in both genera share the same 1-oxo-2-ene-5α-hydroxy-6α,7α-epoxy substitution pattern in rings A and B. In this case, the phytochemical evidence coincides with the phylogenetic proposal. *Salpichroa* and *Jaborosa* have traditionally been placed in tribe Jaboroseae (*9*). However, the phylogenetic evidence proposes *Salpichroa* in a clade informally named "Salpichroina", from which *Jaborosa* is excluded. Again, chemical information supports this proposal.

Despite the fragmentary chemical contribution described in this section of the chapter, it is evident that a large and species-rich study in Solanaceae in both molecular and phytochemical aspects would provide a better comprehension of the relationships among the species contained therein.

Acknowledgments We thank CONICET, Universidad de Buenos Aires and Universidad de Córdoba for financial support.

References

1. Lavie D, Glotter E, Shvo Y (1965) Constituents of *Withania somnifera* Dun. The Structure of Withaferin A. J Chem Soc: 7517
2. Kupchan SM, Doskotch RW, Bollinger P, MacPhail AT, Sim GA, Renauld JAS (1965) The Isolation and Structural Elucidation of a Novel Steroidal Tumor Inhibitor from *Acnistus arborescens*. J Am Chem Soc **87**: 5805

3. Ray AB, Gupta M (1994) Withasteroids, a Growing Group of Naturally Occurring Steroidal Lactones. Prog Chem Org Nat Prod **63**: 1
4. Anjaneyulu ASR, Rao DS, Lequesne PW (1998) Withanolides, Biologically Active Natural Steroidal Lactones: A Review. Stud Nat Prod Chem **20**: 135
5. Veleiro AS, Oberti JC, Burton G (2005) Chemistry and Bioactivity of Withanolides from South American Solanaceae. Stud Nat Prod Chem **32**: 1019
6. Su B-N, Gu J-Q, Kang Y-H, Park E-J, Pezzuto JM, Kinghorn AD (2004) Induction of the Phase II Enzyme, Quinone Reductase, by Withanolides and Norwithanolides from Solanaceous Species. Mini-Rev Org Chem **1**: 115
7. Budhiraja RD, Krishan P, Sudhir S (2000) Biological Activity of Withanolides. J Sci Ind Res **59**: 904
8. D'Arcy WG (1991) Solanaceae III. Taxonomy, Chemistry, Evolution. Royal Botanic Gardens, Kew. In: Hawkes JG, Lester RN, Nee M, Estrada N (eds): The Solanaceae since 1976, with a Review of Its Biogeography. Royal Botanic Gardens, Kew, U.K., p 75
9. Hunziker AT (2001) Genera Solanacearum. The Genera of Solanaceae Illustrated, Arranged According to a New System, Koeltz Scientific Books, Konigstein, Germany
10. Olmstead RG, Bohs L, Abdel Migid H, Santiago-Valentín E, García VF, Collier SM (2008) A Molecular Phylogeny of the Solanaceae. Taxon **57**: 1159
11. Choudhary MI, Yousuf S, Nawaz SA, Ahmed S, Atta-ur-Rahman (2004) Cholinesterase Inhibiting Withanolides from *Withania somnifera*. Chem Pharm Bull **52**: 1358
12. Misra L, Lal P, Sangwan RS, Sangwan NS, Uniyal GC, Tuli R (2005) Unusually Sulfated and Oxygenated Steroids from *Withania somnifera*. Phytochemistry **66**: 2702
13. Benjumea D, Martin-Herrera D, Abdala S, Gutierrez-Luis J, Quinones W, Cardona D, Torres F, Echeverri F (2009) Withanolides from *Withania aristata* and Their Diuretic Activity. J Ethnopharmacol **123**: 351
14. Choudhary MI, Abbas S, Jamal SA, Atta-ur-Rahman (1996) *Withania somnifera* - a Source of Exotic Withanolides. Heterocycles **42**: 555
15. Jayaprakasam B, Nair MG (2003) Cyclooxygenase-2 Enzyme Inhibitory Withanolides from *Withania somnifera* Leaves. Tetrahedron **59**: 841
16. March J (1992): Advanced Organic Chemistry Reactions, Mechanisms, and Structure. John Wiley & Sons, New York, p 755
17. Atta-ur-Rahman, Yousaf M, Gul W, Qureshi S, Choudhary MI, Voelter W, Hoff A, Jens F, Naz A (1998) Five New Withanolides from *Withania coagulans*. Heterocycles **48**: 1801
18. Nur-e-Alam M, Yousaf M, Qureshi S, Baig I, Nasim S, Atta-ur-Rahman, Choudhary MI (2003) A Novel Dimeric Podophyllotoxin-Type Lignan and a New Withanolide from *Withania coagulans*. Helv Chim Acta **86**: 607
19. Kuroyanagi M, Shibata K, Umehara K (1999) Cell Differentiation Inducing Steroids from *Withania somnifera* L. (Dun.). Chem Pharm Bull **47**: 1646
20. Abou-Douh AM (2002) New Withanolides and Other Constituents from the Fruit of *Withania somnifera*. Arch Pharm **335**: 267
21. Zhao J, Nakamura N, Hattori M, Kuboyama T, Tohda C, Komatsu K (2002) Withanolide Derivatives from the Roots of *Withania somnifera* and Their Neurite Outgrowth Activities. Chem Pharm Bull **50**: 760
22. Sahai M, Ali A, Ray AB, Slatkin DJ, Kirson I (1983) Withaperuvin D, a Novel Withanolide from *Physalis peruviana*. J Chem Res (S): 152
23. Neogi P, Sahai M, Ray AB (1987) Withaperuvins F and G, Two Withanolides of *Physalis peruviana* Roots. Phytochemistry **26**: 243
24. Anjaneyulu ASR, Rao DS (1997) New Withanolides from the Roots of *Withania somnifera*. Indian J Chem B **36**: 424
25. Lal P, Misra L, Sangwan RS, Tuli R (2006) New Withanolides from Fresh Berries of *Withania somnifera*. Z Naturforsch, B: Chem Sci **61**: 1143
26. Misra L, Mishra P, Pandey A, Sangwan RS, Sangwan NS, Tuli R (2008) Withanolides from *Withania somnifera* Roots. Phytochemistry **69**: 1000

27. Matsuda H, Murakami T, Kishi A, Yoshikawa M (2001) Structures of Withanosides I, II, III, IV, V, VI, and VII, New Withanolide Glycosides, from the Roots of Indian *Withania somnifera* Dunal. and Inhibitory Activity for Tachyphylaxis to Clonidine in Isolated Guinea-Pig Ileum. Bioorg Med Chem **9**: 1499
28. Pramanick S, Roy A, Ghosh S, Majumder HK, Mukhopadhyay S (2008) Withanolide Z, a New Chlorinated Withanolide from *Withania somnifera*. Planta Med **74**: 1745
29. Jayaprakasam B, Strasburg GA, Nair MG (2004) Potent Lipid Peroxidation Inhibitors from *Withania somnifera* Fruits. Tetrahedron **60**: 3109
30. Atta-ur-Rahman, Shabbir M, Yousaf M, Qureshi S, Dur-e-Shahwar, Naz A, Choudhary MI (1999) Three Withanolides from *Withania coagulans*. Phytochemistry **52**: 1361
31. Abdeljebbar LH, Humam M, Christen P, Jeannerat D, Vitorge B, Amzazi S, Benjouad A, Hostettmann K, Bekkouche K (2007) Withanolides from *Withania adpressa*. Helv Chim Acta **90**: 346
32. Maurya R, Akanksha, Jayendra, Singh AB, Srivastava AK (2008) Coagulanolide, a Withanolide from *Withania coagulans* Fruits and Antihyperglycemic Activity. Bioorg Med Chem Lett **18**: 6534
33. Vande Velde V, Lavie D (1981) New Withanolides of Biogenetic Interest from *Withania somnifera*. Phytochemistry **20**: 1359
34. Atta-ur-Rahman, Dur-e-Shahwar, Naz A, Choudhary MI (2003) Withanolides from *Withania coagulans*. Phytochemistry **63**: 387
35. Huang C-F, Ma L, Sun L-J, Ali M, Arfan M, Liu J-W, Hu L-H (2009) Immunosuppressive Withanolides from *Withania coagulans*. Chem Biodivers **6**: 1415
36. Choudhary MI, Dur-e-Shahwar, Parveen Z, Jabbar A, Ali I (1995) Antifungal Steroidal Lactones from *Withania coagulance*. Phytochemistry **40**: 1243
37. Jahan E, Perveen S, Fatima I, Malik A (2010) Coagulansins A and B, New Withanolides from *Withania coagulans* Dunal. Helv Chim Acta **93**: 530
38. Atta-ur-Rahman, Choudhary MI, Yousaf M, Gul W, Qureshi S (1998) New Withanolides from *Withania coagulans*. Chem Pharm Bull **46**: 1853
39. Kumar A, Ali M, Mir SR (2004) A New Withanolide from the Roots of *Withania somnifera*. Indian J Chem, Sect B **43B**: 2001
40. Atta-ur-Rahman, Abbas S, Dur-e-Shahwar, Jamal SA, Choudhary MI (1993) New Withanolides from *Withania* sp. J Nat Prod **56**: 1000
41. Atta-ur-Rahman,, Shabbir M, Dur-e-Shahwar, Choudhary MI, Voelter W, Hohnholz D (1998) New Steroidal Lactones from *Withania coagulance*. Heterocycles **47**: 1005
42. Atta-ur-Rahman, Choudhary MI, Qureshi S, Gul W, Yousaf M (1998) Two New Ergostane-Type Steroidal Lactones from *Withania coagulans*. J Nat Prod **61**: 812
43. Ahmad S, Malik A, Muhammad P, Gul W, Yasmin R, Afza N (1998) A New Withanolide from *Physalis peruviana*. Fitoterapia **69**: 433
44. Ahmad S, Malik A, Afza N, Yasmin R (1999) A New Withanolide Glycoside from *Physalis peruviana*. J Nat Prod **62**: 493
45. Khan PM, Ahmad S, Rubnawaz H, Malik A (1999) The First Report of a Withanolide from the Family Labiatae. Phytochemistry **51**: 669
46. Ali M, Shuaib M, Ansari SH (1997) Withanolides from the Stem Bark of *Withania somnifera*. Phytochemistry **44**: 1163
47. Subbaraju GV, Vanisree M, Rao CV, Sivaramakrishna C, Sridhar P, Jayaprakasam B, Nair MG (2006) Ashwagandhanolide, a Bioactive Dimeric Thiowithanolide Isolated from the Roots of *Withania somnifera*. J Nat Prod **69**: 1790
48. Mulabagal V, Subbaraju GV, Rao CV, Sivaramakrishna C, DeWitt DL, Holmes D, Sung B, Aggarwal BB, Tsay H-S, Nair M (2009) Withanolide Sulfoxide from Ahswagandha Roots Inhibits Nuclear Transcription Factor-Kappa-B, Cyclooxygenase and Tumor Cell Proliferation. Phytother Res **23**: 987
49. Xu Y-m, Marron MT, Seddon E, McLaughlin SP, Ray DT, Whitesell L, Gunatilaka AAL (2009) 2,3-Dihydrowithaferin A-3β-*O*-Sulfate, a New Potential Prodrug of Withaferin A from Aeroponically Grown *Withania somnifera*. Bioorg Med Chem **17**: 2210

50. Lan Y-H, Chang F-R, Pan M-J, Wu C-C, Wu S-J, Chen S-L, Wang S-S, Wu M-J, Wu Y-C (2009) New Cytotoxic Withanolides from *Physalis peruviana*. Food Chem **116**: 462
51. Dinan LN, Sarker SD, Sik V (1997) 28-Hydroxywithanolide E from *Physalis peruviana*. Phytochemistry **44**: 509
52. Ahmad S, Malik A, Yasmin R, Ullah N, Gul W, Khan PM, Nawaz HR, Afza N (1999) Withanolides from *Physalis peruviana*. Phytochemistry **50**: 647
53. Ahmad S, Yasmin R, Malik A (1999) New Withanolide Glycosides from *Physalis peruviana* L. Chem Pharm Bull **47**: 477
54. Maldonado E, Alvarado VE, Torres FR, Martinez M, Perez-Castorena AL (2005) Androstane and Withanolides from *Physalis cinerascens*. Planta Med **71**: 548
55. Damu AG, Kuo P-C, Su C-R, Kuo T-H, Chen T-H, Bastow KF, Lee K-H, Wu T-S (2007) Isolation, Structures, and Structure-Cytotoxic Activity Relationships of Withanolides and Physalins from *Physalis angulata*. J Nat Prod **70**: 1146
56. Lee S-W, Pan M-H, Chen C-M, Chen Z-T (2008) Withangulatin I, a New Cytotoxic Withanolide from *Physalis angulata*. Chem Pharm Bull **56**: 234
57. Abe F, Nagafuji S, Okawa M, Kinjo J (2006) Trypanocidal Constituents in Plants 6. Minor. Withanolides from the Aerial Parts of *Physalis angulata*. Chem Pharm Bull **54**: 1226
58. He Q-P, Ma L, Luo J-Y, He F-Y, Lou L-G, Hu L-H (2007) Cytotoxic Withanolides from *Physalis angulata* L. Chem Biodivers **4**: 443
59. Glotter E (1991) Withanolides and Related Ergostane-Type Steroids. Nat Prod Rep **8**: 415
60. Choudhary MI, Yousaf S, Ahmed S, Samreen, Yasmeen K, Atta-ur-Rahman (2005) Antileishmanial Physalins from *Physalis minima*. Chem Biodivers **2**: 1164
61. Nawaz HR, Riaz M, Malik A, Khan PM, Ullah N (2000) Withanolides and Alkaloid from *Ajuga parviflora*. J Chem Soc Pak **22**: 138
62. Khan PM, Malik A, Ahmad S, Nawaz HR (1999) Withanolides from *Ajuga parviflora*. J Nat Prod **62**: 1290
63. Khan PM, Nawaz HR, Ahmad S, Malik A (1999) Ajugins C and D, New Withanolides from *Ajuga parviflora*. Helv Chim Acta **82**: 1423
64. Nawaz HR, Malik A, Khan PM, Ahmed S (1999) Ajugins E and F: Two Withanolides from *Ajuga parviflora*. Phytochemistry **52**: 1357
65. Nawaz HR, Malik A, Muhammad P, Ahmed S, Riaz M (2000) Chemical Constituents of *Ajuga parviflora*. Z Naturforsch, B: Chem Sci **55**: 100
66. Nagafuji S, Okabe H, Akahane H, Abe F (2004) Trypanocidal Constituents in Plants 4. Withanolides from the Aerial Parts of *Physalis angulata*. Biol Pharm Bull **27**: 193
67. Li Y-Z, Pan Y-M, Huang X-Y, Wang H-S (2008) Withanolides from *Physalis alkekengi* var. *francheti*. Helv Chim Acta **91**: 2284
68. Misico RI, Veleiro AS, Burton G, Oberti JC (1997) Withanolides from *Jaborosa leucotricha*. Phytochemistry **45**: 1045
69. Nicotra VE, Gil RR, Vaccarini C, Oberti JC, Burton G (2003) 15,21-Cyclowithanolides from *Jaborosa bergii*. J Nat Prod **66**: 1471
70. Misico RI, Gil RR, Oberti JC, Veleiro AS, Burton G (2000) Withanolides from *Vassobia lorentzii*. J Nat Prod **63**: 1329
71. Silva GL, Burton G, Oberti JC (1999) 18,20-Hemiacetal-Type and Other Withanolides from *Dunalia brachyacantha*. J Nat Prod **62**: 949
72. Alfonso D, Kapetanidis I (1994) Withanolides from *Iochroma gesnerioides*. Phytochemistry **36**: 179
73. Maldonado E, Torres FR, Martínez M, Pérez-Castorena AL (2004) 18-Acetoxywithanolides from *Physalis chenopodifolia*. Planta Med **70**: 59
74. Perez-Castorena A-L, Oropeza RF, Vazquez AR, Martinez M, Maldonado E (2006) Labdanes and Withanolides from *Physalis coztomatl*. J Nat Prod **69**: 1029
75. Carcamo C, Fajardo V (1993) (−)-Jaboromagellonine: New Withanolide from Seeds of *Jaborosa magellanica*. Heterocycles **36**: 1771
76. Ramacciotti NS, Nicotra VE (2007) Withanolides from *Jaborosa kurtzii*. J Nat Prod **70**: 1513

77. Cirigliano A, Veleiro AS, Oberti JC, Burton G (1995) A 15β-Hydroxywithanolide from *Datura ferox*. Phytochemistry **40**: 611
78. Veleiro AS, Cirigliano AM, Oberti JC, Burton G (1999) 7-Hydroxywithanolides from *Datura ferox*. J Nat Prod **62**: 1010
79. Yang B, Wang Q, Xia Y, Feng W, Kuang H (2007) Withanolide Compounds from the Flower of *Datura metel* L. Helv Chim Acta **90**: 1522
80. Kuang H, Yang B, Tang L, Xia Y, Dou D (2009) Baimantuoluosides A - C, Three New Withanolide Glucosides from the Flower of *Datura metel* L. Helv Chim Acta **92**: 1315
81. Bhat BA, Dhar KL, Puri SC, Qurishi MA, Khajuria A, Gupta A, Qazi GN (2005) Isolation, Characterization and Biological Evaluation of *Datura* Lactones as Potential Immunomodulators. Bioorg Med Chem **13**: 6672
82. Wube AA, Wenzig E-M, Gibbons S, Asres K, Bauer R, Bucar F (2008) Constituents of the Stem Bark of *Discopodium penninervium* and Their LTB_4 and COX-1 and −2 Inhibitory Activities. Phytochemistry **69**: 982
83. Cordero CP, Morantes SJ, Páez A, Rincón J, Aristizábal FA (2009) Cytotoxicity of Withanolides Isolated from *Acnistus arborescens*. Fitoterapia **80**: 364
84. Bravo B JA, Sauvain M, Gimenez T A, Balanza E, Serani L, Laprevote O, Massiot G, Lavaud C (2001) Trypanocidal Withanolides and Withanolide Glycosides from *Dunalia brachyacantha*. J Nat Prod **64**: 720
85. Lischewski M, Nguyen Thi Bich H, Porzel A, Adam G, Massiot G, Lavaud C (1992) Withanolide Glycosides from *Dunalia australis*. Phytochemistry **31**: 939
86. Yokosuka A, Mimaki Y, Sashida Y (2003) Chantriolides A and B, Two New Withanolide Glucosides from the Rhizomes of *Tacca chantrieri*. J Nat Prod **66**: 876
87. Liu H-Y, Ni W, Xie B-B, Zhou L-Y, Hao X-J, Wang X, Chen C-X (2006) Five New Withanolides from *Tacca plantaginea*. Chem Pharm Bull **54**: 992
88. Yokosuka A, Mimaki Y (2007) New Glycosides from the Rhizomes of *Tacca chantrieri*. Chem Pharm Bull **55**: 273
89. Manickam M, Awasthi SB, Oshima Y, Hisamichi K, Takeshita M, Sahai M, Ray AB (1994) Additional C-21-Oxygenated Withanolides from *Datura fastuosa*. J Chem Res (S): 306
90. Manickam M, Srivastava A, Ray AB (1998) Withanolides from the Flowers of *Datura fastuosa*. Phytochemistry **47**: 1427
91. Manickam M, Kumar S, Sinha-Bagchi A, Sinha SC, Ray AB (1994) Withametelin H and Withafastuosin C, Two New Withanolides from the Leaves of *Datura* Species. J Indian Chem Soc **71**: 393
92. Pan Y, Wang X, Hu X (2007) Cytotoxic Withanolides from the Flowers of *Datura metel*. J Nat Prod **70**: 1127
93. Yang B, Wang Q, Xia Y, Feng W, Kuang H (2008) Baimantuoluolines D-F, Three New Withanolides from the Flower of *Datura metel* L. Helv Chim Acta **91**: 964
94. Manickam M, Awasthi SB, Sinha-Bagchi A, Sinha SC, Ray AB (1996) Withanolides from *Datura tatula*. Phytochemistry **41**: 981
95. Srivastava A, Manickam M, Sinha-Bagchia A, Sinhaa SC, Ray AB (1996) Withasteroids. 28. Novel Withanolides from the Flowers of *Datura tatula*. Nat Prod Sci **2**: 9
96. Manickam M, Ray AB (1996) Structure of Withatatulin E, a Minor Withanolide of *Datura tatula*. Indian J Chem, Sect B **35B**: 1311
97. Gil RR, Misico RI, Sotes IR, Oberti JC, Veleiro AS, Burton G (1997) 16-Hydroxylated Withanolides from *Exodeconus maritimus*. J Nat Prod **60**: 568
98. Minguzzi S, Barata LES, Shin YG, Jonas PF, Chai H-B, Park EJ, Pezzuto JM, Cordell GA (2002) Cytotoxic Withanolides from *Acnistus arborescens*. Phytochemistry **59**: 635
99. Ma C-Y, Williams ID, Che C-T (1999) Withanolides from *Hyoscyamus niger* Seeds. J Nat Prod **62**: 1445
100. Habtemariam S, Gray AI, Waterman PG (1993) 16-Oxygenated Withanolides from the Leaves of *Discopodium penninervium*. Phytochemistry **34**: 807
101. Maldonado E, Amador S, Martinez M, Perez-Castorena AL (2010) Virginols A-C, Three New Withanolides from *Physalis virginiana*. Steroids **75**: 346

102. Habtemariam S, Gray AI (1998) Withanolides from the Roots of *Discopodium penninervium*. Planta Med **64**: 275
103. Kennelly EJ, Gerhaeuser C, Song LL, Graham JG, Beecher CWW, Pezzuto JM, Kinghorn AD (1997) Induction of Quinone Reductase by Withanolides Isolated from *Physalis philadelphica* (Tomatillos). J Agric Food Chem **45**: 3771
104. Su B-N, Misico RI, Park EJ, Santarsiero BD, Mesecar AD, Fong HHS, Pezzuto JM, Kinghorn AD (2002) Isolation and Characterization of Bioactive Principles of the Leaves and Stems of *Physalis philadelphica*. Tetrahedron **58**: 3453
105. Gu J-Q, Li W, Kang Y-H, Su B-N, Fong HHS, van Breemen RB, Pezzuto JM, Kinghorn AD (2003) Minor Withanolides from *Physalis philadelphica*: Structures, Quinone Reductase Induction Activities, and Liquid Chromatography (LC)-MS-MS Investigation as Artifacts. Chem Pharm Bull **51**: 530
106. Cardona D, Quinones W, Torres F, Velez ID, Orozco-P CI, Garzon J, Echeverri F (2005) Structure and Leishmanicidal Activity of Larnaxolide A and B, New Withanolides from *Larnax glabra* (Standl.) Sawyer. Actual Biol (Medellin, Colomb) **27**: 81
107. Hsieh P-W, Huang Z-Y, Chen J-H, Chang F-R, Wu C-C, Yang Y-L, Chiang MY, Yen M-H, Chen S-L, Yen H-F, Luebken T, Hung W-C, Wu Y-C (2007) Cytotoxic Withanolides from *Tubocapsicum anomalum*. J Nat Prod **70**: 747
108. Riaz N, Malik A, Nawaz SA, Muhammad P, Choudhary MI (2004) Cholinesterase-Inhibiting Withanolides from *Ajuga bracteosa*. Chem Biodivers **1**: 1289
109. Ma L, Xie C-M, Li J, Lou F-C, Hu L-H (2006) Daturametelins H, I, and J: 3 New Withanolide Glycosides from *Datura metel* L. Chem Biodivers **3**: 180
110. Zhu XH, Takagi M, Ikeda T, Midzuki K, Nohara T (2001) Withanolide-Type Steroids from *Solanum cilistum*. Phytochemistry **56**: 741
111. Zhu X-H, Ando J, Takagi M, Ikeda T, Nohara T (2001) Six New Withanolide-Type Steroids from the Leaves of *Solanum cilistum*. Chem Pharm Bull **49**: 161
112. Zhu X-H, Ando J, Takagi M, Ikeda T, Yoshimitsu A, Nohara T (2001) Four Novel Withanolide-Type Steroids from the Leaves of *Solanum cilistum*. Chem Pharm Bull **49**: 1440
113. Niero R, Da Silva IT, Tonial GC, Camacho BDS, Gacs-Baitz E, Delle Monache G, Delle Monache F (2006) Cilistepoxide and Cilistadiol, 2 New Withanolides from *Solanum sisymbiifolium*. Nat Prod Res Part A **20**: 1164
114. Vankar PS, Srivastava J, Molcanov K, Kojic-Prodic B (2009) Withanolide A Series Steroidal Lactones from *Eucalyptus globulus* Bark. Phytochemistry Lett **2**: 67
115. Siddiqui BS, Afreen S, Begum S (1999) Two New Withanolides from the Aerial Parts of *Datura innoxia*. Aust J Chem **52**: 905
116. Siddiqui BS, Hashmi IA, Begum S (2002) Two New Withanolides from the Aerial Parts of *Datura innoxia*. Heterocycles **57**: 715
117. Siddiqui BS, Arfeen S, Afshan F, Begum S (2005) Withanolides from *Datura innoxia*. Heterocycles **65**: 857
118. Siddiqui BS, Arfeen S, Begum S, Sattar FA (2005) Daturacin, a New Withanolide from *Datura innoxia*. Nat Prod Res **19**: 619
119. Bonetto GM, Gil RR, Oberti JC, Veleiro AS, Burton G (1995) Novel Withanolides from *Jaborosa sativa*. J Nat Prod **58**: 705
120. Nicotra VE, Ramacciotti NS, Gil RR, Oberti JC, Feresin GE, Guerrero CA, Baggio RF, Garland MT, Burton G (2006) Phytotoxic Withanolides from *Jaborosa rotacea*. J Nat Prod **69**: 783
121. Nicotra VE, Gil RR, Oberti JC, Burton G (2007) Withanolides with Phytotoxic Activity from *Jaborosa caulescens* var. *caulescens* and *J. caulescens* var. *bipinnatifida*. J Nat Prod **70**: 808
122. Usubillaga A, de Castellano G, Zabel V, Watson WH (1980) Acnistins, a New Class of Steroidal Lactones from *Acnistus ramiflorum* Miers, X-Ray Structure of Acnistin E. J Chem Soc, Chem Commun: 854

123. Luis JG, Echeverri F, Quiñones W, González AG, Torres F, Cardona G, Archbold R, Rojas M, Perales A (1994) Unambiguous ^{13}C NMR Assignment of Acnistins and Absolute Configuration of Acnistin A. Steroids **59**: 299
124. Luis JG, Echeverri F, García F, Rojas M (1994) The Structure of Acnistin B and the Immunosuppressive Effects of Acnistins A, B, and E. Planta Med **60**: 348
125. Luis JG, Echeverri F, Gonzalez AG (1994) Acnistins C and D, Withanolides from *Dunalia solanacea*. Phytochemistry **36**: 1297
126. Luis JG, Echeverri F, Gonzalez AG (1994) Acnistins F-H, Withanolides from *Dunalia solanacea*. Phytochemistry **36**: 769
127. Habtemariam S, Skelton BW, Waterman PG, White AH (2000) 17-Epiacnistin-A, a Further Withanolide from the Leaves of *Discopodium penninervium*. J Nat Prod **63**: 512
128. Kiyota N, Shingu K, Yamaguchi K, Yoshitake Y, Harano K, Yoshimitsu H, Ikeda T, Nohara T (2007) New C28 Steroidal Glycosides from *Tubocapsicum anomalum*. Chem Pharm Bull **55**: 34
129. Luis JG, Echeverri F, Quinones W, Gonzalez AG, Torres F, Cardona G, Archbold R, Perales A (1994) Withajardins, Withanolides with a New Type of Skeleton Structure of Withajardins A, B, C and D. Absolute Configuration of Withajardin C. Tetrahedron **50**: 1217
130. Echeverri F, Quinones W, Forres F, Cardona G, Archbold R, Luis JG, Gonzalez AG (1995) Withajardin E, a Withanolide from *Deprea orinocensis*. Phytochemistry **40**: 923
131. Kiyota N, Shingu K, Yamaguchi K, Yoshitake Y, Harano K, Yoshimitsu H, Miyashita H, Ikeda T, Tagawa C, Nohara T (2008) New C28 Steroidal Glycosides from *Tubocapsicum anomalum*. Chem Pharm Bull **56**: 1038
132. Glotter E, Abraham A, Guenzberg G, Kirson I (1977) Naturally Occurring Steroidal Lactones with a 17α-Oriented Side Chain. Structure of Withanolide E and Related Compounds. J Chem Soc, Perkin Trans 1: 341
133. Tomassini TCB, Barbi NS, Ribeiro IM, Xavier DCD (2000) Genero *Physalis* - Uma Revisao Sobre Vitaesteroides. Quim Nova **23**: 47
134. Fang L, Chai H-B, Castillo JJ, Soejarto DD, Farnsworth NR, Cordell GA, Pezzuto JM, Kinghorn AD (2003) Cytotoxic Constituents of *Brachistus stramoniifolius*. Phytother Res **17**: 520
135. Karikas GA, Gupta MP, Ravelo AG, Gonzales AG (1998) Physalin B from *Witheringia hunzikeri*. Fitoterapia **69**: 468
136. Pérez-Castorena AL, García M, Martínez M, Maldonado E (2004) Physalins from *Physalis solanaceus*. Biochem Syst Ecol **32**: 1231
137. Ripperger H, Kamperdick C (1998) First Isolation of Physalins from the Genus *Saracha* of Solanaceae. Pharmazie **53**: 144
138. Jacobo-Herrera NJ, Bremner P, Marquez N, Gupta MP, Gibbons S, Munoz E, Heinrich M (2006) Physalins from *Witheringia solanacea* as Modulators of the NF-κB Cascade. J Nat Prod **69**: 328
139. Qiu L, Zhao F, Jiang Z-H, Chen L-X, Zhao Q, Liu H-X, Yao X-S, Qiu F (2008) Steroids and Flavonoids from *Physalis alkekengi* var. *franchetii* and Their Inhibitory Effects on Nitric Oxide Production. J Nat Prod **71**: 642
140. Sunayama R, Kuroyanagi M, Umehara K, Ueno A (1993) Physalin and Neophysalins from *Physalis alkekengi* var. *francheti* and Their Differentiation Inducing Activity. Phytochemistry **34**: 529
141. Qiu L, Jiang Z-H, Liu H-X, Chen L-X, Yao X-S, Qiu F (2008) A Pair of 3-Epimeric Physalins from *Physalis alkekengi* L. var. *franchetii*. J Asian Nat Prod Res **10**: 881
142. Makino B, Kawai M, Kito K, Yamamura H, Butsugan Y (1995) New Physalins Possessing an Additional Carbon-Carbon Bond from *Physalis alkekengi* var. *francheti*. Tetrahedron **51**: 12529
143. Kawai M, Yamamoto T, Makino B, Yamamura H, Araki S, Butsugan Y, Saito K (2001) The Structure of Physalin T from *Physalis alkekengi* var. *francheti*. J Asian Nat Prod Res **3**: 199

144. Makino B, Kawai M, Iwata Y, Yamamura H, Butsugan Y, Ogawa K, Hayashi M (1995) Physalins Possessing an Endoperoxy Structure from *Physalis alkekengi* var. *francheti*. Structural Revision of Physalin K. Bull Chem Soc Jpn **68**: 219
145. Choudhary MI, Yousuf S, Samreen, Ahmed S, Atta-ur-Rahman (2007) New Leishmanicidal Physalins from *Physalis minima*. Nat Prod Res **21**: 877
146. Kuo P-C, Kuo T-H, Damu AG, Su C-R, Lee E-J, Wu T-S, Shu R, Chen C-M, Bastow KF, Chen T-H, Lee K-H (2006) Physanolide A, a Novel Skeleton Steroid, and Other Cytotoxic Principles from *Physalis angulata*. Org Lett **8**: 2953
147. Chen R, Liang J-Y, Liu R (2007) Two Novel Neophysalins from *Physalis alkekengi* L. var. *franchetii*. Helv Chim Acta **90**: 963
148. Makino B, Kawai M, Ogura T, Nakanishi M, Yamamura H, Butsugan Y (1995) Structural Revision of Physalin H Isolated from *Physalis angulata*. J Nat Prod **58**: 1668
149. Chen R, Liang JY, Yang Y, Liu R (2007) Chemical Constituents from *Physalis alkekengi* and Structural Revision of Physalin G. Chin J Nat Med **5**: 186
150. Sen G, Pathak HD (1995) Physalin L, a 13,14-Seco-16,24 Cyclosteroid from *Physalis minima*. Phytochemistry **39**: 1245
151. Kawai M, Makino B, Yamamura H, Butsugan Y (1996) Upon "Physalin L" Isolated from *Physalis minima*. Phytochemistry **43**: 661
152. Veras ML, Bezerra MZB, Braz-Filho R, Pessoa ODL, Montenegro RC, Do Ó Pessoa C, De Moraes MO, Costa-Lotufo LV (2004) Cytotoxic Epimeric Withaphysalins from Leaves of *Acnistus arborescens*. Planta Med **70**: 551
153. Veras ML, Bezerra MZB, Lemos TLG, Uchoa DEDA, Braz-Filho R, Chai HB, Cordell GA, Pessoa ODL (2004) Cytotoxic Withaphysalins from the Leaves of *Acnistus arborescens*. J Nat Prod **67**: 710
154. Ma L, Gan X-W, He Q-P, Bai H-Y, Arfan M, Lou F-C, Hu L-H (2007) Cytotoxic Withaphysalins from *Physalis minima*. Helv Chim Acta **90**: 1406
155. Sahai M, Kirson I (1984) Withaphysalin D, a New Withaphysalin from *Physalis minima* Linn. var. *indica*. J Nat Prod **47**: 527
156. Veleiro AS, Oberti JC, Burton G (1992) A Ring D Aromatic Withanolide from *Salpichroa origanifolia*. Phytochemistry **31**: 935
157. Veleiro AS, Burton G, Bonetto GM, Gil RR, Oberti JC (1994) New Withanolides from *Salpichroa origanifolia*. J Nat Prod **57**: 1741
158. Tettamanzi MC, Veleiro AS, Oberti JC, Burton G (1998) New Hydroxylated Withanolides from *Salpichroa origanifolia*. J Nat Prod **61**: 338
159. Tettamanzi MC, Veleiro AS, de la Fuente JR, Burton G (2001) Withanolides from *Salpichroa origanifolia*. J Nat Prod **64**: 783
160. Tettamanzi MC, Veleiro AS, Oberti JC, Burton G (1996) Ring D Aromatic Ergostane Derivatives from *Salpichroa origanifolia*. Phytochemistry **43**: 461
161. Gill HK, Smith RW, Whiting DA (1990) Ring D Expansion and Aromatisation in the Biosynthesis of Nic-1, an Antifeedant Steroid from *Nicandra physaloides*. J Chem Soc, Perkin Trans 1: 2989
162. Monteagudo ES, Burton G, Gros EG, Gonzalez CM, Oberti JC (1989) A 19-Hydroxywithanolide from *Jaborosa leucotricha*. Phytochemistry **28**: 1514
163. Misico RI, Oberti JC, Veleiro AS, Burton G (1996) New 19-Hydroxywithanolides from *Jaborosa leucotricha*. J Nat Prod **59**: 66
164. Veleiro AS, Trocca CE, Burton G, Oberti JC (1992) A Phenolic Withanolide from *Jaborosa leucotricha*. Phytochemistry **31**: 2550
165. Kirson IA, Cohen M, Greenberg M, Gottlieb HE, Varenne P, Abraham A (1979) Ixocarpalactone A and B. Two Unusual Naturally Occurring Steroids of the Ergostane Type. J Chem Res (S): 103
166. Huang Y, Müehlbauer A, Henkel T, Liu J-K (2003) Two New Taccalonolides from Tropic Plant *Tacca subflaellata*. Chin Chem Lett **14**: 68
167. Huang Y, Liu J-K, Mühlbauer A, Henkel T (2002) Three Novel Taccalonolides from the Tropical Plant *Tacca subflaellata*. Helv Chim Acta **85**: 2553

168. Fang S-T, Li B, Liu J-K (2009) Two New Withanolides from *Physalis peruviana*. Helv Chim Acta **92**: 1304
169. Lavie D, Besalle R, Pestchanker MJ, Gottlieb HE, Frolow F, Giordano OS (1987) Trechonolide A, a New Withanolide Type from *Trechonaetes laciniata*. Phytochemistry **26**: 1791
170. Parvez M, Fajardo V, Shamma M (1988) (+)-Jaborosalactone M, a Hemiketal Withanolide from *Jaborosa magellanica*. Acta Crystallogr, Sect C: Cryst Struct Commun **44**: 553
171. Cirigliano AM, Veleiro AS, Misico RI, Tettamanzi MC, Oberti JC, Burton G (2007) Withanolides from *Jaborosa laciniata*. J Nat Prod **70**: 1644
172. Pecci A, Alvarez LD, Veleiro AS, Ceballos NR, Lantos CP, Burton G (2009) New Lead Compounds in the Search for Pure Antiglucocorticoids and the Dissociation of Antiglucocorticoid Effects. J Steroid Biochem Mol Biol **113**: 155
173. Baggio RF (2005). Personal communication
174. Garcia ME, S. P, Navarro-Vázquez A, Phillips DD, Gayathri C, Krakauer H, Stephens PW, Nicotra VE, Gil RR (2009) Stereochemistry Determination by Powder X-Ray Diffraction Analysis and NMR Spectroscopy Residual Dipolar Couplings. Angew Chem Int Ed **48**: 5670
175. Tettamanzi MC, Biurrun FN, Cirigliano AM (2007) A New Antifeedant Withanolide from *Jaborosa lanigera*. Z Naturforsch, B: Chem Sci **62**: 573
176. Monteagudo ES, Oberti JC, Gros EG, Burton G (1990) A Spiranic Withanolide from *Jaborosa odonelliana*. Phytochemistry **29**: 933
177. Cirigliano AM, Veleiro AS, Oberti JC, Burton G (2002) Spiranoid Withanolides from *Jaborosa odonelliana*. J Nat Prod **65**: 1049
178. Cirigliano AM, Misico RI (2005) Spiranoid Withanolides from *Jaborosa odonelliana* and *Jaborosa runcinata*. Z Naturforsch, B: Chem Sci **60**: 867
179. Cirigliano AM, Veleiro AS, Bonetto GM, Oberti JC, Burton G (1996) Spiranoid Withanolides from *Jaborosa runcinata* and *Jaborosa araucana*. J Nat Prod **59**: 717
180. Shen J, Chen Z, Gao Y (1996) Taccalonolides from *Tacca plantaginea*. Phytochemistry **42**: 891
181. Chen Z-l, Shen J-h, Gao Y-s, Wichtl M (1997) Five Taccalonolides from *Tacca plantaginea*. Planta Med **63**: 40
182. Yang J-Y, Zhao R-H, Chen C-X, Ni W, Teng F, Hao X-J, Liu H-Y (2008) Taccalonolides W - Y, Three New Pentacyclic Steroids from *Tacca plantaginea*. Helv Chim Acta **91**: 1077
183. Mühlbauer A, Seip S, Nowak A, Tran VS (2003) Five Novel Taccalonolides from the Roots of the Vietnamese Plant *Tacca paxiana*. Helv Chim Acta **86**: 2065
184. Su B-N, Park EJ, Nikolic D, Santarsiero BD, Mesecar AD, Vigo JS, Graham JG, Cabieses F, van Breemen RB, Fong HHS, Farnsworth NR, Pezzuto JM, Kinghorn AD (2003) Activity-Guided Isolation of Novel Norwithanolides from *Deprea subtriflora* with Potential Cancer Chemopreventive Activity. J Org Chem **68**: 2350
185. Su B-N, Park EJ, Nikolic D, Vigo JS, Graham JG, Cabieses F, Van Breemen RB, Fong HHS, Farnsworth NR, Pezzuto JM, Kinghorn AD (2003) Isolation and Characterization of Miscellaneous Secondary Metabolites of *Deprea subtriflora*. J Nat Prod **66**: 1089
186. Ma L, Ali M, Arfan M, Lou L-G, Hu L-H (2007) Withaphysanolide A, a Novel C-27 Norwithanolide Skeleton, and Other Cytotoxic Compounds from *Physalis divericata*. Tetrahedron Lett **48**: 449
187. Shingu K, Marubayashi N, Ueda I, Yahara S, Nohara T (1990) Two New Ergostane Derivatives from *Tubocapsicum anomalum* (Solanaceae). Chem Pharm Bull **38**: 1107
188. Kovganko NV, Kashkan ZhN (1997) Advances in the Chemical Synthesis of Withanolides. Chem Nat Compd **33**: 133
189. Mareggiani G, Picollo MI, Zerba E, Burton G, Tettamanzi MC, Benedetti-Doctorovich MOV, Veleiro AS (2000) Antifeedant Activity of Withanolides from *Salpichroa origanifolia* on *Musca domestica*. J Nat Prod **63**: 1113

190. Bado S, Mareggiani G, Amiano N, Burton G, Veleiro AS (2004) Lethal and Sublethal Effects of Withanolides from *Salpichroa origanifolia* and Analogues on *Ceratitis capitata*. J Agric Food Chem **52**: 2875
191. Misra L, Lal P, Chaurasia ND, Sangwan RS, Sinha S, Tuli R (2008) Selective Reactivity of 2-Mercaptoethanol with 5β,6β-Epoxide in Steroids from *Withania somnifera*. Steroids **73**: 245
192. Yokota Y, Bargagna-Mohan P, Ravindranath PP, Kim KB, Mohan R (2006) Development of Withaferin A Analogs as Probes of Angiogenesis. Bioorg Med Chem Lett **16**: 2603
193. Choudhary MI, Yousuf S, Samreen, Shah SAA, Ahmed S, Atta-ur-Rahman (2006) Biotransformation of Physalin H and Leishmanicidal Activity of its Transformed Products. Chem Pharm Bull **54**: 927
194. Wijeratne EMK, Xu Y, Marron MT, Whitesell L, Gunatilaka AAL (2008) Isolation and Synthesis of Analogs of the Anticancer Natural Product Withaferin A for Structure-Activity Relationship Studies. Abstracts, 42nd Western Regional Meeting of the American Chemical Society, Las Vegas, NV, United States, September 23–27.
195. Jha S, Bandyopadhyay M, Chaudhuri KN, Ghosh S, Ghosh B (2005) Biotechnological Approaches for the Production of Forskolin, Withanolides, Colchicine and Tylophorine. Plant Genet Resour **3**: 101
196. Ray S, Jha S (2001) Production of Withaferin A in Shoot Cultures of *Withania somnifera*. Planta Med **67**: 432
197. Sangwan RS, Das Chaurasiya N, Lal P, Misra L, Uniyal GC, Tuli R, Sangwan NS (2007) Withanolide a Biogeneration in *in Vitro* Shoot Cultures of Ashwagandha (*Withania somnifera* Dunal), a Main Medicinal Plant in Ayurveda. Chem Pharm Bull **55**: 1371
198. Sharada M, Ahuja A, Suri KA, Vij SP, Khajuria RK, Verma V, Kumar A (2007) Withanolide Production by *in Vitro* Cultures of *Withania somnifera* and its Association with Differentiation. Biologia Plantarum **51**: 161
199. Madina BR, Sharma LK, Chaturvedi P, Sangwan RS, Tuli R (2007) Purification and Physico-Kinetic Characterization of 3β-Hydroxy Specific Sterol Glucosyltransferase from *Withania somnifera* (L) and its Stress Response. Biochim Biophys Acta **1774**: 392
200. Madina BR, Sharma LK, Chaturvedi P, Sangwan RS, Tuli R (2007) Purification and Characterization of a Novel Glucosyltransferase Specific to 27*β*-Hydroxy Steroidal Lactones from *Withania somnifera* and its Role in Stress Responses. Biochim Biophys Acta **1774**: 1199
201. Elliger CA, Waiss AC, Jr. (1989) Insect Growth Inhibitors from *Petunia* and Other Solanaceous Plants. In: Arnason JT, Philogene BJR, Morand P (eds): Pesticides of Plant Origin, ACS Symposium Series No. 387. American Chemical Society, Washington DC, p 188
202. Waiss AC, Elliger CA, Haddon WF, Benson M (1993) Insect Inhibitory Steroidal Saccharide Esters from *Physalis peruviana*. J Nat Prod **56**: 1365
203. Elliger CA, Haddon WF, Harden L, Waiss AC, Wong RY (1994) Insect Inhibitory Steroidal Saccharide Esters from *Physalis peruviana*. J Nat Prod **57**: 348
204. Baumann TW, Meier CM (1993) Chemical Defense by Withanolides During Fruit Development in *Physalis peruviana*. Phytochemistry **33**: 317
205. Mareggiani G, Picollo MI, Veleiro AS, Tettamanzi MC, Benedetti-Doctorovich MOV, Burton G, Zerba E (2002) Response of *Tribolium castaneum* (Coleoptera, Tenebrionidae) to *Salpichroa origanifolia* Withanolides. J Agric Food Chem **50**: 104
206. Vaccarini CE, Bonetto GM (2000) Antifeedant Activity Evaluation of Withanolides from *Jaborosa integrifolia*. Molecules **5**: 422
207. Enriz RD, Baldoni HA, Zamora MA, Jauregui EA, Sosa ME, Tonn CE, Luco JM, Gordaliza M (2000) Structure-Antifeedant Activity Relationship of Clerodane Diterpenoids. Comparative Study with Withanolides and Azadirachtin. J Agric Food Chem **48**: 1384
208. Garcia ES, Castro DP, Ribeiro IM, Tomassini TCB, Azambuja P (2006) *Trypanosoma rangeli*: Effects of Physalin B on the Immune Reactions of the Infected Larvae of *Rhodnius prolixus*. Exp Parasitol **112**: 37

209. Castro DP, Figueiredo MB, Ribeiro IM, Tomassini TCB, Azambuja P, Garcia ES (2008) Immune Depression in *Rhodnius prolixus* by Seco-Steroids, Physalins. J Insect Physiol **54**: 555
210. Castro DP, Figueiredo MB, Genta FA, Ribeiro IM, Tomassini TCB, Azambuja P, Garcia ES (2009) Physalin B Inhibits *Rhodnius prolixus* Hemocyte Phagocytosis and Microaggregation by the Activation of Endogenous PAF-Acetyl Hydrolase Activities. J Insect Physiol **55**: 532
211. Dinan L, Whiting P, Alfonso D, Kapetanidis I (1996) Certain Withanolides from *Iochroma gesnerioides* Antagonize Ecdysteroid Actin in a *Drosophila melanogaster* Cell Line. Entomol Exp Appl **80**: 415
212. Savchenko T, Whiting P, Germade A, Dinan L (2000) Ecdysteroid Agonist and Antagonist Activities in Species of the Solanaceae. Biochem Syst Ecol **28**: 403
213. Dinan L, Savchenko T, Whiting P, Sarker SD (1999) Plant Natural Products as Insect Steroid Receptor Agonists and Antagonists. Pestic Sci **55**: 331
214. Dinan L, Bourne PC, Meng Y, Sarker SD, Tolentino RB, Whiting P (2001) Assessment of Natural Products in the *Drosophila melanogaster* BII Cell Bioassay for Ecdysteroid Agonist and Antagonist Activities. Cell Mol Life Sci **58**: 321
215. Vaccarini CE, Bonetto GM (2000) Selective Phytotoxic Activity of Withanolides from *Iochroma australe* to Crop and Weed Species. J Chem Ecol **26**: 2187
216. Vieira NC, Espíndola LS, Santana JM, Veras ML, Pessoa ODL, Pinheiro SM, de Araújo RM, Lima MAS, Silveira ER (2008) Trypanocidal Activity of a New Pterocarpan and Other Secondary Metabolites of Plants from Northeastern Brazil Flora. Bioorg Med Chem **16**: 1676
217. Atta-ur-Rahman, Samreen, Atia-tul-Wahab, Choudhary MI (2008) Discovery of Leishmanicidal Agents from Medicinal Plants. Pure Appl Chem **80**: 1783
218. Cardona D, Quiñones W, Torres F, Robledo S, Vélez ID, Cruz V, Notario R, Echeverri F (2006) Leishmanicidal Activity of Withajardins and Acnistins. An Experimental and Computational Study. Tetrahedron **62**: 6822
219. Sen N, Banerjee B, Das BB, Ganguly A, Sen T, Pramanik S, Mukhopadhyay S, Majumder HK (2006) Apoptosis is Induced in Leishmanial Cells by a Novel Protein Kinase Inhibitor Withaferin A and is Facilitated by Apoptotic Topoisomerase I-DNA Complex. Cell Death Differ **14**: 358
220. Kannan ND, Kulandaivelu G (2007) Novel Method to Isolate Withaferin A from *Withania somnifera* Roots and Its Bioactivity. Allelopathy J **20**: 213
221. Silva MTG, Simas SM, Batista TG, Cardarelli P, Tomassini TCB (2005) Studies on Antimicrobial Activity, in Vitro, of *Physalis angulata* L. (Solanaceae) Fraction and Physalin B Bringing out the Importance of Assay Determination. Mem Inst Oswaldo Cruz **100**: 779
222. Januário AH, Rodrigues Filho E, Pietro RCLR, Kashima S, Sato DN, França SC (2002) Antimycobacterial Physalins from *Physalis angulata* L. (Solanaceae). Phytother Res **16**: 445
223. Vieira AT, Pinho V, Lepsch LB, Scavone C, Ribeiro IM, Tomassini T, Ribeiro-dos-Santos R, Soares MBP, Teixeira MM, Souza DG (2005) Mechanisms of the Anti-Inflammatory Effects of the Natural Secosteroids Physalins in a Model of Intestinal Ischaemia and Reperfusion Injury. Br J Pharmacol **146**: 244
224. Singh D, Aggarwal A, Maurya R, Naik S (2007) *Withania somnifera* Inhibits NF-κB and AP-1 Transcription Factors in Human Peripheral Blood and Synovial Fluid Mononuclear Cells. Phytother Res **21**: 905
225. Kaileh M, Vanden Berghe W, Heyerick A, Horion J, Piette J, Libert C, De Keukeleire D, Essawi T, Haegeman G (2007) Withaferin A Strongly Elicits IκB Kinase Hyperphosphorylation Concomitant with Potent Inhibition of Its Kinase Activity. J Biol Chem **282**: 4253
226. Ichikawa H, Takada Y, Shishodia S, Jayaprakasam B, Nair MG, Aggarwal BB (2006) Withanolides Potentiate Apoptosis, Inhibit Invasion, and Abolish Osteoclastogenesis through Suppression of Nuclear Factor-κB (Nf-κB) Activation and NF-κB-Regulated Gene Expression. Mol Cancer Ther **5**: 1434

227. Punetha H, Gaur AK, Pant AK, Mishra DP (2006) Cyclooxygenase (Cox) Inhibitory Activity of Withanolides from *Withania somnifera* (L.) Dunal as Revealed by Molecular Docking. Bioinf Trends **1**: 41
228. Manickam M, Padma P, Chansouria JPN, Ray AB (1997) Evaluation of Antistress Activity of Withafastuosin D, a Withanolide of *Datura fastuosa*. Phytother Res **11**: 384
229. Goel RK, Maiti RN, Manickam M, Ray AB (1997) Effect of Withafastuosin E on Prostanoid Synthesis by Human Intestinal Mucosa 'in Vitro'. Fitoterapia **68**: 345
230. Maiti RN, Manickam M, Ray AB, Goel RK (1997) Effect of Withafastuosin E on Gastric Mucosal Offensive and Defensive Factors in Rats. Indian J Exp Biol **35**: 751
231. Bhattacharya A, Ghosal S, Bhattacharya SK (2001) Anti-Oxidant Effect of *Withania somnifera* Glycowithanolides in Chronic Footshock Stress-Induced Perturbations of Oxidative Free Radical Scavenging Enzymes and Lipid Peroxidation in Rat Frontal Cortex and Striatum. J Ethnopharmacol **74**: 1
232. Bhattacharya SK, Satyan KS, Ghosal S (1997) Antioxidant Activity of Glycowithanolides from *Withania somnifera*. Indian J Exp Biol **35**: 236
233. Habtemariam S (1997) Cytotoxicity and Immunosuppressive Activity of Withanolides from *Discopodium penninervium*. Planta Med **63**: 15
234. Mesaik MA, Zaheer Ul H, Murad S, Ismail Z, Abdullah NR, Gill HK, Atta-ur-Rahman, Yousaf M, Siddiqui RA, Ahmad A, Choudhary MI (2006) Biological and Molecular Docking Studies on Coagulin-H: Human Il-2 Novel Natural Inhibitor. Mol Immunol **43**: 1855
235. Soares MBP, Bellintani MC, Ribeiro IM, Tomassini TCB, Ribeiro dos Santos R (2003) Inhibition of Macrophage Activation and Lipopolysaccaride-Induced Death by Seco-Steroids Purified from *Physalis angulata* L. Eur J Pharmacol **459**: 107
236. Soares MBP, Brustolim D, Santos LA, Bellintani MC, Paiva FP, Ribeiro YM, Tomassini TCB, Ribeiro dos Santos R (2006) Physalins B, F and G, Seco-Steroids Purified from *Physalis angulata* L., Inhibit Lymphocyte Function and Allogeneic Transplant Rejection. Int Immunopharm **6**: 408
237. Yang H, Shi G, Dou QP (2007) The Tumor Proteasome is a Primary Target for the Natural Anticancer Compound Withaferin A Isolated from "Indian Winter Cherry". Mol Pharmacol **71**: 426
238. Mandal C, Dutta A, Mallick A, Chandra S, Misra L, Sangwan RS (2008) Withaferin A Induces Apoptosis by Activating P38 Mitogen-Activated Protein Kinase Signaling Cascade in Leukemic Cells of Lymphoid and Myeloid Origin through Mitochondrial Death Cascade. Apoptosis **13**: 1450
239. Stan SD, Hahm E-R, Warin R, Singh SV (2008) Withaferin A Causes FOXO3a- and Bim-Dependent Apoptosis and Inhibits Growth of Human Breast Cancer Cells *In Vivo*. Cancer Res **68**: 7661
240. Jayaprakasam B, Zhang Y, Seeram NP, Nair MG (2003) Growth Inhibition of Human Tumor Cell Lines by Withanolides from *Withania somnifera* Leaves. Life Sci **74**: 125
241. Damasceno Rocha D, Gadelha Militão GC, Veras ML, Deusdênia Loiola Pessoa O, Rocha Silveira E, Negreiros Nunes Alves AP, Odorico de Moraes M, Pessoa C, Veras Costa-Lotufo L (2006) Selective Cytotoxicity of Withaphysalins in Myeloid Leukemia Cell Lines Versus Peripheral Blood Mononuclear Cells. Life Sci **79**: 1692
242. Chen W-Y, Chang F-R, Huang Z-Y, Chen J-H, Wu Y-C, Wu C-C (2008) Tubocapsenolide A, a Novel Withanolide, Inhibits Proliferation and Induces Apoptosis in MDA-MB-231 Cells by Thiol Oxidation of Heat Shock Proteins. J Biol Chem **283**: 17184
243. Chang H-C, Chang F-R, Wang Y-C, Pan M-R, Hung W-C, Wu Y-C (2007) A Bioactive Withanolide Tubocapsanolide A Inhibits Proliferation of Human Lung Cancer Cells Via Repressing Skp2 Expression. Mol Cancer Ther **6**: 1572
244. Magalhães HIF, Veras ML, Pessoa ODL, Silveira ER, Moraes MO, Pessoa C, Costa-Lotufo LV (2006) Preliminary Investigation of Structure-Activity Relationship of Cytotoxic Physalins. Lett Drug Design Discovery **3**: 9

245. Magalhães HIF, Veras ML, Torres M, Rocha, Alves APNN, Pessoa ODL, Silveira ER, Costa-Lotufo LV, de Moraes MO, Pessoa C (2006) In-Vitro and in-Vivo Antitumour Activity of Physalins B and D from *Physalis angulata*. J Pharm Pharmacol **58**: 235
246. Hosoya T, Arai MA, Koyano T, Kowithayakorn T, Ishibashi M (2008) Naturally Occurring Small-Molecule Inhibitors of Hedgehog/Gli-Mediated Transcription. ChemBioChem **9**: 1082
247. Choi JK, Murillo G, Su B-N, Pezzuto JM, Kinghorn AD, Mehta RG (2006) Ixocarpalactone A Isolated from the Mexican Tomatillo Shows Potent Antiproliferative and Apoptotic Activity in Colon Cancer Cells. FEBS J **273**: 5714
248. Uma Devi P (1996) *Withania somnifera* Dunal (Ashwagandha): Potential Plant Source of a Promising Drug for Cancer Chemotherapy and Radiosensitization. Indian J Exp Biol **34**: 927
249. Sharada AC, Solomon FE, Devi PU, Udupa N, Srinivasan KK (1996) Antitumor and Radiosensitizing Effects of Withaferin A on Mouse Ehrlich Ascites Carcinoma in Vivo. Acta Oncol **35**: 95
250. Uma Devi P, Kamath R (2003) Radiosensitizing Effect of Withaferin A Combined with Hyperthermia on Mouse Fibrosarcoma and Melanoma. J Radiat Res **44**: 1
251. Kinghorn AD, Su BN, Lee D, Gu JQ, Pezzuto JM (2003) Cancer Chemopreventive Agents Discovered by Activity-Guided Fractionation: An Update. Curr Org Chem **7**: 213
252. Kang Y-H, Pezzuto JM, Helmut S, Lester P (2004) Induction of Quinone Reductase as a Primary Screen for Natural Product Anticarcinogens: Methods Enzymol, vol. 382, p 380. Elsevier, Inc., San Diego.
253. Misico RI, Song LL, Veleiro AS, Cirigliano AM, Tettamanzi MC, Burton G, Bonetto GM, Nicotra VE, Silva GL, Gil RR, Oberti JC, Kinghorn AD, Pezzuto JM (2002) Induction of Quinone Reductase by Withanolides. J Nat Prod **65**: 677
254. Panjamurthy K, Manoharan S, Menon VP, Nirmal MR, Senthil N (2008) Protective Role of Withaferin-A on 7,12-Dimethylbenz(a)Anthracene-Induced Genotoxicity in Bone Marrow of Syrian Golden Hamsters. J Biochem Mol Toxic **22**: 251
255. Mohan R, Hammers H, Bargagna-Mohan P, Zhan X, Herbstritt C, Ruiz A, Zhang L, Hanson A, Conner B, Rougas J, Pribluda V (2004) Withaferin A Is a Potent Inhibitor of Angiogenesis. Angiogenesis **7**: 115
256. Bargagna-Mohan P, Ravindranath Padma P, Mohan R (2006) Small Molecule Anti-Angiogenic Probes of the Ubiquitin Proteasome Pathway: Potential Application to Choroidal Neovascularization. Invest Ophthalmol Vis Sci **47**: 4138
257. Vandenberghe I, Créancier L, Vispé S, Annereau J-P, Barret J-M, Pouny I, Samson A, Aussagues Y, Massiot G, Ausseil F, Bailly C, Kruczynski A (2008) Physalin B, a Novel Inhibitor of the Ubiquitin-Proteasome Pathway, Triggers NOXA-Associated Apoptosis. Biochem Pharmacol **76**: 453
258. Tinley TL, Randall-Hlubek DA, Leal RM, Jackson EM, Cessac JW, Quada JC, Jr., Hemscheidt TK, Mooberry SL (2003) Taccalonolides E and A: Plant-Derived Steroids with Microtubule-Stabilizing Activity. Cancer Res **63**: 3211
259. Risinger AL, Jackson EM, Polin LA, Helms GL, LeBoeuf DA, Joe PA, Hopper-Borge E, Luduena RF, Kruh GD, Mooberry SL (2008) The Taccalonolides: Microtubule Stabilizers That Circumvent Clinically Relevant Taxane Resistance Mechanisms. Cancer Res **68**: 8881
260. Risinger AL, Mooberry SL (2010) Taccalonolides: Novel Microtubule Stabilizers with Clinical Potential. Cancer Lett **291**: 14
261. Tohda C, Kuboyama T, Komatsu K (2005) Search for Natural Products Related to Regeneration of the Neuronal Network. NeuroSignals **14**: 34
262. Kuboyama T, Tohda C, Zhao J, Nakamura N, Hattori M, Komatsu K (2002) Axon- or Dendrite-Predominant Outgrowth Induced by Constituents from Ashwagandha. NeuroReport **13**: 1715
263. Kuboyama T, Tohda C, Komatsu K (2005) Neuritic Regeneration and Synaptic Reconstruction Induced by Withanolide A. Br J Pharmacol **144**: 961

264. Kuboyama T, Tohda C, Komatsu K (2006) Withanoside IV and Its Active Metabolite, Sominone, Attenuate Aβ(25–35)-Induced Neurodegeneration. Eur J Neurosci **23**: 1417
265. Choudhary MI, Nawaz SA, Zaheer-ur-Haq, Lodhi MA, Ghayur MN, Jalil S, Riaz N, Yousuf S, Malik A, Gilani AH, Atta-ur-Rahman (2005) Withanolides, a New Class of Natural Cholinesterase Inhibitors with Calcium Antagonistic Properties. Biochem Biophys Res Commun **334**: 276
266. Jiao M, Luna-Cavazos M, Bye R (2002) Allozyme Variation in Mexican Species and Classification of *Datura* (Solanaceae). Plant Syst Evol **232**: 155
267. Luna-Cavazos M, Bye R, Jiao M (2009) The Origin of *Datura metel* (Solanaceae): Genetic and Phylogenetic Evidence. Gen Resour Crop Evol **56**: 263

Author Index

A
Abbas, S., 217, 218
Abdala, S., 217
Abdel Migid, H., 217
Abdeljebbar, LH., 218
Abdul Rahman, 54
Abdullah, NR., 227
Abe, F., 219
Abou-Douh, AM., 217
Abraham, A., 222, 223
Achmad, F., 54
Adam, G., 220
Adams, TE., 58
Adeline, M-T., 53
Afreen, S., 221
Afriastini, JJ., 53–55
Afshan, F., 221
Afza, N., 218, 219
Aggarwal, A., 226
Aggarwal, BB., 218, 226
Ahmad, A., 227
Ahmad, S., 144, 218, 219
Ahmed, S., 217, 219, 223, 225
Ahuja, A., 225
Akahane, H., 219
Akamatsu, K., 125
Akanksha, 218
Akinniyi, JA., 55
Alfonso, D., 219, 226
Ali, A., 217
Ali, I., 218
Ali, M., 218, 224
Altmann, K-H., 51
Alvarado, VE., 219
Alvarez, LD., 224
Alves, APNN., 228
Amador, S., 220
Amiano, N., 225
Amodei, S., 56
Amzazi, S., 218
Ando, J., 221
Andres, H., 121
Anjaneyulu, ASR., 189, 217
Annereau, J-P., 228
Ansari, SH., 218
Aoki, H., 118
Arai, MA., 228
Arai, T., 118
Araki, S., 222
Arbieva, ZH., 56
Archbold, R., 222
Arfan, M., 218, 223, 224
Arison, BH., 118, 121
Aristizábal, FA., 220
Armirotti, A., 56
Armstrong, HM., 124
Arnason, JT., 55, 225
Arnold, R., 56
Asano, M., 118
Aschauer H., 120
Ashley, G., 119
Askin, D., 122, 123, 125
Asres, K., 220
Aszody, A., 120
Atia-tul-Wahab., 226
Atta-ur-Rahman, 198, 217–219, 223, 225–227, 229
Aubert, G., 58
Aussagues, Y., 228
Ausseil, F., 228
Awang, K., 53
Awasthi, SB., 220
Axel, G., 57
Azambuja, P., 196, 225, 226

A.D. Kinghorn, H. Falk, J. Kobayashi (eds.), *Progress in the Chemistry of Organic Natural Products, Vol. 94*, DOI 10.1007/978-3-7091-0748-5,

B
Bacher, M., 52, 121–123
Bado, S., 225
Baggio, RF., 221, 224
Baguet, A., 58
Bai, H-Y., 223
Baig, I., 217
Bailly, C., 228
Baker, H., 119
Balakrishna, K., 52
Balanza, E., 220
Baldoni, HA., 225
Ballard, JM., 121
Balmanno, K., 57
Balunas, MJ., 51
BaMaung, NY., 124
Bandyopadhyay, M., 225
Banerjee, B., 226
Barata, LES., 220
Barbi, NS., 222
Barboza, G., 127, 211, 212, 214, 215
Bargagna-Mohan, P., 225, 238
Barret, J-M., 238
Bastow, KF., 219, 223
Batchelor, MJ., 125
Batista, TG., 226
Bauer, R., 220
Baumann, B., 52
Baumann, K., 59, 118, 119, 121–125
Baumann, TW., 225
Baumruker, T., 119
Bavandi, A., 120
Beattie, TR., 123
Becker, EB., 56
Becker, JW., 68
Beecher, CWW., 221
Begum, S., 221
Bekkouche, K., 218
Bellintani, MC., 227
Beltrán, G., 211
Benedetti-Doctorovich, MOV., 224, 225
Benjouad, A., 218
Benjumea, D., 217
Benson, M., 225
Bernard, Y., 58
Besalle, R., 224
Bezerra, MZB., 223
Bhat, BA., 220
Bhattacharya, A., 227
Bhattacharya, SK., 227
Biehl, ML., 227
Biggers, MS., 125
Billich, A., 118, 120
Biurrun, FN., 224
Bleumink, M., 56
Blocker, LW., 125
Bohnenstengel, FI., 52, 54, 55
Bohs, L., 217
Bollinger, P., 216
Bonetto, GM., 221, 223–226, 228
Bonini, P., 56
Bonni, A., 56
Bordeleau, ME., 56
Borris, RP., 118
Bourdeau, A., 56
Bourne, PC., 226
Brader, G., 52
Bravo, BJA., 220
Braz-Filho, R., 223
Brecht, V., 53
Brecker, L., 54
Brem, B., 52, 56
Bremner, P., 222
Bringmann, G., 52, 54, 55
Bruce, I., 58
Brustolim, D., 227
Bucar, F., 220
Büchau, A., 120
Buchheit, KH., 124
Buckland, BC., 121
Budhiraja, RD., 217
Bulusu, MARC., 59, 118, 122, 123
Burkhard, P., 68
Burtin, P., 120
Burton, G., 127, 217, 219–221, 223–225, 228
Butler, MS., 51
Butsugan, Y., 222, 223
Bye, R., 229
Byrne, K., 118

C
Cabieses, F., 224
Cai, B., 56
Cai, SJ., 121
Cai, X-H., 53, 54
Camacho, BDS., 221
Cammisuli, S., 124
Carcache-Blanco, EJ., 55
Carcamo, C., 219
Cardarelli, P., 226
Cardona, D., 217, 221, 226
Cardona, G., 222
Cariou, K., 58
Carney, JR., 119
Caron, PR., 121

Carreras, CW., 119
Carrier, M., 56
Carter, GW., 123, 124
Castillo, JJ., 222
Castro, DP., 225, 226
Ceballos, NR., 224
Cederbaum, F., 57
Cencic, R., 56, 58
Cessac, JW., 228
Chai, H., 52–56
Chai, HB., 51, 53, 55, 220, 222, 223
Chaidir, 54
Chan, HK., 68
Chandra, S., 227
Chang, F-R., 219, 221, 227
Chang, H-C., 227
Chang, SH., 56
Chansouria, JPN., 227
Chantrapromma, K., 55
Chao, ED., 123
Chase, MW., 52
Chaturvedi, P., 225
Chaudhuri, KN., 225
Chaurasia, ND., 225
Che, C-T., 220
Chen, C-M., 165, 219, 223
Chen, C-X., 220, 224
Chen, H-D., 53
Chen, J-H., 221, 227
Chen, K., 125
Chen, L-X., 222
Chen, R., 223
Chen, S-L., 219, 221
Chen, SM., 56
Chen, SST., 118
Chen, T-H., 219, 223
Chen, TS., 118
Chen, W-Y., 227
Chen, Y-W., 124
Chen, Z., 224
Chen, Z-L., 224
Chen, Z-T., 219
Cheng, Y-J., 54
Chiang, C-C., 52
Chiang, MY., 221
Chiarini, F., 212, 214, 215
Chiaroni, A., 54
Chibout, SD., 120
Chin, YW., 51–55
Chiu, SF., 23, 55
Cho, H., 125
Choi, DB., 125
Choi, JK., 228
Choudhary, MI., 164, 217–219, 221, 223, 225–227, 229
Chow, K., 121
Christen, P., 218
Christians, U., 119
Chumkaew, P., 55
Chung, J., 119
Chung, L., 119
Chung, RCK., 51
Chung, Y., 125
Cirigliano, AM., 178, 220, 224, 228
Clardy, J., 120, 121
Clark, RF., 123, 124
Clemons, PA., 123
Cocucci, AA., 215
Cohen, M., 223
Cole, SH., 125
Coleman, RS., 123
Collier, SM., 217
Coltella, N., 57
Colwell, LF., 119
Condon, SM., 125
Conner, B., 228
Connolly, JD., 55
Connolly, MJ., 125
Cook, SJ., 57
Cooke, NG., 57
Cooper, K., 125
Cooper, ME., 123
Cordell, GA., 51–55, 220, 222, 223
Cordero, CP., 220
Cordier, A., 120
Corley, EG., 124
Cosa, MT., 211, 212, 214
Costa-Lotufo, LV., 223, 227, 228
Cozzolino, F., 56
Cragg, GM., 51
Créancier, L., 228
Cresteil, T., 58
Cruz, V., 226
Cryan, JG., 124
Cui, B., 52, 56

D

D'Arcy, WG., 217
Da Silva, IT., 221
Damasceno Rocha, D., 227
Damont, A., 121, 122
Damonte, G., 56
Damu AG., 219, 223
Danishefsky, SJ., 121, 123, 126
Darnaedi, D., 53, 55

Das, BB., 226
Das Chaurasiya, N., 225
Davey, AE., 57
de Araújo, RM., 226
de Castellano, G., 221
De Chiara, G., 56
De Keukeleire, D., 226
de la Fuente, JR., 223
De Moraes, MO., 223, 228
Dean, DC., 124
Dean, FM., 54
Debatin, K-M., 52
Delle Monache, F., 221
Delle Monache, G., 221
Demain, AL., 126
DeMarco, A., 124
Demirs, JT., 56
Denessiouk, K., 57
Désaubry, L., 47, 49, 58
Desmond, R., 123, 124
Deusdênia Loiola Pessoa, O., 227
Devi, PU., 228
DeWitt, DL., 218
Dhar, KL., 220
Di Renzo, MF., 57
Diedrichs, N., 57, 58
Dinan, L., 144, 219, 226
Diorazio, LJ., 57
Dirr, R., 57
Do Ó Pessoa, C., 223
Dobler, MR., 38, 47, 57
Donald, DK., 123
Donovan, C., 125
Doskotch, RW., 216
Dou, D., 220
Dou, QP., 227
Dreyer, M., 52, 55
Duh, C-Y., 54, 55
Dumont, FJ., 123, 124
Dumontet, V., 53, 54
Duong, AT., 53
Duong, TN., 53
Dur-e-Shahwar, 218
Dutta, A., 227
Duval, F., 55
Dyatmiko, W., 54

E
Ebada, SS., 1
Ebel, R., 52–55
Ebelin, ME., 120
Echeverri, F., 199, 217, 221, 222, 226
Ecker, R., 120
Edjlalipour, M., 120
Edmunds, AJF., 119, 121
Edrada, RA., 52–54
Egan, MAM., 124
Egan, RS., 121
El Sous, M., 58
Elbe-Buerger, A., 120
Elliger, CA., 225
Emerson, K., 124
Emmer, G., 122, 123
Engelmeier, D., 52
Enriz, RD., 225
Enz, A., 119, 124
Erchen, J., 120
Eriksson, JE., 57
Espíndola, LS., 226
Essawi, T., 226
Estrada, N., 217
Evans, CG., 123
Ewete, F., 55

F
Fahrngruber, H., 120
Fairchild, CR., 54
Fajardo, V., 219, 224
Fang, L., 222
Fang, S-T., 224
Fardis, M., 119
Farmer, JD., 121
Farnsworth, NR., 51–55, 222, 224
Fatima, I., 218
Fehr, T., 118, 119, 124
Feifel, R., 120
Feng, L., 119
Feng, W., 220
Feresin, GE., 221
Ferraina, RA., 125
Fesik, SW., 121, 123
Fey, TA., 124
Fialla, R., 119
Fichtinger, P., 119
Figueiredo, MB., 226
Fisher, MJ., 121
Fitzgibbon, MJ., 121
Fleissner, G., 118
Fleming, MA., 121
Födinger, D., 119
Foley, MA., 123
Fong, HHS., 221, 224
Formenti, SC., 56
Fozard, JR., 124
Frahm, AW., 53
França, SC., 226

Frank, W., 53
Friedman, J., 121
Frolow, F., 224
Frontier, JA., 43, 58
Frydenvang, K., 123
Fu, B., 58
Fuhr, M., 54
Fuhrer, W., 119
Fujita, E., 52
Fuzzati, N., 54

G
Gacs-Baitz, E., 221
Gadelha Militão, GC., 227
Gaiddon, C., 58
Gailliot, FP., 118, 121
Galet, S., 119
Galicia-Vázquez, G., 56
Gallo, R., 120
Gallucci, JC., 55
Galluzzi, L., 56
Gan, X-W., 223
Ganguly, A., 226
Gao, Y., 224
Garaci, E., 56
Garcia, ES., 225, 226
García, F., 222
García, M., 222
Garcia, ME., 224
García, VF., 217
Garland, MT., 221
Garzon, J., 221
Gaspard, C., 53
Gaur, AK., 227
Gauvin, DM., 124
Gayathri, C., 224
Gaynor, RB., 56
Gbewonyo, K., 118
Gegnas, LD., 125
Gehling, M., 52
Genta, FA., 226
Gerard, B., 56–58
Gerhaeuser, C., 221
Germade, A., 226
Gestwicki, JE., 123
Ghayur, MN., 229
Ghosal, S., 227
Ghosh, B., 225
Ghosh, S., 218, 225
Giaisi, M., 52, 56
Gibbons, GS., 123
Gibbons, S., 220, 222
Giger, R., 119
Gil, RR., 127, 219, 221, 223, 224, 228
Gilani, AH., 229
Gill, HK., 223, 227
Gillespie, RJ., 125
Gimenez, T A., 220
Giordano, OS., 224
Gladstone, BG., 123
Gleason, JL., 125
Glotter, E., 216, 219, 222
Goel, RK., 227
Goh, SH., 54
Gold, BG., 119
Golec, JMC., 125
Gonzalez, AG., 222
Gonzalez, CM., 223
Goomber, S., 55
Gordaliza, M., 225
Goto, T., 118
Gottlieb, HE., 223, 224
Goulet, MT., 123, 124
Grabowski, EJJ., 124
Graham, JG., 221, 224
Grassberger, MA., 118–125
Gray, AI., 220–221
Greenberg, M., 223
Greenspan, PD., 54
Greger, H., 52–54, 56
Greig, G., 120
Grethe, S., 57
Griffith, JP., 121
Gros, EG., 223, 224
Gschwind, L., 119
Gu, JQ., 217, 221, 228
Guadliana, MA., 125
Gubbins, E., 121
Guenzberg, G., 222
Guerrero, CA., 221
Gul, W., 217–219
Gunatilaka, AAL., 218, 225
Gunawardana, IWK., 123, 124
Gunning, PJ., 51
Gupta, A., 220
Gupta, M., 185, 217
Gupta, MP., 222
Güssregen, B., 54
Gutierrez-Luis, J., 217

H
Haag, M., 118
Habtemariam, S., 220–222, 227
Hadacek, F., 52

Haddon, WF., 225
Hadi, AHA., 53, 54
Hadi, H., 53
Haecker, H., 118
Haegeman, G., 226
Hahm, E-R., 227
Haidl, E., 118, 121, 124
Haidl, G., 121
Hale, KJ., 125
Hall, IH., 52
Hall, RG., 57
Hamashima, T., 125
Hammers, H., 228
Han, SH., 57
Hane, K., 121
Hansen, L., 123
Hanson, A., 228
Hanson, DC., 125
Hao, X-J., 53, 220, 224
Harano, K., 222
Harden, L., 225
Hartmann, B., 120
Hartmann, O., 122
Hashida, M., 125
Hashimoto, M., 118
Hashmi, IA., 221
Hatanaka, H., 118
Hattori, M., 217, 228
Hausott, B., 56
Hawkes, JG., 217
Hawkins, BC., 58
Hayashi, M., 223
Hayashi, N., 52
He, F-Y., 219
He, Q-P., 219, 223
Hebert, AA., 120
Hedgecock, CJR., 125
Hedin, PA., 51
Heinrich, M., 222
Helms, GL., 228
Helmut, G., 57
Helmut, S., 228
Hemes, JD., 68
Hemscheidt, TK., 228
Hengsawad, V., 55
Henkel, T., 223
Henry, CL., 124
Henry, R., 123
Herbstritt, C., 228
Herold, M., 52
Herr, I., 52
Hersperger, R., 124
Heuer, C., 122
Heyerick, A., 226
Hiestand, P., 119, 122
Hietakangas, V., 57
Higashimoto, Y., 56
Highsmith, TK., 125
Hiort, J., 54
Hirner, S., 58
Hisamichi, K., 220
Ho, G-J., 124
Hodkey, DW., 124
Hoetzenecker, W., 120
Hofer, M., 53
Hofer, O., 52–54
Hoff, A., 217
Höfle, G., 51
Högenauer, K., 121, 122
Hohnholz, D., 218
Hollingworth, RM., 51
Holloway, G., 58
Holmes, D., 218
Holmes, MA., 124
Holt, DA., 123
Holter, W., 120
Holze, I., 119
Holzman, TF., 121
Honda, H., 118
Hopper-Borge, E., 228
Horion, J., 226
Horvath, A., 123–125
Hosoya, K., 125
Hosoya, T., 228
Hostettmann, K., 54, 218
Hsiao, K., 121
Hsieh, GC., 123, 124
Hsieh, P-W., 184, 221
Hsu, SC., 57
Hu, L-H., 218, 219, 221, 223, 224
Hu, X., 220
Huang, C-F., 218
Huang, H-C., 52
Huang, T-F., 54
Huang, X-Y., 219
Huang, Y., 172, 223
Huang, Z-Y., 221, 227
Hultsch, T., 119, 120
Humam, M., 218
Hung, PD., 52, 54, 55
Hung, W-C., 221, 227
Huntington, MF., 124
Hunziker, AT., 217
Hwang, BY., 54, 56

I

Ichikawa, H., 201, 226
Ikeda, T., 221, 222
Imanaka, H., 118

Imiyabir, Z., 54
Inada, A., 53, 55
Inamine, ES., 118
Inamura, N., 118
Inatomi, Y., 53, 55
Ireland, RE., 125
Irving, E., 57
Ishibashi, F., 6, 23, 54
Ishibashi, M., 228
Ismail, Z., 227
Isman, MB., 51, 54, 55
Iwami, M., 118
Iwata, Y., 223

J
Jabbar, A., 218
Jackson, EM., 228
Jacobo-Herrera, NJ., 222
Jahan, E., 218
Jalil, S., 229
Jamal, SA., 217, 218
Janaki, S., 52
Januário, AH., 226
Jaroszewski, JW., 123
Jauregui, EA., 225
Jayaprakasam, B., 217, 218, 226, 227
Jayendra, 218
Jeannerat, D., 218
Jeck, R., 122
Jens, F., 217
Jha, S., 225
Jiang, Z-H., 222
Jiao, M., 229
Joe, D., 122, 123
Joe, PA., 228
Johnson, MS., 57
Jonas, PF., 220
Jones, AB., 126
Jones, G., 57
Jones, SD., 125
Jones, TK., 122, 123, 125
Jones, WP., 51
Jongbunprasert, V., 55
Joycharat, N., 53
Junker, B., 118

K
Kahn, Y., 55
Kaileh, M., 226
Kalchhauser, H., 52
Kalish, VJ., 121
Kalthoff, FS., 119, 120
Kamath, R., 228
Kamperdick, C., 222
Kang, Y-H., 217, 221, 228
Kannan, ND., 226
Kapetanidis, I., 219, 226
Kaplan, L., 119
Kardono, LBS., 53–55
Karikas, GA., 222
Karplus, PA., 120
Karuso, P., 121
Kashima, S., 226
Kashkan, ZN., 185, 224
Katajamäki, T., 57
Katamna, C., 57
Kato, S., 55
Kaunisto, A., 57
Kaur, H., 55
Kawai, M., 123, 124, 166, 222, 223
Kehren, J., 120
Keil, E., 57
Kelley, CJ., 55
Kennelly, EJ., 221
Kessler, H., 119, 121
Khajuria, A., 220
Khajuria, RK., 225
Khan, PM., 218, 219
Khoo, ML., 58
Khozirah, KS., 54
Kiet, LC., 52, 54, 55
Kiew, R., 51
Kihara, N., 121, 122
Kim, BJ., 56
Kim, EE., 121
Kim, J., 121
Kim, KB., 225
Kim, S., 52, 55, 56
King, ML., 5, 52
Kinghorn, AD., 51–56, 153, 172, 181, 205, 217, 221, 222, 224, 228
Kinjo, J., 219
Kino, T., 118
Kirson, I., 217, 222, 223
Kishi, A., 218
Kishi, H., 56
Kissinger, CR., 121
Kito, K., 222
Kiyota, N., 222
Klicius, J., 119
Knapp, H., 121, 122
Knighton, DR., 121
Knop, J., 119
Ko, F-N., 54

Koch, G., 122
Koch, K., 125
Kochevar, IE., 56
Koda, S., 121
Köhler, R., 52, 56
Kohzuma, S., 57
Kojic-Prodic, B., 221
Kokpol, U., 55
Kollenz, G., 121
Komar, M., 120
Komatsu, K., 217, 228, 229
Kopecka, H., 124
Kopp, T., 120
Koprak, S., 124
Kosaka, M., 118
Kostek, GJ., 125
Koul, O., 55
Kovganko, NV., 185, 224
Kowalsky, E., 120
Kowithayakorn, T., 228
Koyama, Y., 118
Koyano, T., 55, 228
Krakauer, H., 224
Krammer, PH., 52, 55–57
Kraus, GA., 38, 57
Krause, R., 124
Kreuz, S., 57
Krishan, P., 217
Kroemer, G., 56
Kruczynski, A., 228
Kruh, GD., 228
Kuang, H., 220
Kuboyama, T., 217, 228, 229
Kuczynski, D., 121
Kudelski, A., 119
Kuesters, E., 118, 122
Kulandaivelu, G., 226
Kumar, A., 218, 225
Kumar, S., 220
Kumar, V., 54
Kuo, P-C., 173, 219, 223
Kuo, T-H., 219, 223
Kupchan, SM., 216
Kuroda, A., 118
Kuroyanagi, M., 217, 222
Kusters, E., 122
Kyburz, E., 119

L
Laakso, LF., 125
Lai, MZ., 57
Lai, Y-H., 54
Lajkiewicz, 1
Lal, P., 217, 225
Lan, Y-H., 219
Lane, BC., 123, 124
Lane, WS., 121
Lantos, CP., 224
Laprevote, O., 220
Larochette, N., 56
Lavaud, C., 220
Lavie, D., 174, 216, 218, 224
Lavrik, IN., 56
Leal, RM., 228
LeBoeuf, DA., 228
Lee, D., 228
Lee, E-J., 223
Lee, K-H., 52, 219, 223
Lee, SK., 56
Lee, S-W., 219
Leiva, S., 211, 214
Lemos, TLG., 223
Lepre, CA., 121
Lepsch, LB., 226
Lequesne, PW., 217
Leroy, E., 53
Lester, P., 228
Lester, RN., 217
Lewis, CT., 121
Lewis, DE., 55
Li, B., 224
Li, H., 58
Li, J., 221
Li, M., 214
Li, N., 58
Li, Q., 56
Li, W., 221
Li, Y., 54, 124
Li, Y-Z., 219
Li-Weber, M., 1, 52, 55–57
Liang, JY., 223
Libert, C., 226
Lien, T., 118
Likhitwitayawuid, K., 53
Lima, MAS., 226
Lin, WH., 53, 54
Linde, RG., 126
Lindqvist, L., 56
Ling, H-C., 52
Liou, M-J., 54
Lipipum, V., 52
Lipsky, P., 55
Lischewski, M., 220
Liu, B., 214
Liu, H-X., 222

Liu, H-Y., 151, 220, 224
Liu, J., 121
Liu, J-K., 223, 224
Liu, J-W., 218
Liu, L., 124, 125
Liu, R., 223
Liu, WJ., 58
Lodhi, MA., 229
Lohse, O., 124
Lou, F-C., 221, 223
Lou, L-G., 219, 224
Lowe, SW., 56
Lucibello, M., 56
Luco, JM., 225
Luduena, RF., 228
Luebken, T., 221
Luengo, JI., 123
Luger, TA., 120
Luis, JG., 222
Lukacs, G., 123
Luly, JR., 123, 124
Luna-Cavazos, M., 229
Luo, J-Y., 219
Luo, X-D., 53, 54

M
Ma, A., 55
Ma, C-Y., 220
Ma, L., 154, 184, 219, 221, 223, 224
Ma, YQ., 53
Macian, F., 56
MacPhail, AT., 216
Madani, L., 54
Madina, BR., 225
Magalhães, HIF., 204, 227, 228
Magnus, P., 41, 58
Mahlknecht, U., 56
Maibach, HI., 119
Maiti, RN., 227
Majumder, HK., 218, 226
Mak, CP., 122
Makino, B., 165, 186, 222, 223
Maldonado, E., 144, 219, 220, 222
Malik, A., 146, 154, 218, 219, 221, 229
Mallick, A., 227
Malona, JA., 58
Mandal, C., 227
Manickam, M., 220, 227
Mano, T., 57
Manoharan, S., 228
March, J., 217
Marcocci, ME., 56
Marcy, AI., 68
Mareggiani, G., 224, 225
Marian, B., 56
Marinec, PS., 123
Marks, TM., 124
Marquez, N., 222
Marron, MT., 218, 225
Marsh, K., 124
Martel, RR., 119
Martin, M-T., 53, 54
Martin-Herrera, D., 217
Martínez, M., 219, 220, 222
Martland, A., 120
Marubayashi, N., 224
Marusawa, H., 118
Masler, EP., 51
Massiot, G., 220, 228
Massy-Westropp, RA., 55
Mathre, DJ., 124
Matsuda, H., 218
Maurya, R., 218, 226
Mazzoni, L., 124
McAlpine, J., 123
McAlpine, SR., 124
McCauley, JA., 125
McDougal, NT., 57
McKeever, BM., 68
McLaughlin, SP., 218
McManemin, GJ., 121
McNamara, J., 124
McPhail, AT., 52
Meadows, RP., 121
Mehta, RG., 228
Mehta, RR., 56
Meier, CM., 225
Meingassner, JG., 119, 120, 122
Meiser, BM., 119, 125
Melchers, F., 119
Melillo, DG., 124
Melvin, LS., 125
Meng Y., 226
Menon, VP., 228
Mereiter, K., 53
Merling, A., 52
Mesaik, MA., 227
Mesecar, AD., 53, 54, 221, 224
Messer, K., 55
Meyer, C., 55
Mi, Q., 51, 53, 54, 56
Midzuki, K., 221
Mier, JW., 57
Mierke, DF., 121
Miller, L., 124

Miller, RR., 121
Mills, SG., 123, 125
Mimaki, Y., 220
Minguzzi, S., 220
Mir, SR., 218
Mishra, DP., 227
Mishra, P., 217
Misico, RI., 127, 219–221, 223, 224, 228
Misra, L., 187, 217, 225, 227
Miyamoto, J., 51
Miyashita, H., 222
Miyata, S., 118
Moenius, T., 121, 122
Mohamad, K., 53
Mohan, R., 188, 207, 225, 228
Molcanov, K., 221
Molleyres, L-P., 54
Mollison, KW., 123, 124
Monaghan, RL., 118
Monkhe, TV., 54
Monteagudo, ES., 178, 223, 224
Montenegro, RC., 223
Mooberry, SL., 207, 228
Moomaw, EW., 121
Moore, H., 120
Moore, HD., 120
Moore, JM., 121
Moraes, MO., 227
Morand, P., 225
Morantes, SJ., 220
Mori, T., 125
Morisaki, M., 118
Morris, RE., 119
Motamedi, H., 121
Mou, Y., 57
Muellner, AN., 52
Muhammad, P., 218, 219, 221
Mühlbacher, J., 52, 55
Mühlbauer, A., 223, 224
Mühleisen, A., 52
Mukhopadhyay, S., 218, 226
Mulabagal, V., 218
Mulholland, DA., 54
Müller, KD., 119
Müller, R., 51
Müller, WW., 52
Mulzer, J., 51
Munoz, E., 222
Murad, S., 227
Muraguchi, A., 56
Murakami, T., 218
Murata, H., 53, 55
Murdoch, R., 125
Murillo, G., 228
Musser, P., 119
Myasoedov, NF., 121

N

Nagaev, IY., 121
Nagafuji, S., 219
Nagata, T., 56
Naidoo, N., 54
Naik, S., 226
Nair, MG., 201, 203, 217, 218, 226, 227
Najdar, H., 53
Nakamura, N., 217, 228
Nakanishi, M., 223
Nakanishi, T., 53, 55
Nakatsuka, M., 125
Namiki, Y., 121, 122
Nasim, S., 217
Natishan, TK., 121
Navarro-Vázquez, A., 224
Navia, MA., 121
Nawaz, HR., 219
Nawaz, SA., 217, 221, 229
Naz, A., 217, 218
Nebigil, CG., 58
Nee, M., 217
Negreiros Nunes Alves, AP., 227
Nell, B., 120
Neogi, P., 217
Nettesheim, DG., 121, 123
Newborg, MF., 125
Newman, DJ., 51
Nguyen Thi Bich, H., 220
Ni, W., 220, 224
Nicol, RW., 55
Nicotra, VE., 127, 159, 162, 174, 219, 221, 224, 228
Nielsen, PG., 123
Niero, R., 221
Nikolic, D., 224
Nimtz, M., 54
Nirmal, MR., 228
Nishikawa, M., 125
Nishiyama, M., 118
Nohara, T., 155, 221, 222, 224
Notario, R., 226
Nowak, A., 224
Nugroho, BW., 20, 52–55
Nur-e-Alam, M., 217
Nussbaumer, P., 119, 122, 123

O
O'Leary, DJ., 57
O'Shea, JJ., 55
Oberbauer, R., 120
Oberhauser, B., 121
Oberti, JC., 127, 217, 219–221, 223, 224, 228
Ochiai, M., 52
Odorico de Moraes, M., 227
Ogawa, K., 223
Ogura, T., 223
Ohba, S., 55
Ohse, T., 55
Ok, HO., 123
Oka, T., 125
Okabe, H., 219
Okawa, M., 219
Okuhara, M., 118
Olejniczak, ET., 121
Olewinski, R., 118
Olmstead, RG., 217
Omobuwajo, OR., 54
Or, YS., 123, 124
Oropeza, RF., 219
Orozco-P, CI., 221
Oshima, Y., 220
Otsuka, M., 57
Overbeek, DL., 123
Owen, DJ., 58

P
Páez, A., 220
Pacher, T., 52, 53
Padma, P., 227
Païs, M., 53, 54
Paiva, FP., 227
Palamara, AT., 56
Palfi, K., 52
Pan, M-H., 219
Pan, M-J., 219
Pan, M-R., 227
Pan, Y., 151, 157, 220
Pan, Y-M., 219
Pandey, A., 217
Panjamurthy, K., 206, 228
Panka, DJ., 57
Pannell, CM., 51–53
Pant, AK., 227
Parge, HE., 121
Park, EJ., 217, 220, 221, 224
Parsons, WH., 123, 124
Parveen, Z., 218
Parvez, M., 174, 224
Pathak, HD., 166, 223
Paul, C., 120
Pawlus, AD., 55
Pecci, A., 224
Pelletier, J., 56, 58
Pelletier, LA., 121
Pengsuparp, T., 52
Penn, G., 118
Perales, A., 222
Pérez-Castorena, AL., 219, 220, 222
Perromat, G., 54
Perveen, S., 218
Pessoa, C., 227, 228
Pessoa, ODL., 223, 226–228
Pestchanker, MJ., 224
Peter, K., 54
Peterson, LB., 124
Petros, AM., 121, 123
Pezzuto, JM., 51–54, 56, 205, 217, 220–222, 224, 228
Phillips, DD., 224
Philogène, BJR., 55, 225
Picollo, MI., 224, 225
Pietro, RCLR., 226
Piette, J., 226
Pinheiro, SM., 226
Pinho, V., 226
Pleiss, U., 122
Pointinger, S., 53, 54
Polin, LA., 228
Pollman, MJ., 57
Ponelle, M., 119, 124
Pong, M., 124
Porco, JA Jr., 1, 39, 44, 48, 56–58
Porn-Ares, MI., 57
Porzel, A., 220
Poukkula, M., 57
Pouny, I., 228
Pramanick, S., 218, 226
Prantz, K., 51
Pribluda, V., 228
Prijono, D., 53
Prince, CZ., 57
Proksch, P., 1, 52–56
Promdang, S., 53
Punetha, H., 227
Puri, SC., 220
Puripattanavong, J., 53
Purushothaman, KK., 55
Putz, E., 119

Q
Qazi, GN., 220
Qin, Z., 43, 58

Qiu, F., 222
Qiu, L., 164, 165, 222
Quada, JC., 228
Quentmeier, H., 55
Quiñones, W., 217, 221, 222, 226
Qureshi, S., 217, 218
Qurishi, MA., 220

R
Rachman, I., 55
Ragan, JA., 125
Ragot, JP., 40, 57, 58
Ramacciotti, NS., 219, 221
Ramchandani, M., 125
Randall-Hlubek, DA., 228
Rao, CV., 218
Rao, DS., 217
Rappersberger, K., 119, 220
Ravelo, AG., 222
Ravindranath, PP., 225, 228
Ray, AB., 157, 185, 217, 220, 227
Ray, DT., 218
Ray, S., 225
Reamer, RA., 121–125
Reddy, J., 118
Reeves, CR., 118
Reider, PJ., 124
Renauld, JAS., 216
Reutrakul, V., 52
Revill, WP., 119
Reynolds, KA., 126
Rhoades, TA., 124
Riaz, M., 219
Riaz, N., 221, 229
Ribeiro, IM., 222, 225–227
Ribeiro, N., 58
Ribeiro, YM., 227
Ribeiro dos Santos, R., 226, 227
Riche, C., 54
Richter, L., 120
Rieger D., 124
Rincón J., 220
Rindlisbacher, A., 54
Ripperger, H., 220
Risinger, AL., 228
Riswan, S., 53–55
Rivero-Cruz, JF., 53
Rizzacasa, MA., 46, 58
Robert, F., 56
Robinson, DJ., 119, 125
Robledo, S., 226
Rocha Silveira, E., 227, 228
Rochais, C., 122, 123
Roche, SP., 58
Rodrigues Filho, E., 226
Rodríguez, R., 214
Roenigk, HH., 119
Rojas, M., 222
Roper, TD., 125
Rosa, R., 124
Rose, WC., 54
Rosini, P., 56
Rotonda, J., 68
Rougas, J., 228
Roux, D., 53
Roy, A., 218
Rozamus, LW., 123
Rubnawaz, H., 218
Ruiz, A., 228
Rupprecht, KM., 123
Russo, T., 56
Ryu, SW., 56

S
Sahai, M., 217, 220, 223
Saifah, E., 52, 53, 55
Saito, K., 222
Saito, S., 56
Salim, AA., 52, 55
Sammakia, T., 125
Samreen, 219, 223, 225, 226
Samson, A., 228
Samuel, R., 52
Sangji, S., 57
Sanglier, JJ., 118, 119
Sangwan, NS., 217, 225
Sangwan, RS., 217, 225, 227
Santana, JM., 226
Santarsiero, BD., 53, 54, 221, 224
Santiago-Valent'in, E., 217
Santisuk, T., 52
Santos, LA., 227
Sarada, A., 55
Sarker, SD., 219, 226
Sashida, Y., 220
Satasook, C., 54, 55
Sato, DN., 226
Sattar, FA., 221
Satyan, KS., 227
Saulnier, MG., 54
Sauvain, M., 220
Savage, GP., 58
Savchenko, T., 226
Saw, LG., 51

Sawyer, PS., 125
Scammells, PJ., 58
Scavone, C., 226
Schaeffer, MJ., 57
Schauber, J., 120
Schaus, SE., 57
Scheurich, P., 57
Schiebel, HM., 119
Schilling, W., 119
Schinnerl J., 53
Schirmer, A., 119
Schmieder, P., 119
Schmitz, I., 57
Schneider, C., 52, 54
Schneider, D., 120
Schneider, RJ., 56
Schoop, A., 57
Schopf, RE., 119
Schreiber, SL., 120, 121, 123, 125
Schuler, W., 119, 122, 124, 125
Schulte, G., 125
Schulz, G., 118, 121–125
Schulz, M., 119
Schulze-Osthoff, K., 57
Schuster, M., 57
Schuurman, H., 119
Schweitzer, A., 122, 124
Schwendinger, B., 119
Schwendinger, H., 120
Scott, G., 120
Seddon, E., 218
Seeram, NP., 227
Seger, C., 53, 54
Sehgal, SN., 119
Seip, S., 224
Sen, G., 166, 223
Sen, N., 226
Sen, T., 226
Senthil, N., 228
Serani, L., 220
Seth, A., 123
Setyowati, FM., 53
Sévenet, T., 53, 54
Severin, J., 121
Sewing, KF., 119
Shabbir, M., 218
Shafiee, A., 119, 121
Shah, SAA., 225
Shamma, M., 224
Shamsub, S., 52
Sharada, AC., 228
Sharada, M., 225
Sharma, LK., 225
Sheets, MP., 124
Shen, J., 224
Shepard, RM., 125
Shevchenko, VP., 121
Shi, G., 227
Shibata, K., 217
Shiengthong, D., 55
Shin, YG., 220
Shingu, K., 184, 222, 224
Shinkai, I., 122, 123, 125
Shishodia, S., 226
Shiyama, T., 125
Shono, K., 53
Shorthouse, R., 119
Showalter, RE., 121
Shu, R., 223
Shuaib, M., 218
Shuman, R., 124
Shvo, Y., 216
Siddiqui, BS., 221
Siddiqui, RA., 157, 227
Siegmund, D., 52, 57
Sik, V., 219
Silva, GL., 219, 228
Silva, MTG., 227
Silveira, ER., 226–228
Silvera, D., 56
Sim, GA., 216
Simas, SM., 226
Simpson, J., 55
Sinclair, PJ., 124
Singh, AB., 218
Singh, D., 226
Singh, SV., 227
Sinha, S., 225
Sinha, SC., 220
Sinha-Bagchi, A., 220
Sintchak, MD., 121
Sistonen, L., 57
Sivaramakrishna, C., 218
Skelton, BW., 222
Skytte, DM., 123
Slatkin, DJ., 217
Smith, DB., 125
Smith, H., 121
Smith, III AB., 125
Smith, ML., 124
Smith, RW., 223
Snader, KM., 51
Snyder, JR., 125
Soares, MBP., 226, 227
Soejarto, DD., 51, 222
Soepadmo, E., 51

Sohar, P., 124
Solomon, FE., 228
Sonenberg, N., 58
Song, BJ., 56
Song, LL., 221, 228
Song, Z., 124
Sorano, T., 55
Sosa, ME., 225
Sotes, IR., 220
Souza, DG., 200, 226
Spergel, JM., 120
Sperner, H., 123–125
Spollen, KM., 51
Spring, H., 52
Springer, JP., 68
Sridhar, P., 218
Srinivasan, KK., 228
Srivastava, AK., 218, 220
Srivastava, J., 221
Stan, SD., 227
Standaert, RF., 120, 121
Staruch, MJ., 124
Steck, A., 121–123
Steinhoff, M., 120
Stent, MAH., 58
Stephens, PW., 224
Steube, KG., 53, 55
Stingl, G., 120
Strasburg, GA., 218
Strauch, MJ., 123
Streicher, SL., 121
Strnadt, G., 121, 122
Strohl, WR., 126
Stuetz, A., 59, 119–120
Su, B-N., 53–55, 217, 221, 224, 228
Su, C-R., 219, 223
Subbaraju, GV., 218
Sudhir, S., 217
Suenaga, T., 118
Suhara, T., 57
Sukarieh, R., 56
Sukumalanand, P., 55
Sumaryono, W., 54
Sun, L-J., 218
Sunayama, R., 164, 222
Sunderkoetter, C., 120
Sung, B., 218
Suparakchinda, N., 53
Suri, KA., 225
Susan, A., 121
Suttisri, R., 52
Svitkin, Y., 58
Swanson, SM., 51–56
Sy, JO., 57
Szumiloski, JL., 123

T

Tagawa, C., 222
Takada, Y., 226
Takagi, M., 221
Takahashi, T., 125
Takakura, Y., 125
Takeshita, M., 220
Takeuchi, T., 57
Tan, BKH., 54
Tanaka, A., 125
Tanaka, H., 118, 123
Tang, L., 220
Tarnowski, MA., 123
Taylor, DAH., 54
Taylor, P., 68
Taylor, RJK., 34, 57
Teichmann, K., 53
Teixeira, MM., 226
Tempczyk, A., 121
Tempête, C., 53
Teng, C-M., 54
Teng, F., 224
Teodoro, JG., 56
Testa, B., 119
Tettamanzi, MC., 177, 223–225, 228
Thede, K., 40, 57, 58
Thoison, O., 54
Thompson, AS., 124
Thompson, DG., 51
Thomson, JA., 121
Thuaud, F., 58
Tinley, TL., 228
Tohda, C., 217, 228, 229
Toledo, J., 211
Tolentino, RB., 226
Tomasetto, C., 58
Tomassini, TCB., 222, 225–227
Tong, D., 119
Tonial, GC., 221
Tonn, CE., 225
Torcia, M., 56
Torres, F., 217, 221, 222,
Torres, FR., 219
Torres, M., 228
Towers, GHN., 54
Tran, VS., 224
Treiber, MK., 52
Tremblay, ML., 56
Trevillyan, JM., 124

Tri, MV., 53
Tricotet, T., 122, 123
Trocca, CE., 223
Trost, BM., 5, 36, 54
Tsay, F-R., 124
Tsay, H-S., 218
Tschaen, DM., 123, 124
Tsukada, K., 56
Tu, NP., 124
Tucker, E., 119
Tucker, KD., 121
Tuli, R., 192, 217, 225
Turkeri, G., 58
Tyldesley, M., 120

U
Uchoa, DEDA., 223
Udupa, N., 228
Ueda, I., 224
Ueffing, N., 57
Uehling, DE., 125
Ueno, A., 222
Ullah, N., 219
Uma Devi, P., 228
Umehara, K., 55, 57, 217, 222
Ungphakorn, A., 55
Uniyal, GC., 217, 225
Usubillaga, A., 159, 221

V
Vaccarini, CE., 219, 225, 226
Vajrodaya, S., 52, 53
Van Breemen, RB., 221, 224
Van Duyne, GD., 120, 121
Vande Velde, V., 218
Vanden Berghe, W., 226
Vandenberghe, I., 228
Vanisree, M., 218
Vankar, PS., 221
Varenne, P., 223
Vazquez, AR., 219
Veleiro, AS., 168, 219–225, 228
Vélez, ID., 221, 226
Venaskulchai, B., 55
Veras, ML., 167, 223, 226–228
Verma, IM., 56
Verma, V., 225
Vezina, C., 119
Vieira, AT., 226
Vieira, NC., 226
Vigo, JS., 224
Vij, SP., 225
Vijayasekaran, V., 52
Villalobos, A., 121, 126
Vispé, S., 228
Viswanathan, S., 52
Vit, P., 120
Vite, GD., 54
Vitorge, B., 218
Vittal, JJ., 54
Voda, J., 119
Voelter, W., 217, 218
Voges, R., 122
Volante, RP., 122, 123, 125

W
Wagner, R., 124
Wagner, T., 121, 122
Wahab, S., 55
Waiss, AC Jr., 25
Wajant, H., 52, 57
Walde, I., 120
Waldstaetten, P., 122, 123
Walker, C., 124
Walkinshaw, MD., 68
Walsh, K., 57
Wang, B-G., 53
Wang, C-Y., 53
Wang, H-S., 219
Wang, J., 119
Wang, MA., 58
Wang, Q., 220
Wang, S., 119
Wang, S-K., 54, 55
Wang, S-S., 219
Wang, W., 57
Wang, X., 220
Wang, Y., 122
Wang, Y-C., 227
Wang, Y-Y., 54
Wang-Fan, W., 122
Warin, R., 227
Watanabe, T., 38, 57
Waterman, PG., 220, 222
Watson, WH., 221
Weavers, RT., 55
Weber, C., 52
Weber, HP., 121, 122
Weber, S., 53
Weber-Roth, S., 122
Weishaeupl, C., 119
Weissman, I., 121
Wendel, HG., 56

Wenzig, E-M., 220
Werner, FJ., 119
White, AH., 222
Whitesell, L., 218, 225
Whiting, DA., 223
Whiting, P., 226
Whittern, DN., 123
Wichtl, M., 224
Wicker, LS., 118
Wieckhusen, D., 122
Wiedeman, PE., 123, 124
Wiederrecht, GJ., 68, 124
Wijeratne, EMK., 225
Wild, R., 54, 56
Williams, ID., 225
Wilusz, MB., 124
Winiski, A., 118
Winkler, T., 54
Wioland, C., 119
Wiriyachitra, P., 55
Wirth, T., 52
Witte, L., 52–54
Wolff, B., 119
Wolff, K., 119–120
Wong, F., 124
Wong, RY., 225
Wray, V., 52–55
Wu, C-C., 219, 221, 227
Wu, J., 119
Wu, M-J., 219
Wu, S-J., 219
Wu, T-S., 54, 219, 223
Wu, X-H., 54
Wu, Y-C., 219, 221, 227
Wube, AA., 220
Wyvratt, MJ., 123, 124

X
Xavier, DCD., 222
Xia, Y., 220
Xia, Z., 56
Xie, B-B., 220
Xie, B-J., 53
Xie, C-M., 221
Xie, Q., 123
Xie, ZQ., 58
Xu, RX., 121
Xu, Y., 225
Xu, Y-J., 54
Xu, YM., 218

Y
Yahara, S., 224
Yamaguchi, K., 222
Yamamoto, T., 55, 222
Yamamoto, Y., 56
Yamamura, H., 222, 223
Yang, B., 151, 157, 220
Yang, BV., 54
Yang, H., 227
Yang, J-Y., 224
Yang, S-P., 53
Yang, Y., 223
Yang, Y-L., 221
Yao, X-S., 222
Yasmeen, K., 219
Yasmin, R., 218, 219
Yasuda, T., 121
Yeh, JH., 57
Yen, H-F., 221
Yen, M-H., 221
Yokosuka, A., 151, 220
Yokota, Y., 225
Yoshikawa, M., 218
Yoshimitsu, A., 221
Yoshimitsu, H., 222
Yoshimura, N., 125
Yoshino, T., 56
Yoshitake, Y., 222
Yousaf, M., 217, 218, 227
Yousuf, S., 217, 223, 225, 229
Yue, J-M., 53
Yura, H., 125

Z
Zabel, V., 221
Zaheer, UH., 227, 229
Zamora, MA., 225
Zamzami, N., 56
Zehender, H., 124
Zenke, G., 119, 122, 124, 125
Zerba, E., 224, 225
Zhan, X., 228
Zhang, L., 228
Zhang, Y., 227
Zhao, F., 222
Zhao, J., 217
Zhao, M., 124
Zhao, P-J., 54
Zhao, Q., 222
Zhao, R-H., 224

Zhou, J., 53
Zhou, L-Y., 220
Zhou, Y., 119
Zhu, JY., 52, 56
Zhu, XH., 221
Zhuang, S., 56
Zimmer, R., 124, 125
Zimmerlin, AG., 124
Zink, DL., 118
Zollinger, M., 124

Subject Index

A
Acetylcholinesterase (AChE) inhibitors, 208
10-*O*-Acetyledulirin A, 16
1-*O*-Acetylrocaglamide, 26
Acnistins, 132, 133, 159
  antileishmanial activity, 199
Acnistus arborescens, 149
  acnistins, 159
  cytotoxicity, 211
  exodeconolides, 152
  trypanocidal activity, 197
Activation-induced-cell-death (AICD), 33
Aglaforbesin derivatives, 17
Aglaforbesins, 15, 19
Aglaia argentea, 10
Aglaia dasyclada, 16
Aglaia duperreana, 9, 24
Aglaia edulis, 16, 21
Aglaia elaeagnoidea, 10, 11, 25
Aglaia elliptica, 12
Aglaia elliptifolia, 4
Aglaia forbesii, 3
Aglaia foveolata, 11, 17
Aglaia harmsiana, 9
Aglaia odorata, 3, 4, 10
Aglaia ponapensis, 16
Aglaia roxburghiana, 9, 12
Aglaia spectabilis, 10, 11
Aglaia spp. (Meliaceae), 1
  activities, 4
Aglaia tomentosa, 3
Aglaiastatin, 12, 28, 38
Aglaiformosanin, 12
Aglains, 12, 17
Aglaroxins, 12, 28
Aglaxiflorin A, 16
Ajuga bracteosa, bracteosins, 154, 208
Ajuga parviflora, coagulin R, 132, 141, 146
Ajuga spp., withanolides, 132, 146
Allergic contact dermatitis (ACD), 62
Allescheria boydii, withanolide, 200
Angiogenesis inhibitors, withanolides, 207
Anomanolides, 168
Antascomycins, 60
Antiangiogenic activity, withanolides, 214
Antifeedants, withanolides, 202
Antifungal, withaferin A, 207
Antileishmanial activity, 206
Antistress, withafastuosin, 210
Apoptosis induction, rocaglamides, 31
Ascomycin, 60
  derivatives, anti-inflammatory, 62
  structure, 66
Ashwagandha, 128
Ashwaghandanolide, 143
Aspergillus niger, withaferin A, 200
Azadirachta indica, 24
Azadirachtin, 24

B
Bacillus subtilis, withaferin A, 199
Baimantuoluolines, 152, 157
Baimantuoluosides, 149
Benzo[*b*]oxepines, 18
Brachistus stramoniifolius, physalins, 163
Bracteosins, 154
  AChE/BChE inhibition, 208
Butyrylcholinesterase (BChE), 208

C
Calcineurin inhibitors, 63
Chagas disease, withanolides, 197
Chantriolides, 151
Chenopodium album, effect of withanolides, 197
Cholinesterase inhibition, 208
Choroidal neovascularization, 207

Cilistediol, 156
Cilistepoxide, 156
Cilistols, 155
Cinerolide, 171
Coagulansin, 139, 140
Coagulin, 135, 141
Cunninghamella elegans, isophysalin, 191
Curvularia lunata, withanolide, 200
Cyclo-ascomycins, 80, 117
Cyclofloveoglin, 17
Cyclooxygenase–2 (COX–2) inhibition, 201
Cyclopenta[b]benzofurans, 4
  synthesis, 34
Cyclopenta[*b*]tetrahydrobenzofuran, 6
Cyclopenta[*bc*]benzopyran(2,5-methano–1-benzoxepin), 12
Cyclophysalins, 165, 189
Cyclorocaglamide, 12
Cyclosporin A,, 60
Cyclowithanolides, 162

D
Datura fastuosa, withafastuosin D, anxiolytic, 202
Datura ferox, 149, 214
Datura inoxia, 158, 214
Datura metel, 154, 157, 192
  cytotoxicity, 204
Datura metel var. *fastuosa*, 151
Datura quercifolia, 149
Datura spp., 129
Datura stramonium var. *tatula*, 152
Daturalactones, 149, 201
Daturalicin, 157
Daturametelins, 154, 157
Datureae, 213
Death inducing signaling complex (DISC), 31
Dehydroedulirin A, 16
Dehydroedulisone, 20
9-Deoxoascomycin, 84
4-Deoxywithaperuvin, 135
  antibacterial, 199
Deprea orinocensis, withajardins, 199
Desacetylpyrimidaglains, 17
Desmethylrocaglamide, 6
24-Desoxyascomycin, 94, 117
Dihydro–3β-hydroxywithacnistine, 196
Discopodium penninervium, 149, 153, 160
  17-epiacnistin A, 160
Drechslera rostrata, withanolide, 200
Drosophila melanogaster, ecdysteroid-responsive, 196
Dunalia brachyacantha, 150, 153
  trypanocidal activity, 197
  withaphysalin, 167
Dunalia solanacea, acnistins, 160
  withajardins, 199
Dunawithanines, 150

E
Ecdysteroids, agonists/antagonists, 196
Edulirin A, 16
Edulisones A, 20
4-Epiaglain A, 15
Epoxyphysalin, 199
Epoxywithanolides, 135
Ergostane glycosides, 156
Eriolarynx lorentzii, 148, 212
  withaphysalins, 166
Escherichia coli, withaferin A, 199
Eucalyptus globulus, C_{29} withanolide, 157
  withanolides, 132
Excited-state intramolecular proton transfer (ESIPT), 39
Exodeconolides, 152
Exodeconus maritimus, 152, 214, 216

F
Flavaglines, 1, 4, 5
Forbaglines, 15, 19
Furano-ascomycins, 70

G
Glucosomniferanolide, 140
Growth inhibition, withanolides, 194

H
Helicoverpa armigera, 23, 25
18-Hydroxyascomycin, 99
Hydroxynicandrin, 149
17β-Hydroxywithanolide K, antifungal activity, 200
18-Hydroxywithanolide, 148
Hyoscyameae, 213
Hyoscyamus niger, 214
  16α-acetoxyhyoscyamilactol, 152

I
IFN-γ, 26, 63
IL–4, 26, 63

Iochroma australe, 212
7-oxygenated withanolides, 196
Iochroma fuchsioides, 212
Iochroma gesneroides, 148, 149, 154, 196
Iochrominae, 212
Isofoveoglin, 17
Isothapsakon A, 12, 22
Isotubocaposides 160
Ixabepilone, 2
Ixocarpalactones, 134, 172
cancer chemopreventive, 205
Ixocarpanolide, 137
Ixocarpolactones, cytotoxicity, 204

J
Jaborochlorotriol, 174
Jaboromagellonine, 149
Jaborosa araucana, 178
Jaborosa bergii, 147, 162, 215
Jaborosa caulescens, 159, 175, 215
Jaborosa laciniata, trechonolide, 174
Jaborosa leucotricha, 147, 215
jaborosalactone, 171
Jaborosa odonelliana, feeding-deterrent, 195
jaborosalactone P, 178
Jaborosa reflexa, 215
Jaborosa rotacea, 159, 185, 215
Jaborosa runcinata, 178
Jaborosa sativa, 167, 215
Jaborosa spp., 159, 215
Jaborosalactols, 147, 162
Jaborosalactones, 147, 159
Jaborotetrol, 174, 175

K
Kaempferol, 22
12-Ketowithanolides, 149
Khaya (African mahogany), 3

L
Lactuca sativa, effect of withanolides, 197
Larnax glabra, 154
Larnax subtriflora, subtrifloralactones, 206
trechonolides, 177
Leishmania spp., withanolides, 197, 198
Leishmanicidal activity, 198
Lycieae, 213
Lycium barbarum, 214
Lycium chinense, 214

M
Macrophilin, 62, 67
Margaranthus solanaceous, physalins, 163
Marikarin, 12
Meliaceae, 1
3'-Methoxypannellin, 11
Methyl rocaglate, 6
Microsporum canis, withanolide, 200
Microtubule stabilizing activity, 207
Mycobacterium tuberculosis, physalin, 200

N
NAD(P)H:quinone reductase (QR), 205
Neophysalins, 165
Nicandra physalodes, 168, 193
Nicandrenone, 193
18-Norwithanolides, 181

O
Odorine, 12, 15–17, 23
Odorinol, 12, 15–17, 23
Ostrinia nubilalis, 23
Oxomethylendioxyrocaglaol, 26

P
Pannellin–1-*O*-acetate, 11
Peridroma saucia, 23
Perulactones, 134, 172
Phalaris canariensis,, 197
Philadelphicalactone A, cancer chemopreventive, 205
Philadelphicalactones, 153
Phyperunolides, 144
Physachenolides, 144
Physacoztolides, 148
Physagulins, 146, 147
trypanocidal activity, 197, 198
Physaleae, 210–213
Physalin B, inhibitor, ubiquitin-mediated proteasome pathway, 207
Physalins, 132, 133, 163
antileishmanial activity, 198
biotransformations, 189–192
nitric oxide, inhibition of production, 203
photocyclization, 191
photooxygenation, 190
trypanocidal activity, 197
Physalis alkekengi, 203
Physalis angulata, physalins, 164
physanolides, 173

Physalis chenopodifolia, 148
Physalis cinerascens, cinerolide, 171
Physalis coztomatl, 148
Physalis divaricata, physalins/withaphysalins, 184
Physalis minima, antileishmanial activity, 198
withaphysalins, 167
Physalis peruviana, 144
coagulin R, 141
Physalis philadelphica, 153
cancer chemopreventive, 205
ixocarpalactone, 172
Physalis spp., 129
Physalis virginiana, virginols 153
Physanolides, 173
Physapubenolide, 147
Pieris rapae, 23
Pimecrolimus, 59, 63, 100
Piriferine, 12, 15–17, 22
Plantagiolides, 151
Poly(ADP-ribose) polymerase (PARP), 31
Pseudomonas aeruginosa, withaferin A, 199
Putrescine, 16, 22
Pyrimidaglains, 17

Q
Quinone reductase, 206

R
Rapamycin, 60
Ras-ERK-Mnk1 pathway, 30
Retapamulin, 2
Rhizopus stolonifer, physalin H, 189
Rhodnius prolixus, physalins, 196
Rocaglamides, 4, 6, 23
anticancer, 28
anti-inflammatory, 26
biosynthesis 20
derivatives, 5
discovery, 4
inhibition of protein synthesis, 29
insecticidal, 23
pharmacology, 23
structures, 5
synthesis, 34
Rocaglaol, 6, 40
Rocaglates, 5, 47

S
Salpichroa origanifolia, 314
antifeedant, 194
Salpichrolides, 171, 184, 186
antifeedant, 194
Sativolides, 132, 133, 157
Schraderanthus viscosus, physalins, 163
Secofoveoglin, 17
Silvestrol, 28, 30
syntheses, 44
Solanaceae, uncertain taxa, 213
Solaneae, 213
Solanum ciliatum, 3,5-cyclowithanolides, 155
Solanum sisymbriifolium, 156, 214
Sominone, memory deficit, 208
Somniferanolide, 143
Somnifericin, 136
Somniwithanolide, 143
Sorghum halepense, effect of withanolides, 197
Spiranoid-γ-lactones, 134, 178
Spodoptera frugiperda, 25
Spodoptera littoralis, 23
Staphylococcus aureus, withaferin A, 199
Streptomyces hygroscopicus var. *ascomyceticus*, 60
Subtrifloralactones, 132, 134, 182
QR induction, 206
Swietenia (mahogany), 3, 4
Synaptogenesis, 208

T
Tacca chantrieri, 151
microtubule stabilizers, 207
Tacca paxiana, 180
Tacca plantaginea, 151
taccalonolides, 179
Tacca spp., withanolides, 132
Tacca subflabellata, taccalonolides, 178
Taccalonolides, 132, 134, 179
microtubule stabilizing, 207
Tacrolimus, 60
Tetrahydrocyclopenta[*b*]benzofuran, 5
Thapsakones, 16, 22
TNF-α, 26, 63
Trabectedin (ET–743), 2
Trechonolides, 134, 174
Tribolium castaneum, 194
Trihydroxyoxowithadienolide, cancer chemopreventive, 205
Trypanosoma cruzi, withanolides, 197
Trypanosoma rangeli, 198
Tsukubamycins, 84
Tubocapsanolides, 154
cytotoxicity, 203

Tubocapsicum anomalum, 154
acnistins, 159
cytotoxic, 203
17-methyl–18-nor-ergostanes, 184
Tubonolides, 161

V
Vassobia breviflora, 212
Virginols, 153
Viscosalactone B, 201

W
Withacoagulins, 139
Withafastuosins, 151, 157, 202
Withaferin A, 128, 135, 143
antiinflammatory, 200
biotinylated analog, 190
cytotoxicity, 203
Withajardins, 132, 133, 161
antileishmanial activity, 199
Withametelinols, 157
Withametelins, 132, 133, 151, 157
cytotoxicity, 204
Withaminimin, trypanocidal activity, 198
Withangulatins, 145, 204
trypanocidal activity, 198
Withania adpressa, 135
Withania aristata, 135
Withania coagulans, 135
Withania somnifera, 128, 135
Ayurveda, 192
cytotoxicity, 204
glucosyltransferases, 191
Withanolides, 127ff, 139
antiinflammatory, 200
antimicrobial, 199
antiparasitic, 197
biological activities, 192
biotransformations, 185, 189
cancer-related activities, 203
chemotaxonomy, 209
classification, 132
CNS-related activities, 208
cytotoxicity, 203
epoxides, 192
glucocorticoid activities, 200
immunosuppressive/immunomodulatory, 202
insecticidal, 193
δ-lactone/δ-lactol side chain, 132
γ-lactone side chain, 134, 172
modified, 157
non-solanaceous, 132
photochemical transformations, 208
phytotoxic, 196
Solanaceae, 129
spiranoid at C–22, 184
trypanocidal activity, 197
unmodified, 135
Withanone, 205
Withanosides, 137
Withaperuvins, 135, 196
Withaphysacarpin, 153, 154
cancer chemopreventive, 205
Withaphysalins, 132, 163, 166
trypanocidal activity, 197
Withaphysanolide, 184
Witharifeen, 157
Witharistatin, 135
Withasomniferols, 137
Witheringia solanacea, physalins, 163

Z
Ziconotide, 2